The role of DOK7 and its variants in colorectal cancer

By

Lucy Kate Satherley

Cardiff-China Medical Research Collaborative

Cardiff University School of Medicine

December 2016

Thesis submitted to Cardiff University for the application of degree of Doctor of Philosophy (PhD)

The role of DOK7 and its variants in colorectal cancer

Student:	Lucy Kate Satherley
Student Number:	990334242
Supervisors:	Professor WG Jiang
	Miss R Hargest
	Doctor L Ye

Cardiff-China Medical Research Collaborative

Cardiff University School of Medicine

Heath Park

Cardiff

Wales

UK

CF14 4XN

December 2016

Declaration

This work has not been submitted in substance for any other degree or award at this or any other university or place of learning, nor is being submitted concurrently in candidature for any degree or other award.

Signed……Date……

Statement 1

This thesis is being submitted in partial fulfilment of the requirements for the degree of PhD

Signed……Date……

Statement 2

This thesis is the result of my own independent work/investigation, except where otherwise stated. Other sources are acknowledged by explicit references. The views expressed are my own.

Signed……Date……

Statement 3

I hereby give consent for my thesis, if accepted, to be available for photocopying and for interlibrary loan, and for the title and summary to be made available to outside organisations.

Signed……Date……

Dedication

To my wonderful parents

For inspiring in me a love of learning and for your unfailing love and support, this thesis is dedicated to you with all my love and thanks for all you have done for me.

Acknowledgements

I would like to thank my supervisors, Professor Wen G. Jiang and Miss Rachel Hargest, firstly, for providing me with the opportunity to participate in laboratory based research and secondly, for their guidance and support over the last four years.

I would also like to thank all the staff and students at the Cardiff-China Medical Research Collaborative for making me feel so welcome. It has been such a privilege to combine clinical medicine and science and your help, advice, support and friendship has made my time as a PhD student so enjoyable. In particular, I would like to thank my laboratory supervisor Dr. Lin Ye for his friendship, support, encouragement and advice.

I am also very grateful to my clinical colleagues, particularly those in the Department of Surgery at the University Hospital of Wales in Cardiff, who have allowed me to dedicate time to my research and also to Cardiff and Vale NHS Trust for employing me as a clinical fellow during my PhD studies. I would also like to especially thank my consultant colleagues at the Breast Centre in University Hospital Llandough (Ms Eleri Davies, Ms Donna Egbeare, Mr Sumit Goyal and Professor Helen Sweetland) whose support and encouragement has ensured I have been able to write up, submit, defend and complete my thesis whilst continuing my higher surgical training.

Finally, I would like to dedicate this work to my family, especially my parents, and to my husband Guy, and to thank them for their never-ending love, support and encouragement through all the challenges of working full-time and simultaneously undertaking a full-time PhD!

Publications and Presentations undertaken during the period of research

Published papers

LK Satherley, PH Sun, K Ji, M Mason, R Hargest, WG Jiang, L Ye. Prostate apoptosis response-4 (PAR4) suppresses growth and invasion of breast cancer cells and is positively associated with patient survival. *Anticancer Research* 2016 **36**:1227-1236 (Impact factor = 1.895).

MFA Malik, **LK Satherley**, EL Davies, L Ye, WG Jiang. Expression of Semaphorin 3C in breast cancer and its impact on adhesion and invasion of breast cancer cells. *Anticancer Research* 2016 **36**:1281-1286 (Impact factor = 1.895).

S Shao, PH Sun, **LK Satherley**, X Gao, K Ji, Y Feng, Y Jia, J Ji, WG Jiang, L Ye. Reduced RanBPM expression is associated with distant metastasis in gastric cancer and chemoresistance. *Anticancer Research* 2016 **36**: 1295-1304 (Impact factor = 1.895).

J Li, L Ye, PH Sun, **LK Satherley**, R Hargest, Z Zhang, WG Jiang. MTA1 is up-regulated in colorectal cancer and is inversely correlated with lymphatic metastasis. *Cancer Genomics and Proteomics* 2015 11-12;**12**(6):339-345 (Impact factor = 2.800).

LK Satherley, L Ye, WG Jiang, R Hargest. Tumour suppressor genes in gastric carcinogenesis: An up-to-date review of genetic and epigenetic changes in the development of gastric adenocarcinoma. *Transl Gastrointest Cancer* 2015;**4**(4):294-307.

WG Jiang, L Ye, F Ruge, PH Sun, AJ Sanders, K Ji, J Lane, L Zhang, **L Satherley**, HP Weeks, X Zhi, Y Gao, C Wei, Y Wu, MD Mason. Expression of Sonic Hedgehog (SHH) in human lung cancer and the impact of YangZheng XiaoJi on SHH-mediated biological function of lung cancer cells and tumour growth. *Anticancer Research* 2015 Mar;**35**(3):1321-31 (Impact factor = 1.895).

WG Jiang, L Ye, F Ruge, S Owen, T Martin, PH Sun, AJ Sanders, J Lane, **L Satherley**, HP Weeks, Y Gao, C Wei, Y Wu, MD Mason. YangZheng XiaoJi exerts anti-tumour growth effects by antagonising the effects of HGF and its receptor, cMET in human lung cancer cells. *J Transl Med* 2015 Aug 27;**13**:280 (Impact factor = 3.694).

Published abstracts

LK Satherley, L Ye, R Hargest, WG Jiang. DOK7 variant expression and function in human colorectal cancer. *Anticancer Research* 2015 **35** (7): 4331 (Impact factor = 1.895).

WG Jiang, L Ye, F Ruge, PH Sun, AJ Sanders, K Ji, J Lane, **L Satherley**, HP Weeks, Y Gao, C Wei, Y Wu, MD Mason. YangZheng Xiaoji sensitises the response to SIS3 inhibitor in human cancer cells, in vitro and in vivo; therapeutic implications. *Anticancer Research* 2015 **35**(7): 4360 (Impact factor = 1.895)

L Satherley, W Jiang, R Hargest, J Torkington, M Davies. Expression of lymphangiogenic factors VEGF-C and VEGF-D and impact of VEGF-D knockout on tubule formation in human colorectal cancer. *Br J Surg* 2015 **102**: 8 (Impact factor = 5.596).

LK Satherley, L Ye, R Hargest, WG Jiang. DOK7 expression in colorectal cancer cells and association with clinical and prognostic outcome. *Br J Surg* 2014 **101**(Suppl 4): 12 (Impact factor = 5.596).

L Satherley, L Ye, R Hargest, WG Jiang. DOK7 expression and association with patient survival. *European Journal of Cancer* 2013 **49**:S158 (Impact factor = 6.163)

Oral Presentations

L Satherley. Dok7 expression in colorectal cancer: Association with tumour pathology and clinical outcome, Institute of Cancer and Genetics PhD seminar Day, Cardiff University, October 2014.

L Satherley, L Ye, R Hargest, WG Jiang. Dok7 expression in colorectal cancer cells and association with clinical and prognostic outcome. MIA Prize session, President's Day meeting, Royal Society of Medicine, June 2014

L Satherley, WG Jiang, R Hargest, J Torkington, ML Davies. Expression of lymphangiogenic factors VEGF-C and VEGF-D and impact of VEGF-D knockout on tubule formation in human colorectal cancer. Association of Surgeons of Great Britain and Ireland (ASGBI) Conference (Short Paper of Distinction), Harrogate, May 2014

L Satherley, L Ye, R Hargest, W Jiang Dok7 expression in colorectal cancer cells and association with clinical and prognostic outcome, SARS conference, Cambridge, January 2014

L Satherley. Medical training in the UK. Cardiff University-Capital Medical University International Centre for Biomedical Research Symposium. Beijing, China, July 2013.

Poster Presentations

L Satherley, L Ye, R Hargest, WG Jiang. Downstream of tyrosine kinase 7 (DOK7) variant expression and function in human colorectal cancer. ECCO/ESMO Conference, Vienna, September 2015

C Bunston, PH Sun, **L Satherley**, K Ji, C Hao, J Ji, WG Jiang, L Ye. Capillary morphogenesis gene 2 is overexpressed by local advanced pancreatic tumours and the corresponding therapeutic potential. China-UK Cancer (CUKC) Conference, Cardiff, July 2015

L Satherley, L Ye, R Hargest, WG Jiang. DOK7 variant expression and function in human colorectal cancer. China-UK Cancer (CUKC) Conference, Cardiff, July 2015

WG Jiang, L Ye, F Ruge, PH Sun, AJ Sanders, K Ji, J Lane, **L Satherley**, HP Weeks, Y Gao, C Wei, Y Wu, MD Mason. YangZheng Xiaoji sensitises the response to SIS3 inhibitor in human cancer cells, in vitro and in vivo; therapeutic implications. China-UK Cancer (CUKC) Conference, Cardiff, July 2015

L Satherley, L Ye, R Hargest, WG Jiang. Dok 7 expression in colorectal cancer cells and association with clinical and prognostic outcome. BASO/Cardiff University teaching day, June 2014

L Satherley, L Ye, R Hargest, WG Jiang. Psoriasin expression in human colorectal cancer. Digestive Diseases Week, Chicago, May 2014

L Satherley, L Ye, R Hargest, WG Jiang. DOK7 expression in colorectal cancer cells and association with patient survival. European Cancer Congress, Amsterdam, September 2013.

Abbreviations

α-SMA	alpha smooth muscle actin
Abl	Abelson murine leukaemia viral oncogene
ABS	antibiotics
AChE	acetylcholine esterase
AChR	acetylcholine receptor
ACPGBI	Association of Coloproctology of Great Britain and Ireland
AICR	American Institute for Cancer Research
AJCC	American Joint Committee on Cancer
Akt	v-Akt murine thymoma viral oncogene (also known as PKB)
Ang-1	angiopoietin-1
AP-1	activator protein 1
APC	adenomatous polyposis coli
APER	abdomino-perineal excision of the rectum
APS	ammonium persulphate
AFP	alpha-fetoprotein
ATP	adenosine triphosphate
B-ALL	B-cell acute lymphoblastic leukaemia
bcr	breakpoint cluster region
BCR	B-cell antigen receptor
BCR-ABL	BCR-ABL fusion gene
BM	basement membrane
bp	base pairs
BRCA	Breast cancer gene
BRAF	proto-oncogene B-Raf

BSA	bovine serum albumin
BSS	balanced salt solution
Btk	Bruton's tyrosine kinase
CA-125	cancer antigen 125
CA 19-9	cancer antigen 19-9
$CaCl_2$	calcium chloride
Cas	Crk-associated substrate adaptor protein
Cbl	Casitas B-lineage lymphoma protein ligase
CD	cluster of differentiation
cDNA	complementary DNA
CEA	carcinoembryonic antigen
ChAT	choline acetyltransferase
CLL	chronic lymphocytic leukaemia
CML	chronic myeloid leukaemia
CMS	congenital myasthenic syndrome
CO_2	carbon dioxide
CPEx	cardiopulmonary exercise
CRC	colorectal cancer
Crk	v-Crk avian sarcoma virus CT10 oncogene homolog
Crk-L	v-Crk avian sarcoma virus CT10 oncogene homolog-like
CRM	circumferential resection margin
Csk	c-Src tyrosine kinase
CT	computed tomography
C-terminal	carboxyl-terminal
DAB	diaminobenzidine
DABSYL	4-(4'-dimethylaminophenylazo) sulfonic acid
DC™	Detergent compatible
DCC	deleted in colorectal carcinoma

DEPC	Diethylpyrocarbonate
dH_2O	distilled water
DMEM	Dulbecco's Modified Eagle medium
DMSO	dimethylsulphoxide
DNA	deoxyribonucleic acid
dNTP	deoxynucleotide
DOK	downstream of kinase
ECACC	European Collection of Authenticated Cell Cultures
E-cadherin	epithelial cadherin
ECIS®	electric cell-substrate impedance sensing
ECM	extracellular matrix
EDTA	ethylenediaminetetraacetic acid
EGF	epidermal growth factor
EGFR	epidermal growth factor receptor
Elk	ETS transcription factor
EMR	endoscopic mucosal resection
EMT	epithelial-mesenchymal transition
EphB2	EPH receptor B2
Epo	erythropoietin
ErbB2	Erb-B2 receptor tyrosine kinase 2 (also known as HER-2)
ERK	extracellular signal-regulated kinase
ESD	endoscopic submucosal dissection
EXO1	exonuclease 1
FAK	focal adhesion kinase
FAP	familial adenomatous polyposis
FcepsilonRI	high affinity IgE receptor
FCS	foetal calf serum
FGF	fibroblast growth factor

FOLFOX	folinic acid + fluorouracil + oxaliplatin
FOLFIRI	folinic acid + fluorouracil + irinotecan
Fos	FBJ murine osteosarcoma viral oncogene homolog
FOXO3a	Forkhead Box O3
Fyn	FYN proto-oncogene
Gab	Grb2-associated-binding protein
GAP	GTPase activating protein
GAPDH	glyceraldehyde 3-phosphate dehydrogenase
GATA	GATA transcription factor
GDNF	glial cell derived neurotrophic factor
GDP	guanosine diphosphate
GPVI	glycoprotein VI platelet
GRB2	growth factor receptor bound protein 2
GTP	guanosine triphosphate
H_2O	water
HAI	hepatocyte growth factor activator inhibitor type 1
HBSS	Hank's balanced salt solution
HCl	hydrochloric acid
Hepes	4(2-hydroxyethyl)-1-piperazine-ethanesulphonic acid
HER2	Erb-B2 receptor tyrosine kinase 2 (also known as ErbB2)
HGF	hepatocyte growth factor
HGFA	hepatocyte growth factor activator
HGFR	hepatocyte growth factor receptor (also known as c-Met)
hMLH1	MutL homolog 1
hMSH2	MutS homolog 2
HNPCC	hereditary non-polyposis colorectal cancer
H. pylori	*Helicobacter pylori*
HPV	human papillomavirus

HRAS	Harvey rat sarcoma viral oncogene homolog
HRP	Horseradish peroxidase
IARC	International Agency for Research on Cancer
Ick	intestinal cell (MAK-like) kinase
IFN-γ	interferon gamma
IgE	Immunoglobulin E
IGF	insulin-like growth factor
IGF-1	Insulin-like growth factor 1
IGFBP	Insulin-like growth factor-binding protein
IGF-IR	Insulin-like growth factor 1 receptor
IgG	Immunoglobulin G
IgM	Immunoglobulin M
IL	interleukin
IP	immunoprecipitation
IRS	insulin receptor substrate
JAK	Janus kinase
JNK	c-Jun N-terminal kinases
Jun	Jun proto-oncogene
KCl	potassium chloride
KH_2PO_4	monopotassium phosphate
Kit	KIT proto-oncogene receptor tyrosine kinase
KRAS	Kirsten rat sarcoma viral oncogene homolog
LAT	linker of activated T cells
LB	Lysogeny broth/Luria-Bertani medium
Lck	lymphocyte-specific protein tyrosine kinase
LGM	limb girdle myasthenia
LPS	lipopolysaccharide
Lrp4	lipoprotein receptor related protein 4

Lyn	tyrosine protein kinase Lyn
mAbs	monoclonal antibodies
MAPK	mitogen-activated protein kinase
MCMV	murine cytomegalovirus
mCRC	metastatic colorectal cancer
MDT	multidisciplinary team
MEK	MAPK/ERK kinase
MDT	multidisciplinary team
Met	hepatocyte growth factor receptor (also known as HGFR)
min	minute
MMP	matrix metalloproteinase
MMR	mismatch repair
mnd2	motor neuron degeneration 2
MR	magnetic resonance
mRNA	messenger RNA
MSH3	MutS homolog 3
MSH6	MutS homolog 6
MuSK	muscle specific kinase
Myc	v-Myc avian myelocytomatosis viral oncogene homolog
NaCl	sodium chloride
Na_2HPO_4	disodium phosphate
Na_3VO_4	sodium orthovanadate
NaOH	sodium hydroxide
Nck	cytoplasmic protein NCK
NES	nuclear export signal
NF-κB	nuclear factor kappa-light-chain-enhancer of activated B cells
NICE	National Institute for Health and Care Excellence
NK	natural killer

NMJ	neuromuscular junction
NPI	Nottingham Prognostic Index
NRAS	Neuroblastoma RAS viral oncogene homolog
NT	neurotrophin
N-terminal	amino-terminal
p53	tumour protein p53
PAGE	polyacrylamide gel electrophoresis
Pak	p21 protein (Cdc42/Rac)-activated kinase
PBS	phosphate buffered saline
PCR	polymerase chain reaction
PDGF	platelet-derived growth factor
PDPL	podoplanin
PET	positron emission tomography
PH	pleckstrin homology
Ph+	Philadelphia chromosome positive
Ph-	Philadelphia chromosome negative
Ph1	Philadelphia chromosome
PI3K	phosphatidylinositol 3-kinase
PKB	v-Akt murine thymoma viral oncogene (also known as Akt)
PLC-γ	phospholipase C, gamma
PMP	platelet-derived microparticles
PMS1	PMS1 homolog 1, mismatch repair system component
PMS2	PMS1 homolog 2, mismatch repair system component
PMSF	phenylmethylsulfonyl fluoride
Prox-1	Prospero Homeobox 1
PSA	Prostate-specific antigen
PTB	phosphotyrosine binding
PtdIns5P	phosphatidylinositol 5-phosphate

PTK	protein tyrosine kinase
PxxP	proline-rich
qPCR	quantitative real-time PCR
Raf	Raf proto-oncogene serine/threonine-protein kinase
Rap	Rap GTP-binding protein
Ras	Rat sarcoma
RasGAP	Ras GTPase activating protein
RET	RET proto-oncogene
RNA	ribonucleic acid
RNase	ribonuclease
ROS	reactive oxygen species
RPMI	Roswell Park Memorial Institute
rRNA	ribosomal RNA
RTK	receptor tyrosine kinase
RT	reverse transcription
RT-PCR	reverse transcription polymerase chain reaction
SCF	stem cell factor
SDF-1	stromal cell-derived factor 1
SDS	sodium dodecyl sulphate
SH2	Src homology 2
SH3	Src homology 3
Shc1	Src homology 2 domain containing transforming protein 1
SHIP	Src homology 2 domain-containing inositol 5'-phosphatase
SHP-1	protein tyrosine phosphatase, non-receptor type 6
SHP-2	protein tyrosine phosphatase, non-receptor type 11
SIGGAR	Special Interest Group in Gastrointestinal and Abdominal Radiologists
siRNA	small interfering RNA
Snail1	zinc finger protein SNAI1

SLP-65	B-cell linker protein
Slug	snail family zinc finger 2
SMAD	SMAD family member
SOC	super optimal broth catabolite repression
SOS	SOS Ras/Rac guanine nucleotide exchange factor 1
Src	SRC proto-oncogene, non-receptor tyrosine kinase
ssRNA	single stranded ribonucleic acid
STAT	signal transducer and activator of transcription
Syk	spleen tyrosine kinase
TBE	Tris-Boric acid-EDTA
T-bet	T-box transcription factor TBX21
TBS	Tris buffered saline
TCR	T cell receptor for antigen
Tec	Tec protein tyrosine kinase
Tek	Tek receptor tyrosine kinase
TEMED	tetramethylethylenediamine
TGF-α	transforming growth factor alpha
TGF-β	transforming growth factor beta
Th2	T helper lymphocytes, type 2
TLR	toll like receptor
T_m	melting temperature
TNF-α	tumour necrosis factor alpha
TNM	tumour node metastasis
TRAP	thrombin receptor activating peptide
Tris	tris(hydroxymethyl)aminomethane
TRITC	tetramethylrhodamine
Trk	tropomyosin-related kinase
tRNA	transfer RNA

Tween 20	polyethylene glycol sorbitan monolaurate
Twist1	Twist related protein 1
Tyr	tyrosine
UICC	Union for International Cancer Control
UV	ultraviolet
Vav	proto-oncogene Vav
VEGF	vascular endothelial growth factor
WCRF	World Cancer Research Fund
WHO	World Health Organisation
Wnt	Wnt family member
XELOX	capecitabine + oxaliplatin
Yes	YES proto-oncogene 1, Src family tyrosine kinase
Zap-70	Zeta chain of T cell receptor associated protein kinase 70kDa
ZnCl	zinc chloride
ZO1	zona occludens-1

Abstract

The downstream of tyrosine kinase (Dok) protein family has seven members, Dok 1-7. The precise role of these proteins is not entirely clear although some authors have suggested a potential tumour suppressor role. The aims of this clinically oriented PhD were to determine the expression profile and role of DOK7 in human colorectal cancer, to determine whether DOK7 expression is associated with tumour pathology and clinical outcome data, to determine the functional role of DOK7 in colorectal cancer cells and to evaluate DOK7 coordinated cell signalling in colorectal cancer.

Initial work revealed that DOK7 mRNA expression is significantly reduced in colorectal cancer tissue compared with normal colorectal tissue and is associated with overall survival in patients with colorectal cancer. DOK7 is variably expressed in colorectal cancer cell lines with high expression in HRT-18 cells and low expression in HT-115 and RKO cells. Difficulties in obtaining DOK7 knockdown and expression subsequently revealed that DOK7 has several splice variants coding for different isoforms.

Further work investigating DOK7 variants 1-3 (DOK7V1-3) revealed that DOK7V1 mRNA expression is significantly reduced in colorectal cancer tissue compared with normal colorectal tissue and is associated with disease-free status and length of disease-free survival. In contrast, DOK7V2 and DOK7V3 mRNA expression is significantly increased in colorectal cancer tissue compared with normal colorectal tissue.

Functional assays using a DOK7V2 overexpression model did not show a significant difference in colorectal cancer cell growth, adhesion or invasion in RKO DOK7V2 overexpression cells compared to the control cell line.

However, antibody based protein microarray revealed that DOK7V2 overexpression is associated with significant changes in the expression and phosphorylation (activation) of numerous proteins in RKO cells. Cell signalling pathways potentially implicated include PI-3K-Akt, mTOR, MAPK, Jak/STAT and angiogenesis signalling pathways.

Our findings suggest that DOK7 plays an important role in colorectal carcinogenesis and that DOK7 isoforms may play different and possibly opposing roles. Protein microarray data provides a number of potential avenues for further work to elucidate the interaction of Dok7 with other cell signalling proteins and may help identify future potential therapeutic targets.

Table of Contents

Chapter 1: General Introduction & Review of the Literature

1.1 Colorectal cancer

1.1.1 Introduction

Colorectal cancer is one of commonest cancers worldwide, with 1,361,000 cases in 2012 (1). It remains the third commonest cancer in men (746,000 cases in 2012, 10.1% of all cancers) and the second commonest cancer in women (614,000, 9.2% of all cancers) (1). The estimated age-standardised incidences of colorectal cancer per 100,000 of the population by gender from the most recent GLOBOCAN figures are illustrated in Figure 1.1.

A.

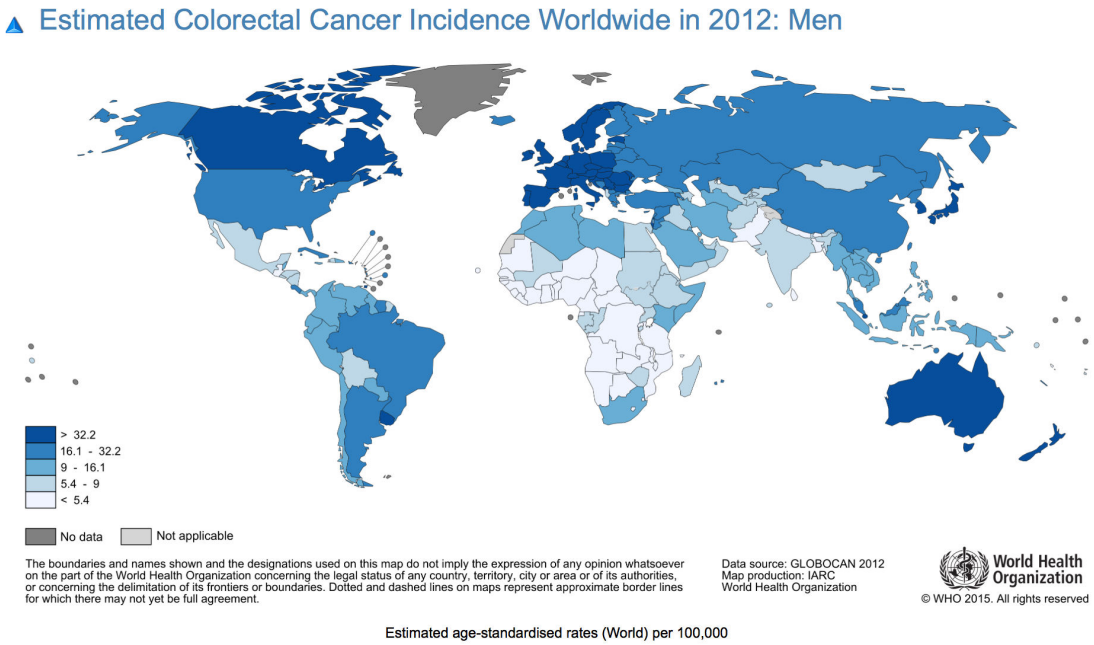

B.

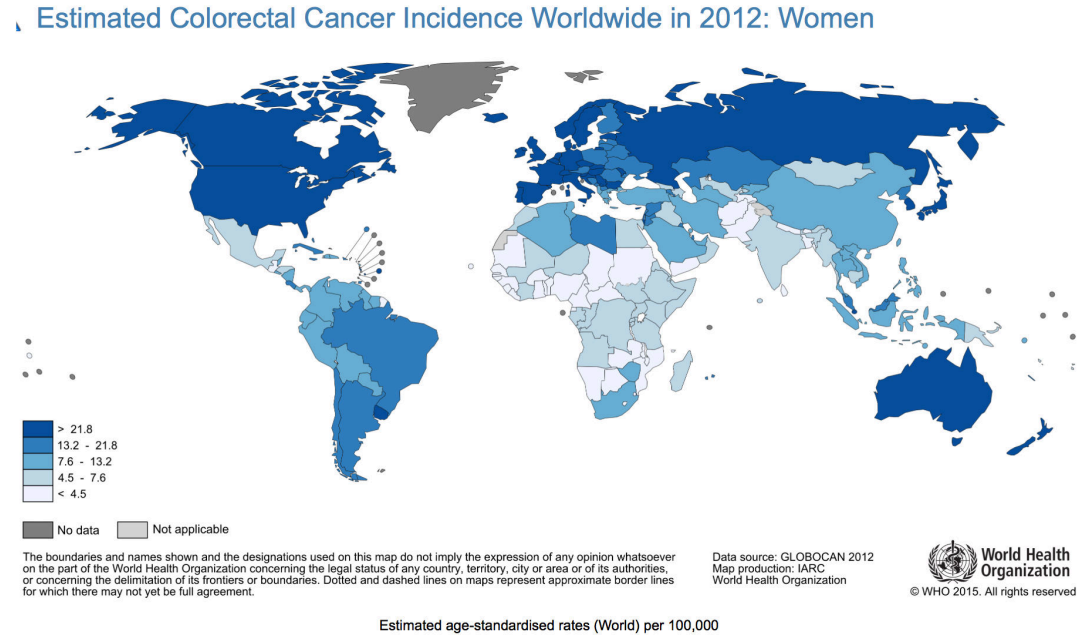

Figure 1.1 Age-standardised colorectal cancer incidence worldwide in 2012 A. Age-standardised incidence per 100,000 men B. Age-standardised incidence per 100,000 women. Map from most recent GLOBOCAN figures (IARC) 2012 (1)

There is wide geographical variation in incidence, with the majority of cases (54.2%) occurring in more developed countries (1). The highest incidence rates are seen in Australia and New Zealand, with the lowest incidence seen in Western Africa (1). Potential causes for the geographical variation seen include differences in diet (particularly with regard to consumption of meat, fibre and animal fats), levels of physical activity and obesity and possibly differences in genetic susceptibility to dietary carcinogens (2, 3).

In the UK, colorectal carcinoma is the fourth commonest cancer with 41,300 newly diagnosed cases in 2014 and accounts for 12% of all new cancers diagnosed in the UK per year (4). It is the third most common cancer in both men (22,800 cases diagnosed in 2014, 12% of all nale cancers) and women (18,400 cases diagnosed in 2014, 10% of all female cancers) (4). The crude incidence rate for men and women in the UK is 72 and 56 per 100,000 respectively, giving a male: female ratio of approximately 12:10 (4). In the UK, the European Age-Standardised incidence of colorectal cancer has risen by 6% over the last decade and World Health Organisation figures predict that the incidence of colorectal cancer will continue to rise, with a forecasted incidence of 58,119 in the year 2035 (1, 4). In the UK, the European age-standardised incidence rates of bowel cancer in people aged 60-69 years rose by 14% between 2004-2006 and 2008-2012 (4). It is likely that this is due to the introduction of bowel screening during that period (4).

In 2012, the lifetime risk of developing bowel cancer was 1 in 14 for men and 1 in 19 for women, highlighting the important public health problem that this cancer poses (4).

1.1.2 Mortality

Five-year survival rates for colorectal cancer have doubled over the last 40 years. For men with bowel cancer, 1-year age standardised net survival has increased from 47% to 77% and the 5-year age-standardised net survival has increased from 25% to 59% over the time period from 1971-1972 to 2010-2011 (5). For women with bowel cancer, 1-year age-standardised net survival has increased from 45% to 74% and 5-year age-standardised net survival has increased from 24% to 58% over the same time period (5). The most recent Cancer Research UK figures for the age-standardised one-, five- and ten-year net survival rates for adults with bowel cancer in England and Wales are shown in Table 1.1.

Table 1.1 Age-standardised one-, five- and ten-year net survival for adults aged 15-99 with bowel cancer in England and Wales in 2010-2011. Data from Cancer Research UK: Bowel cancer survival statistics (5).

Net survival	1-year survival (%)	5-year survival (%)	10-year survival (%)
Men	77.4	59.2	56.0
Women	73.9	58.2	57.2
Both sexes	75.7	58.7	56.6

Despite improvements in survival, colorectal cancer resulted in 694,000 deaths worldwide in 2012 (1). In the UK, it remains the second commonest cause of cancer related death accounting for 10% of all cancer deaths and in 2014, 15,900 patients died of the disease – 44 each day (6). Worldwide, mortality rates from colorectal cancer vary with the highest estimated mortality rates seen in Central and Eastern Europe and the lowest in Western Africa (1).

Within Europe, 5-year survival is highest in Central European countries (over 60%), followed by Northern Europe and Italy, with levels significantly lower in the UK and Slovenia (around 50%) and lowest in Eastern European countries (7). It has been suggested that poorer colorectal cancer survival in the UK may be due to more advanced disease at presentation, although this assertion has been challenged (8, 9). Nevertheless, a significant proportion of patients present with advanced disease (at the time of diagnosis, 55% of patients have stage III or IV disease and 26% have metastases) and this is related to survival outcomes (4).

Currently, there is great variation worldwide in screening strategies for colorectal cancer and their implementation (10). Strategies for screening include non-invasive stool tests such as guaiac faecal occult blood test (gFOBT) and faecal immunochemical test for haemoglobin (FIT), and invasive tests such as flexible sigmoidoscopy, colonoscopy and CT colonography (10). More recently, newer screening strategies to detect DNA, RNA or protein in blood or stool have become available alongside imaging tests such as colon capsule endoscopy and magnetic resonance colonography (10). Globally, there are also differences in the delivery of screening with some countries offering an organised screening programme and others, taking a more opportunistic approach. Generally, the implementation of organised screening programmes has been higher in Western countries with higher incidences of colorectal cancer (10). Analysis of 2012 GLOBOCAN incidence and mortality statistics has revealed that countries with formal colorectal cancer screening programmes have lower than expected mortality-to-incidence ratios for colorectal cancer whereas countries with no screening programmes have higher than expected mortality-to-incidence ratios (11). This suggests that global differences in screening strategies may have an effect on global variations in colorectal cancer mortality.

Five-year relative survival by stage at diagnosis is shown in Table 1.2. As the data shows, survival decreases markedly with increasing stage of disease, highlighting the importance of early diagnosis.

Table 1.2 Five-year relative survival (%) by stage of disease at diagnosis in adults aged 15-99 presenting with colorectal cancer in the former Anglia Cancer Network, UK from 2006-2010. Data from Cancer Research UK: Bowel cancer survival statistics (5).

Stage	Men	Women
Stage I	94.6	100.2
Stage II	83.5	85.9
Stage III	62.6	62.7
Stage IV	6.9	8.1
All Stages	58.2	61.1
Stage not known	18.7	15.1

Advanced colorectal cancers may present as an emergency. Recent data from Public Health England shows that 25% of colorectal cancers present as an emergency and that this is associated with reduced survival (12). One-year relative survival is estimated to be 49% for patients presenting as an emergency compared to 82% for those patients presenting via the urgent suspected two-week wait outpatient clinic (12). Factors contributing to a late or emergency presentation include patient factors such as older age, female gender, high deprivation index, and unmarried, divorced or widowed marital status and hospital or physician associated factors such as incomplete colonic imaging, false-negative investigations, inappropriate surgical treatment, administrative delays and the commencement of iron therapy in patients with iron deficiency anaemia without investigation to establish a cause for blood loss (13, 14).

Overall, differences in cancer survival rates may be attributed to four main factors: (1) stage at diagnosis, which may be influenced by diagnostic delay (2) the outcomes of treatments including surgery, chemotherapy, hormonal therapy or radiotherapy, (3) patient factors such

as age, fitness, co-morbidities and socio-economic factors and (4) the characteristics of the tumour (15).

1.1.3 Anatomy of the colon and rectum

The large intestine is approximately 1.5m in length and extends from the caecum to the anus (16). It comprises the caecum, appendix, colon, rectum and anal canal and its primary function is to absorb fluid from the bowel content resulting in formed stools (16). This study focuses on cancers affecting the large intestine from the caecum to the rectum (referred to interchangeably as colorectal or bowel cancers) but excludes those affecting the anal canal (anal cancers).

The large intestine begins at the caecum, located in the right iliac fossa (16). Bowel content enters the caecum from the terminal ileum via the ileocaecal valve (16). From the caecum, the large intestine continues upwards as the ascending colon and then bends to the left at the right colic flexure (or hepatic flexure) becoming the transverse colon which runs transversely across the upper abdomen (16). In the left upper quadrant, the large intestine bends downwards at the left colic flexure (or splenic flexure) and continues as the descending colon (16). At the pelvis, it becomes the sigmoid colon and at the third sacral vertebra the sigmoid colon ends and the large intestine continues as the rectum (16). The large intestine has a number of structural characteristics that help to differentiate it from the small intestine. It has a wider lumen, it's longitudinal muscle is separated into three bands called taeniae coli, it has appendices of fat on its outer surface called appendices epiploicae and it is drawn into sacculations giving rise to colonic haustra (16).

The caecum, transverse colon and sigmoid colon are intraperitoneal structures, meaning that they are mobile within the peritoneal cavity and the transverse and sigmoid colon are also

suspended on a mesocolon (16). By comparison, the ascending and descending colon and the rectum are retroperitoneal structures (16).

The blood supply to the colon is split according to the embryological origin of the large intestine. The large intestine from the caecum as far round as the latter two-thirds of the transverse colon arises from the embryonic midgut and is therefore supplied by branches of the superior mesenteric artery, namely the ileocolic artery (giving rise to the anterior and posterior caecal arteries, the appendicular artery and the colic artery), the right colic artery and the middle colic artery (16). The remainder of the large intestine from the latter one-third of the transverse colon as far down as the dentate line arises from the embryological hindgut and consequently is supplied by branches of the inferior mesenteric artery, namely the left colic artery, the sigmoidal arteries and the superior rectal artery (16). The blood supply of the lower one-third of the anal canal arises from branches of the internal iliac artery, namely the middle rectal artery and the internal pudendal artery which gives rise to the inferior rectal artery (16). The superior and inferior mesenteric veins provide the venous drainage of the large intestine above the dentate line and drain the territories supplied by the corresponding arteries into the portal vein. Venous blood from the lower one-third of the anal canal drains into the internal iliac veins and from there into the common iliac veins and subsequently the inferior vena cava. Consequently the rectum is one of several sites in the body where there are porto-systemic anastomoses.

1.1.4 Anatomical site of colorectal cancer

The majority of bowel cancers occur in the left side of the bowel with around 57% of cases diagnosed between 2007-2009 being located in the descending colon, sigmoid colon, rectosigmoid junction or rectum (4). The anatomical distribution of bowel cancers diagnosed in Great Britain between 2007-2009 is illustrated in Figure 1.2.

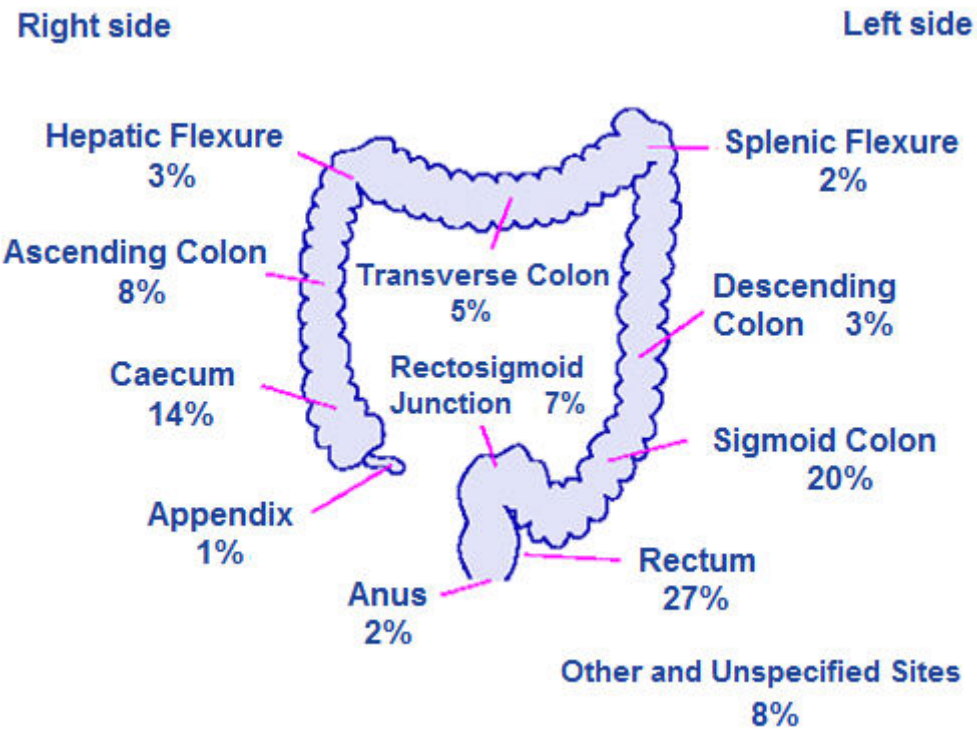

Figure 1.2 Anatomical distribution of large bowel cancers diagnosed in Great Britain between 2007-2009. Figure obtained from Cancer Research UK: Bowel cancer incidence statistics (4).

Although left-sided bowel cancers remain more prevalent, several authors report a shift towards more proximal tumours over recent decades in several countries emphasizing the importance of complete colonic assessment (17-20). Furthermore, previous studies have identified a number of differences in the presentation, prognosis and underlying genetic and epigenetic changes between proximal and distal colonic tumours leading some authors to speculate that left- and right-sided colonic cancers may represent different tumours (21). For example, microsatellite instability is more common in tumours located proximal to the splenic flexure whereas chromosomal instability is more common in more distal tumours (22, 23). The causes of these differences in tumours of different anatomical location and the apparent "proximal shift" of colon cancer are uncertain but causes may include differences in embryological origin or physiology or differences in exposure to environmental factors or susceptibility to dietary factors or alcohol (23).

1.1.5 Histopathological features of colorectal cancer

More than 95% of colorectal cancers are adenocarcinomas, which originate in the glandular lining of the bowel wall. Most adenocarcinomas arise within pre-existing adenomatous polyps or adenomas, which have an estimated prevalence of around 35% in Western countries and around 10-15% in Asia and Africa (24). Adenomas can be further classified according to their architecture as tubular, villous, tubulovillous or serrated (24). It is estimated that around 5% of adenomatous polyps become malignant over a period of 5-10 years and features associated with higher malignant potential include villous architecture, large size, and high-grade epithelial dysplasia (24).

Histological subtypes of colorectal adenocarcinomas include mucinous adenocarcinomas, which account for 5-15% of all colorectal cancers, and signet ring tumours, which account for

around 1% of colorectal cancers (25, 26). These are treated in the same way as other adenocarcinomas (25).

Other rare types of colorectal cancer include squamous cell carcinomas, carcinoid tumours, sarcomas and lymphomas (25). The full WHO histological classification of tumours of the colon and rectum is shown in Table 1.3. The work discussed in this thesis focuses on colorectal adenocarcinomas and therefore, these rarer types will not be discussed further.

Table 1.3 WHO histological classification of tumours of the colon and rectum. Adapted from Hamilton SR, Aaltonen LA (Eds.): World Health Organisation Classification of Tumours. Pathology and Genetics of Tumours of the Digestive System. IARC Press: Lyon 2000 (27).

Epithelial tumours Adenoma	Tubular Villous Tubulovillous Serrated	**Non-epithelial tumours** Lipoma Leiomyoma Gastrointestinal stromal tumour Leiomyosarcoma Angiosarcoma Kaposi sarcoma Malignant melanoma Others	
Intraepithelial neoplasia (dysplasia)	Low-grade glandular intraepithelial neoplasia High-grade glandular intraepithelial neoplasia	Malignant lymphomas	Marginal zone B-cell lymphoma of MALT type Mantle cell lymphoma Diffuse large B-cell lymphoma Burkitt lymphoma Burkitt-like/atypical Burkitt-lymphoma
Carcinoma	Adenocarcinoma Mucinous adenocarcinoma Signet-ring cell carcinoma Small cell carcinoma Squamous cell carcinoma Adenosquamous carcinoma Medullary carcinoma Undifferentiated carcinoma	**Secondary tumours** **Polyps** Hyperplastic (metaplastic) Peutz-Jeghers	
Carcinoid	EC-cell, serotonin-producing neoplasm L-cell glucagon-like peptide and PP/PYY producing tumour Others	Juvenile	
Mixed carcinoid-adenocarcinoma			
Others			

1.1.6 Histopathological grading of colorectal cancer

The histopathological grading of colorectal cancers is based on the extent of glandular appearance (27). Well-differentiated tumours are those in which glandular structures are exhibited in >95% of the tumour, moderately differentiated tumours are those in which glandular structures are seen in 50-95% of the tumour and poorly differentiated tumours are those in which 5-50% of the tumour has glandular structures (27). Mucinous and signet-ring cell carcinomas are considered to be poorly differentiated carcinomas.

1.1.7 Colorectal cancer spread

Colorectal carcinomas may breach the muscularis propria and spread directly to involve adjacent structures or perforate, resulting in transcoelomic spread to the peritoneal cavity (27). Alternatively, spread may occur via the blood or lymphatic vessels resulting in systemic disease. Common distant metastatic sites include the liver and lungs.

1.1.8 Adenoma-carcinoma sequence

The process of colorectal cancer development from normal tissue is amongst the best understood of all cancers. It has long been recognised that colorectal carcinomas often arise from pre-existing benign tumours known as adenomas, and the age-linked incidence of cancer suggests that tumour development occurs as a result of mutations acquired in a multistep fashion (28).

Over recent decades, the molecular and histopathological changes occurring during various stages of tumour development from tiny adenoma to advanced metastatic carcinoma have been studied and we now understand colorectal carcinogenesis to be a complex multistep

process that involves numerous genetic and epigenetic modifications. This knowledge has generated a model of colorectal cancer development usually referred to as the adenoma-carcinoma sequence.

The genetic model of colorectal tumourigenesis proposed by Fearon and Vogelstein is shown in Figure 1.3. Tumourigenesis occurs as a result of accumulated (inherited or acquired) genetic mutations in oncogenes (such as Ras) and tumour suppressor genes (such as those found on chromosomes 5q, 17p and 18q) resulting in their activation and suppression, respectively (29). Although temporal relationships in the occurrence of genetic mutations can be inferred from studies of normal, adenomatous and carcinomatous tissue, it is the progressive accumulation of these defects, rather than their order of occurrence, that is most crucial to the process of tumourigenesis (29).

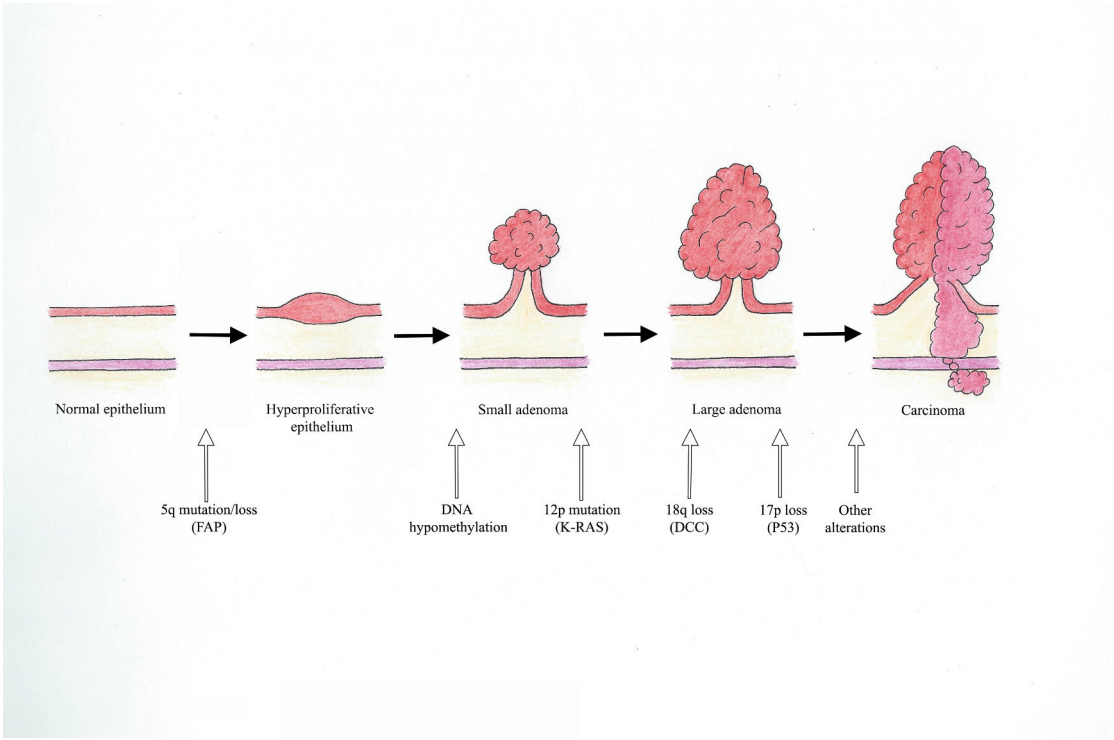

Figure 1.3 Genetic model for colorectal tumourigenesis. Adapted from 'A Genetic Model for Colorectal Tumourigenesis' Fearon & Vogelstein (1990) (29).

1.1.9 Aetiology and risk factors

The development and progression of colorectal cancer is dependent on the complex interaction of genetic, epigenetic and environmental factors.

1.1.9.1 Genetic/epigenetic factors

The genetic factors contributing to colorectal cancer development can be divided into those relating to chromosomal instability, where there are mutations in oncogenes or tumour suppressor genes, and those relating to microsatellite instability, due to mutations in mismatch repair genes. Epigenetic changes such as hyper/hypomethylation may also play a role in cancer development by altering the stability of the genome, increasing the rate of accumulation of genetic defects within the cell (29).

1.1.9.1.1 Oncogenes in colorectal cancer

Oncogenes are activated by "gain of function" mutations resulting in over, or aberrant, expression of their gene product resulting in the subsequent stimulation of cell growth or inhibition of cell death (30).

1.1.9.1.1.1 *Ras (Rat sarcoma)* oncogenes

The *Ras* proteins are involved in cell signal transduction acting as effectors in the mitogen-activated protein kinase (MAPK) pathway downstream of epidermal growth factor receptor (EGFR) (31). EGFR is a tyrosine kinase receptor that, via its interaction with its ligand epidermal growth factor (EGF) stimulates cell proliferation, differentiation and survival (32,

33). The ras proteins were discovered as a result of observations made by Jennifer Harvey in 1964, that the injection of mice with Moloney's leukaemogenic virus resulted in the development of tumours (34).

The three human *ras* genes, HRAS, KRAS and NRAS, are the commonest oncogenes implicated in human cancer and studies have shown that mutations of the *ras* genes are important in the development of pancreatic, thyroid and lung cancer, amongst other human cancers (32, 35, 36).

The first studies of the Ras oncogenes in colorectal cancer date back to the early 1980s when Feinberg and Vogelstein reported the hypomethylation of HRAS and KRAS in colonic adenocarcinomas (37). Later, in 1984, Spandidos and Kerr confirmed that KRAS and HRAS are overexpressed in pre-malignant adenomatous polyps and malignant colorectal tumours (38).

Ras gene mutations are found in over a third of colorectal cancers, as well as in over 50% of adenomas greater than 1cm in size suggesting they precede cancer development and play a role in the early stages of tumourigenesis (33, 39, 40). However, *ras* gene mutations are less common in small adenomas less than 1cm, where prevalence is less than 10% (40). Mutations of the KRAS gene result in activation of the MAPK pathway and in metastatic colorectal cancer, they have been shown to predict treatment resistance to anti-EGFR monoclonal antibodies (31).

1.1.9.1.2 Tumour suppressor genes in colorectal cancer

Tumour suppressor genes are affected by "loss of function" mutations in cancer resulting in reduced expression of a gene product that usually stimulates apoptosis or differentiation, or

which inhibits cell growth (30). Knudson hypothesized that both maternal and paternal copies of a tumour suppressor gene must be inactivated in order to eliminate their function but in practice, it is likely that some tumour suppressor genes act in a dominant negative fashion, exerting their phenotypic effect even in the presence of a wild-type allele (29).

1.1.9.1.2.1 Adenomatous polyposis coli (APC) gene

The adenomatous polyposis coli (APC) gene is a tumour suppressor gene located on chromosome 5q21 (41). It encodes a 312kDa protein, involved in the control of cell proliferation and differentiation via the Wnt signalling pathway, which is inactivated in the early stages of colorectal cancer (30). In patients with familial adenomatous polyposis (FAP), there is an inherited mutation in the APC gene but mutation or loss of this gene may also occur sporadically at an early stage in the process of colorectal tumourigenesis in patients without FAP (29).

1.1.9.1.2.2 p53

The TP53 gene is located on chromosome 17p. Loss of p53 is observed in over 75% of colorectal cancers (and a smaller proportion of colorectal adenomas) and is associated with the presence of distant metastases and cancer-related death (40, 42).

1.1.9.1.2.3 Deleted in colorectal cancer (DCC) gene

The deleted in colorectal cancer (DCC) gene is a tumour suppressor gene located on chromosome 18q (29). Loss of this allele is found in over 70% of colorectal carcinomas, 47% of advanced adenomas, but less than 15% of early adenomas (40).

1.1.9.1.3 Microsatellite instability

Microsatellite instability occurs as a result of impaired DNA mismatch repair (MMR), such that the correction of spontaneous errors occurring during DNA replication does not take place. Consequently, cells with defective MMR accumulate errors and contain novel microsatellite sequences in their DNA. Microsatellites are repeated sequences of up to six base pairs in length, which usually occur in introns but may also occur in coding regions.

Inactivation of DNA MMR is associated with hereditary non-polyposis colorectal cancer (HNPCC) and is also seen in around 20% of sporadic colorectal cancers (43). The majority of patients with HNPCC have a germline mutation in one of the MMR genes (hMSH2 or hMLH1), whereas the majority of sporadic MSI cases are due to hypermethylation of the hMLH1 promoter (43). Germline mutations in hMSH6 are also seen but are associated with late-onset familial colorectal cancer and extra-colonic tumours (43).

1.1.9.1.4 Inherited colorectal cancer syndromes

The two most common inherited colorectal cancer syndromes are HNPCC and FAP, which together account for approximately 5% of all colorectal cancers (44). Other inherited syndromes associated with an increased risk of colorectal cancer include Peutz-Jeghers syndrome and Juvenile polyposis syndrome. As well as these defined inherited syndromes, around 20% of bowel cancers are associated with hereditary factors, likely due to as-yet-undiscovered susceptibility genes with lower penetrance (45, 46).

1.1.9.1.4.1 Familial adenomatous polyposis (FAP)

Familial adenomatous polyposis is an autosomal dominant condition, caused by a germline mutation in the APC gene on chromosome 5, that accounts for less than 1% of bowel cancers (47). It is characterised by the development of hundreds of thousands of adenomatous polyps in the colon and rectum beginning in childhood or adolescence. Colorectal cancer develops in almost 100% of patients by the age of 50, with an average age of onset of 39 years (48). Depending on the nature of the mutation, extra-colonic manifestations may also be found and these include gastric and duodenal polyps, desmoid tumours, osteomas, retinal lesions and brain tumours (30). Classical FAP, described above, differs clinically from attenuated FAP (a subtype of FAP) in that attenuated FAP is associated with the later development of colonic polyps, reduced polyp number and the later development of colorectal cancer.

In patients with classical FAP, colectomy is recommended once adenomas emerge to prevent the almost inevitable development of colorectal cancer. Operative strategies include colectomy with ileorectal anastomosis, total proctocolectomy with permanent ileostomy or restorative proctocolectomy with pouch formation.

1.1.9.1.4.2 Hereditary non-polyposis colorectal cancer (HNPCC)

Hereditary non-polyposis colorectal cancer (HNPCC, also known as Lynch syndrome) is the commonest cause of inherited colorectal cancer and is also associated with an increased risk of other cancers including endometrial, ovarian, gastric, pancreatic, small bowel, ureteric and renal cancer (49). It accounts for 1-4% of colon cancers (47). HNPCC occurs due to inherited mutations in one of seven mismatch repair genes, shown in Table 1.4. Currently predictive testing in the UK focuses on four of these genes: MLH1, MSH2, MSH6 and PMS2 (50). Individuals at risk due to their family history or identified by predictive genetic testing are

offered additional bowel screening by colonoscopy, are educated about the symptoms of bowel cancer and are offered prophylactic colectomy.

Table 1.4 Mismatch repair genes associated with HNPCC and their associated frequency in HNPCC. Data obtained from Medscape: Hereditary Colorectal Cancer webpage (51).

Mismatch repair gene	Chromosomal location	Frequency of HNPCC cases
MSH2	2p16	45-50%
MLH1	3p22.3	20%
MSH6	2p16	10%
PMS2	7p22.1	1%
PMS1	2q32.2	Rare
MSH3	5q14.1	Rare
EXO1	1q43	Rare
Unidentified genes		20-25%

1.1.9.2 Individual patient factors

1.1.9.2.1 Age

The incidence of colorectal cancer is strongly related to age. Ninety five percent of patients diagnosed with bowel cancer are aged 50 or over, and roughly half of these (43% of all cases) are aged over 75 years (4). The age-specific incidence for colorectal cancer in the UK is shown in Figure 1.4.

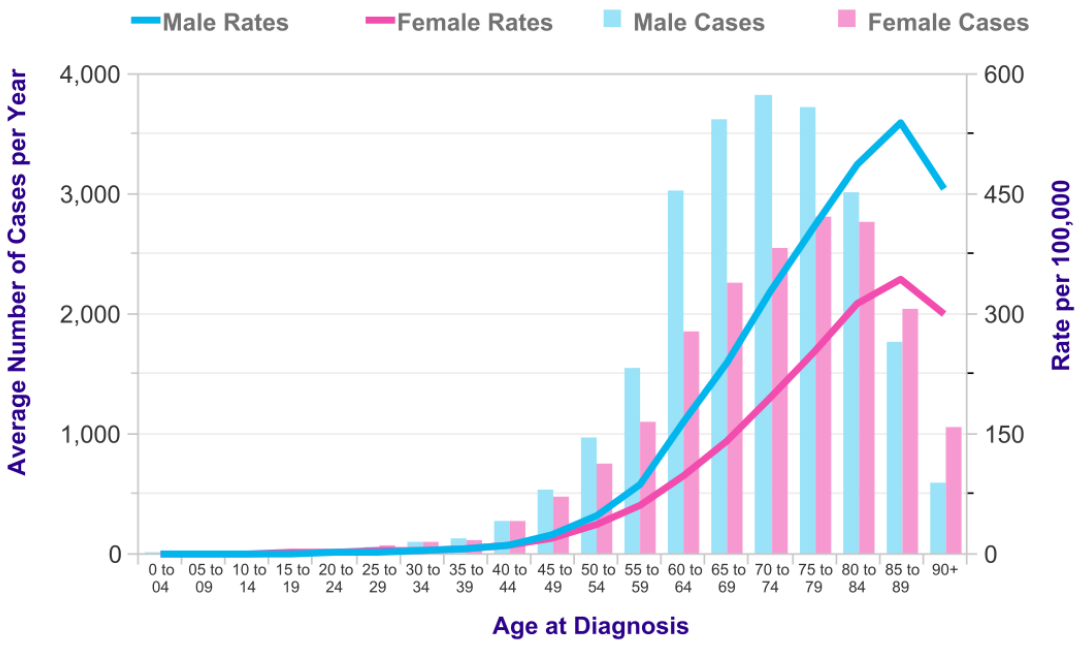

Figure 1.4 Average number of new cases per year and age-specific incidence rate for bowel cancer in the UK (2010-2012). Source: cruk.org/cancerstats (4).

1.1.9.2.2 Socio-economic factors

There is an association between increasing socio-economic deprivation and bowel cancer incidence in men in England but no evidence for a similar association in females (4).

1.1.9.2.3 Ethnicity

The age-standardised incidence of bowel cancer is significantly higher in white males and females than for Asians or Black men and women (4).

1.1.9.3 Lifestyle and other risk factors

It is estimated that 54% of cases of bowel cancer are associated with lifestyle or other environmental risk factors (52) The lifestyle or environmental factors associated with bowel cancer risk are shown in Table 1.5.

Table 1.5 Lifestyle or environmental risk factors implicated in colorectal cancer.

Risk factor	Effect on bowel cancer risk [a]	Percentage of bowel cancers in UK attributable to factor
X radiation [b] Gamma radiation [b]	Increases risk	2%
Drinking alcohol [c]	Increases risk	11%
Tobacco smoking	Increases risk	8%
Red/processed meat	Increases risk	21%
Overweight/obesity	Increases risk	13%
Abdominal fatness	Increases risk	NQ
Height	Increases risk	NQ
Haem iron	Possibly increases risk	NQ
Cheese	Possibly increases risk	NQ
Dietary sugars	Possibly increases risk	NQ
Dietary animal fat	Possibly increases risk	NQ
Asbestos	May increase risk	NQ
Schistosoma japonicum	May increase risk	NQ
Physical activity [d]	Decreases risk	3% due to inadequate physical activity
Dietary fibre	May decrease risk	12% due to inadequate dietary fibre
Garlic	May decrease risk	NQ
Calcium	May decrease risk	NQ
Milk	May decrease risk	NQ
Non-starchy vegetables	Possibly decrease risk	NQ
Fruit	Possibly decrease risk	NQ
Dietary folate	Possibly decrease risk	NQ
Dietary/supplementary selenium	Possibly decrease risk	NQ
Fish	Possibly decrease risk	NQ
Dietary vitamin D	Possibly decrease risk	NQ

NQ = not quantified
[a] As classified by the World Cancer Research Fund/American Institute for Cancer Research (WCRF/AICR)
[b] Evidence sufficient for colon but limited for rectum
[c] Evidence convincing for males and probable for females
[d] Evidence stronger for colon than rectum

1.1.9.4 Medical conditions

The risk of developing colorectal cancer is increased in individuals with colorectal adenomas, inflammatory bowel disease, complicated diverticulitis, previous cancer, sarcoidosis, gallstones, metabolic syndrome and type II diabetes, though risk is actually lower in diabetics taking metformin. Furthermore, infection with the human papillomavirus (HPV) and Helicobacter pylori (H. pylori) are also associated with elevated bowel cancer risk.

1.1.9.4.1 Inflammatory bowel diseases

Patients with inflammatory bowel diseases have an increased risk of colorectal cancer (pooled standardized incidence ratio 1.7, 95% CI =1.2-2.2) with risk highest in those patients with IBD diagnosis before age 30, those with extensive disease and those with longer disease duration (53).

1.1.10 Diagnosis of colorectal cancer

The diagnosis of colorectal cancer begins with thorough history taking and a systematic examination of the patient, which includes a digital rectal examination and rigid sigmoidoscopy. The majority of patients present symptomatically, although the introduction of bowel screening in recent years will inevitably result in increasing numbers of diagnoses in asymptomatic individuals.

1.1.10.1 Mode of presentation and symptomatology

1.1.10.1.1 Bowel screening

The English Bowel Cancer Screening pilot conducted between 2000 and 2002 assessed the feasibility of a faecal occult blood (FOB) screening tool for the detection of colorectal cancer. This study revealed that the positive predictive value of FOB screening was 10.9% for cancer and 35% for adenoma (54). Of all screen detected cancers, 48% were Dukes' stage A and only 1% had metastasised at the time of diagnosis (54). The NHS Bowel Cancer Screening programme was subsequently introduced in England in 2006, in Scotland in 2007 and in 2007 in Wales.

The current Bowel Screening Wales programme invites men and women aged 60 to 74 for screening every two years (55). The initial test kit is a guaiac faecal occult blood (FOB) test kit, which is completed by participants at home and returned to the screening laboratory. Participants with a negative FOB are returned to routine recall, those with equivocal results are sent a faecal immunochemical test to complete and those with a positive FOB result are invited for telephone assessment with Specialist Screening Practitioners who assess their fitness for colonoscopy. If the participant is fit, they are offered a colonoscopy in their local assessment centre and dependent on the results of the colonoscopy, they are then returned to routine colonoscopy entered into a polyp surveillance programme or, if cancer is diagnosed, they are referred to the multidisciplinary team. Those unfit for colonscopy are usually offered a CT scan.

The aim of the Bowel Screening Wales programme is to reduce deaths from bowel cancer by 15% in the group of people invited for screening by the year 2020 (55). In the most recent Annual Statistical Report published in January 2017, uptake for invited participants was

54.4% (55). Of 164,400 test kits that were validated, 151,800 were given a definitive result of which 98.7% were negative and 1.3% were positive (55). Attendance at index colonoscopy or flexible sigmoidoscopy was 97.3% and of these procedures, the cancer detection rate was 12.0%, the polyp detection rate was 67.0% and the adenoma detection rate was 52.8% (55). In the year 2015-2016, a total of 205 participants were diagnosed with cancer and 1149 had polyps detected and removed (55).

1.1.10.1.2 Symptomatic presentation

Colorectal cancer may present with symptoms including change in bowel habit, rectal bleeding, abdominal pain and weight loss or symptomatic anaemia.

1.1.10.1.2.1 Emergency symptomatic presentation

Unfortunately, 21% of all patients with colorectal cancer present as an emergency with a tendency for this group to represent the more elderly, frail, co-morbid patients and those with advanced disease (56). Consequently, the mortality in this group is much higher and 1 in 7 (13.7%) of those undergoing emergency surgical resection do not survive beyond the first 90 post-operative days (57). Increasing bowel cancer awareness amongst the general population and bowel screening are strategies aimed at reducing these numbers.

1.1.11 Investigation of suspected colorectal cancer

1.1.11.1 Colonoscopy

Colonoscopy is the 'gold standard' investigation for suspected colorectal cancer and National Institute for Health and Care Excellence (NICE) guidelines, updated in 2014, state that it should be offered as the first-line investigation for all patients suspected to have colorectal cancer who do not have a major comorbidity (58). Colonoscopy offers several advantages over alternative diagnostic investigations, not least the opportunity to obtain histological diagnosis by biopsy.

Magnetic endoscopic imaging devices (MEIs) are adjuncts to colonoscopy that demonstrate the configuration of the colonoscopy in three dimensions. The aim of these devices is to allow the colonoscopist to adjust the colonoscope to prevent looping thereby potentially reducing pain and increasing caecal intubation rates. A recent systematic review and meta-analysis of 13 randomised studies found that use of MEI increased the caecal intubation rate, particularly for procedures performed by inexperienced colonoscopists (59). Although procedure time and pain were reduced, the difference was not felt by the authors to be clinically significant (59). Moreover, further studies to determine the effect on complication rate and cost-benefit analyses are required.

1.1.11.2 Computerised tomography pneumocolon (CT pneumocolon)

CT pneumocolon (also known as CT colonography) approaches colonoscopy in terms of its sensitivity and specificity and in the short term, is more acceptable to patients (60). However, 30% of CT pneumocolons will detect a lesion that requires a colonoscopy for further

evaluation and longer-term follow up suggests that overall, there is greater patient satisfaction with colonoscopy as the first line investigation (60).

1.1.11.3 Minimal-preparation CT

Minimal-preparation CT is a valuable tool in the investigation of frail or elderly patients with suspected colorectal cancer who are not fit enough to undergo colonoscopy or CT pneumocolon (61). A study of 1077 CT studies in 1031 patients found that CT correctly identified 83/98 colorectal cancers, with a sensitivity of 85% (CI: 78-92%) and a specificity of 91% (CI: 90-93%)(61).

1.1.11.4 Flexible sigmoidoscopy

Flexible sigmoidoscopy is used to investigate fresh rectal bleeding or other symptoms suggestive of anal outlet pathology in patients for whom there is a low suspicion of malignancy.

1.1.11.5 Barium enema

The results of the multicentre Special Interest Group in Gastrointestinal and Abdominal Radiology (SIGGAR) 1 trial show that CT colonography is significantly better at detecting colorectal cancer than barium enema (62). Therefore, the Royal College of Radiologists no longer recommends the use of barium enema as a method of investigation for patients with symptoms suggestive of colorectal cancer (63).

1.1.12 Staging of colorectal cancer

Staging is essential in determining what treatment strategies are appropriate, whether treatment will be curative or palliative in intent and the patient's likely prognosis. In addition, proper staging is essential in recording and comparing outcomes and in determining the success of established or novel treatments. There are a number of staging systems in use, namely Dukes' staging, Tumour Node Metastasis (TNM) classification or the Union for International Cancer Control (UICC) stage grouping.

1.1.12.1 Dukes' staging

Cuthbert Dukes (1890-1977) was a Pathologist at St. Mark's hospital in London who specialised in the pathology of rectal cancer and pioneered work on familial polyposis of the colon resulting in the establishment of the national polyposis registry (64). In 1932, he developed the Dukes' classification for rectal cancers (see Table 1.6), although it was extended for broader use across all colorectal cancers in due course.

Table 1.6 Dukes' staging of rectal cancer (65).

Stage	Definition
A	Growth confined to the rectum, no extra-rectal spread, no lymphatic metastases
B	Spread by direct continuity into extra-rectal tissues, no lymph node spread
C	Lymphatic metastases present

"Modified" Dukes' classification includes an additional stage 'D' which is defined by the presence of distant metastasis. Dukes' stage is closely associated with survival as illustrated in Table 1.7.

Table 1.7 Colorectal cancer 5-year relative survival rate by Dukes' stage at diagnosis, England 1996-2002.

Dukes stage at diagnosis	Percentage of cases	5 year relative survival
A	8.7%	93.2%
B	24.2%	77.0%
C	23.6%	47.7%
D	9.2%	6.6%
Unknown	34.3%	35.4%

Source: Cancer Research UK, Original data: Colorectal Survival by Stage, NCIN Publication, accessed May 2012.

1.1.12.2 TNM classification

The most common staging system used for colorectal cancer is the TNM (tumour/node/metastasis) system developed by the American Joint Committee on Cancer (AJCC) and updated most recently as its 7th edition in 2010. A number is assigned to each of the three categories based on the degree of bowel wall invasion (T), involvement of lymph nodes (N) and presence of metastatic disease (M). The TNM staging definitions for colorectal cancer are shown in Table 1.8.

Table 1.8 TNM Colon and Rectum Cancer Staging Definitions. From AJCC Colon and Rectum Cancer Staging 7th Edition (66).

Primary Tumour (T)	
Tx	Primary tumour cannot be assessed
T0	No evidence of primary tumour
Tis	Carcinoma in situ
T1	Tumour invades submucosa
T2	Tumour invades muscularis propria
T3	Tumour invades into pericolorectal tissues
T4a	Tumour penetrates to surface of visceral peritoneum
T4b	Tumour directly invades/is adherent to other organs
Regional lymph nodes (N)	
Nx	Regional lymph nodes cannot be assessed
N0	No regional lymph node metastasis
N1	Metastasis in 1-3 regional lymph nodes
N1a	Metastasis in one regional lymph node
N1b	Metastasis in 2-3 regional lymph nodes
N1c	Tumour in subserosa, mesentery, non peritonealised pericolic/perirectal tissue without regional nodal metastasis
	Metastasis in 4 or more regional lymph nodes
N2	Metastasis in 4-6 regional lymph nodes
N2a	Metastasis in 7 or more regional lymph nodes
N2b	
Distant metastasis (M)	
M0	No distant metastasis
M1	Distant metastasis
M1a	Metastasis confined to one organ or site
M1b	Metastases in more than one organ/site or peritoneum

Note: cTNM = clinical classification, pTNM = pathological classification, rTNM = classification of recurrent disease

1.1.12.3 UICC stage grouping for colorectal cancer

The TNM stage can be further grouped into UICC/AJCC stage grouping. This, along with its association with Dukes' staging is shown in Table 1.9.

Table 1.9 UICC stage and its association with TNM stage and Dukes' stage. Taken from AJCC 7th Edition Colon and Rectum Cancer Staging (66).

Stage	T	N	M	Dukes' stage
0	Tis	N0	M0	-
I	T1	N0	M0	A
	T2	N0	M0	A
IIA	T3	N0	M0	B
IIB	T4a	N0	M0	B
IIC	T4b	N0	M0	B
IIIA	T1-2	N1/N1c	M0	C
	T1	N2a	M0	C
IIIB	T3-T4a	N1/N1c	M0	C
	T2-T3	N2a	M0	C
	T1-T2	N2b	M0	C
IIIC	T4a	N2a	M0	C
	T3-T4a	N2b	M0	C
	T4b	N1-N2	M0	C
IVA	Any T	Any N	M1a	-
IVB	Any T	Any N	M1b	

1.1.13 Staging investigations

1.1.13.1 Computerised tomography

All patients with colorectal cancer should undergo contrast-enhanced CT scan of the chest, abdomen and pelvis for the purposes of staging (67).

1.1.13.2 Magnetic resonance (MR) imaging

In addition to CT scan, all patients with rectal cancer should also undergo MR imaging to determine whether the circumferential resection margin (CRM) is threatened by the tumour (67). Furthermore, the Royal College of Radiologists recommends MR imaging with liver-specific contrast agents as the technique of choice in staging patients with colorectal liver metastases, as MR has greater sensitivity for the detection of metastatic disease than either CT or positron emission tomography CT (PET-CT) (68).

1.1.13.3 Endorectal ultrasound scan (USS)

Endorectal USS can be a useful adjunct to MRI imaging in patients with potentially resectable rectal cancer or can be used as an alternative in patients in whom MRI is contraindicated (67).

1.1.13.4 Positron emission tomography –CT (PET-CT)

18-fluorodeoxyglucose positron emission tomography-CT (^{18}FDG PET-CT) may be used for the further assessment of extra-hepatic metastases that may be amenable to radical surgery and a recent meta-analysis has confirmed that it is a useful tool to help predict survival outcomes in patients with colorectal cancer liver metastases (67, 69).

1.1.13.5 Stratification of local recurrence risk of rectal cancers

The risk of local recurrence of rectal cancers can be predicted by MRI as shown in Table 1.10. A high risk of systemic recurrence may also be predicted by the presence of extramural vascular invasion on MRI (67).

Table 1.10 Risk of local recurrence for rectal tumours based on characteristics of tumour predicted by MRI. Taken from NICE guideline CG131 (Colorectal cancer: The diagnosis and management of colorectal cancer) (67).

Risk of local recurrence	Characteristic of rectal tumour predicted by MRI
High risk	Threatened (<1mm) or breached CRM
	Low tumours with inter-sphincteric or levator involvement
Moderate risk	cT3b or greater without threatened CRM
	Suspicious lymph node without threatened CRM
	Extramural vascular invasion
Low risk	cT1/cT2/cT3a without lymph node involvement

1.1.14 Management of colorectal cancer

1.1.14.1 The role of the multidisciplinary team

The multidisciplinary team (MDT) is central to the modern management of colorectal cancer. The team, which includes surgeons, gastroenterologists, colorectal nurse specialists, radiologists, oncologists and pathologists, meet regularly to discuss new cases, decide management plans, record patient outcomes and undertake data collection for purposes of local and national audit. The MDT is usually surgeon led, with patients being assigned to, and being the responsibility of, a named consultant surgeon though their care may be transferred to the oncologists as required. During the MDT meeting, information is shared and through collaborative decision-making, recommendations for the patient's management are made. These recommendations can then be discussed with the patient enabling them to make informed decisions about their care.

The aim of the MDT is to enable timely diagnosis and treatment, to ensure evidence-based recommendations for patient management, to allow continuity of care, to facilitate information exchange, to identify patients who may be eligible for inclusion in trials and to provide education and learning to members (70). The evidence for the effectiveness of cancer MDT meetings is weak and limited but there are more studies that suggest MDTs have a positive impact than those suggesting they have a negative impact (70). One large study looking at patients with all cancers found that MDT meetings were associated with a significant improvement in 5 year survival and in another study looking at colorectal cancer in particular, MDT working was associated with an increase in recruitment of patients to trials (71, 72). Given the fact that MDT meetings are the cornerstone of cancer management in current UK practice, it seems unlikely that further randomised controlled trials will be undertaken.

1.1.14.2 Surgery for colorectal cancer

Surgical resection remains the cornerstone of curative management of locally confined colorectal cancers and the most recent National Bowel Cancer Audit shows that just over 60% of patients with colorectal cancer undergo major resectional surgery (57).

Although the proportion of patients undergoing major resection has remained around 60-65% over the last 5 years, the 90-day mortality rate has decreased from 5.8% to 3.8% overall (73). Over this time period, the proportion of colorectal cancer patients has remained at just over 21% and 16% of patients with a colorectal cancer have their major resectional surgery performed as an urgent or emergency procedure (73). Emergent/urgent surgery is associated with an increased 90-day mortality of 12.1% compared to 2.3% for those patients undergoing elective or scheduled surgery (73).

1.1.14.2.1 Selection of patients for surgery

The suitability for surgery of a patient with colorectal cancer depends both of the stage of the disease and also on the patients fitness for surgery. Cardiopulmonary exercise (CPEx) testing is a non-invasive assessment of a patients exercise capacity that is used to estimate their fitness prior to undertaking major resectional surgery.

1.1.14.2.2 Surgical approaches

The surgical resection of a colorectal cancer can be undertaken via an open or laparoscopic approach. Laparoscopic surgery is associated with reduced length of hospital stay and NICE and the Association of Coloproctology of Great Britain and Ireland (ACPGBI) recommend

that laparoscopic resection should be offered as an alternative to open resection to suitable patients (57). In 2011/2012, 40% of bowel resections in England and Wales were performed via a laparoscopic approach, compared to 25% in 2008/2009 (57).

1.1.14.2.3 Resection of hepatic metastases

Historically, the presence of liver metastases was tantamount to a death sentence. Fortunately, this is no longer the case and now nearly 7% of all patients with distant colorectal metastases confined to the liver are being considered for liver resection with curative intent (67).

1.1.14.3 Colonic stents for acute large bowel obstruction

In patients presenting as an emergency with acute left-sided colonic obstruction, a colonic stent can be employed to manage the obstruction in patients with unresectable disease or who are unfit for major surgery, or can be used as a 'bridge' to manage relieve obstruction and convert an emergency admission to a planned resection (73).

1.1.14.4 Chemotherapy

Adjuvant chemotherapy with capecitabine monotherapy or combination therapy with oxaliplatin, 5-fluorouracil and folinic acid is offered to patients with high risk Stage II and Stage III colon cancer (67).

Neo-adjuvant chemotherapy is offered to patients with advanced and metastatic colorectal cancer. Current NICE guidelines suggest folinic acid plus fluorouracil plus oxaliplatin (FOLFOX) as first-line treatment followed by either irinotecan alone or folinic acid plus

fluorouracil plus irinotecan (FOLFIRI) as second-line treatment (67). Alternatively, capecitabine plus oxaliplatin (XELOX) may be used as first-line treatment followed by FOLFIRI as second-line treatment (67).

1.1.14.5 Neo-adjuvant therapy for rectal cancer

The use of neo-adjuvant therapy in rectal cancer depends on the risk of local recurrence predicted from staging MR imaging. Patients with low risk rectal cancer do not require neo-adjuvant therapy and proceed directly to surgical resection (67). For patients with high-risk rectal tumours, neo-adjuvant chemoradiotherapy with an interval prior to surgery is advised to allow tumour response and shrinkage (67).

The management of those with moderate risk rectal cancers is more contentious. There are essentially two options for this group, (i) short-course pre-operative radiotherapy followed by immediate surgery and (ii) pre-operative chemoradiotherapy with an interval before surgery. Current NICE guidelines recommend the former option in those with moderate-risk rectal tumours and the latter option in those with borderline moderate/high risk MR findings (67).

1.1.14.6 Biological agents in the treatment of metastatic colorectal cancer

1.1.14.6.1 Anti-EGFR monoclonal antibody

Anti-EGFR monoclonal antibodies (mAbs), such as cetuximab, now play a role in the management of patients with metastatic colorectal cancer (mCRC). Current NICE guidelines recommend the use of anti-EGFR mAbs in patients with EGFR-expressing KRAS wild-type mCRC in combination with chemotherapy, or as a single agent in patients who have failed chemotherapy (74).

A recent study by Sorich *et al* suggests that patients with KRAS exon 3 and 4, and NRAS exon 2, 3 and 4 mutations may also benefit less from anti-EGFR mAbs than patients who are wild-type for these additional RAS activating mutations and that testing for these further mutations should form part of patient work up when deciding whether anti-EGFR therapy is appropriate (31).

1.1.14.7 Palliation of advanced disease

Palliation of symptoms is the primary aim of treatment for patients with advanced colorectal cancer and may encompass palliative surgery or stenting to prevent or alleviate obstruction, chemotherapy, radiotherapy and medications including analgesics and antiemetics.

1.1.14.8 Challenges in the management of colorectal cancer

Despite advances in treatment, colorectal cancer accounts for a significant proportion of cancer related deaths. It is likely that this is due, in part at least, to the high proportion of patients presenting with advanced disease or as an emergency. Population based screening is one strategy aimed at addressing this problem but limitations of current UK screening include the possibility of false negative FOB test, cost and the fact that colonoscopy is invasive and is associated with complications such as bleeding and colonic perforation.

There is a real need to develop non-invasive or minimally invasive diagnostic tests, which could identify patients at higher risk of developing colorectal cancer or identify those with early changes or early stage cancer, which is associated with better prognosis. Consequently there has been increasing interest in the development of blood or faecal-based biomarker tests that can detect the presence of altered genes associated with colorectal cancer.

Biomarkers are defined as 'molecular indicators of exposure or disease state'(75). In cancer, they may arise from the tumour itself or from the response of the body to cancer and may have a role in identifying populations at increased risk, in cancer prevention, diagnosis and prognosis and in predicting tumour responsiveness to therapy and the risk of relapse.
There has been huge interest in the identification of genetic, epigenetic and proteomic biomarkers in relation to all cancers and a number of biomarkers have been identified which are shown in Table 1.11.

Table 1.11 Examples of cancer biomarkers

Biomarker	Name	Disease
AFP	Alpha-fetoprotein	Liver cancer
BCR-ABL	Philadelphia chromosome	Chronic myeloid leukaemia
BRCA1/BRCA2	Breast cancer 1/Breast cancer 2	Breast/ovarian cancer
BRAF V600E	Proto-oncogene B-Raf	Melanoma/colorectal cancer
CA-125	Cancer antigen 125	Ovarian cancer
CA19-9	Cancer antigen 19-9	Pancreatic cancer
CEA	Carcinoembryonic antigen	Colorectal cancer
EGFR	Epidermal growth factor receptor	Non-small cell lung cancer
HER-2	Human epidermal growth factor receptor 2	Breast cancer
KIT	Proto-oncogene c-Kit	Gastrointestinal stromal tumour
PSA	Prostate specific antigen	Prostate cancer
S100	S100 protein	Melanoma

One recently identified biomarker is Septin9 DNA, which is hypermethylated in colorectal cancer. A molecular DNA test for this (Epi proColon®) was the first blood-based test for colorectal cancer screening to be approved by the FDA in April 2016. It is hoped that further biomarkers will be identified that may aid not only in the diagnosis of colorectal cancer, but in its management, either by stratifying patients according to their likely response to adjuvant therapies or through the development of novel molecular therapies.

This thesis is concerned with the investigation of an adaptor protein called Dok-7, its association with colorectal cancer with a view to its potential use as a diagnostic and prognostic marker in colorectal cancer and its potential as a novel therapeutic target. The Dok proteins are discussed in detail in Section 1.3.

1.1.14.9 Follow up

All patients with colorectal cancer undergoing treatment with curative intent should be offered follow up starting with clinical follow up 4-6 weeks after treatment. Within the first three years after treatment, patients should undergo two CT scans of the chest, abdomen and pelvis and serum carcinoembryonic antigen (CEA) should be checked every six months (67). Surveillance colonoscopy is usually performed 1 year and 5 years after initial treatment (67).

1.2 The Hallmarks of Cancer and the molecular basis of cancer progression

1.2.1 The Hallmarks of Cancer

In their seminal paper 'The Hallmarks of Cancer' published in Nature in 2000, Hanahan and Weinberg identified a number of characteristics shared by cancer cells (76). These characteristics are (i) self-sufficiency in growth signals, (ii) insensitivity to antigrowth signals, (iii) evasion of apoptosis, (iv) limitless replicative potential, (v) sustained angiogenesis and (vi) tissue invasion and metastasis (76). As previously discussed, outcomes in patients with colorectal cancer are closely related to stage of disease, which is defined by the degree of local tumour invasion and the presence of local and distant metastases, and the majority of cancer-related deaths occur as a consequence of metastatic disease.

1.2.2 The molecular basis of cancer progression

1.2.2.1 Epithelial-mesenchymal transition

Enhanced cancer cell motility plays an important role in both invasion and metastasis (77). Firstly, primary tumour cells invade local tissues in a process known as epithelial-mesenchymal transition (EMT). EMT is seen during normal foetal and postnatal development and is regulated by transcription factors such as Twist1, Snail1 and Slug, which inhibit E-cadherin expression, zonaoccludens 1 (ZO1) and Beta4-integrin (78). It results in the reorganisation of cytoskeletal structures and the upregulation of fibroblast markers and genes such as vimentin, N-cadherin, Twist and α-smooth muscle actin (α-SMA). Cells consequently become more mobile, plastic, isolated and resistant to apoptosis. Several molecules have been

implicated in EMT, including TGF-β, which has been shown to induce EMT in embryonic epithelial cells.

1.2.2.2 Invasion

Tumour cells invade through the basement membrane and degrade the extracellular matrix to invade into blood and lymphatic vessels in a process controlled by the matrix metalloproteinases. These are endopeptidases that are involved in normal tissue remodelling during growth and wound healing. Altered expression of MMPs has been identified in colorectal cancer (79). Normally, cells detaching from the extracellular matrix lose cell-matrix interactions and consequently undergo programmed cell death in a process known as anoikis but successfully metastasising cancer cells are able to evade anoikis.

1.2.2.3 Migration

Migration is stimulated by scatter factors including hepatocyte growth factor (HGF). Initially recognised as a promoter of hepatocyte cell growth, HGF is now understood to play an important role in cell growth and cell motility for a range of epithelial cells (80). The activity of hepatocyte growth factor increases after injury, suggesting an important role in normal wound healing and organ regeneration and higher levels of the HGF receptor (cMet) have been found in metastatic lesions compared with primary tumours (80). As the tumour progresses, it will encounter normal blood vessels and new vessel growth is induced by angiogenic factors. Tumour cells invade the blood vessels and are transported through the circulatory system until they reach an appropriate microenvironment. Angiogenesis is important in order for tumour cells to become established at this metastatic site and to enable subsequent growth.

1.2.2.4 Haematogenous and lymphatogenous spread

As they spread, tumour cells migrate and invade into local tissues including local blood or lymphatic vessels (intravasation) and the development of new blood and lymphatic vessels (angiogenesis and lymphangiogenesis) is induced by angiogenic and lymphangiogenic factors. Tanigawa et al (1997) found that the degree of new vessel formation around colorectal tumour was the most important predictor of haematogenous metastatic development (81).

Angiogenesis is the biological process by which new capillaries are formed (82). It is essential in normal embryological development and post-embryonic angiogenesis is minimal in adult life though certain sites retain angiogenic activity, such as the corpus lutea in the ovaries, the endometrium of the uterus and there are high levels of angiogenic activity during the proliferative phase of wound healing (83, 84). However, inappropriate angiogenesis may occur in pathological states such as in rheumatoid arthritis, diabetic retinopathy and in cancer.

Angiogenic factors are secreted by tumours, resulting in the stimulation of new vessel growth, improving the delivery of nutrients and oxygen to the growing tumour (85, 86). These new vessels provide nutrients to the growing tumour, are poorly developed compared to normal vessels facilitating penetration and embolization increasing the metastatic potential of the tumour, and support the survival and growth of metastatic tumour deposits.

The development of the embryological vascular system involves a complex process of differentiation, proliferation, migration and maturation resulting in the formation of an organized network of vessels (87). Several molecules are involved in the regulation of angiogenesis including the VEGF family, Delta/Notch, Slit/Robo, neuropilin and HGF. Once the vascular tree is complete, the balance of stimulating and inhibiting factors stabilizes and

angiogenesis is usually limited to normal physiological processes like reproduction and wound healing. Post-embryonic angiogenesis is also induced by fibroblast growth factor (FGF), angiogenin, TGF-α, TGF-β, platelet derived growth factor (PDGF), TNF-α, interleukins, chemokines and angiopoietins (85).

Bevacizumab (Avastin®) is a humanized variant of a murine anti-human monoclonal antibody targeting VEGF-A; a prime angiogenic molecule involved in the development of blood supply for both the primary tumour and secondary tumour deposits. The FDA has approved bevacizumab for the first- and second-line treatment of metastatic colorectal cancer in combination with chemotherapy (88). However, current NICE guidelines do not recommend bevacizumab for patients with metastatic colorectal cancer who have not been previously treated with the drug.

Lymphangiogenesis is the process of lymphatic system development. The lymphatic system comprises a network of thin-walled, blind-ending vessels lines with a single layer of lymphatic endothelial cells. They originate from the same embryological tissue as the arteriovenous system. They collect extravasated fluid, proteins and electrolytes from extracellular fluid, returning this lymphatic fluid back to the arteriovenous system. The lymphatic system is also part of the immunosurveillance system, presenting foreign antigens to lymphocytes in lymph nodes scattered along the lymphatic vascular chain.

In 1902, Sabin proposed a mechanism of lymphangiogenesis whereby lymphatic vessel development is subsequent to blood vessel development and which involved the sprouting of lymphatic vessels from venous endothelium of nearby veins. Subsequent work found that the expression of Prox-1 by venous endothelial cells within the embryo reflects the site of budding and sprouting of lymphatic cells that give rise to the primary lymphatic system.

1.2.2.5 Development of distant metastases

Once the cancer cell reaches a suitable metastatic site, they leave the blood/lymphatic system (extravasation) and lodge in the target organ. They may then enter a period of metastatic dormancy for months or even years before subsequent growth and progression.

There are two major theories relating to tumour invasion and the development of metastases. Firstly, Paget's seed and soil theory, which states that a specific organ microenvironment is required for the development of metastases. Secondly, Ewing's anatomical theory states that invasion and metastases depend on the regional lymphovascular system. In practice, both of these factors play a role. Regional metastases usually follow the anatomy of the regional blood and lymphatic vessels whilst distant metastases often show a preference for certain organ microenvironments. Furthermore, the ability of the cancer cell to establish metastases depends not only on the tumour cell itself but also on factors relating to the microenvironment of the potential metastatic site. For example, the release of chemokines by host tissues may aid tumour cell migration.

1.3 The Dok proteins

Tyrosine phosphorylation of proteins by protein tyrosine kinases (PTKs) is a reversible process that plays an important role in the regulation of a variety of cellular functions including cell growth, differentiation and cell motility. Activation of PTKs by extracellular stimuli results in the phosphorylation of both the PTK as well as other substrates including trans-membrane receptors and downstream adaptor proteins (89). These proteins then either recruit or inhibit further downstream molecules, thereby regulating tyrosine kinase signalling pathways (89, 90). Aberrations in this process of tyrosine phosphorylation and downstream signal transduction are associated with many types of cancer. Consequently, there has been an effort to investigate and understand this complex process in order to evaluate its potential as a target for therapeutic intervention.

Downstream of kinase (Dok) proteins possess structural characteristics typical of adapter proteins and, like other adapter molecules, they associate with activated cell-surface receptors and aid in the docking of downstream signalling molecules, facilitating intracellular signal transduction.

1.3.1 Introduction to the Dok protein family

The first of the downstream of kinase (Dok) protein family, Dok-1, was identified by Ellis *et al* in 1990 (91). Since then, a total of seven members of this family of enzymatically inert adaptor proteins have been identified, so called Dok-1-7, which are subdivided into three subgroups (Dok-1-3, Dok-4-6 and Dok-7). All of the Dok proteins share structural characteristics typical of adapter proteins and, like other adapter molecules, they associate with activated cell-surface receptors and aid in the docking of downstream signalling molecules, facilitating intracellular signal transduction (90, 92, 93).

The discovery of Dok-1 occurred in 1990 when Ellis *et al* identified a 62kDa protein that co-precipitated with p21rasGTPase-activating protein (GAP) and acted as a target for activated protein tyrosine kinases including v-Abl and v-Src (91). This protein, initially called p62, was found to be tyrosine phosphorylated by tyrosine kinases in response to extracellular stimuli such as epidermal growth factor (EGF) and the extent of its phosphorylation was associated with cellular transformation (91). Later, Carpino *et al* reported that a constitutively tyrosine phosphorylated 62kDa protein, corresponding to the protein identified by Ellis *et al*, associates with GAP in p210 (bcr-abl) expressing haematopoietic progenitor cells isolated from chronic myeloid leukaemia (CML) patients (94). They found that activation of the receptor tyrosine kinase c-Kit resulted in tyrosine phosphorylation of this protein and its subsequent association with GAP, with affinity dependent on the degree of tyrosine phosphorylation (94, 95). They named the protein p62 (dok) due to its role in signal transduction pathways downstream of receptor tyrosine kinases, and this later became known as Dok-1 (94).

The discovery of the Dok-1 occurred in the context of CML, a disease characterized by the t(9;22) Philadelphia chromosome (Ph1) and its resultant fusion oncogene, Bcr-Abl (94). This oncogene expresses a chimeric protein p210(bcr-abl) that has enhanced tyrosine kinase activity resulting in the activation of several downstream signalling pathways including mitogen-activated protein kinase (MAP)/Extracellular-signal-regulated kinases (ERK), Myc, Jun, STAT, PI3K and NF-κB (96).

Later work established that Dok-1 was the major phosphorylation substrate not only for p210bcr-abl oncoprotein, but also for many other receptor and cytoplasmic tyrosine kinases, including v-Abl, v-Src, EGF receptor (EGFR), insulin/insulin-like growth factor 1 (IGF-1) receptors and platelet derived growth factor receptor (PDGFR) (91, 94, 95, 97-100). Within the next decade, Dok-2 (Dok-R/p56 (dok-2)), a 56kDa protein comprising 412 amino acids with 35% homology to Dok-1, and Dok-3 (Dok-L) were subsequently identified (101, 102).

Owing to structural and functional similarities, Dok-1, Dok-2 and Dok-3 form a subgroup within the Dok protein family (102, 103).

Dok-4 and Dok-5 were discovered in 2001 by Grimm *et al*, followed by Dok-6, which was discovered by Crowder *et al* in 2004 and these three Dok family members form a subgroup, which appears to be phylogenetically distinct from Dok-1, Dok-2 and Dok-3 on the basis of differences in expression and function (104, 105).

The most recent member of the Dok protein family, Dok-7, was identified by Okada et al in 2006 (106). They found that this cytoplasmic adaptor protein plays an essential role in neuromuscular junction (NMJ) formation, a process which is organised by the tyrosine kinase muscle specific kinase (MuSK) and its extracellular activator, agrin (107). Dok-7 is both a substrate of MuSK and an essential activator of MuSK kinase activity as well as being required for acetylcholine receptor (AChR) clustering (89, 106, 108). Moreover, Dok-7 is required by agrin to activate MuSK and is also necessary for the correct localisation of MuSK in muscle (107). Therefore, NMJ formation requires agrin, derived from neurons, as well as MuSK, Dok-7 and a protein called low-density lipoprotein receptor-related protein 4 (Lrp4), all of which arise from muscle (108-110). Other authors subsequently demonstrated that overexpression of Dok-7 is associated with increased activation of MuSK and NMJ formation and that in agrin deficient mice; Dok-7 expression enhances MuSK activation and restores NMJ formation (107, 109, 110).

1.3.2 Dok protein structure

The Dok proteins share a common structure, shown in Figure 1.5, that bears some similarity to the insulin receptor substrate (IRS) family of proteins, which act downstream of the insulin and IGF-1 receptors mediating signal transduction to the phosphatidylinositol 3-kinase (PI3K) and mitogen-activated protein kinase (MAPK) pathways (102).

A.

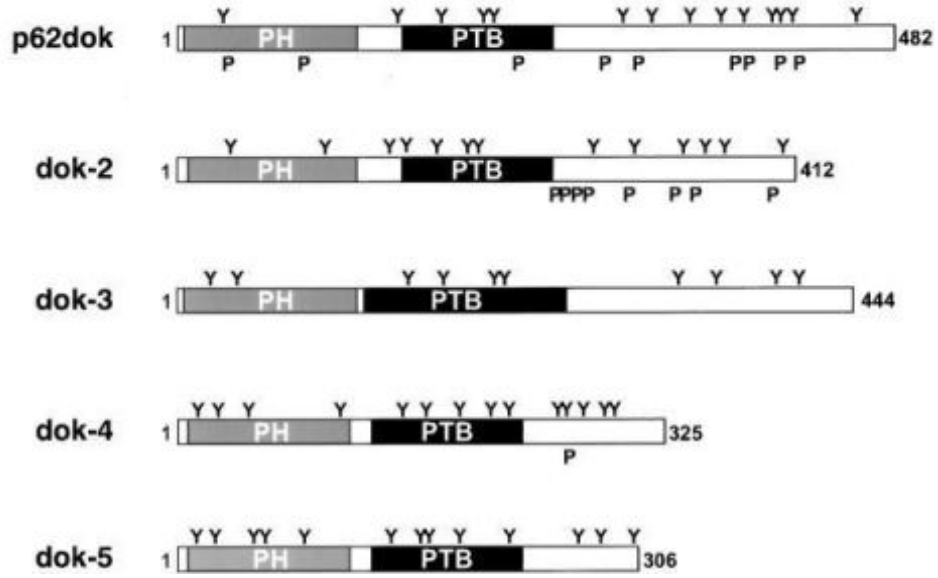

B.

Figure 1.5 Protein structure of DOKs. A. Function domains of DOK protein family members 1-5. PH (grey) and PTB (black) domains are shown and positions of tyrosine residues (Y) and PXXP motifs (P) are indicated. Illustration taken from Grimm et al (104) B. Phylogenetic tree of human DOK proteins. The phylogenetic analysis was performed using the ClustalW (http://www.ebi.ac.uk/clustalw/), and the dendrogram tree was plotted using the Treeview (Version 1.6.6, http://taxonomy.zoology.gla.ac.uk/rod/treeview.html).

The MAP kinase pathway is a signalling cascade initiated by the binding of a ligand, such as epidermal growth factor (EGF) to the extracellular binding site of a receptor tyrosine kinase (RTK). Binding of the ligand results in the dimerization of two subunits of the RTK. This in turn catalyses the phosphorylation of the intracellular portion of each RTK subunit and enables growth factor receptor bound protein 2 (GRB2) to bind to the phosphorylated RTK, which in turn binds the protein SOS. SOS can then bind onto the membrane-bound protein RAS, which in its inactive form is bound to GDP. Binding of SOS to Ras catalyses the conversion of GDP into GTP and the activation of the Ras protein. Once activated, Ras is able to bind to several effector proteins, including the kinase B-Raf. Active B-Raf phosphorylates and activates kinases MEK1 and MEK2, which in turn, phosphorylate and activate ERK1 and ERK2. Ultimately this cascade of phosphorylation and activation results in the activation of activator protein 1 (AP-1) transcription factors, including jun and fos. These transcription factors then form a heterodimer in the cell nucleus and bind to AP-1 motifs in the DNA resulting in the expression of genes involved in cell proliferation.

The Dok family proteins, like other docking/scaffolding proteins, characteristically contain protein-protein interaction motifs such as multiple tyrosine residues (111). When phosphorylated, these tyrosine residues act as binding sites for Src homology 2 (SH2) domain containing signalling proteins, such as growth factor receptor-bound protein 2 (Grb2), PI3K and the SHP-2 tyrosine phosphatase (111).

Initial work investigating the structure of Dok-1 revealed prominent tyrosine residues and nearby SH2 binding sites, suggesting its likely role as a signalling molecule (94, 95). Since then, the structure of the Dok family proteins has been elucidated and is characterized by three distinct regions: an amino (N-) terminal pleckstrin homology (PH) domain, a central phosphotyrosine-binding (PTB) domain and a carboxyl (C-) terminal, which contains multiple sites for tyrosine phosphorylation and proline-rich (PxxP) motifs which may enable the docking of SH2 and SH3 containing proteins (89, 101-103, 112).

The N-terminal PH domain is a region containing around 120 amino acids. This domain is found in many proteins involved in cell signalling and is thought to regulate signal transduction by mediating the association of the PH domain containing protein with the cell membrane (113). Studies of Dok-1 isoforms suggest that the N-terminal plays an important role in determining the cellular localization of Dok-1 throughout the cytoplasm, and in Dok-2, the PH domain acts to stabilise Dok-2-EGFR binding and tyrosine phosphorylation of Dok-2 (93, 114). Phosphorylation of Dok-4 by receptor tyrosine kinase RET or cytosolic tyrosine kinase Fyn requires both its PH and PTB domains and results in the inhibition of Elk-1 activation (115). This effect, as well as the negative regulation of T cell activation, requires the PH domain of Dok-4 (116). The PH domain has also been shown to be important for the constitutive localization of Dok-4 and Dok-6 at the cell membrane (117). Itoh *et al* found that the mitochondrial location of Dok-4, and c-Src with which it associates, is dependent on the N-terminal and PTB domains and identified a putative mitochondrial targeting sequence in the N terminal of Dok-4 and Dok-5 (118). Expression of Dok-4 in endothelial mitochondria enhances TNF-α-induced reactive oxygen species (ROS) production and NF-κB production (118). In Dok-7, the N-terminal PH domain enables the nuclear import of Dok-7 (119).

Phosphotyrosine-binding (PTB) domains are found in a range of signalling and cytoskeletal proteins (120). Previous authors have shown that Dok-1 and Dok-2 associate with activated EGFR via their PTB domains and that the inhibition of Src tyrosine kinase-induced cellular transformation by Dok-1 is dependent on the Dok-1 PTB domain as well as the presence of C-terminal tyrosine phosphorylation sites (especially residues 336-363) (93, 112, 121). Upon tyrosine phosphorylation, Dok-1 and Dok-2 interact homotypically and heterotypically to form oligomers via the PTB domain and this oligomerisation is essential for Dok phosphorylation and function (122). For example, the PTB domain and the amino terminal tyrosine 146 (Tyr (146)) residue enable Dok-1 to form homodimers, which are essential for the inhibition of Src transformation (112).

The PTB domain of the Dok proteins has also been shown to play a key role in the formation of Dok-1 and Dok-5 homomeric and heteromeric associations, the interactions of Dok-1, Dok-2 and Dok-3 with SH2-containing inositol 5'-Phosphatase (SHIP)-1, the interaction of Dok-2 with receptor tyrosine kinases such as erbB-2 (HER2/neu) and Tek (Angiopoietin-1 receptor), and for the recruitment and phosphorylation of Dok-2 by activated EGFR, an interaction that is stabilized by the PH domain (93, 103, 123-126).

Dok-3 binds to, and is phosphorylated by, Abl tyrosine kinase via its PTB domain (102). Overexpression of Dok-3 reduces v-Abl-induced MAPK activation in a PTB dependent fashion but has no effect on constitutively activated Ras- and EGF-induced MAPK activation (102).

Unlike Dok-1, the PTB domain of Dok-4 and Dok-5 does not bind tyrosine phosphorylation sites in EGFR and when compared to Dok-1, the PTB domain of Dok-4 binds poorly to Ret with additional C-terminal residues being required for its binding (121, 125). However, the PTB domain of Dok-4 does bind SHIP-1, via phosphorylated NPXY motifs and SHIP-1 facilitates coupling of Abl to Dok-4 (125). In Dok-5, the PTB domain interacts with Tropomyosin receptor kinase (Trk) B/C resulting in the activation of the MAPK pathway and in Dok-6, the PTB domain binds to the NPQY motif of TrkC (127, 128). TrkC is involved in nervous system development and this interaction with Dok-6 promotes neurotrophin 3 (NT-3) mediated neurite outgrowth in cortical neurons (105, 128). Dok-7 interacts with the juxtamembrane region of MuSK via its PTB domain and both PH and PTB domains are required for MuSK activation (106, 119, 129).

The C-terminal of Dok-1 and Dok-2 (but not Dok-3) contains repeated YxxP motifs, which are involved in the interaction of the Dok proteins with SH domain-containing molecules, as well as providing multiple sites for tyrosine phosphorylation (102, 130). It is here that Dok-1 is tyrosine phosphorylated by p210 (bcr-abl) and specifically, Tyr (362) and Tyr (398) are

major sites for phosphorylation and for interaction of Dok-1 with GAP (131, 132). Tyr (362) is also involved in the interaction between Dok-1 and non-catalytic region of tyrosine kinase adaptor protein 1 (Nck) (132), whilst Tyr (336) and Tyr (340) are necessary for the negative regulation of Ras-Erk signalling and cellular transformation, though they are not required for p210rasGAP (RasGAP) binding (133). Dok-2 interacts with c-Abl in an interaction that is mediated by SH3 and a PMMP motif in the proline-rich tail of Dok-2 and which is enhanced by the SH2 domain (134). Through this interaction, the tyrosine phosphorylation and kinase activity of c-Abl is increased, with a corresponding increase in activity relating to cytoskeletal reorganization (134).

Hamuro *et al* found that the C-terminal region of Dok-7 contains a chromosome region maintenance 1-dependent nuclear export signal (NES) and that the NES-mediated cytoplasmic location of Dok-7 is necessary for regulating its interaction with MuSK (119). The C-terminal of Dok-7 contains SH2 target motifs required for MuSK activation, and phosphorylation of tyrosine residues in this region by agrin results in the recruitment of the adapter proteins Crk and Crk-L which are required for normal NMJ formation (119, 129). Crk also contains N-terminal SH2 and C-terminal SH3 domains implicated in the positive and negative regulation of cellular transformation respectively (135). Overall, the PH, PTB, SH2 motifs and C-terminal NES are all important for Dok-7/MuSK signalling and disruption in these elements may give rise to NMJ synaptopathy (119).

1.3.3 Genetic loci of DOK genes

DOK1 has been mapped to human chromosome 2p13, in a region that is translocated in chronic lymphocytic leukaemia (CLL), B-cell acute lymphoblastic leukaemia (B-ALL), basal cell papilloma and keratoacanthoma (136-140). DOK2 has been localised to chromosome 8p21.3, DOK3 to chromosome 5q35.3, DOK4 to chromosome 16q21, DOK5 to chromosome

20q13.2 and DOK6 to chromosome 18q22.2. DOK7 is located on the short arm of chromosome 4 at position 16.3 extending from base pair 3,463,305 to base pair 3,494,481. It comprises 7 exons (141).

1.3.4 Expression profile of DOKs

The expression profile of DOKs in the human body by tissue type is shown in Table 1.12.

Table 1.12 Expression profile of *DOKs* by tissue type (TPM, transcripts per million)

	DOK1	***DOK2***	***DOK3***	***DOK4***	***DOK5***	***DOK6***	***DOK7***
Adipose tissue	**155**	**233**	0	77	**77**	0	0
Adrenal gland	30	0	0	30	0	0	0
Ascites	0	0	0	50	0	0	0
Bladder	0	0	0	0	0	0	0
Blood	**114**	**139**	**302**	0	0	0	8
Bone	13	13	0	69	27	0	0
Bone marrow	41	0	61	41	0	0	0
Brain	10	1	16	**153**	**83**	**25**	10
Cervix	41	0	0	20	0	0	0
Connective tissue	67	**114**	33	60	67	20	0
Ear	0	0	0	0	0	**124**	0
Embryonic tissue	14	0	4	61	18	0	0
Eye	9	19	4	19	14	28	9
Heart	33	0	33	33	11	0	**33**
Intestine	25	4	12	**116**	8	0	0
Kidney	23	4	9	66	18	4	4
Larynx	0	0	0	0	0	0	0
Liver	4	9	0	19	0	0	0
Lung	14	29	20	38	2	0	5
Lymph	0	0	203	0	0	0	0
Lymph node	44	0	178	11	0	0	0
Mammary gland	39	0	13	19	0	0	19
Mouth	15	15	15	0	0	0	30
Muscle	9	0	0	56	18	9	9
Nerve	0	0	0	0	0	0	0
Oesophagus	0	0	0	0	0	0	0
Ovary	9	9	0	49	**226**	9	29
Pancreas	28	14	0	84	0	4	14
Parathyroid	0	0	0	0	0	**48**	0
Pharynx	0	49	0	49	0	0	0
Pituitary gland	0	0	0	60	0	0	**60**
Placenta	42	28	10	14	0	28	0
Prostate	5	0	0	21	0	0	0
Salivary gland	0	0	0	0	0	0	0
Skin	18	0	0	42	9	0	4
Spleen	18	74	**468**	37	0	0	**37**
Stomach	0	20	10	52	0	0	0
Testis	6	2	16	64	0	11	4
Thymus	12	50	125	25	12	0	0
Thyroid	0	0	21	21	0	0	0
Tonsil	58	0	**763**	0	0	0	0
Trachea	0	0	19	0	0	0	0
Umbilical cord	**72**	0	0	0	0	0	0
Uterus	25	21	25	43	4	0	17
Vascular	19	0	0	**116**	19	0	0

Note: TPMs in bold are top three organs/tissues which express higher levels of the *DOKs.* This is a summative table adapted from approximate expression pattern from the EST profile at http://www.ncbi.nlm.nih.gov/UniGene.

Although Dok-1, Dok-2 and Dok-3 are preferentially expressed in several haematopoietic cells, immune cells, the spleen and the lung, they are also found in other tissues (90, 94, 101, 130, 142-144).

Dok-1 is abundantly expressed in all layers of the primate dorsolateral prefrontal cortex, both in neurons and in the endothelial cells of cerebral blood vessels (145). Since its distribution is similar to that of the IGF-1 receptor, Smith *et al* suggest that Dok-1 may be a downstream target of IGF signalling in this area of the brain, which is involved in learning and memory (145). Dok-1 is also expressed in stem cell factor (SCF)/erythropoietin (Epo)-dependent erythroid progenitor cells from cord blood where it is implicated in signalling downstream of the c-kit/SCF receptor (146). Dok-2 is highly expressed in lymphoid tissues whilst Dok-3 is highly expressed in bone marrow and haematopoietic cell types including B cells, macrophages, mast cells and myeloid cells (102, 130, 147). Dok-4 and Dok-5 are expressed in human T cells (148).

Dok-4 is also expressed in many non-haematopoietic tissues including the brain, heart, intestine, liver, kidney and lung (115). Both Dok-4 and Dok-5 are found in neuronal tissue and Dok-5 is highly expressed in skeletal muscle and brain tissue (104, 149, 150). Dok-6 is highly expressed in the developing central nervous system whilst Dok-7 is preferentially expressed in muscle tissue and, like MuSK, it co-localises with AChRs at the postsynaptic area of NMJs (105, 106).

1.3.5 Role of Dok proteins in normal physiological processes and benign disease

1.3.5.1 Role of Dok proteins in allergy/inflammation

Dok-1 plays an important role in the regulation of airway inflammation and may, therefore, present a potential therapeutic target in asthma and other atopic diseases (151). In the ovalbumin-induced murine model of asthma, overexpression of Dok-1 is associated with a reduction in inflammatory cell number, airway hyper-responsiveness, Th2 cytokine expression and mucus response (151). Furthermore, Dok-1 overexpression is associated with stimulation of Signal Transducer and Activator of Transcription 4 (STAT-4) and T-bet transcription factors and inhibition of STAT-6 and GATA-3 transcription factors (151). Consistent with these findings, Dok-1/Dok-2/Dok-3 triple knockout mice exhibit increased airway hyper-responsiveness and Th2 cytokine expression in response to methacholine inhalation suggesting that Dok-1, Dok-2 and Dok-3 play an anti-inflammatory role in the lung (152).

Consistent with this, treatment of mast cells with dexamethasone is associated with upregulation of Dok-1 expression and phosphorylation, increased recruitment of RasGAP by Dok-1 and reduced activation of the MAPK pathway in antigen stimulated mast cells suggesting that Dok-1 may mediate the anti-allergic effects of dexamethasone (153).

Work by Abramson *et al* found that Dok-1 and Dok-2 play a role in the signalling cascade downstream of type 1 Fcepsilon receptors (FcepsilonRI) which ultimately results in the production of inflammatory mediators as well as changes in cell adhesion and morphology (154). Phosphorylation of Dok-1 by Fcepsilon results in its association with RasGAP and overexpression of Dok-1 results in reduced Ras/Raf/Erk signalling and reduced de novo synthesis of the cell signalling protein Tumour Necrosis Factor-alpha (TNF-α) (154).

Aggregation of FcepsilonRIs allows Dok-1 and Dok-2 to act as a scaffold for the association of further molecules including Nck, Crk-L and Cas, which are known to play a role in cytoskeletal rearrangement (154). Furthermore, the formation of Dok-Grb2-SHIP complexes inhibits mast cells and may therefore play a role in the modulation of human allergic diseases (155).

1.3.5.2 Role of Dok proteins in bone disease

Interestingly, a previous study by Kawamata *et al* has suggested that Dok-1 and Dok-2 may play a role in bone homeostasis (156). Their study found that deficiency of Dok-1 and Dok-2 was associated with a reduction in trabecular and cortical bone mass, increased periosteal and endosteal perimeters of the mid shaft of long bones and enhanced osteoclast number and activity, with resultant osteopenia (156).

1.3.5.3 Role of Dok proteins in haemostasis

The Dok proteins have also been implicated in platelet function and thrombosis. Dok-1 is one of several signalling proteins phosphorylated in activated platelets and both Dok-1 and Dok-3 are involved in platelet signalling downstream of the integrin alpha(IIb)beta(3), which is required for platelet aggregation (157, 158). Platelet spreading on fibrinogen is associated with increased tyrosine phosphorylation of Dok-1 and Dok-3, resulting in their interaction with Grb2 and SHIP-1 (158). Dok-2 is also thought to play a role in platelet adhesion, haemostasis and thrombosis signalling cascades and Dok-2 deficiency has been linked with accelerated thrombus formation (159, 160).

1.3.5.4 Role of Dok proteins in embryological development

In Drosophila flies, a homolog of Dok has been shown to play a crucial role in embryonic dorsal closure and loss of Dok is associated with defects in this process, suggesting that Dok may play a potential role in embryonic development (161).

1.3.5.5 Role of Dok proteins in endometrial physiology

Dok-1 has been found in the endometrium at all stages of the menstrual cycle, with higher levels seen during the proliferative phase than during the secretory phase (162).

1.3.5.6 Role of Dok proteins in neuromuscular disorders

Congenital myasthenic syndromes (CMS) arise as a result of genetic defects in the NMJ resulting in muscle weakness and other symptoms including fatigue (163). Mutations in the Dok-7 gene result in abnormal NMJ structure and give rise to a specific subtype of CMS characterised by "limb girdle" pattern fatiguable muscle weakness that accounts for 10-15% of CMS (89, 164-168).

Patients with Dok-7 CMS show great phenotypic variability, though most have small NMJs and end plate structural abnormalities (169, 170). Although Dok-7 plays a role in the organization of AChRs, the density and phosphorylation of AChR in Dok-7 CMS is normal (170). In the normal NMJ, each motor nerve impulse results in the release of neurotransmitter molecules from the presynaptic bouton, the effect of which is amplified by voltage-gated sodium channels in the highly folded postsynaptic membrane (171). Patients with Dok-7

CMS have abnormally small NMJs with reduced postsynaptic folding resulting in impaired neurotransmission (89, 171).

Most patients with Dok-7 CMS have at least one allele with a frameshift mutation in DOK7 exon 7 that causes truncation of the C-terminal of Dok-7 and impairs Dok-7 induced MuSK activation (89, 119, 167). Recently, however, mutations in the N-terminal PH or central PTB domains have also been identified (89, 119).

Unlike other forms of CMS, patients with Dok-7 CMS do not usually respond clinically to acetylcholine esterase (AChE) inhibitors but ephedrine is an effective treatment (165, 172). Interestingly, recent studies have shown that treatment with salbutamol, a selective B2-adrenergic agonist, is effective in patients with Dok-7 CMS (173, 174).

Furthermore, an exciting recent study by Arimura *et al* showed that in a mouse model of Dok-7 myasthenia, administration of DOK7 gene therapy resulted in enlargement of NMJs and an increase in muscle strength and survival (175).

Previous work by Jang *et al* has also found that the region of the motor neuron degeneration 2 (mnd2) mutation on mouse chromosome 6, and the corresponding region on human chromosome 2, encodes three genes, one of which is Dok-1 suggesting that this Dok family member may also play a potential role in neuromuscular disorders (176).

1.3.6 Tyrosine kinase signalling in cancer

Protein kinases, named from the Greek κινειν meaning "to move", are protein enzymes that catalyse the movement of phosphate molecules from ATP to a target protein. The first protein kinase was identified in 1959 and since then, protein phosphorylation has come to be

recognized as one of the most important mechanisms regulating protein activity and, by extension, a variety of cellular processes, including cell differentiation, migration, transformation, transduction of intracellular signals and the cell cycle (177). In fact, we now know that over 30% of mammalian cell proteins can be modified by phosphorylation (178). Protein kinases can be sub-divided into a number of groups including the protein tyrosine kinases (PTKs), which catalyse the transfer of phosphate molecules to tyrosine residues in target proteins.

Tyrosine phosphorylation of proteins by PTKs is a reversible process that plays an important role in the regulation of a variety of cellular functions, including cell proliferation, differentiation and cell motility. These effects are mediated by the binding of other proteins to the phosphorylated protein and the initiation of downstream signalling cascades. The signals downstream of PTKs can be upregulated or downregulated depending on the signalling proteins involved and this positive or negative regulation is crucial to normal cell physiology and the maintenance of homeostasis (179).

Protein tyrosine kinases can be further sub-divided into the receptor tyrosine kinases (RTKs), which are involved in trans-membrane signalling, and the cytoplasmic/non-receptor tyrosine kinases (CTKs), which participate in intracellular signal transduction. Following stimulation, PTKs become activated resulting in autophosphorylation and the phosphorylation of other molecules such as cytoplasmic adapter proteins. This leads to the recruitment or inhibition of other downstream signalling proteins (89).

Currently, 58 RTKs have been identified and these are grouped into 20 subfamilies, shown in Table 1.13. Each RTK contains an extracellular domain for ligand binding, a trans-membrane helix and a cytoplasmic portion containing the tyrosine kinase domain, a C-terminal and a juxtamembrane regulatory region (180). RTKs play an important regulatory role in numerous cellular processes including cell survival, cell proliferation, differentiation, cell migration and

cell cycle control (181, 182). Deregulation of RTKs occurs in a range of human diseases and aberrant RTK activation (due to autocrine activation, chromosomal translocations, overexpression of RTKs or gain-of-function mutations) is associated with cancer (180). The CTKs, shown in Table 1.14, contain SH2 and/or SH3 domains, which enable them to bind to phosphorylated tyrosines on other proteins, including the RTKs (183).

Table 1.13 Receptor tyrosine kinase subfamilies and their family members

Subfamily	**Family members**
ErbB	EGFR, ErbB2, ErbB3, ErbB4
Ins	InsR, IGF1R, InsRR
PDGF	PDGFRα, PDGFRβ, CSF1R/Fms, Kit/SCFR, Flt3/Flk2
VEGF	VEGFR1/Flt1, VEGFR2/KDR, VEGFR3/Flt4
FGF	FGFR1, FGFR2, FGFR3, FGFR4
PTK7	PTK7/CCK4
Trk	TrkA, TrkB, TrkC
Ror	Ror1, Ror2
MuSK	MuSK
Met	Met, Ron
Axl	Axl, Mer, Tyro3
Tie	Tie1, Tie2
Eph	EphA1-8, EphA10, EphB1-4, EphB6
Ret	Ret
Ryk	Ryk
DDR	DDR1, DDR2
Ros	Ros
LMR	LMR1, LMR2, LMR3
ALK	ALK, LTK
STYK1	SuRTK106/STYK1

Table 1.14 Cytoplasmic/non-receptor tyrosine kinase (CTK) subfamilies and their family members

Subfamily	Family members
Src	Src, Fyn, Yes, Blk, Yrk, Frk/Rak, Fgr, Hck, Lck, Srm, Lyn
Csk	Csk
Tec	Tec, Btk, Itk/Emt/Tsk, Bmx, Txk/Rlk
Abl	Abl, Abl2/Arg
Syk	Syk, Zap-70
Ack	Ack1/Tnk2, Ack2, DACK, Tnk1, ARK-1, DPR2, Kos1
JAK	JAK1, JAK2, JAK3, Tyk2
FAK	FAK, PYK2/CAK-β/RAFTK/CADTK
FER	Fer, Fes

So-called docking, or adaptor proteins, play a key role in the transduction of signals from activated tyrosine kinases (103). These docking proteins, including the Dok family, typically have an N-terminal PH domain, which mediates interaction with the cell membrane, and a PTB domain that binds an autophosphorylation site in the RTK. The docking protein is thus recruited to the RTK and becomes tyrosine phosphorylated by its kinase domain. As a consequence of this, binding sites become available to recruit additional SH2 containing signalling molecules and thus the adapter protein functions as a 'scaffold' for the formation of protein complexes (184, 185).

Aberrant tyrosine phosphorylation is associated with many types of cancer and other human diseases and provides a potential target for therapeutic intervention. The epidermal growth factor receptor (EGFR) is an RTK belonging to the ErbB family. Binding of a ligand, such as epidermal growth factor (EGF), results in dimerization of EGFR either with another EGFR monomer or with another ErbB family monomer and consequently autophosphorylation of its intracellular portion (186). This results in the activation of numerous downstream signalling pathways including PI3K and the MAPK pathway resulting in increased cell survival, invasion, proliferation, migration, adhesion and angiogenesis (186, 187).

The Ras proteins are involved cell signal transduction in the MAPK pathway downstream of EGFR and are known to play a role in cell growth, differentiation and survival (31-33). They were discovered as a result of observations made by Jennifer Harvey in 1964, that the injection of mice with Moloney's leukaemogenic virus resulted in the development of tumours (34). The three human Ras genes, HRAS, KRAS and NRAS, are all oncogenes commonly implicated in human cancer and previous studies have shown that they are important in the development of pancreatic, thyroid and lung cancer, amongst other human malignancies (32, 35, 36).

The first studies of the Ras oncogenes in colorectal cancer date back to the early 1980s when Feinberg and Vogelstein reported the hypomethylation of HRAS and KRAS in colonic adenocarcinomas (37). Later, in 1984, Spandidos and Kerr confirmed that KRAS and HRAS are overexpressed in pre-malignant adenomatous polyps and malignant colorectal tumours (38). We now know that RAS gene mutations are found in over a third of colorectal cancers, as well as in over 50% of adenomas over 1cm in size suggesting that they may play a role in tumourigenesis (33, 39, 40). However, RAS gene mutations are less common in small adenomas less than 1cm, where prevalence is less than 10% (40). KRAS, which activates MAPK via the oncogene BRAF to promote cell growth and survival, is mutated in 45% of colorectal cancers and, in metastatic colorectal cancer; KRAS status has been shown to predict treatment resistance to anti-EGFR monoclonal antibodies (31, 188, 189). The BRAF oncogene, which encodes the B-Raf protein that occurs downstream of Ras in the Ras/Raf/MAPK pathway, is itself mutated in around 10-15% of colorectal cancers (188).

Activation of the PI3K pathway plays a key role in the promotion of cancer cell proliferation and survival both via the activation of Akt and Akt-independent pathways such as Bruton tyrosine kinase (Btk), the PTK Tec, serum- and glucocorticoid-regulated kinases and small GTPase regulators (190). PI3K signalling may be aberrantly activated in cancer as a result of RTK activation or as a result of somatic mutations in genes coding for proteins involved in

the signalling pathway (190). For example, mutations in PI3K pathway genes occur in almost 40% of colorectal tumours (191). Previous analysis of human colorectal cancers has identified mutations in several genes encoding PI3K pathway proteins, including the serine/threonine kinases 3-phosphoinositide-dependent protein kinase 1 (PDK1), Akt2 and p21-activated kinase 4 (Pak 4), the non-serine/threonine kinases insulin-related receptor (INSRR), the RTK ErbB4, phosphatase and tensin homolog (PTEN), IRS2 and phosphatidylinositol-4,5-bisphosphate 3-kinase catalytic subunit alpha (PIK3CA), which encodes the p110α catalytic subunit (191). Mutations in PIK3CA are found in around 30% of colorectal cancers, but in few adenomas (and then generally in advanced tubulovillous adenomas measuring over 5cm diameter), suggesting that they arise late in the process of colorectal tumourigenesis (192). PTEN is a protein tyrosine phosphatase that functions as a tumour suppressor. Mutations of PTEN occur in approximately 20% of colorectal cancers, with a higher frequency (30%) found in tumours with microsatellite instability (MSI), compared to that found in tumours that are microsatellite stable (MSS) (9%) (193).

Monoclonal antibodies against RTKs approved by the FDA for colorectal cancer therapy include cetuximab (Erbitux) and panitumumab (Vectibix), which both target EGFR, and bevacizumab (Avastin®), which targets VEGF and inhibits angiogenesis (180). The clinical effectiveness of monoclonal anti-TKR antibodies is limited by the fact that patients may develop drug resistance (180). Therapeutic agents targeted at the PI3K-Akt signalling pathway present a potential solution to this problem and include the PI3K inhibitors, the Akt inhibitors, the mechanistic target of rapamycin (mTOR) inhibitors and drugs that work via a combination of these methods and may in the future include novel agents targeting other signalling molecules such as the adaptor proteins (180, 190).

1.3.7 Dok protein-coordinated signal transduction and cellular functions

The main interacting partners of the Dok proteins are shown in Table 1.15.

Table 1.15 Main interacting partners of the DOK proteins

	Interacting proteins
DOK1	RASA1, ABL1, NCK1, TEC, SRC, LCK, GRB10, KIT, FYN, SHC1
DOK2	TEK, RASA1, NCK1, CRK, LCK, ABL1, IL4R, SRC, LYN, IL2RA
DOK3	GRB2, CSK, LYN, INPP5D, SRC, ABL1, FYN, LCK, RET, DOK7
DOK4	RET, FYN, RAP1A, GDNF, TEK, GFRA1, CRK, NDUFA9, SRC, COX5A
DOK5	RET, GDNF, NTRK3, GFRA1, IGFBP5, INSR, FYN, IGF1R, NTRK2, COX5A
DOK6	SRC, RET, GDNF, GFRA1, NTRK3, COX5A, TMX3, CCDC102B, OSBPL1A, DOK7
DOK7	MUSK, RAPSN, AGRN, FLAD1, DRAGT1, FLVCR2, NTRK3, NTRK2, RRP7A, ACHE

Note: RASA1 (RAS p21 protein activator (GTPase activating protein) 1); ABL1, c-abl oncogene 1; NCK1, NCK adaptor protein 1; TEC, tec protein tyrosine kinase; SRC, v-src sarcoma (Schmidt-Ruppin A-2) viral oncogene homolog; LCK, lymphocyte-specific protein tyrosine kinase; GRB10, growth factor receptor-bound protein 10; KIT, v-kit Hardy-Zuckerman 4 feline sarcoma viral oncogene homolog; FYN, FYN oncogene related to SRC, FGR, YES; SHC1, SHC (Src homology 2 domain containing) transforming protein 1; TEK, TEK tyrosine kinase; CRK, v-crk sarcoma virus CT10 oncogene homolog; IL4R, interleukin 4 receptor; LYN, v-yes-1 Yamaguchi sarcoma viral related oncogene homolog; IL2RA, interleukin 2 receptor, alpha; GRB2, growth factor receptor-bound protein 2; CSK, c-src tyrosine kinase; INPP5D, inositol polyphosphate-5-phosphatase; RET, ret proto-oncogene; RAP1A, a member of RAS oncogene family ; GDNF, glial cell derived neurotrophic factor; TEK, TEK tyrosine kinase; GFRA1, GDNF family receptor alpha 1; NDUFA9, NADH dehydrogenase (ubiquinone) 1 alpha subcomplex, 9; COX5A, cytochrome c oxidase subunit Va; NTRK3, neurotrophic tyrosine kinase, receptor, type 3; IGFBP5, insulin-like growth factor binding protein 5; INSR, insulin receptor; IGF1R, insulin-like growth factor 1 receptor; NTRK2, neurotrophic tyrosine kinase, receptor, type 2; TMX3, thioredoxin-related transmembrane protein 3; CCDC102B, coiled-coil domain containing 102B; OSBPL1A, oxysterol binding protein-like 1A; MUSK, muscle, skeletal, receptor tyrosine kinase; RAPSN, receptor-associated protein of the synapse; AGRN, agrin; FLAD1, FAD1 flavin adenine dinucleotide synthetase homolog; DRAGT1, dolichyl-phosphate (UDP-N-acetylglucosamine) N-acetylglucosaminephosphotransferase 1; FLVCR2, feline leukaemia virus subgroup C cellular receptor family, member 2; RRP7A, ribosomal RNA processing 7 homolog A; ACHE, acetylcholinesterase.

Dok-1, Dok-2 and Dok-3 comprise a subfamily of Dok proteins with overlapping functions that are substrates for a wide variety of RTKs. They are tyrosine phosphorylated in response to a variety of growth factors and cytokines, such as EGF, allowing them to bind SH2 domain containing proteins such as Nck, Src homology region 2 domain containing phosphatase-1 (SHP-1), SHIP-1 and RasGAP phosphatases (93, 101, 134, 194, 195). RasGAP is a GTPase activating protein that exerts a negative regulatory role in the Ras/Raf/MEK/MAPK signalling pathway (94, 101, 124). Dok-1, Dok-2 and Dok-3 are therefore able to negatively regulate signalling pathways downstream of RTKs and CTKs and are consequently implicated in a range of physiological and pathological cellular processes.

Many studies have shown that Dok-1 is highly phosphorylated in many cells containing activated tyrosine kinases, suggesting that it is a substrate of several tyrosine kinases, including EGFR, c-Kit, EphB2 and v-Abl (91, 95, 196). Once phosphorylated, Dok-1 has been shown to interact with a number of downstream signalling proteins including RasGAP, Crk-L and Nck (94, 95, 196, 197). Tyrosine phosphorylation of Dok-1 is also induced by insulin (which also promotes the association of phosphorylated Dok-1 with RasGAP and Nck) and by cell adhesion to extracellular matrix proteins (198).

In terms of their impact on cell function, initial studies of the Dok proteins in found that they negatively regulated cell growth; either through inhibition of EGF induced ERK activation or via the inhibition of c-Src induced cell transformation (112, 124, 147). In addition, Dok-1 has also been shown to be a negative regulator of growth factor induced cell proliferation, differentiation and transformation (94, 95, 97, 112, 199-202). Despite these negative effects, however, overexpression of Dok-1 is actually associated with enhanced cell migration (198).

Since then, numerous studies have confirmed that Dok-1, Dok-2 and Dok-3 negatively regulate Ras/Raf/MEK/MAPK signalling downstream of protein tyrosine kinases (203). All three interact with SHIP1, an SH2 domain containing inositol-5-phosphatase that regulates

levels of lipid second messengers, and Csk, which negatively regulates c-Src family kinases (99, 103, 177, 204-206). SHIP1 negatively regulates haematopoiesis and associates with BCR/ABL, PI3K and Crk-L adaptor protein, all of which are involved in the regulation of cell migration (207). The expression of SHIP1 is reduced by BCR/ABL tyrosine kinase oncogene (207).

Phosphorylation of Dok-2 by EGFR occurs in response to EGF stimulation and results in the subsequent binding of SH2 domain containing molecules such as RasGAP and Nck (93). The recruitment of RasGAP and SHIP1 by Dok-2 leads to the subsequent inhibition of the Ras/Raf/MEK/MAPK and PI3K/Akt signalling pathways and consequently affects cytokine expression (93, 94, 142-144, 194, 208, 209).

In endothelial cell lines, Dok-2 is co-expressed with Tek, an endothelial cell-specific RTK that is crucial in murine embryonic vascular development and which plays a key role in angiogenesis and cell migration (124, 210, 211). Following the activation of Tek by Angiopoietin-1 (Ang-1), Dok-2 interacts with Tek via its PTB domain and is phosphorylated, resulting in the recruitment of RasGAP, Nck, Pak and Crk to the activated Tek receptor at the cell membrane (124, 210). Overexpression of Dok-2 has been shown to increase endothelial cell migration via this mechanism (210). The binding and phosphorylation of Dok-2 is mediated by an Ang1-dependent autophosphorylation site Tyr (1106) on Tek, as well as the PTB and PH domains of Dok-2 (211).

Dok-2 acts as a signalling molecule in activated platelets and has been found in platelet-derived microparticles (PMPs) obtained from thrombin activated platelets (212, 213). PMPs are microvesicles generated in response to platelet activation which are found in elevated levels in a range of diseases, including cancer, where they increase expression of adhesion molecules, stimulate cytokine release and induce angiogenesis and metastasis (214). Dok-2 is also involved in collagen receptor, glycoprotein VI (GPVI) signalling in human platelets

stimulated by thrombin receptor activating peptide (TRAP), suggesting a potential role in platelet aggregation and activation (212). Dok-2 also interacts with the RTK HER2, an EGFR, the overexpression of which is associated with poor prognosis in human breast cancer (123). In macrophages, Dok-2 has been shown to negatively regulate c-myc signal transduction and cytokine induced cell proliferation (195). C-Myc is a phosphoprotein involved in cell proliferation, cellular transformation and apoptosis and has been shown to be mutated in many cancers (215).

Previous studies have shown that attenuation of MAPK activation can occur independently of RasGAP (93, 201). Phosphorylation of Dok-2 in response to EGF stimulation attenuates MAPK and Akt activity via Dok-2's SH3-dependent interaction with (and inhibition of) c-Src and the recruitment of Csk, a negative regulatory kinase (99, 103). Dok-2, therefore, acts as a scaffold molecule for c-Src and Csk to negatively regulate EGFR signalling (103). Further evidence for a tumour suppressor role of the Dok proteins is offered in the finding that Dok-2 in association with c-Src and Csk can abolish the protective effect of c-Src in facilitating breast cancer cell evasion of anoikis (103). Moreover, Dok-1 inhibits PDGF-induced mitogenesis by tethering signalling molecules to the cell membrane, firstly by attenuating c-myc induction through the recruitment of Csk to active Src kinases and secondly, by inhibiting Ras/Raf/MEK/MAPK activation by interaction with RasGAP (216). Dok-1 also increases activin A-induced B-cell apoptosis via its association with Smads, inhibits activation of the c-fos proto-oncogene promoter, inhibits cellular transformation by Src tyrosine kinase and also binds to RET proto-oncogene negatively regulating downstream pathways including RasGAP/ERK and Nck/ Jun N-terminal protein kinase (JNK) pathways (112, 149, 217, 218). Overall, these studies suggest that Dok-1 and Dok-2 act as negative regulators of growth-factor induced cell proliferation and are likely tumour suppressors (216).

Consistent with this negative role in cell signalling pathways, previous studies in both haematopoietic and non-haematopoietic cells have shown that loss of Dok-1 is associated with increased cell proliferation in response to growth factor treatment, sustained Ras and Ras/Raf/MEK/MAPK activation after removal of growth factor treatment and the promotion of oncogenic cellular transformation (97, 202). However, on the contrary, Hosooka *et al* found that inhibition of endogenous Dok-1 tyrosine phosphorylation in metastatic mouse melanoma cells resulted in reduced cell spreading, migration, growth and Ras activation (77).

Unlike Dok-1 and Dok-2, Dok-3 does not bind RasGAP to negatively regulate Ras-Erk pathway (102, 203). Upon tyrosine phosphorylation, Dok-3 binds Grb2 via SH2 domains, inhibiting the ability of Grb2 to form complexes with Sos, a Ras activator (203). Therefore, by sequestering Grb2, Dok-3 inhibits the Ras-Erk pathway independently of RasGAP (203). Dok-3 also regulates JNK and calcium mobilization via its interaction with SHIP-1 and Grb2 (144). In CML, Grb2/Grb 2-associated-binding protein (Gab2)/Src homology domain-containing transforming protein 1 (Shc1) and Dok-1/Dok-2 complexes assemble on the BCR-ABL1 core in a phosphorylation-dependent fashion (219). These can then interact with SH2 domain containing molecules to influence downstream pathways including PI3K, ERK and Akt. Overexpression of Dok-3 is associated with reduced v-Abl induced MAPK activation and reduced v-Abl associated transforming activity but has no effect on constitutively activated Ras- or EGF-induced MAPK activation (102).

Dok-4 also inhibits tyrosine kinase signalling in epithelial cells (115). Phosphorylated Dok-4 associates with RasGAP, Crk, Src and Fyn but not PI3K p85, Grb2, Shp-2, Nck or phospholipase C gamma Src homology 2 domains (150). Dok-5 does not associate with RasGAP, Nck or Src homology 2 domains nor does it activate MAPK (104, 149, 150). Both Dok-4 and Dok-5 are substrates for the IGF-1 receptors and the RTK c-Ret, with which they are co-expressed in neuronal tissues, but are not phosphorylated by PDGFR beta or IGF-IR (104, 115). By comparison, although Dok-6 is phosphorylated in response to Ret activation,

the affinity of the Dok-6 PTB domain for c-Ret is much lower with correspondingly less impact on Ret signalling (105, 117). Activation of c-Ret is associated with neuronal differentiation, resulting in axonal outgrowth and activation of MAPK (104). Consequently, both Dok-4 and Dok-6 promote GDNF-dependent neurite outgrowth during neuronal development (220). Dok-4 is also a substrate for non-receptor tyrosine kinases Fyn, Src and Jak2 (115).

The Dok proteins act mainly to negatively regulate signalling downstream of kinases, but Dok-4 has both positive as well as negative regulatory functions and Baldwin *et al* hypothesised that the N-terminus and C-terminus of Dok-4 exerts opposing inhibitory and stimulatory properties respectively (221).

The expression of Dok-5 in cardiac muscle increases significantly during cardiomyocyte differentiation (222). In mice studies they identified that Dok-5 expression is associated with enhanced cardiomyocyte differentiation and that FOXO3a, a downstream substrate of PI3K/PKB, inhibits Dok-5 expression by transcriptional repression (222). In mouse spinal tissues, Dok-5 is involved in NT-3 signalling that blocks TrkC-induced apoptosis (223).

1.3.8 Dok proteins in immune function

Immunoreceptors mediate their effects by inducing tyrosine phosphorylation of target intracellular proteins either via intrinsic PTK activity or via recruitment and activation of CTKs, such as the Src family (130). Src family kinases phosphorylate tyrosine residues within the intracellular motif enabling spleen tyrosine kinase (Syk)/Zap-70-related PTKs to bind to the immunoreceptor, activating further downstream signalling molecules including phospholipase C (PLC)-γ, PI3K and Ras and ultimately activating immune functions (130). These functions are negatively regulated by protein tyrosine phosphatases (PTPs) such as

SHP-1, SHP-2, Csk and the Src homology 2 domain-containing inositol 5'-phosphatase (SHIP) (130).

Signals transduced by the B cell antigen receptor (BCR) control B cell development and function (224). Antigen binding to BCR results in BCR phosphorylation and the recruitment and activation of Syk via SH2 domains (224). This results in the subsequent phosphorylation of adapter protein SLP-65 and recruitment of Btk and PLC- γ2 (224). Another tyrosine kinase important to BCR signal transduction is the Ick/yes-related novel protein tyrosine kinase (Lyn), which has been shown to have both positive and negative effects on BCR signalling (225-227).

Several studies have shown that the Dok proteins play important roles in immune cell signalling (194). Dok-1 has been shown to play a role both in B cells and in T cells and consequently, is important in the regulation of both the humoral and cell-mediated adaptive immune response. In B-cells, Tec mediates signalling between BCR and Dok-1, which functions with SHIP to regulate BCR signal transduction (217, 228, 229). In T cells, Dok-1 is recruited to the plasma membrane by cluster of differentiation 45 (CD45) resulting in negative regulation of the Janus kinase (JAK)/STAT signalling pathway and has also been found to play an important role in stromal cell-derived factor-1 (SDF-1alpha/CXCL12) induced chemotaxis in T cells (230, 231). Both Dok-1 and SHIP are tyrosine phosphorylated in response to T cell stimulation and are required for the regulation of CD4+CD25+ T cell development (232).

Dok-3 is highly expressed in B cells where it is located at the inner aspect of the plasma membrane (233). Following BCR activation, Dok-3 is tyrosine phosphorylated, probably by the Src family kinase Lyn (130). This results in the recruitment of inhibitory molecules SHIP and Csk leading to the negative regulation of B cell activation and downstream signalling pathways such as the JNK signalling cascade (130, 234, 235). Dok-3 also plays a key role in

the negative feedback regulation of intracellular calcium signalling downstream of BCR (233). Upon phosphorylation, Dok-3 binds cytosolic Grb2 via SH2 domains (224, 235). This in turn phosphorylates Dok-3 and results in the formation of further Dok-3/Grb2 complexes, decreasing PLC- γ2 activation, inositol-1,4,5-triphosphate production and mobilization of calcium (224, 233). Dok-3 also promotes plasma cell differentiation by regulating the expression of programmed cell death 1 ligands (236). Via these effects, Dok-3 is thought to affect cell proliferation, differentiation and apoptosis (237, 238). Previous authors have shown that Dok-3/Grb2 attenuates BCR signal transduction by decreasing Lyn dependent phosphorylation of Syk and thus attenuating its tyrosine kinase activity (224). Moreover, they found that Dok-3/Grb2 complex formation is necessary for the organization of BCR microclusters into discrete microsignalosomes and for phosphorylation of SHIP1 which is required for signal transduction (224).

Along with Grb2 and Casitas B-lineage Lymphoma (Cbl) proto-oncogene, Dok-3 has been shown to play a key role firstly, in the recruitment of dynein to BCR microclusters following antigen recognition and secondly, in the subsequent movement of BCR microclusters on microtubules to gather antigen (130, 239). Dok-3, Grb2 and Cbl are recruited to antigen containing BCR microclusters in a Grb2 dependent fashion and localize dynein, allowing movement on microtubules and internalization of the microcluster (140, 239). It has been suggested by Schnyder *et al* that Lyn and Syk signalling is initiated by antigen recognition along with the formation of BCR microclusters and that this results in the recruitment of other mediators such as Vav and PLC-γ2, which are involved in the organisation of the actin cytoskeleton (239). Studies in mice have shown that mice lacking in Dok-3 displayed normal B-cell development but had a higher level of IgM antibodies in their sera, exhibited an enhanced humoral immune response to T cell-independent type I and II antigens, hyperproliferated, had an increased level of calcium signalling and enhanced activation of nuclear factor kappa-light-chain-enhancer of activated B cells (NF-κB), JNK and p38MAPK (240). Moreover, lack of Dok-3 was associated with reduced phosphorylation of SHIP-1

(240). Overall, these results suggest that Dok-3 is involved in the negative regulation of BCR signalling (240).

Dok-1 and Dok-2 (though not Dok-3) are expressed in T cells and are tyrosine phosphorylated following stimulation by CD2 or CD28, but not CD3, resulting in the negative regulation of downstream signalling (122, 130, 241, 242). CD2 induced phosphorylation of Dok-1 is dependent on Src family kinases, such as Lck and Fyn, and results in the association of Dok-1 with Crk-L (242). The latter association is dependent on the ZAP70/Syk family kinases (242). Overexpression of Dok-1 in immortalized T cells inhibits CD2 mediated signalling resulting in reduced calcium mobilisation, reduced phospholipase C gamma 1 phosphorylation and reduced activation of Erk1/2 (241).

Dok-1 and Dok-2 negatively regulate T cell receptor for antigen (TCR) signalling, which plays a crucial role in the immune response, via formation of signalling complexes involving SHIP-1 and Grb-2 (243). These interact with linker of activated T cells (LAT) to attenuate TCR signalling and negatively regulate Akt and ZAP-70 (122, 241, 243, 244). Like Dok-1, Dok-2 also negatively regulates T cell development via its interaction with RasGAP and Nck, and expression of Dok-2 in bone marrow cells is associated with reduced capacity for cytokine-induced colony formation (245). In irradiated mice, Dok-2 expression is associated with reduced repopulation of lymphoid and thymic tissue and a reduction in mature peripheral T cells (245).

Dok-1 and Dok-2 are associated with Tec, a protein tyrosine kinase expressed in T cells (246). They provide negative regulation of Tec via downregulation of its tyrosine phosphorylation and downstream signalling pathways, which include the Ras pathway (246). Previously, Yoshida *et al* found that Tec induces Dok-1 hyperphosphorylation, and that Tec associates with Dok-1 in a phosphorylation-dependent manner (217).

Stem cell factor (SCF) is a cytokine involved in cell survival, proliferation, differentiation and migration that binds to c-Kit, resulting in the activation of PI3-K (247). This phosphorylates and activates Tec and Dok-1 which form a complex with Lyn (247). Dok-1 is phosphorylated by both Tec and Lyn, enabling the binding of several downstream signalling molecules activated by SCF including Abl, Crk-L, SHIP and PLCγ-1 via SH2 binding domains (247). Thus, Dok-1 acts as a "scaffold molecule" in c-Kit signalling pathways (247). Previous studies have shown that stimulation of Mo7 cells with SCF induced PI3K dependent tyrosine phosphorylation of Dok-1 and the recruitment of Dok-1 to the membrane (an event that is essential for the ability of Dok-1 to function as a negative regulator of cell proliferation) (248). C-Kit associates with Dok-1 via its juxtamembrane region and C-terminal tail (248). Both tyrosine phosphorylation of c-Kit and the association of c-Kit with Dok-1 are promoted by Lyn (248).

Stimulation of the T cell receptor by an antigen results in the recruitment of ZAP-70, a protein tyrosine kinase recruited to the T cell receptor that plays a key role in T cell activation (244). Both Dok-1 and Dok-2 attenuate activation of the Akt pathway and ZAP-70 (243, 244). Lack of Dok-1 and Dok-2 is associated with elevated T cell response to TCR stimulation, with an increase in ZAP-70 activation and cytokine production (244). By contrast, forced expression of Dok-1 or Dok-2 is associated with suppression of TCR stimulated ZAP-70 activation (244). Murine studies have shown that mice lacking Dok-1 and Dok-2 have elevated antibody titres and develop lupus-like renal disease (244).

Interestingly, Guittard *et al* found that this negative regulatory role in T cell function and the tyrosine phosphorylation of Dok-1 and Dok-2 depends on the presence of their PH domain (249). These PH domains act as lipid/protein-interacting modules, binding to the phosphoinositide, phosphatidylinositol 5-phosphate (PtdIns5P) to regulate T cell response (249). Overexpression of Dok-1 or Dok-2 inhibits ZAP-70 activation whilst overexpression of both Dok-1 and Dok-2 reduces IL-2 production in activated T-cells (244, 246). Double

knockdown of Dok-1 and Dok-2 by siRNA increases TCR-induced Il-2 secretion and prolongs TCR-mediated Akt activation (243). In mouse models, lack of Dok-1 and Dok-2 is associated with an amplified response to thymus-dependent (but not thymus-independent) antigens, increased T cell response to TCR stimulation and consequently, increased ZAP-70 activation, cell proliferation and cytokine production (244). Inhibition of T cell receptor signal transduction by zanolimumab, an anti-CD4 monoclonal antibody, is partly due to activation of p56Ick, a CD4-associated tyrosine kinase which relays inhibitory signals downstream via Dok-1 and SHIP-1 (250).

Dok-1 and Dok-2 (though not other Dok family members) are both expressed in Natural killer (NK) cells and act as negative regulators of NK-cell function (194). Activation of the NK cell results in tyrosine phosphorylation of Dok-1 and Dok-2 (194). Celis-Guitirrez *et al* found that Dok-1/Dok-2 double knockout mice had reduced peripheral NK cells and exhibited impaired NK-cell development compared to wild-type mice, possibly due to impaired apoptosis during NK cell maturation (194). They suggest that Dok-1 and Dok-2 downregulate NK cell activation induced by NK cell surface activating receptors but that they upregulate NK cell activation and interferon gamma (IFN-γ) production induced by the cytokines interleukin (IL)-12 and IL-18 (194). *In vivo* studies show that Dok-1/Dok-2 double knockout mice had delayed control of murine cytomegalovirus (MCMV) replication (194). Despite these negative regulatory roles in immune signalling events, Dok-1 has also been shown to play a positive regulatory role both in IL-4 signalling, increasing IL-4-induced CD4+ T cell and B cell proliferation and also the IgE response to T cell-dependent antigen (251).

In astrocytes and microglia, toll like receptor (TLR) 2 increased Dok-1 and Dok-2 tyrosine phosphorylation whilst knockdown of Dok-1 and Dok-2 increased TLR2-induced ERK activation (208). In astrocytes, silencing of Dok-1 and Dok-2 resulted in increased NF-κB activation and IL-6 production suggesting that Dok-1 and Dok-2 both negatively regulate TLR2-induced inflammatory signalling cascades in astrocytes (208). By comparison, in

microglia, knockdown of Dok-1 (but not Dok-2) reduced TLR2-induced NF-κB activation and Il-6 production suggesting that TLR2-induced pro-inflammatory signalling is differentially regulated by Dok-1 and Dok-2 in different types of glial cells (208).

Evidence on the role of the Dok proteins in the macrophage response to infection is somewhat conflicting. Mashima *et al* found that Dok-1 and Dok-2 play a negative regulatory role in macrophage responses, but work by Alvarez de Celis *et al* suggests that Dok-1 and Dok-2 positively regulate the response of bone marrow derived macrophages to infection with *Leishmania* (252).

In mouse macrophages stimulated with bacterial lipopolysaccharide (LPS), lack of Dok-1 or Dok-2 was associated with increased sensitivity to LPS, increased activation of Erk (though not other MAP kinases or NF-κB), with consequent increase in the production of the proinflammatory cytokine TNF-α and nitric oxide production (253). Overexpression of Dok-1 or Dok-2 by contrast inhibited LPS-induced Erk activation and reduced TNF-α production (253). Therefore, it seems Dok-1 and Dok-2 also negatively regulate innate immunity cell signalling downstream of TLR4 (253). However, Dok-3 has been shown to play a positive role in the TLR3 signalling cascade which is also part of the innate immune system (254).

1.3.9 Aberrant expression and function of Dok proteins in cancer

Many of the early studies investigating the Dok proteins in relation to malignant disease focused on their role in leukaemia but they have subsequently been found to play a role in several other human cancers. The expression profile of in different tumours is shown in Table 1.16.

Table 1.16 Expression profile of *DOK*s in different tumours (TPM, transcripts per million)

	DOK1	***DOK2***	***DOK3***	***DOK4***	***DOK5***	***DOK6***	***DOK7***
Adrenal tumour	**79**	0	0	79	0	0	0
Bladder carcinoma	0	0	0	0	0	0	0
Breast (mammary gland) tumour	42	0	10	10	0	0	**32**
Cervical tumour	57	0	0	0	0	0	0
Chondrosarcoma	**60**	24	12	**132**	36	12	0
Colorectal tumour	17	0	8	97	0	0	0
Gastrointestinal tumour	0	0	8	33	0	0	0
Germ cell tumour	22	15	53	60	15	15	0
Glioma	0	0	27	74	93	18	0
Head and neck tumour	7	22	7	22	0	0	0
Kidney tumour	14	0	14	43	14	14	14
Leukaemia	**84**	**63**	**243**	21	0	0	0
Liver tumour	10	0	0	10	0	0	0
Lung tumour	19	9	19	38	0	0	0
Lymphoma	0	0	**263**	0	0	0	0
Oesophageal tumour	0	0	0	0	0	0	0
Ovarian tumour	0	0	0	39	288	13	**39**
Pancreatic tumour	9	0	0	57	0	0	0
Primitive neuroendocrine tumour	31	0	0	559	7	0	0
Prostate cancer	0	0	0	9	0	0	0
Retinoblastoma	21	0	0	0	0	43	0
Skin tumour	31	0	0	55	0	0	7
Soft tissue/muscle tumour	0	0	0	63	39	15	7
Uterine tumour	33	11	44	44	11	0	**44**

Note: TPMs in bold are top three tumours which express higher levels of *DOKs*. This is a summative table adapted from approximate expression pattern from the EST profile at http://www.ncbi.nlm.nih.gov/UniGene.

1.3.9.1 Role of the Dok proteins in leukaemia

Several studies have shown that the Dok proteins act as leukaemia suppressors in mice, and both Dok-1 and Dok-2 are downregulated in CML (142, 143, 255). In experimental studies, Dok-1/Dok-2 double deficient mice display an increase in myeloid progenitor cells, the development of CML-like myeloproliferative disease, splenomegaly and hypercellularity of the peripheral blood and bone marrow (142, 143). At a cellular level, Dok-1 and/or Dok-2 knockout mice exhibit increased activation of both MAPK/Erk and Akt pathways, greater proliferative response to cytokines and reduced apoptosis, with these effects being more pronounced in the double deficient, as compared with single knockout, mice (97, 143).

Further murine studies performed by Niki *et al* have confirmed that double Dok-1/Dok-2 knockout results in aberrant haematopoiesis, Ras/MAPK activation and the development of CML-like myeloproliferative disease with increased proliferation, reduced apoptosis and accelerated leukaemia and blast crisis onset (142). They did not however demonstrate any effect on haematopoiesis with single Dok-1 or Dok-2 knockout (142).

In CML, the C-terminal portion of Dok-1 is constitutively phosphorylated by elevated kinase activity from p210 (bcr-abl) expression. This results in the inhibition of RasGAP activity, activation of the Ras signalling pathway and, in mouse models infected with a p210bcr-abl retrovirus, loss of Dok-1 was associated with a shorter latent period before the onset of fatal myeloproliferative disease (97, 131). Interestingly, work by Janas and Van Aelst has demonstrated that oncogenic tyrosine kinases including p210 (bcr-abl) and Src target Dok-1 for degradation by the ubiquitin-proteasome pathway, thereby overcoming the Dok-1's inhibitory effects to promote cell transformation (202). Treatment of CML cells with Imatinib, a specific BCR-ABL kinase inhibitor, results in a 90% reduction in the phosphorylation of BCR-ABL, SHIP-2 and Dok-2 as well as the regulation of other proteins

such as SHIP-1, SH2 containing protein (SHC) and Casitas B-lineage lymphoma proto-oncogene (BBL) (177).

Previous studies have shown that Dok-1 and Dok-2 are recruited by CD200R, an inhibitory receptor expressed on haematopoietic progenitor cells and involved in myeloid cell regulation (209). Knockout of CD200R does not affect myeloid progenitor number or their proliferative capacity suggesting that the development of leukaemia seen in Dok-1/Dok-2 double knockout mice is not due to absence of CD200 mediated CD200R signalling alone (209).

1.3.9.2 Role of the Dok proteins in lung cancer

Research published in 2010 identified Dok-1, Dok-2 and Dok-3 as lung tumour suppressors (90). In mouse models, loss of Dok-1, Dok-2 and Dok-3 results in aberrant proliferation of alveolar type II cells and bronchoalveolar stem cells with subsequent development of lung cancer (90). The penetrance and latency of these effects are dependent on the number of lost Dok alleles, with the highest penetrance, shortest latent period and poorest survival times witnessed in triple knockout mice (90). In humans, lung adenocarcinoma is associated with loss or downregulation of Dok-2 whilst *in vivo* and *in vitro* studies have shown that Dok-2 suppresses lung cancer cell proliferation and reduced Akt and Erk phosphorylation (90). Moreover, Dok-2 is haploinsufficient in its tumour suppressor function so heterozygosity alone may promote lung cancer (90).

Knockout of Dok1/Dok-2/Dok-3 in mice is associated with the development of lung adenocarcinomas with histological features including nuclear polymorphism, vascular invasion, multiple tumour nodules and inflammatory infiltrates (90). In the majority of cases, tumours were well differentiated and although lymph nodes were not sampled routinely,

incidental lymph node metastases were not found (90). In terms of intracellular signalling, the mutant mice also exhibited abnormal Akt and Erk phosphorylation and activation (90). Chromosome 8p21.3, the location of the DOK2 gene, is one of the commonest regions deleted in human lung cancer (256). Berger *et al* found that 37% of human lung adenocarcinoma and 33% of human non-small cell lung cancers are associated with loss of one copy of the DOK2 gene (90). DOK2 mRNA is significantly downregulated in primary lung adenocarcinoma, lymph node metastases and lung cancer cell lines compared with normal lung tissue whilst forced Dok-2 expression in a lung cancer cells results in reduced growth rate and reduced Akt and Erk phosphorylation (90). Although Dok-3 expression was reduced in lung cancer lymph node metastases compared with normal lung, no difference was observed in the level of DOK1 or DOK3 mRNA in primary lung cancer tissue (90).

1.3.9.3 Role of the Dok proteins in breast cancer

In breast cancer, Dok-2 and Dok-6 expression are both inversely associated with TNM stage and Nottingham Prognostic Index score suggesting a potential tumour suppressor role (257). In keeping with this, a recent study has shown that disease-free survival in breast cancer patients is associated with higher levels of Dok-2 and Dok-6 expression (257). In 2013, Heyn *et al* published their study which examined DNA extracted from the whole blood of monozygotic twin pairs who were discordant for breast cancer using high-resolution DNA methylation analysis (258). They found that the Dok-7 promoter region in the blood of the twin with breast cancer was consistently hypermethylated compared to the blood of the paired healthy twin and this finding was also observed in primary breast cancer tissue and breast cancer cell lines (258). Interestingly, they also found that hypermethylation of the Dok-7 promoter occurs years before tumour diagnosis, suggesting that Dok-7 may have a potential role as a blood based biomarker of early disease or disease predisposition (258).

1.3.9.4 Role of the Dok proteins in colorectal cancer

To date, there have been very few studies investigating the role of the Dok proteins in colorectal cancer. A recently published paper found that loss of Dok-2 expression was more common in colorectal cancer tissues than in normal colorectal tissue (259). Furthermore, the absence of Dok-2 expression was associated with poorer five-year overall survival rate and disease recurrence in patients with colorectal cancer (259). Other authors have identified Dok3 as a potential therapeutic target in colorectal cancer cells (94).

1.3.9.5 Role of the Dok proteins in skin cancer

A recent study by Huang *et al* identified Dok-1 among several differentially expressed molecular markers in melanoma compared to normal skin tissue, suggesting its potential use as a diagnostic or prognostic marker in skin cancer (260).

1.3.9.6 Role of the Dok proteins in reticuloendothelial system cancer

Histiocytic sarcoma is a rare, aggressive malignant proliferation of histiocytic cells, which is associated with a poor prognosis (261). In a murine model, knockout of Dok-1 and/or Dok2 results in half of the mice developing a histiocytic sarcoma of macrophage origin (143). In mice experiments conducted by Mashima *et al,* triple knockout of Dok-1/Dok-2/Dok-3 was associated with the development of aggressive histiocytic sarcoma with multiple organ invasion and metastases, earlier mortality secondary to sarcoma as well as aberrant accumulation and proliferation of macrophage tumour precursor cells in the lung (261).

1.3.9.7 Role of the Dok proteins in ovarian cancer

Mercier *et al* found that a 5'-non-coding DNA region upstream of the DOK1 translation start codon was hypermethylated in primary serous epithelial ovarian cancer compared to normal ovarian tissue (262). Despite this, Dok-1 expression was not reduced and was in fact overexpressed in these tumours with the level of expression significantly correlated with improved progression-free survival and response to a cisplatin (262). Functional studies performed by the same group found that Dok-1 expression was associated with increased proliferation and migration of epithelial ovarian cancer cells (262).

1.3.10 Novel potential application of Dok proteins

The Dok family proteins are a group of structurally related adapter proteins that play a key role in cell signalling pathways downstream of PTKs. Consequently, they have been shown to play diverse roles in the control of cell functions including cell growth, differentiation and cell motility, and aberrations in Dok-protein co-ordinated cell signalling have been implicated in a range of both benign and malignant human diseases. A recent study by Heyn *et al* has suggested that the Dok proteins may have a potential role as blood based biomarkers in human cancer providing a compelling reason to investigate the role of these proteins and their potential use as diagnostic and therapeutic targets further. This thesis is concerned with the expression and role of Dok-7 in colorectal cancer.

Table 1.12 and Table 1.16 provide an overview of DOK7 expression and distribution in different tissues/organs and tumours but there are limitations of using this information due to technical bias and the limited number of samples being tested and included in the database. The work in this thesis is based on the initial determination of DOK7 expression in our laboratories, which suggested aberrant DOK7 expression in human colorectal cancer. This

initial work was provoked by the important role of receptor tyrosine kinases in cancer and DOK7 protein's regulatory role in RTK signalling pathways. It is hoped that by determining the expression of DOK7 in colorectal cancer we might determine its potential use as a diagnostic or prognostic marker and through developing a greater understanding of its links with candidate RTKs and signalling pathways, we may determine whether it has any further value as a therapeutic target, for example through gene therapy or antibody therapy.

Aims and objectives

The aim of this clinically oriented PhD is to determine the expression profile and role of DOK7 in human colorectal cancer. The central hypothesis of the study is that DOK7 has an important role in colorectal cancer and that it is likely to play a tumour suppressive role.

The objectives of the PhD are as follows:

- To evaluate the existing literature relating to the DOK family proteins, particularly in relation to human cancers
- To determine the expression profile of DOK7 in human colorectal cancer cell lines
- To determine whether DOK7 expression is associated with tumour pathology and clinical outcome data obtained from a clinical cohort
- To determine the functional role of DOK7 in colorectal cancer cells through functional assay analysis of transgenic cells.
- To evaluate DOK7 coordinated cell signalling in colorectal cancer focusing on altered signalling events in colorectal cancer cells with altered DOK7 expression and to determine relevant signalling pathways and responsive genes. Therefore, we aim to propose an action model of DOK7 in colorectal cancer highlighting its diagnostic and therapeutic value.

Chapter 2: Materials and Methods

2.1 Materials

2.1.1 Cell lines

Human cancer cell lines were freshly acquired from the European Collection of Authenticated Cell Cultures (ECACC, Salisbury, UK) or the American Type Culture Collection (ATCC, Middlesex, UK). All cell lines were verified at source for identity and were low passage on acquisition. This study used four colorectal cancer cell lines: RKO, HT-115, HRT-18 and Caco-2. These cell lines were chosen because they are commonly used in studies of human colorectal cancer, there is considerable experience in their use within the host laboratories, and because this panel of cell lines includes both colonic and rectal cancer cells and well and poorly differentiated cell types.

Full details of the cells used in the study are shown in Table 2.1. Human endothelial cell line (HECV) was purchased from Interlab (Milan, Italy).

Table 2.1. Details of colorectal cancer cell lines used in this study

	RKO	HT-115	HRT-18	Caco-2
Species	Human	Human	Human	Human
Tissue	Colon	Colon	Rectum	Colon
Gender	-	-	Male	Male
Age	-	-	67	72
Morphology	Epithelial	Epithelial	Epithelial like	Epithelial
Growth mode	Adherent	Adherent	Adherent	Adherent
Characteristics	Poorly differentiated	Highly invasive	-	Moderately well differentiated adenocarcinomas consistent with colonic primary grade II
Country	UK	UK	UK	UK

2.1.2 General compounds

The general compounds used in this study and their sources are listed in Table 2.2 (See Appendix 1).

2.1.3 General plastic consumables, hardware and software

The general plastic consumables, hardware and software used in this study and their sources are listed in Table 2.3 (See Appendix 2).

2.1.4 Antibodies

The primary and secondary antibodies used in this study are shown in Table 2.4 and Table 2.5 respectively (See Appendix 3).

2.1.5 Primers

The primers used in this study were designed using the Beacon Design software programme (Biosoft International, Palo Alto, CA, USA) and synthesised by either Invitrogen (Paisley, UK) or Sigma (Poole, UK). The sequences of the primers used for conventional RT-PCR and qPCR are shown in Table 2.6 (See Appendix 4).

2.1.6 Preparation of reagents, buffers and standard solutions

2.1.6.1 Solutions used in cell culture

2.1.6.1.1 Preparation of complete cell culture medium

Cell lines were cultured and maintained in the specific cell culture media recommended by the ECACC/ATCC.

For RKO and HECV cells, 50ml of heat inactivated foetal calf serum (FCS) and 5ml antibiotics were added to 500ml DMEM/F12 with 2mM L-glutamine. For HT115 cells, 75ml of heat inactivated FCS and 5ml antibiotics were added to 500ml DMEM/F12 with 2mM L-glutamine. HRT-18 cells were maintained in RPMI media supplemented with 50ml of heat inactivated FCS and 5ml antibiotics. All media were stored at 4°C and used within one month of preparation.

2.1.6.1.2 Antibiotics

An antibiotic solution for use in cell culture was prepared by dissolving 3.3g penicillin, 5g streptomycin and 12.5mg Amphotericin B in dimethyl sulfoxide (DMSO) in 500ml Balanced Salt Solution (BSS). The solution was filtered prior to use and stored at -20°C. Five millilitres of this antibiotic solution were added to each 500ml of culture media as described above.

2.1.6.1.3 Balanced Salt Solution (BSS)

A stock solution of BSS (137mM NaCl, 2.6mM KCl, 1.7mM Na_2HPO_4 and 8mM KH_2PO_4) was prepared by dissolving 79.5g NaCl, 2.2gKCl, 1.1g Na_2HPO_4 and 2.1g KH_2PO_4 in 10 litres of distilled water (dH_2O). The pH was adjusted to 7.2 with 1M NaOH and the solution was stored at room temperature until use.

2.1.6.1.4 Ethylenediaminetetraacetic acid (EDTA)

A 0.05M stock solution was prepared by dissolving 40g NaCl, 1g KCl, 5.72g Na_2HPO_4, 1g KH_2PO_4 and 1.4g EDTA in 5 litres of dH_2O. The pH was adjusted to 7.4 using 1M NaOH and the solution was autoclaved before use.

2.1.6.1.5 Trypsin/EDTA solution

A 25mg/ml stock solution of trypsin/EDTA solution was prepared by dissolving 500mg trypsin in 20ml 0.05M EDTA. The solution was filtered through a 0.2µm mini-start filter and stored at -20°C. A working solution was prepared by further dissolving 250µl of the stock trypsin/EDTA solution in 10ml of 0.05M EDTA. The working solution was stored at 4°C until use.

2.1.6.1.6 Phosphate-buffered saline (PBS)

To prepare 1L of 1 x PBS, (137mM NaCl, 2.7mM KCl, 10mM Na_2HPO_4, 1.8mM KH_2PO_4) was prepared by dissolving 8g NaCl, 0.2g KCl, 1.44g Na_2HPO_4 and 0.24g KH_2PO_4 in 800ml of H_2O. The pH was adjusted to 7.4 with HCl and H_2O added to make up the volume to 1L.

The solution was then alliquoted and sterilized by autoclaving for 20 minutes at 15psi ($1.05kg/cm^2$) on a liquid cycle before being stored at room temperature.

2.1.6.2 Solutions used in molecular biology

2.1.6.2.1 Tris-Boric acid-EDTA (TBE) electrophoresis buffer

A five-times concentration stock solution of TBE (1.1M Tris; 900mM Borate; 25mM EDTA) was prepared by dissolving 540g Tris-Cl, 275g boric acid and 46.5g EDTA in 10 litres of dH_2O. The pH was adjusted to 8.3 using 1M NaOH and the solution was stored at room temperature until use. A working solution was prepared by diluting 200ml of the stock solution in 800ml of dH_2O.

2.1.6.2.2 Diethylpyrocarbonate (DEPC) water

Diethylpyrocarbonate (DEPC) is used to inactivate RNase enzymes that may contaminate water or laboratory equipment, thereby reducing the risk of RNA degradation. A stock solution of DEPC water was prepared by dissolving 500µl of DEPC in 9500µl dH_2O. The solution was autoclaved prior to use.

2.1.6.2.3 Loading buffer

Loading buffer was prepared by dissolving 25mg bromophenol blue and 4g sucrose in 10ml of dH_2O. The buffer was stored at 4°C until use.

2.1.6.3 Solutions used for gene transfer techniques

2.1.6.3.1 LB agar

LB agar was prepared by dissolving 10g tryptone, 5g yeast extract, 15g agar and 10g NaCl in 1 litre of dH_2O. The pH was adjusted to 7.0 and the media was autoclaved and stored at 4°C until use.

2.1.6.3.2 Preparation of LB agar dishes

In order to prepare LB agar dishes the LB agar was first melted in a microwave. Upon reaching a liquid state, the agar was allowed to cool to approximately 65°C and the appropriate antibiotic for colony selection was added. The agar solution was then poured into $10cm^2$ Petri dishes, which were left to cool. Once the agar had solidified, the plates were stored at 4°C until required.

2.1.6.3.3 LB broth

LB broth was prepared by dissolving 10g tryptone, 10g NaCl and 5g yeast extract in 1 litre of dH_2O. The pH was adjusted to 7.0 and then the media was autoclaved prior to storage at 4°C until use. Appropriate antibiotics for colony selection were added prior to use.

2.1.6.4 Solutions used for protein extraction and Western blotting

2.1.6.4.1 Protease and phosphatase inhibitors

The protease and phosphatase inhibitors used in this study are shown in Table 2.7.

Table 2.7. Protease and phosphatase inhibitors and their stock concentrations

Name	Protease/phosphatase inhibited	Stock concentration
Phenylmethylsulfonyl fluoride (PMSF) 100mM in isopropanol, stored at -20°C	Serine, cysteine proteases	100mM
Leupeptin 1mg/ml in H2O, stored at -20°C	Lysosomal	1mg/ml
EDTA	Metalloproteases requiring Mg2+ and Mn2+	
Sodium fluoride	Serine/threonine phosphatases	
Aprotinin 1mg/ml in H_2O, stored at -20°C	Trypsin, chymotrypsin, plasmin	1mg/ml
Sodium orthovanadate (Na_3VO_4)	Tyrosine phosphatases	200mM

2.1.6.4.2 Inhibitor buffer

A (x3) solution of inhibitor buffer was prepared by mixing 2.76g sodium nitrate, 630g sodium fluoride, 5.58g EDTA, 10g $Na_2H_2PO_4$ and $3x10^5$ units aprotinin made up to 1L with dH_2O. The solution was stored at 4°C until use.

2.1.6.4.3 Cell lysis buffer

A stock solution of cell lysis buffer was prepared by dissolving 2mM $CaCl_2$, 0.5% Triton X-100, 1mg/ml aprotinin, 1mg/ml leupeptin and 10mM sodium orthovanadate in 50ml dH_2O . The solution was stored at 4°C until use. A working solution was prepared by diluting 10ml stock solution in 6.6ml inhibitor buffer, 200µl PMSF, 80µl 10mM $CaCl_2$, 3ml of 10% Triton X-100 made up to 20ml with dH_2O.

2.1.6.4.4 Tris Buffered Saline (TBS)

A (x10) stock solution (200mM Tris; 1.37M NaCl) was prepared by dissolving 24.228g Tris-Cl and 80.06g NaCl in 1 litre dH_2O. The pH was adjusted to 7.4 using hydrochloric acid (HCl) and the solution was stored at room temperature until use.

2.1.6.4.5 Ammonium Persulphate (APS)

A 10% APS solution was prepared by dissolving 1g APS in 10ml dH_2O. The solution was stored at 4°C until use.

2.1.6.4.6 Running buffer

A (x10) stock solution was prepared by dissolving 303g Tris, 100g SDS and 1.44kg glycine in 10 litres dH_2O. The pH was adjusted to 8.3 using NaOH and the solution was stored at room temperature. A working solution was prepared by diluting 100ml of the stock solution with 900ml dH_2O prior to use.

2.1.6.4.7 Transfer buffer

Transfer buffer was prepared by dissolving 15.15g Tris, 72g glycine and 1L methanol in 4 litres dH_2O.

2.1.6.4.8 Preparation of 0.1% Coomassie blue

This was prepared by dissolving 1g coomassie blue, 400ml methanol and 100ml acetic acid and making the volume up to 1 litre with dH_2O. The solution was filtered and stored at room temperature until use.

2.1.6.5 Preparation of SDS-PAGE gels

2.1.6.5.1 Resolving gel

A 10% resolving gel for SDS-polyacrylamide gel electrophoresis (SDS-PAGE) was prepared using 7.9ml dH_2O, 6.7ml 30% acrylamide mix, 5ml 1.5M Tris (pH 8.8), 200µl 10% SDS, 200µl APS and 8µl Tetramethylethylenediamine (TEMED) per gel.

2.1.6.5.2 Stacking gel

A 5% stacking gel for SDS-PAGE was prepared using 6.8ml dH_2O, 1.7ml 30% acrylamide mix, 1.25ml 1.5M Tris (pH 6.8), 100µL 10% SDS, 100µL APS and 10µL TEMED per gel.

2.2 Methods

2.2.1 Cell culture

2.2.1.1 Preparation of cell media

Cell lines were cultured and maintained according to ECACC/ATCC recommendations. RKO cells were maintained in Dulbecco's Modified Eagle's Medium/Nutrient F-12 Ham (DMEM-F12, Sigma-Aldrich, Dorset, UK) media supplemented with 10% heat-inactivated foetal calf serum (FCS, PAA Laboratories, Coelbe, Germany) and antibiotics. HT-115 cells were maintained in DMEM-F12 media supplemented with 15% FCS and antibiotics. HRT-18 cells were maintained in Roswell Park Memorial Institute (RPMI, Sigma-Aldrich, Dorset, UK) media supplemented with 10% FCS and antibiotics. HECV cells were maintained in DMEM-F12 media supplemented with 10% FCS and antibiotics. For the purposes of this thesis, these media will be referred to as 'normal media' throughout.

2.2.1.2 Cell maintenance and storage

Cells were cultured in $25cm^2$ or $75cm^2$ tissue culture flasks depending on the required application. The flasks were placed horizontally in an incubator humidified to 98% with a water tray at a temperature of 37°C with 5% CO_2 in air. The flask caps were loosened to facilitate gaseous exchange.

Transfected cell lines were cultured in normal media for 24 hours following transfection and then transferred into blasticidin selection media (normal media supplemented with 5µg/ml

blasticidin S). Following selection of transfected cells, cells were maintained in blasticidin maintenance media (normal media supplemented with 0.5µg/ml blasticidin S).
Cells were inspected regularly using the light microscope to assess viability, confluence and to monitor for infection. Cells were routinely passaged once confluence exceeded 80%. All experimental work in this study was carried out using cells with a total passage number of 20 or less.

All cell work was carried out in a Class II Laminar Flow Cabinet with disposable sterile and/or autoclaved equipment.

2.2.1.3 Cell detachment and cell counting

The tissue culture flask was removed from the incubator and the waste medium was removed using a glass pipette and vacuum aspirator. The flask was washed briefly with 2ml of PBS buffer to remove any remaining FCS as this may inhibit the action of trypsin.

Approximately 500µl trypsin/EDTA solution (Trypsin 0.01% (w/v) and EDTA 0.05% (w/v) in HBSS buffer) per 25cm^2 of tissue culture flask surface area was added to the flask and the flasks were capped and returned to the incubator for 5-10 minutes at 37°C to facilitate cell detachment. Flasks were visually inspected under the light microscope to ensure complete cell detachment.

Following cell detachment, 5ml of the appropriate media was added to each flask to neutralise the trypsin and wash the detached cells from the flask surface. This cell/medium mixture was transferred to a sterile 30ml universal container and centrifuged at 1,800rpm for 10 minutes. The media was then aspirated and discarded and the cell pellet re-suspended in media for re-culturing or immediate use in experimental work.

Cell counts were performed using the Tali™ Image-based cytometer. The Tali™ Image-based cytometer is a benchtop assay platform that uses optics and image analysis to perform cell counting assays as well as apoptosis and cell viability assays. In order to perform a cell count, 25µl sample was pipetted into the sample loading area of a disposable Tali™ cellular analysis slide and the slide was inserted into the slide port of the Tali™ cytometer. The image adjustment knob was used to focus the cells prior to image capture. Multiple repeat cell counts were taken from each sample to reduce error.

2.2.1.4 Storage of cell lines in liquid nitrogen and cell resuscitation

In order to prepare cells for storage, they were detached from the flask as described above, centrifuged and the cell pellet was re-suspended in the appropriate medium with 10% dimethylsulphoxide (DMSO) at a density of $1x10^6$ cells/ml. This cell suspension was rapidly transferred into 1ml labelled cryotubes and frozen down to -80°C using a Mr. Frosty™ Freezing container which uses 100% isopropyl alcohol to cool cells at a rate of approximately -1°C per minute. For longer-term storage, cells were transferred to dewars containing liquid nitrogen maintained at -196°C.

To resuscitate frozen cells, a cryotube was removed from liquid nitrogen and thawed rapidly in a 37°C water bath. The cell suspension was then transferred into a 30ml universal container containing 5ml of pre-warmed medium and then centrifuged at 1800rpm for 8 minutes. The medium was removed by vacuum aspiration to remove any DMSO and the cell pellet resuspended in 5ml normal media. Centrifugation and resuspension in fresh media was repeated once more prior to seeding in a $25cm^2$ tissue culture flask. The flask cap was loosened to facilitate gaseous exchange and the flask was placed horizontally in an incubator at 37°C, 98% humidification and 5% CO_2.

2.2.2 Methods for RNA isolation and quantification

2.2.2.1 Total RNA isolation

Isolation of total RNA was performed according to the manufacturer's instructions provided with TRI Reagent® as described below.

2.2.2.1.1 Preparation of tissue samples

Tissue samples were homogenized in TRI Reagent® (1ml per 50-100mg of tissue) in a homogeniser.

2.2.2.1.2 Preparation of monolayer cells

Cells were cultured in a monolayer to a confluence of approximately 80% (5-10x10^5 cells). The medium was removed with a vacuum aspirator and the cells washed gently with BSS solution, which was aspirated before 1ml TRI Reagent® per 10cm2 culture flask surface area was added to lyse the cells. The cell lysate was passed through a pipette several times to form a homogenous lysate and then transferred to a 1.8ml eppendorf tube.

2.2.2.1.3 Phase separation

The sample was then left to stand for 5 minutes at room temperature to ensure dissociation of nucleoprotein complexes.

Two hundred microliters of chloroform (per 1ml TRI Reagent®) was then added to each tube. The tube was closed tightly and shaken vigorously for 15 seconds before being allowed to stand for 2-15 minutes at room temperature. The mixture was then centrifuged at 12,000 x *g* for 15 minutes at 4°C, separating the sample into three phases: a red organic phase containing protein, a white interphase containing DNA and a colourless upper aqueous phase containing RNA.

2.2.2.1.4 Isolation of RNA

The upper aqueous phase was carefully removed and transferred to a fresh eppendorf tube. Five hundred microliters of 2-propanol (per 1ml TRI Reagent®) was then added to the sample, mixed and then left to stand for 5-10 minutes at room temperature. The sample was then centrifuged at 12,000 x *g* for 10 minutes at 4°C resulting in an RNA pellet forming at the bottom of the tube. The white interphase and red organic phase were discarded unless required for subsequent DNA isolation for cell identity verification.

The supernatant was removed using a pipette and the RNA pellet was washed by adding 1ml 75% ethanol in DEPC water (per 1ml TRI Reagent®). The sample was vortexed then centrifuged at 7,500 x *g* for 5 minutes at 4°C. The RNA pellet was briefly air dried at 55°C for 5-10 minutes in a drying oven to evaporate most of the ethanol without drying the pellet completely in order to aid solubility. Finally, 30-50µL of DEPC water was added to the RNA pellet and the pellet dissolved by repeated pipetting for 10-15 minutes. The RNA was then quantified prior to storage at -80°C.

2.2.2.2 Quantification of RNA

The resulting single stranded RNA (ssRNA) in µg/µg was quantified by measuring its absorbance at a wavelength of 260nm using a Uv1101 Biotech spectrophotometer (WPA, Cambridge, UK) set to detect single strand RNA (ssRNA) with a dilution factor of 1:10. The photometer was calibrated between samples using DEPC water as a blank.

The concentration of RNA samples was then standardised to 0.5µg/µl using DEPC water to make up the total volume and the samples were stored at -80°C until further use.

2.2.2.3 Synthesis of cDNA using reverse transcription of RNA

Reverse transcription (RT) is a process whereby complementary DNA (cDNA) is generated from an RNA template enabling subsequent analysis by polymerase chain reaction (PCR). Together, these processes are known as RT-PCR.

Single stranded cDNA was synthesised from total RNA using a High Capacity cDNA Reverse Transcription Kit (Applied Biosystems, Paisley, UK).

2.2.2.3.1 Preparation of 2X RT Master Mix

The 2X RT Master Mix was prepared on ice using the kit components described in Table 2.8.

Table 2.8. Components for 2xRT Master mix (per 20µL reaction)

Component	Volume per reaction (µL)
10x RT Buffer	2µL
25xdNTP mix (100nM)	0.8µL
10xRT Random primers	2µL
MultiScribe™ Reverse Transcriptase	1µL
RNase Inhibitor	1µL
Nuclease-free H_20	3.2µL
Total volume per reaction	10µL

2.2.2.3.2 Preparation of cDNA RT reactions

The cDNA RT reactions were prepared by mixing 10µL 2xRT Mastermix and 0.5µg of total RNA diluted in 10µL DEPC water in a 200µL PCR tube to give a total reaction volume of 20µL. The tube/plate was then sealed, briefly centrifuged to spin down the contents and eliminate air bubbles and placed on ice prior to performing reverse transcription.

2.2.2.3.3 Performing reverse transcription

The reaction was carried out in a T-Cy Thermocycler using the conditions shown in Table 2.9, which are optimized for use with the High Capacity cDNA Reverse Transcription kits.

Table 2.9 Thermal cycler conditions for reverse transcription

	Temperature (°C)	Time (minutes:seconds)
Step 1	25	10:00
Step 2	37	80:00
Step 3	85	05:00
Step 4	4	∞

The resulting 20µl of cDNA product was diluted 1:4 with 60µl PCR water and either used immediately for PCR or stored at -20°C until required.

2.2.2.4 Polymerase chain reaction (PCR)

Polymerase chain reaction (PCR) is a technique, first developed by Kary Mullis in 1983, that is used to amplify a single or a few copies of DNA, producing thousands or millions of copies of a the DNA sequence.

The components required for a PCR reaction include a DNA template containing the target DNA that is to be amplified, a heat resistant DNA polymerase such as Taq polymerase which synthesizes DNA from nucleotides, short DNA fragments called primers which contain complementary sequences to the 3' ends of the sense and anti-sense strand of the target DNA and which act as a starting point for DNA formation by the DNA polymerase, deoxynucleoside triphosphates (dNTPs) from which the polymerase can synthesis new DNA strands and a thermal cycler, which provides repeated cycles of heating and cooling to provide the required temperatures for each step of the reaction. The DNA produced by the

PCR acts as a further template for replication resulting in a chain reaction and the exponential amplification of DNA.

2.2.2.4.1 Steps of PCR

The steps in a typical PCR procedure are shown in Table 2.10.

Table 2.10 Steps in a typical PCR procedure

Step	Temperature (°C)	Time	Purpose
Initialisation	94	1-9 min	Only required for DNA polymerases needing heat activation
Denaturation	94	20-30 seconds	Disrupts hydrogen bonds in dsDNA template resulting in single stranded DNA
Annealing	55	20-40 seconds	Allows specific hybridization of the primer to the ssDNA template enabling the polymerase to bind
Extension/elongation	~ 72	20-40 seconds	Synthesis of new DNA strand complementary to template by DNA polymerase leading to exponential amplification
Final elongation	72	5-15 minutes	
Final hold	4	∞	For short-term storage

Notes: Denaturation + annealing + elongation = one cycle. Multiple cycles (usually 20-40) are used. Temperatures used and length of cycle vary and depend in part on the enzyme used for DNA synthesis and the melting temperature (Tm) of the primers.
* Only required for DNA polymerases that require heat activation

2.2.2.4.2. Components and conditions for PCR

Conventional PCR was performed using a total reaction volume of 12µL. The components in each PCR reaction are shown in Table 2.10 and the conditions used are shown in Table 2.11.

Table 2.11. Components in PCR reaction

Component	Volume
2xGoTaq® Green Master Mix (Promega, USA)	6µL
Forward primer (1µM)	1µL
Reverse primer (1µM)	1µL
cDNA	1µL
PCR water	3µL
Total volume per reaction	12µL

A negative control containing no cDNA template (volume replaced with PCR water) was run with each set of test samples and all cDNA samples were simultaneously screened for GAPDH (a house keeping gene) as an internal loading control to check uniformity of sample cDNA levels.

The reaction was set up in individual PCR tubes or 96 well PCR plates which were sealed and placed in an Applied Biosystems® 2720 PCR Thermal Cycler. The conditions used for conventional PCR in this study are shown in Table 2.12.

Table 2.12. Conditions used for conventional PCR

Step	Temperature (°C)	Time (minutes:seconds)	Number of cycles
Initialisation	94	05:00	
Denaturation	94	00:20	32 cycles
Annealing	55	00:20	
Extension/elongation	72	00:40	
Final extension	72	10:00	
Final hold	4	∞	

.

2.2.2.5 Agarose gel electrophoresis and DNA visualisation

Agarose gel electrophoresis uses electricity to move negatively charged DNA towards a positive electrode through an agarose gel matrix. The speed with which DNA moves through the agarose gel depends on the length of the DNA fragments. Electrophoresis therefore, separates DNA by size allowing DNA to be visualized and purified. A DNA ladder containing different DNA fragments of known lengths can be run alongside samples on the gel enabling the size of the DNA in the samples to be determined.

Size separation of PCR products was performed using 1-2% agarose gel depending on the size of the PCR products. A higher agarose percentage was used for small PCR products and a lower percentage was used for larger products. Agarose gel was prepared by adding the appropriate amount (1-2g) of agarose powder to 100ml 1xTBE buffer in a heat resistant flask. The mixture was placed into a microwave and heated until the agarose had completely dissolved. The solution was allowed to cool for 5 minutes before being stained 1:10,000 using SYBR®Safe DNA gel stain (Life Technologies Ltd, Paisley, UK) and poured into electrophoresis gel tray. Well forming combs were lowered into the gel and the gel was

covered to protect the gel from light and left to set at room temperature for approximately 30-45 minutes until the gel was completely solidified.

Once the gel was set, the well forming combs were removed and the agarose gel was placed into the electrophoresis unit. The gel was then immersed in 1xTBE to ensure the gel was completely covered with 5mm fluid. A molecular weight ladder (5µL, PCR DNA ladder, GenScript®, Piscataway, USA) was then loaded into the first lane of the gel with a pipette and then 8µL of each sample was added using the additional wells of the gel. The lid containing the electrodes was then placed onto the unit ensuring the correct orientation and the gel was run at 80-150V, 100mA and 50W using a Gibco BRL Electrophoresis power supply (model 250EX Life Technologies Ltd, Paisley, UK) or 45 minutes to 1 hour, or until the dye line had moved 75-80% of the way down the gel. The electrodes were then disconnected, the gel removed and the DNA fragments visualised using Syngene U:Genius3 fluorescence UV transilluminator (Synoptics Ltd, Cambridge, UK). Images were saved electronically and printed using a thermal printer.

2.2.2.6 Real-time/quantitative PCR (qPCR)

Real-time (or quantitative) PCR is a very sensitive gene analysis technique, which measures PCT amplification as it occurs (i.e. in "real-time") and not just at the end of the reaction, as occurs in conventional PCR. As data is collected during the log phase of PCR (when the quantity of PCR product is proportional to the amount of template), qPCR also provides quantitative data, allowing the exact concentration of amplified DNA in the sample to be calculated. Quantitative PCR has a number of advantages when compared to conventional PCR, it is quick, does not involve a separate DNA separation and visualisation step, it allows high throughput, it is very sensitive, is repeatable, has a broad dynamic range of

quantification and provides more informative results. It is however, more costly and can be sensitive to errors in technique.

2.2.2.6.1 Principles of qPCR

Quantitative PCR is based on the same principles as conventional PCR but a fluorescent label is added to the amplified DNA and the level of fluorescence is measured throughout the PCR cycle. During amplification, the amount of fluorescence produced is directly proportional to the amount of amplified DNA and samples with higher initial copy number of the DNA target will produce a faster rise in fluorescence and the cycle in which the fluorescence is detected (the quantitation cycle, Cq) will occur sooner than for samples with a lower initial copy number.

2.2.2.6.2 Components and conditions for qPCR

Quantitative PCR in the current study was performed using the Amplifluor ™ Universal Detection System (Intergen®, New York, USA). This system is based on molecular energy transfer from an excited fluorophore (fluorescein) to an acceptor moiety (4-(4'-dimethylaminophenylazo) sulfonic acid (DABSYL)) that quenches the fluorescence emission. The fluorophore and acceptor are tethered together via an oligonucleotide primer called UniPrimer™. Amplifluor™ UniPrimer™ hairpin primers are designed in such a way that a fluorescent signal is only generated when the primer is unfolded during its incorporation into an amplification product. The fluorescent signal is generated during unfolding due to the fact that quenching is no longer possible because of the increased distance between the fluorescein and DABSYL moieties. The level of fluorescence directly correlates with the amount of PCR

product during each cycle and can be measured during the reaction (real-time) or at the end of the reaction (endpoint) to give a quantification of PCR product.

Contained within the UniPrimer™ is a 3' 18 base oligonucleotide tail called a Z sequence, which acts as a universal PCR primer. The fluorophore and acceptor are located at the 5' end. In order to use the UniPrimer™, the Z sequence is added to the 5' end of a target-specific primer. The UniPrimer™ can then anneal to the Z' sequence in an amplicon generated in the initial cycles of the PCR reaction. As the UniPrimer™ is incorporated, the hairpin becomes unfolded, quenching can no longer occur and then a fluorescence signal that directly correlates to the amount of amplified DNA is produced. An illustration showing how the Amplifluor™ Universal detection system using UniPrimer™ detection system works is shown in Figure 2.1.

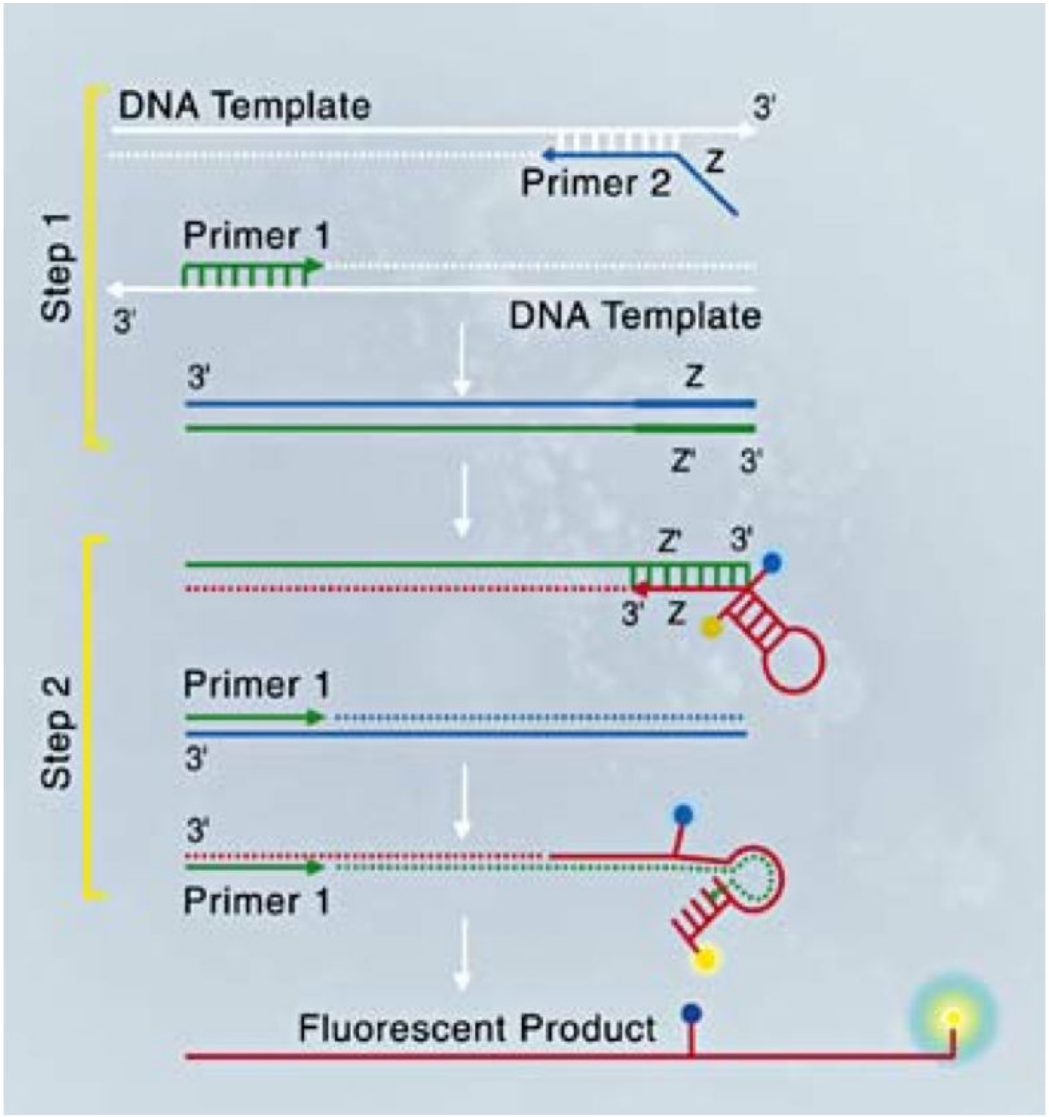

Figure 2.1 Amplifluor™ Universal detection system using UniPrimer™

The components of each qPCR reaction are shown in Table. 2.13. Each sample was loaded into a 96 well plate (Applied Biosystems™, Life Technologies Ltd, Paisley, UK), covered with MicroAmp® Optical Adhesive film (ThermoFisher Scientific, Life Technologies Ltd, Paisley, UK) and run alongside a podoplanin (PDPL) standard of a known transcript number (ranging from 10^8 to 10^1). PDPL is a lymphangiogenesis marker, which acted as a reference control gene to ensure any differences observed were not due to technical errors and allowed normalization of results. The 96 well plate was placed in an iCycler Thermal Cycler which uses a light source to excite the fluorescent molecules in the wells and an image intensifier and a 350,000 pixel charge-coupled device (CCD) detector to image all 96 wells every second and detect fluorescent light. The conditions used for qPCR are shown in Table 2.14.

Table 2.13 Components in each qPCR reaction

Component	Volume
2x iQ™ Supermix	5µL
Forward primer (10pmol/µL)	0.3µL
Reverse primer (1pmol/µL)	0.3µL
Amplifluor™ probe (10pmol/µL)	0.3µL
cDNA	1µL
PCR H_20	3µL
Total volume per reaction	10µL

Table 2.14. Conditions for qPCR

Step	Temperature (°C)	Time (minutes:seconds)	Number of cycles
Initial denaturation	94	05:00	
Denaturation	94	00:10	80-90 cycles
Annealing	55	00:35	
Extension	72	00:20	

Software was used to analyse the data in order to determine the threshold cycle (Ct). The Ct is the number of cycles taken to detect fluorescence (above background fluorescence levels) from the sample in a given well. The Ct value is inversely proportional to the amount of nucleic acid in the sample. The procedure was repeated at least three times.

An example of the amplification plot and standard curve produced using qPCR is shown in Figure 2.2

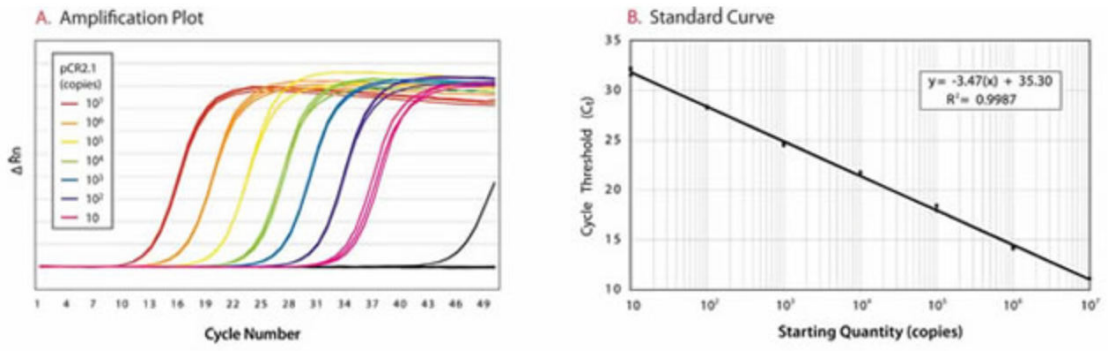

Figure 2.2 Amplification plot and standard curve produced using qPCR and pCR2.1 standard with known transcript numbers from 10^1 to 10^8. A. Amplification plot showing exponential increase in transcript copy number with cycle number B. Standard curve produced by plotting starting copy number against cycle threshold (Ct). From ThermoFisher Scientific https://www.thermofisher.com/order/catalog/product/11733038.

2.2.3 Methods for protein detection

2.2.3.1 Extraction of protein and preparation of cell lysates

The first step in protein extraction and analysis is to collect and lyse cells. Once cells had reached an appropriate confluence, the medium was removed with a vacuum aspirator and the cell monolayer was washed with BSS buffer. A sterile cell scraper was then used to scrape the cells from the flask surface and the resultant suspension was collected in a universal container. The universal container was placed in a centrifuge and the suspension centrifuged at 1,800rpm for 8 minutes to deposit cells in a cell pellet. The supernatant was then removed with a vacuum aspirator and the cell pellet was resuspended in BSS and centrifuged twice. After removal of the supernatant, the cell pellet was resuspended in 200-300µL lysis buffer (depending on pellet size) and transferred to a 1.8ml eppendorf tube. The tube was placed on a Labinco rotating wheel (Woolf laboratories, York, UK) and rotated at room temperature.

After 1 hour, the resulting suspension was centrifuged at 13,000rpm for 15 minutes separating the sample into a supernatant containing proteins, which was transferred to a fresh microfuge tube, and a cell pellet containing cell debris, which was discarded. The protein containing supernatant was then either quantified immediately or stored at -20°C until further use.

2.2.3.2 Quantification of proteins and preparation of protein samples

In order to standardize the concentration of the protein samples prior to their analysis using SDS-PAGE and Western blotting, the protein samples were then quantified using the Bio-Rad DC Protein Assay kit (Bio-Rad Laboratories, Hemel Hempstead, UK). This is a colourimetric assay based on the reaction of protein with an alkaline copper tartrate solution (Reagent A)

and Folin reagent (Reagent B) and is used for the determination of protein concentration following detergent solubilisation. The protein reacts with copper in the alkaline medium resulting in the subsequent reduction of the Folin reagent and the production of a characteristic blue colour with an absorbance between 405-750nm). Bovine serum albumin was used as a standard.

The working reagent (Reagent A') was prepared by adding 20µL of reagent S to each 1ml of reagent A. In a 96-well plate, serial dilutions of a protein standard were prepared using 50mg/ml bovine serum albumin (BSA) and the same lysis buffer that was used for the sample proteins in order to produce standards with a protein concentration gradient of 0.78mg/ml to 50mg/ml. Five microliters of either protein sample or standard were pipetted into fresh wells on a 96 well plate and 25µL of Reagent A' was added to each well followed by 200µL Reagent B. The plate was gently agitated to mix the reagents and then left to rest for 15 minutes at room temperature until the colourimetric reaction had occurred. Absorbances were then read at 750nm using the ELx800 plate reading spectrophotometer (Bio-Tek, Wolf Laboratories, York, UK). A standard curve of protein concentration was prepared by plotting a graph of the BSA standards protein concentration versus absorbance and this was then used to determine the protein concentration of the protein samples. The protein samples were then standardised to a final concentration of 1-2mg/ml using the appropriate amount of lysis buffer. Finally, 2x Lamelli sample buffer concentrate was added 1:1 to each standardised protein sample prior to denaturation by boiling at 100°C for 5-10 minutes. The boiled samples were either used immediately for SDS-PAGE or stored at -20°C

2.2.3.3 Sodium Dodecyl Sulphate Polyacrylamide Gel Electrophoresis (SDS-PAGE)

The percentage gel required depends on the size of the protein of interest. The gel percentages required for different protein sizes are shown in Table 2.15.

Table 2.15 SDS-PAGE gel percentage required for different sizes of proteins. Adapted from 'Western blot protocol" by Abcam (http://www.abcam.com/protocols/general-western-blot-protocol)

Protein size	Gel percentage
4-40kDa	20%
12-45kDa	15%
10-70kDa	12.5%
15-100kDa	10%
25-100kDa	8%

A molecular weight marker was loaded into the first well of the SDS-PAGE gel and equal volumes of the protein samples were loaded into each of the remaining wells. The gel was then run at 100V for 1-2 hours.

2.2.3.4 Transferring proteins from gel to nitrocellulose membrane (Western blotting)

During SDS-PAGE, the equipment required for transferring the proteins from gel to nitrocellulose membrane was prepared. Six sheets of filter paper cut to the same size as the gel were soaked in 1x transfer buffer. Once SDS-PAGE was complete, three of these sheets were then placed one at a time onto the bottom graphite base electrode of a SD20 SemiDry Maxi System blotting unit (SemiDRY, Wolf Laboratories, York, UK). Air bubbles between the sheets were removed by rolling a roller gently over each layer in the stack. A sheet of similarly sized Hybond nitrocellulose membrane (Amersham Biosciences Ltd, Bucks, UK) was placed on top of the filter paper. The SDS-PAGE gel cassette was removed from the cell and the glass plates pried open to expose the gel. The stacking gel was discarded and the resolving gel was carefully placed on top of the nitrocellulose membrane. The remaining three sheets of pre-soaked filter paper were then placed on top of the gel to complete the

stack. The lid of the blotter was then placed on top of the stack and electroblotting was carried out at 15V, 500mA and 8W for 20-60 minutes depending on protein size. The arrangement of paper, gel and nitrocellulose membrane is shown in Figure 2.3.

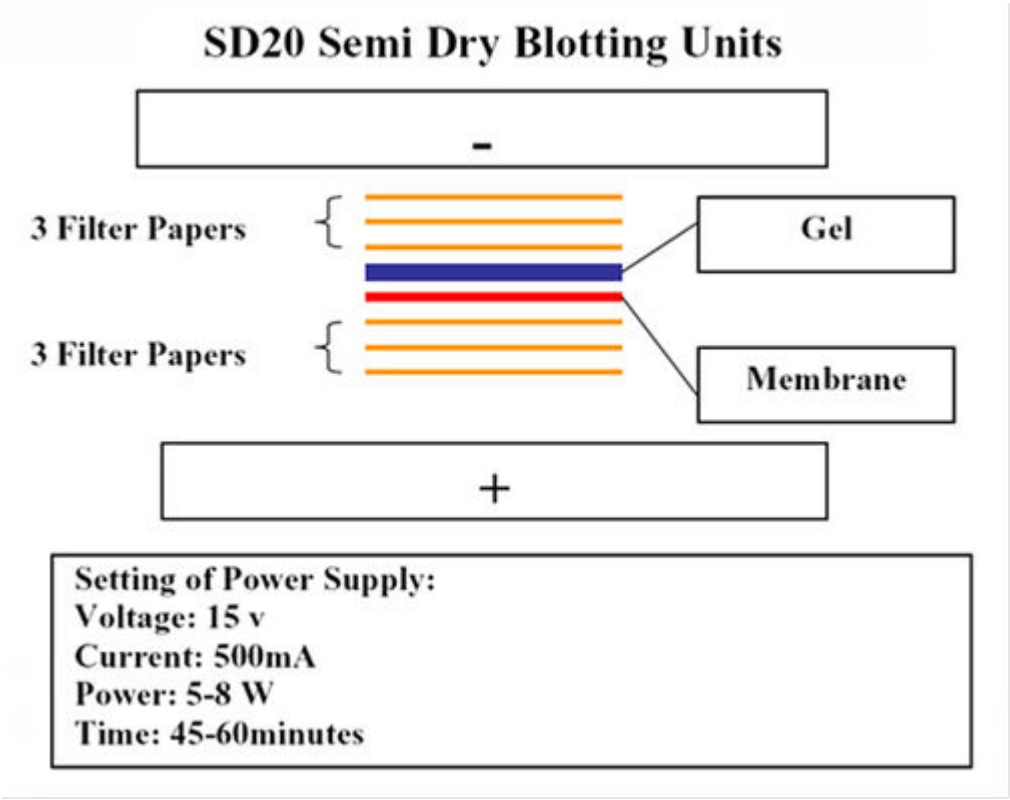

Figure 2.3. Sandwich arrangement of filter paper, nitrocellulose membrane and gel used for Western blotting. Figure taken from the PhD thesis of Dr. L. Ye.

2.2.3.5 Protein staining and blocking of nitrocellulose membrane

Successful transfer of the proteins from gel to membrane was confirmed using Ponceau S staining.

A 10% milk solution was prepared using 10% milk powder and 0.1% polyoxyethylene (20) sorbitanmonolaurate (Tween 20) (Sigma-Aldrich, St. Louis, USA) in 50ml TBS. The nitrocellulose membrane was placed in a 50ml falcon tube (Fisher Scientific, Leicester, UK) with the side of the membrane that had been facing the gel towards the lumen of the tube and filled with 10% milk solution. The tube was left overnight at 4°C for the milk solution to block the membrane.

2.2.3.6 Protein detection using specific immuno-probing

A 3% milk solution was prepared using 3% milk powder and 0.1% Tween 20 in 50ml TBS. A primary antibody solution was prepared using 3% milk solution containing primary antibody diluted 1:500. Secondary antibody solution was prepared using 3% milk solution containing 1:1000 horseradish peroxidase (HRP) conjugated secondary antibody. Tween TBS solution was prepared using 0.2% Tween 20 in TBS.

Following overnight blocking, the nitrocellulose membrane was transferred into a fresh 50ml falcon tube and fresh 10% milk solution was added. The tube was then placed on a roller mixer for one hour at room temperature. Following this, the 10% milk solution was removed and replaced with 10ml 3% milk solution and the tube was returned to the roller mixer for 15 minutes. The 3% milk solution was then poured off and replaced with 5ml primary antibody solution. The tube was returned to the roller mixer to incubate the membrane with the primary antibody for one hour at room temperature. The primary antibody solution was then removed

and the membrane washed twice by adding fresh 3% milk solution and placing the tube on the roller for 15 minutes at room temperature. The membrane was then incubated with 5ml secondary antibody solution for one hour on the roller mixer at room temperature. The membrane was then removed from the secondary antibody solution and washed with 10ml 3% milk solution twice for 15 minutes each time followed by two washes each lasting 15 minutes with Tween TBS solution. Finally, the membrane was washed twice for 15 minutes per wash in TBS to remove any residual detergent.

2.2.3.7 Protein visualization using chemiluminescence

Protein detection was performed using Luminata™ Forte Western HRP chemiluminescence substrate (Millipore, Billerica, MA, USA). This substrate works on the principle that horseradish peroxidase catalyses the oxidation of luminol in the presence of peroxide releasing photons (chemiluminescence) that can be captured by a CCD camera.

The blot was placed protein side up in a plastic weighing boat and 0.1ml of HRP substrate per cm2 of membrane area was added (i.e. for a 7 x 8.4cm blot, 6ml HRP substrate was required). The blot was incubated for 2-5 minutes at room temperature. The excess substrate was then poured off and the blot was transferred using forceps into a fresh weighing boat. The chemiluminescent signal was detected using a UVITEC Imager (UVITEC, Cambridge, UK), which comprises a darkroom and a camera to detect chemiluminescence attached to a computer. Images were viewed and analysed using the UVI band software package (UVITEC, Cambridge, UK).

Glyceraldehyde-3-phosphate dehydrogenase (GAPDH) is a commonly used human "housekeeping gene", the expression of which should not differ between samples. It is used as a reference or endogenous control against which quantification of a gene in tissues can be

normalised to avoid bias caused by RNA extraction and quantification, sample loading (i.e. to ensure there is an equal amount of template), variation in RT efficiency, degradation of RNA, presence of inhibitors in the RNA sample and differences in sample handling. Each Western blot was carried out a minimum of three times.

2.2.4 Antibody based protein microarrays

Antibody based protein microarray was performed using the Kinex™ KAM-880 antibody microarray (Kinexus Bioinformatics Ltd, Canada). This microarray identifies the differential binding of dye-labelled proteins in lysates prepared from cells or tissues in order to provide information on differences in protein expression, phosphorylation and protein-protein interactions. This enables targeted protein work using Western blot to be undertaken and signalling pathway analysis to be performed.

2.2.4.1 Principles of antibody based protein microarrays

The Kinex™ KAM-880 antibody microarray uses 877 antibodies to identify differences in the protein expression levels (using 518 pan-specific antibodies) and phosphorylation states (using 359 phosphosite-specific antibodies) of a range of proteins involved in cell signal transduction. The classes of protein targets on the KAM-880 Antibody Microarray chip are shown in Table 2.16.

Table 2.16 Classes of targeted proteins and phosphosites on the Kinex™ KAM-880 Antibody Microarray chip. Information obtained from Kinex™ KAM-880 Antibody Microarray Service Customer Information Package March 2015 (Kinexus Bioinformatics Ltd, Vancouver, Canada)

Content	Total %	Total N
Total number of pan-specific antibodies	60%	518
Total number of phospho-specific antibodies	40%	359
Total number of antibodies	100%	877
Total number of protein kinase pan-specific antibodies	35%	307
Total number of protein kinase phospho-specific antibodies	23%	200
Total number of protein phosphatase pan-specific antibodies	7%	65
Total number of protein phosphatase phospho-specific antibodies	0.5%	4

N = number

These antibodies are covalently immobilised onto a glass surface coated with a three-dimensional polymer material to ensure high binding efficiency and specificity. In order to ensure consistency in quantity of protein across all fields, each microarray has loading and antibody controls. Semi-quantitative analysis of protein expression and phosphorylation state in two samples (control *vs.* treated) is provided by duplicate measurements of the strength of the fluorescence signals for each target protein. In order to reduce the number of false positive results and to eliminate differential binding that may occur with the use of different dyes, the same fluorescent dye is used to label both the control and test lysate samples and they are analysed simultaneously on the same chip at the same time.

One of the inherent limitations of antibody based protein microarrays is the high rate of false positives due to the fact that non-denaturing conditions are used, giving rise to the possibility that changes observed are due to protein-protein interactions rather than differences in protein expression and phosphorylation. In order to reduce the possibility of false positives, the

Kinex™ KAM-880 antibody microarray uses a chemical digestion step that fragments proteins, disrupting protein complexes without destroying the epitopes recognized by the antibodies. An image of the microarray chip is shown in Figure 2.4.

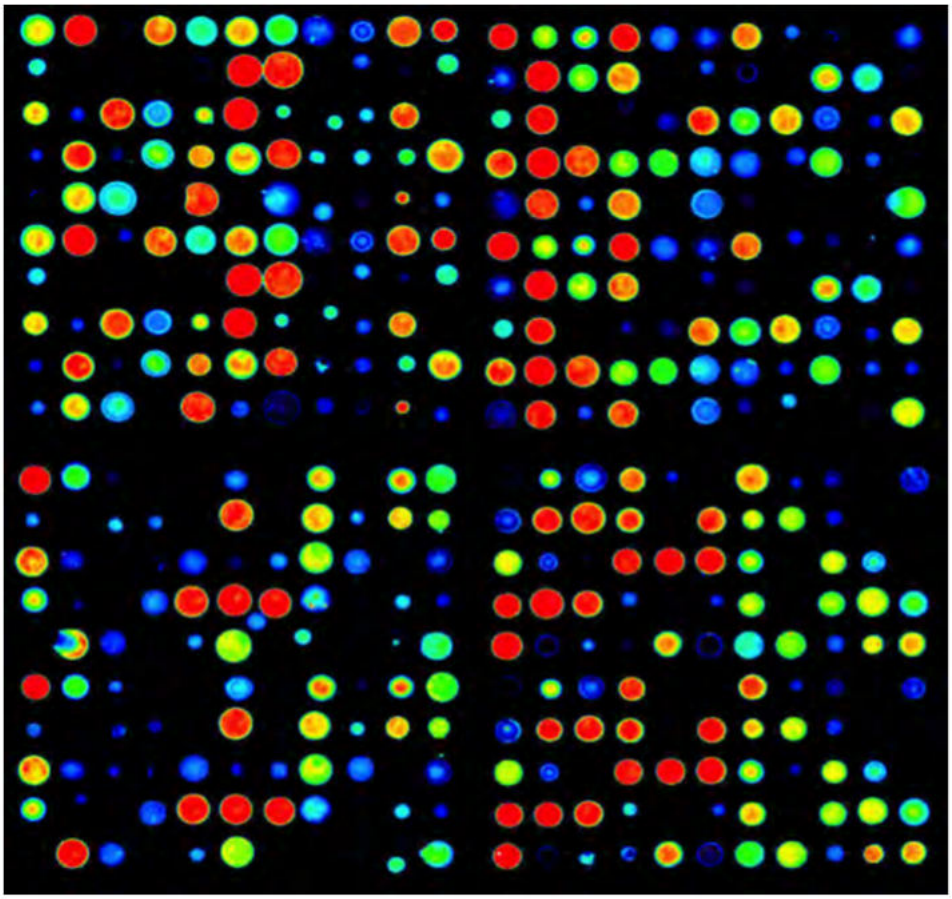

Figure 2.4 Close up scanned image of 4 of 32 grids on a Kinex™ KAM-880 Antibody Microarray chip. High signal intensity is shown in red/orange with lower signal intensities represented by green/blue. Image from Kinex™ KAM-880 Antibody Microarray Service Customer Information Package March 2015 (Kinexus Bioinformatics Ltd, Vancouver, Canada)

Kinex™ KAM-880 Antibody microarray is based on the binding and detection of control and test cell lysate proteins to antibodies. The methodology used in the microarray is illustrated in Figure 2.5.

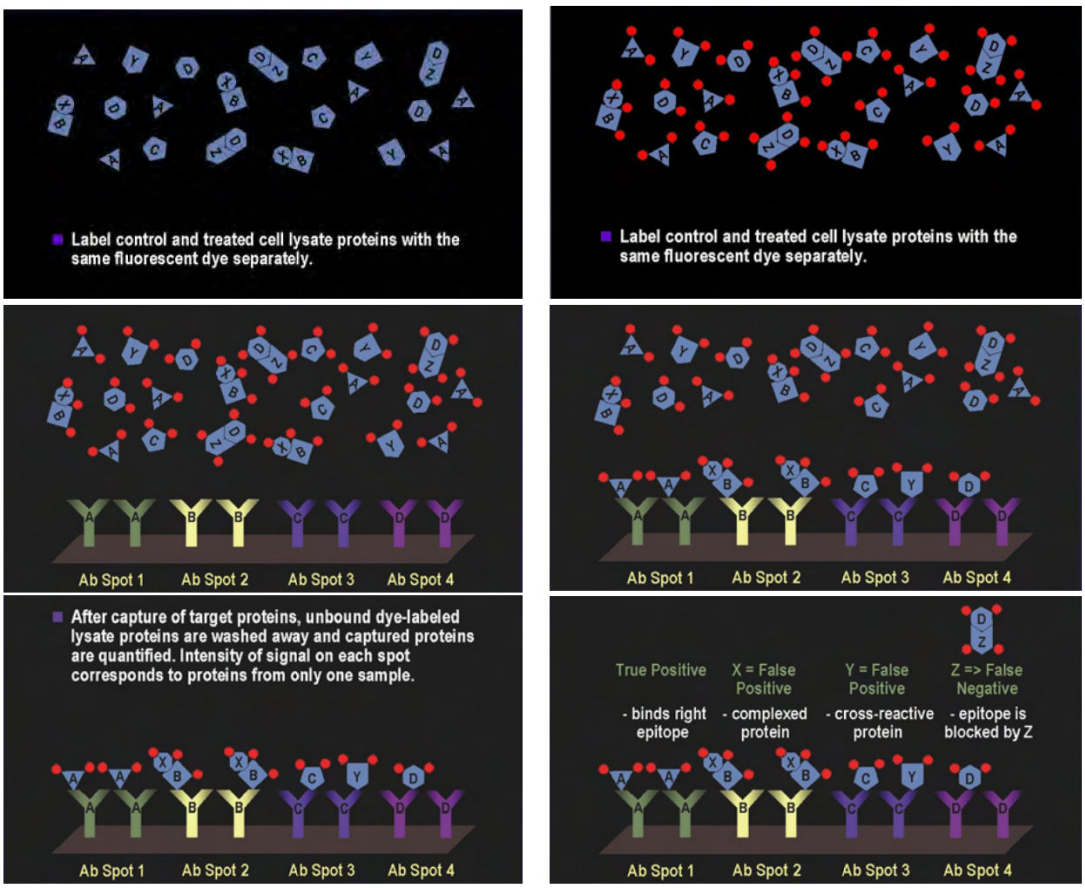

Figure 2.5 Methodology used in Kinex™ KAM-880 Antibody Microarray. Taken from Kinex™ KAM-880 Antibody Microarray Service Customer Information Package March 2015 (Kinexus Bioinformatics Ltd, Vancouver, Canada)

2.2.4.2. Preparation of cell lysate samples for Kinex™ KAM-880 Antibody Microarray

2.2.4.2.1 Preparation of lysis buffer

Lysis buffer was prepared using the ingredients shown in Table 2.17. SDS-PAGE sample buffer was not used as non-denatured proteins are required for analysis. Final pH of the lysis buffer was corrected to 7.2 prior to use.

Table 2.17 Ingredients of lysis buffer for Kinex™ Antibody Microarray

Ingredients	Purpose
20mM MOPS, pH 7.0	Buffer
2mM EGTA	Binds calcium
5mM EDTA	Binds magnesium and manganese
30mM sodium fluoride	Inhibits protein-serine phosphatases
60mM β-glycerophosphate, pH 7.2	Inhibits protein-serine phosphatases
20mM sodium pyrophosphate	Inhibits protein-serine phosphatases
1mM sodium orthovanadate	Inhibit protein-tyrosine phosphatases
1% Triton X-100	Cellular fractionation

Immediately before use, a number of protease inhibitors and DTT were added to the lysis buffer. These are shown in Table 2.18.

Table 2.18 Protease inhibitors and DTT added to lysis buffer for Kinex™ Antibody Microarray

Ingredient	Purpose
1mM phenylmethylsulfonylfluoride	Inhibit proteases
3mM benzamidine	Inhibit proteases
5μM pepstatin A	Inhibit proteases
10μM leupeptin	Inhibit proteases
1mM dithiothreitol	Disrupt disulphate bonds

2.2.4.2.2 Preparation of cell lysates

Verified transfected cells were maintained in blasticidin maintenance medium until required. Once cell culture flasks containing approximately 1-2 x10^6 cells reached approximately 80% confluence, the medium was removed by vacuum aspiration and replaced with normal media supplemented with 5% FCS. The flasks were then returned to the incubator for overnight culture. The following morning, the medium was replaced with fresh normal medium supplemented with 5% FCS and the flasks were returned to the incubator for a further three hours culture prior to harvesting the cells for protein extraction.

At the time of harvest, the medium was removed with vacuum aspiration and the cells were washed twice with 5ml PBS, firstly at room temperature and secondly, with PBS kept refrigerated at 4°C. The cells were then scraped into a universal container and the suspension was pelleted using a centrifuge at 1600 rpm for 5 minutes. The supernatant was discarded and 600μL of the lysis buffer prepared as described in Section 2.2.4.2.1 was added to the cell pellet. The pellet/buffer mix was transferred to a 1.5ml eppendorf tube and rotated on a blood wheel at 4°C for 1 hour.

The lysates were then centrifuged at maximum speed (15,000-17,000 x g) in a benchtop Eppendorf microcentrifuge for 30 minutes at 4°C. The supernatant was then transferred to a 1.5ml microcentrifuge tube and protein quantification using a BSA standard was performed to determine the protein concentration. A minimum of 100µg protein for each lysate with a minimum concentration of 2mg/ml was then transferred into a fresh tube, frozen immediately and shipped by a courier on dry ice to Kinexus in Canada on a Monday. Any remaining lysate was stored at -20°C for future use.

2.2.4.2.3 Analysis of antibody based protein microarray data

Once the intensities of dye-bound proteins on the KAM-880 chip are scanned and quantified by Kinex™, software is used to calculate the average intensities recorded for each pair of antibody spots to calculate the differences between the control and test lysate samples. Data is normalized to account for any differences in lysate protein loading and Z scores and percent changes from control (%CFC) are calculated. Kinexus also undertake a mapping analysis of the results and allow access to the KiNET™ Antibody Microarray (KiNET-AM) Database so that data can be compared with lysates from other model systems analysed with the same methodology.

Using the data report provided by Kinexus, the results of the control and test cell lysates were compared using the Globally Normalised Signal Intensity, %CFC and Z-scores.

2.2.5 Manipulation of gene expression

2.2.5.1 Steps in gene transfer

The manipulation of gene expression by gene transfer involves a number of steps shown in Figure 2.6.

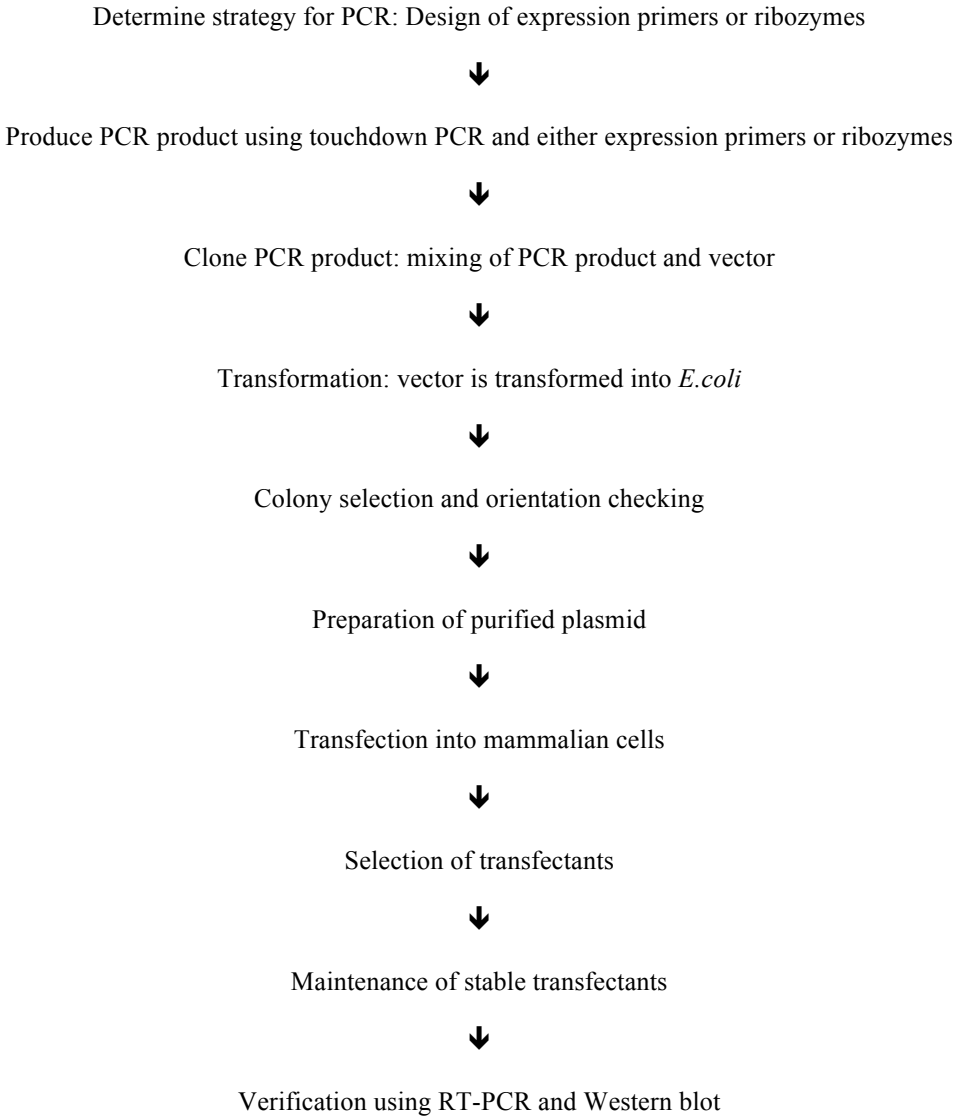

Figure 2.6 Steps in gene transfer

2.2.5.2 Determining the strategy for PCR: Design of expression primers and ribozymes

Ribozymes are RNA molecules capable of cleaving a sequence leading to loss of the molecule at transcript level.

Ribozyme primers based on the secondary structure of the gene transcripts were designed using Zuker's RNA mFold programme and transgenes were created using touchdown PCR.

2.2.5.3 Production of PCR products

Ribozyme transgenes for the knockdown of DOK7 at mRNA level were created using ribozyme primers and touchdown PCR. The components for the reaction are shown in Table 2.19 and the conditions for the PCR are shown in Table 2.20.

Table 2.19 Components used for ribozyme transgene generation

Component	Volume
2xGoTaq® Green Master Mix (Promega, USA)	10µl
Forward primer (1µM)	1µl
Reverse primer (1µM)	1µl
PCR H_2O	8µl

Table 2.20 Conditions used for touchdown PCR

Step	Temperature	Time	Cycle
Initialisation	94°C	5 minutes	1
Denaturation	94°C	10 seconds	48
Annealing	70°C 65°C 60°C 55°C 50°C	15 seconds 15 seconds 15 seconds 15 seconds 15 seconds	
Extension	72°C	20 seconds	
Final extension	72°C	7-10 minutes	1

Following PCR, agarose gel electrophoresis using a 2% agarose gel was used to confirm the presence and size of the resulting transgenes prior to their use in TOPO-TA gene cloning.

2.2.5.4 TOPO-TA gene cloning

Cloning was carried out using the pEF6/V5-His TOPO ® TA Expression Kit (Invitrogen, CA, USA) according to the manufacturers protocol.

2.2.5.4.1 Anatomy of the pEF6/V5-His-TOPO® vector

A schematic representation of the pEF6/V5-His-TOPO® vector illustrating the important regions for gene cloning is shown in Figure 2.7.

A.

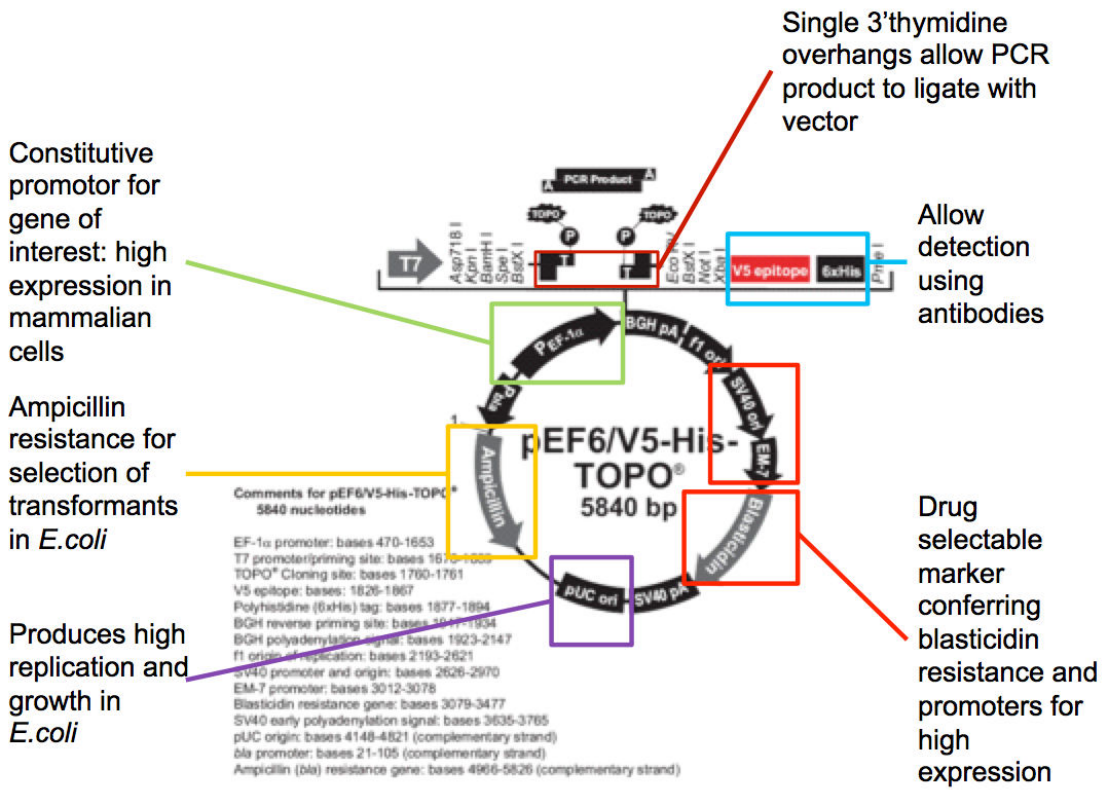

B.

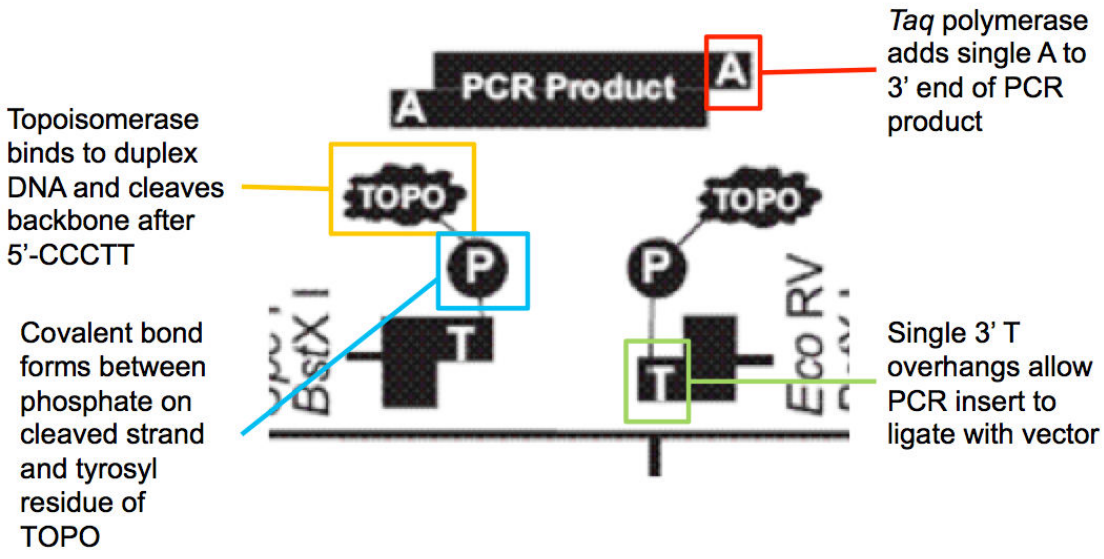

Figure 2.7 Schematic representation of the pEF6/V5-His-TOPO® vector. A. Complete view showing important regions within vector. B. View of PCR product binding site.

2.2.5.4.2 TOPO® cloning reaction

The components of the TOPO® cloning reaction are shown in Table 2.21. These reagents were mixed together in an eppendorf tube and incubated at room temperature for 5 minutes prior to being placed on ice.

Table 2.21 Components of TOPO® cloning reaction

Reagent	Volume
PCR product	4µL
Salt solution	1µL
TOPO® vector	1µL

2.2.5.5 Transformation of chemically competent *E.coli*

Five microlitres of the TOPO® cloning reaction was added to one 50µL vial of OneShot® TOP10 chemically competent *E.coli* (Life Technologies Ltd, Paisley, UK) and tapped gently to mix. The vial was then incubated on ice for 30 minutes. A heat shock of 42°C for 30 seconds was then applied by placing the vial into a pre-heated water bath. The vial was then removed from the water bath, placed on ice and 250µL of pre-warmed S.O.C medium was added to the vial. The vial was then placed in a tube holding foam pad and placed on an orbital shaker in an incubator and shaken at 225-250rpm for 1 hour at 37°C.

Meanwhile, ampicillin selection plates were prepared using LB agar with 100µg/ml ampicillin in a Class II laminar flow cabinet. Refrigerated autoclaved LB agar was placed into a microwave and heated for approximately 10 minutes with occasional agitation until it had become liquid. It was then placed into the cabinet and allowed to cool slightly before use.

Sterile culture dishes, autoclaved LB broth and stock concentration ampicillin (100mg/ml) were placed into the cabinet and the dishes labelled accordingly. Twenty millilitres of LB broth were then added to 30ml of LB agar in a Falcon tube and 50µL of the ampicillin was added to the tube. The tube was tipped back and forth to mix the contents and then approximately 15ml was poured into each culture dish. The dishes were tipped to evenly coat them with the mixture and a sterile pipette tip was used to dispel any bubbles. The dishes were then left to set in the cabinet.

The vial was removed from the incubator and one third of the transformed *E.coli* were then pipetted onto the top of the plate with the remaining two-thirds pipetted onto the bottom of the plate. The bacteria were then spread over the plate using a zig-zag pattern to obtain high and low seeding densities. The lids were placed on the dishes, they were inverted to prevent condensation build up and placed in an incubator at 37°C overnight.

Any remaining transformed bacteria were stored at -80°C until further use.

2.2.5.6 Selection of correctly oriented colonies

After overnight incubation at 37°C, plates were examined for colony growth. Owing to the ampicillin in the selection plate agar, surviving colonies should be those that have successfully taken up the vector, which carries resistance to ampicillin.

2.2.5.6.1 Orientation checking

Orientation checking was performed to ensure the PCR product was inserted into the plasmid with the correct orientation. Using a clean pipette tip, a small sample was taken from each of the 10 selected colonies and orientation was checked by performing three PCR reactions.

The first reaction used a T7F primer and a reverse primer specific to the insert. The T7F primer starts at around 90bp upstream of the inserting site and therefore, if the insert is correctly oriented, the resulting PCR product should be around 100bp bigger than the predicted product size.

The second reaction used T7F primer and a forward primer specific to the inserted sequence. If a PCR product was generated in this reaction, it indicated incorrect insert orientation. If a PCR product was generated for both reactions, it indicated that the colony contained a mixture of plasmids with both correctly and incorrectly inserted sequences.

A final reaction using T7F and BGHR primers was used to verify that the full sequence has been inserted without degradation. All PCR products were visualised using agarose gel electrophoresis to confirm presence and size of PCR product.

The conditions used for the PCR are shown in Table 2.22.

Table 2.22 Conditions for orientation checking PCR

Step	Temperature	Time	Cycle
Initialisation	94°C	10 minutes	1
Denaturation	94°C	20 seconds	25
Annealing	55°C	30 seconds	
Extension	72°C	40 seconds	
Final extension	72°C	7 minutes	1

Following orientation checking, a sterile pipette tip was used to inoculate 10ml fresh LB broth containing 100µg/ml ampicillin with the correctly oriented colonies and these were cultured overnight on an orbital shaker in an incubator at 37°C.

2.2.5.7 Purification and amplification of plasmids

The following day, the universal container was taken from the incubator and checked for turbidity to confirm *E.coli* growth. Plasmids were isolated using the GenElute™ Plasmid Miniprep kit (Sigma-Aldrich Ltd, Dorset, UK), which isolates plasmid DNA from recombinant *E.coli* cultures.

Cells were first harvested by transferring 5ml of the overnight recombinant E.coli culture to a 2ml microcentrifuge tube and pelleting the cells using centrifugation at ≥ 12,000 x g for 1 minute. The supernatant was discarded. The bacterial cell pellet was then resuspended with 200µL of the Resuspension solution and the tube was vortexed to produce a homogeneous solution. Cells were then lysed by adding 200µL of the lysis solution and the contents of the tube were immediately mixed by gentle inversion 6-8 times until the solution became clear and viscous. Cell debris was then precipitated by adding 350µL of the Neutralisation/Binding solution and the tube was inverted 4-6 times to mix gently. The cell debris was then pelleted by centrifuging at ≥ 12,000 g for 10 minutes to produce a cleared lysate.

A GenElute™ Miniprep binding column was prepared by inserting it into a microcentrifuge tube and adding 500µL of column preparation solution to the column. The tube was then centrifuged at ≥ 12,000 x g for 1 minute. The flow-through liquid was discarded and the cleared lysate was transferred to the column and centrifuged at ≥ 12,000 x g for 1 minute. The flow-through liquid was discarded and the column was washed by adding 750µL of the diluted wash solution to the column and centrifuging at ≥ 12,000 x g for 1 minute. The flow

through liquid was discarded and the tube centrifuged again at ≥ 12,000 x g for 2 minutes to remove excess ethanol. The column was transferred to a fresh collection tube and 100µL Elution solution was added prior to centrifuging at ≥ 12,000 x g for 1 minute. The eluate containing DNA was either used immediately or stored at -20°C until further use.

The presence and correct size of plasmid was confirmed using agarose gel electrophoresis using a 1% agarose gel and 3µL product mixed with 2µL loading dye per well.

2.2.5.8 Sequencing of inserts

Where necessary, inserts were submitted for analysis by sequencing using the T7 primer.

2.2.5.9 Transfection of cells using electroporation

Transfection is the process by which foreign DNA is introduced into the nucleus of eukaryotic cells. There are a variety of methods by which transfection can occur, including physical methods, such as electroporation, microinjection and sonoporation, and chemical methods, such as lipofection and co-precipitation. In this study, transfection was performed using electroporation, whereby transfection is induced using a high voltage electrical shock. This shock temporarily destabilizes the cell membrane rendering it highly permeable to exogenous molecules in the surrounding media. Plasmids can therefore move into the cell via pores, which close when the electrical field is turned off.

The components required for transfection are immortalised mammalian cell lines and a mammalian expression vector which contains a bacterial plasmid, the gene of interest, a

mammalian promoter and a selectable marker which allows the selection of stable transfectants in mammalian cells.

The cell lines used for transfection were low passage, free of contamination, grown in appropriate medium according to optimum conditions recommended by the supplier and were transfected when they were approximately 70-80% confluent to optimize gene uptake.

Following plasmid extraction and verification, the plasmids containing transgenes were used to transfect colorectal cancer cells and empty plasmid vectors (pEF) were also transfected into wild type colorectal cancer cells using the same technique in order to provide a control cell line.

Cells were cultured until approximately 80% confluent, harvested, counted and $1x10^6$ cells were resuspended in 1ml normal media. Five hundred microlitres of this cell suspension (500,000 cells in 500µL) was transferred to an electroporation cuvette and 3-5µL of plasmid was added. The solution was gently mixed using a pipette tip and left at room temperature for 5 minutes. The cuvette was then placed into the electroporator and a pulse of 290-310V at 1200vF capacitance and $\infty\Omega$ was applied to the cuvette. The transfected cell solution was then immediately seeded into a fresh cell culture flask containing pre-warmed normal media supplemented with FCS and antibiotics as appropriate for the cell line. These were then placed in an incubator at 37°C with 5% CO_2 for 24-48 hours.

2.2.5.10 Establishing stable transfected mammalian cell lines

Following 24-48 hours incubation of the transfected cells, the medium was removed with a vacuum aspirator and blasticidin selection media (media containing 5µg/ml blasticidin) added to the flask. The selective media was changed every 3-4 days for around 1-2 weeks until distinct blasticidin resistant colonies were seen. Once selected, stable transfectants were maintained in blasticidin maintenance media (media containing 0.5µg/ml blasticidin) until further use. Cells were maintained in this media thereafter and cultured for use in *in vitro* functional assays. Cells transfected with empty plasmid vector (pEF) were selected and maintained in the same fashion.

Following selection, successful gene manipulation was verified using PCR.

2.2.6 *In vitro* functional assays

The stable transfected cell lines produced by gene transfer were used to explore the effect of altered gene expression on mammalian cell function using in vitro cell function assays.

2.2.6.1 *In vitro* growth assay

In vitro growth assays were performed according to the protocol described by Jiang *et al.* in 2005 (263).

Two hundred microlitres of media containing 2,000 cells was seeded into each well of five 96 well plates using at least six repeats for each cell line. The plates were incubated at 37°C and 5% CO_2 for a period of 24, 48, 72, 96 and 120 hours respectively. On the appropriate day of analysis, the media was removed from the wells using vacuum aspiration and the cells were fixed with 4% formalin for 10-20 minutes before being stained with 0.5% crystal violet for 10 minutes. The dye was then washed off with water and the plates left to air dry.

Cell growth was assessed by counting the number of cells under a light microscope prior to solubilisation of the dye with 200µL acetic acid and measuring the absorbance at 540nm using an absorbance reader (BioTek® ELx800, Swindon, UK). Growth was calculated as a percentage using the 24-hour plate as a baseline measurement to control for any seeding differences.

2.2.6.2 *In vitro* Matrigel® adhesion assay

In vitro adhesion assays were performed according to the protocol described by Jiang *et al* (264). Each well of a 96 well plate was coated with 100µl of serum free media containing 5µl (stock concentration 0.05µg/µl) Matrigel® (Corning®, Tewksbury, MA, USA). The plate was then left to dry in a drying cabinet at 55°C for 2 hours until the Matrigel® was completely dry.

The Matrigel® was then rehydrated with 200µl of sterile water and left for 30 minutes at room temperature. The liquid in each well was then removed with a vacuum aspirator leaving the layer of rehydrated Matrigel® at the base of each well. A cell suspension of 20,000 cells in 200µl media was then seeded into each well and the plate was placed in an incubator for 45 minutes at 37°C with 5%CO_2 to allow time for cells to adhere.

After this incubation time, the media was removed using vacuum aspiration and the plate was gently washed with BSS to remove any non-adherent cells. The adherent cells were then fixed with 4% formalin for 10-20 minutes before being stained with 0.5% crystal violet for 10 minutes. The dye was washed off and the plate left to air-dry before capturing images under the microscope and counting cell number.

In order to ensure the same areas of each well were compared, a gridlines 2mm apart were drawn on the underside of each 96 well plate. This divided each well (internal diameter 6mm) into nine areas. Photographs were then taken from three of these nine areas for each well using a microscope-mounted camera with a 160/0.17 AP10PL 0.25 x 10 lens. Each image was then analysed and the number of cells per photograph counted using Image J software. The average cell count across the three images was then calculated using Excel and used to compare adhesion across different cell lines.

Following photography, the grid was removed from the underside of each 96 well plate using 70% ethanol and 200µL acetic acid was added to each well to solubilise the crystal violet dye. The absorbance was measured at 540nm using an absorbance reader (BioTek® ELx800, Swindon, UK).

2.2.6.3 *In vitro* Matrigel® invasion assay

The inner bases of trans-well inserts with an 8µm pore size (Corning™ Falcon™, ThermoFisher Scientific, Loughborough, UK) were each coated with a solution containing 100µl serum free media and 50µg Matrigel® (stock concentration 0.5µg/µl). The inserts were suspended over the wells of a 24 well plate (Nunc™, ThermoFisher Scientific, Loughborough, UK) using sterile forceps and left to dry in a drying oven for 2 hours at 55°C. The Matrigel® was then rehydrated with 200µl sterile water and left for 30 minutes at room temperature until the Matrigel® was completely rehydrated. The water was removed using vacuum aspiration taking care not to damage the Matrigel® layer and 20,000 cells in 200µl media were seeded into each insert. Six hundred microlitres of media were then pipetted into the well surrounding the insert and the plates were placed in an incubator for 72 hours at 37°C with 5%CO_2. The *in vitro* Matrigel® invasion assay is illustrated in Figure 2.8.

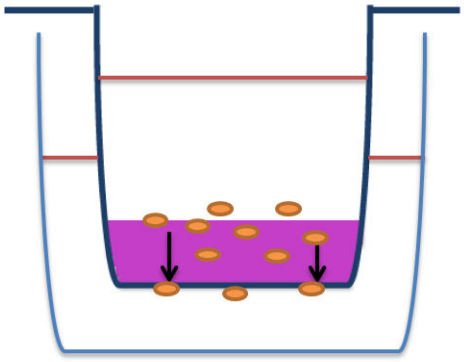

Figure 2.8 *In vitro* Matrigel® invasion assay. (The figure was adapted from MRes thesis of Carly Bunston).

After 72 hours incubation, the Matrigel® layer was carefully removed from the inside of the insert using a cotton bud and cells that had invaded through to the other side of the membrane as well as those that had reached the base of the surrounding well were fixed with 4% formalin for 10-20 minutes prior to staining with 0.5% crystal violet for 10 minutes. The crystal violet was then washed off and the inserts left to air dry. Images were captured of the stained cells and cell counting performed using absorbance as previously described.

2.2.6.4 *In vitro* cell motility assay

Each well of a 24 well plate was seeded with 600µL DMEM-F12 medium containing 10% FCS and antibiotics and 500,000 cells. The plate was incubated at 37C and 5% CO_2 overnight to allow cells to adhere to the plate in a confluent monolayer. The following day, each cell monolayer was wounded in a linear fashion with a sharp sterile pipette tip and photos of the same area of the wounded cells were taken periodically after wounding using the EVOS® Cell Imaging system (Life Technologies, Paisley, UK). Migration distances were measured using Image J software (National Institute of Health, USA).

2.2.7 Clinical cohort study

2.2.7.1 Colorectal cancer cohort patient selection and tissue collection

Primary human colorectal cancer tissue (n=94) and normal colorectal tissue (n=80) were collected during surgery from informed, consenting patients. Of these, 69 pairs of colorectal cancer and normal colorectal tissue were available from the same patient. Tissue was recovered from the operating theatre during the procedure by a researcher and delivered immediately to a Consultant Histopathologist. The Consultant Histopathologist examined the operative specimens and fresh samples of colorectal carcinoma, normal matched colorectal tissue (>10cm away from tumour margin) and mesenteric tissue were obtained. Tissue samples were placed in labelled universal containers, frozen in liquid nitrogen and stored in the research laboratory at -80°C until required. The remaining surgical specimen was fixed and examined by the same Consultant Histopathologist and the subsequent report was obtained for data stratification.

Patients underwent routine clinical, colonoscopic and radiological follow up after the surgery and results were obtained using the hospital clinical portal system and CANISC data. The median follow up period was 65 months.

Ethical approval for the use of tissue was obtained from the South East Wales Local Research Ethics Committee (Reference: 05/WSE03/92).

2.2.7.2 Preparation of tissue samples

Frozen tissue samples were sectioned into 8-10μm sections using a Leica CM1900 Cryostat (Leica Biosystems, Newcastle Upon Tyne, UK). Sections were homogenized to allow RNA extraction.

2.2.7.3 Quantitative PCR analysis of mRNA expression in colorectal cancer tissue

Once extracted, RNA was quantified using a UV spectrophotometer and cDNA was generated as previously described. The quantity of target mRNA transcripts was determined using qPCR as described previously.

2.2.8 Statistical analysis

Mann-Whitney U test for non-parametric data was used to analyse qPCR results. Kruskal-Wallis test was used to analyse the association between T stage and DOK7 level. Survival analyses were performed using Kaplan-Meier survival analysis. Differences were considered to be statistically significant at $p<0.05$.

Chapter 3: Initial assessment of DOK7 in colorectal cancer

3.1 Introduction

Dok-7 is a cytoplasmic adaptor protein that was first identified in 2006 by Okada *et al.* In common with other Dok family members, Dok-7 has SH2 domain target motifs in the C-terminal region along with PH and PTB domains in the N-terminal region (141). The PTB binding domain enables Dok-7 to interact with MuSK resulting in agrin-independent neuromuscular synaptogenesis. Dok-7 is preferentially expressed in skeletal muscle and in the heart and is localised at the post-synaptic neuromuscular junction (141).

The discovery of the Dok proteins and much of the early research on their role occurred in the context of CML but subsequent work has shown that they play a role in a variety of other human cancers, including lung cancer, breast cancer, skin cancer, ovarian cancer and in neurological malignancy. Thus far, the role of Dok-7 in colorectal cancer has not been investigated. However, a recently published study by Heyn *et al*, which investigated DNA methylation in identical twins discordant for breast cancer diagnosis found that the Dok-7 promoter region was hypermethylated in the peripheral blood of twins with breast cancer (265). Moreover, they also found Dok-7 promoter hypermethylation in primary breast cancer tissue and breast cancer cell lines (265). Intriguingly, the authors also reported that hypermethylation of the Dok-7 promoter could be found in peripheral blood years before tumour diagnosis, suggesting that Dok-7 may have potential use as a blood based biomarker (265).

In relation to colorectal cancer, a recent study has demonstrated that Dok-2 expression is reduced in colorectal cancer tissue compared to normal colorectal tissue and that lack of Dok-2 expression is associated with poorer five-year survival and an increased risk of disease recurrence (259). This suggests that the Dok family may play a tumour suppressor role in colorectal cancer but, to date, there have been no studies looking at the expression of Dok-7

in colorectal cancer or its association with clinical and pathological characteristics of the disease or patient outcomes.

The study presented in this chapter aimed to examine the mRNA expression profile of DOK7 in colorectal cancer tissues obtained from a clinical cohort and in colorectal cancer cell lines, with the subsequent aim of developing *in vitro* cell models that would allow us to explore the effect of DOK7 expression on colorectal cancer cell function. Moreover, we analysed the association between DOK7 expression and clinicopathological features of colorectal cancer and patient outcomes using qPCR in order to determine whether DOK7 may have any potential role as a biomarker in colorectal cancer.

3.2 Materials and methods

3.2.1 Materials and methods for determination of DOK7 expression in colorectal cancer patient cohort tissue samples

3.2.1.1 Patient selection

Colorectal cancer tissue and normal colorectal tissue were obtained from patients undergoing curative surgery for colorectal cancer in three hospitals in South Wales; University Hospital of Wales, Llandough Hospital and the Royal Gwent Hospital over the 1 year collection phase of the study.

In order to be included in the study, patients had to meet all of the following criteria; proven colorectal cancer, deemed suitable for surgery with curative intent following MDT discussion and informed pre-operative consent obtained from the patient and the Consultant Surgeon responsible for their care. Lt. Col. Mansel Davies, a research fellow working in the laboratory at the time, identified patients fulfilling these criteria at the time of MDT discussion.

3.2.1.2 Collection of tissue samples

The collection of tissue samples is described in Section 2.2.7.1.

3.2.1.3 Isolation of RNA and cDNA from tissue samples

Frozen tissue samples were sectioned into 8-10μm sections using a Leica CM1900 Cryostat and homogenized. RNA was isolated from the homogenized tissue using TRI Reagent® as described in Section 2.2.2.1, quantified as described in Section 2.2.2.2 and converted into cDNA by reverse transcription using a High Capacity cDNA Reverse Transcription kit as described in Section 2.2.2.3.

3.2.1.4 Quantitative PCR

Quantitative PCR to determine the level of DOK7 mRNA expression was simultaneously performed on all of the cDNA samples obtained from the patient cohort using the DOK7F1 and DOK7ZR1 primers, details of which are listed in Table 2.6. The components and conditions used for qPCR are provided in Section 2.2.2.6.2.

3.2.1.5 Statistical analysis

Data obtained from qPCR was analysed using the Mann-Whitney test for non-parametric data and Kruskal-Wallis test. Survival analysis was performed using Kaplan-Meier survival analysis. The threshold for statistical significance was $p<0.05$. Multivariate analysis was not performed as it was felt that this was not appropriate given the nature of the data.

3.2.2 Materials and methods for determination of DOK7 expression in colorectal cancer cell lines

3.2.2.1 Colorectal cancer cell lines

The details of the colorectal cancer cell lines used in this study are shown in Section 2.1.1. All cells were maintained according to the supplier's instructions. Details of the media used for cell culture are provided in Section 2.1.6.1 and the methods of cell culture used are described in Section 2.2.1.

HECV, a cell line originating from human umbilical cord tissue, was used as a positive control.

3.2.2.2 Primers

The primers used in this study are shown in Table 3.1. Full details of these primers are shown in Table 2.6.

Table 3.1. Primers used for determination of DOK7 expression in colorectal cancer tissues and colorectal cancer cell lines, DOK7 expression, ribozyme synthesis and orientation checking

Gene	Primer
DOK7	DOK7F1 DOK7ZR1
DOK7	DOK7F8 DOK7R8
DOK7	DOK7F9 DOK7R9
DOK7	DOK7exF2 DOK7exR4
DOK7	DOK7rib1F DOK7rib1R
DOK7	DOK7rib2F DOK7rib2R
pEF/His TOPO TA plasmid vector	T7F BGHR
GAPDH	GAPDHF10 GAPDHR10

3.2.2.3 RNA isolation and cDNA synthesis

RNA was isolated from cells using TRI Reagent® (Sigma-Aldrich Inc., Poole. UK) as described in Section 2.2.2.1, and quantified using a spectrophotometer as described in Section 2.2.2.2. Reverse transcription using a High Capacity cDNA Reverse transcription kit was used to synthesis cDNA as described in Section 2.2.2.3.

3.2.2.4 PCR

The synthesised cDNA was screened for DOK7 expression using PCR. The components and conditions used for PCR are described in Section 2.2.2.4.2.

Size separation of the resulting PCR products was performed using 2% agarose gel electrophoresis and visualized using SYBR® Safe DNA gel stain (Life Technologies Ltd, Paisley, UK) and UV transillumination as described in Section 2.2.2.5.

3.2.2.5 qPCR

Quantitative PCR to determine the level of DOK7 mRNA expression was performed on the cDNA samples obtained from the colorectal cell lines using the Amplifluor™ Universal Detection system (Intergen®, New York, USA) as described in Section 2.2.2.6 using the DOK7F1 and DOK7ZR1 primers, details of which are listed in Table 2.6. The components and conditions used for qPCR are described in Section 2.2.2.6.2.

3.2.3 Materials and methods used for the knockdown and overexpression of DOK7

The manipulation of gene expression was performed using techniques described in Section 2.2.5.

3.2.3.1 Generation of DOK7 ribozyme transgenes

Hammerhead ribozymes targeting DOK7 were designed using Zuker's mRNA Fold programme and used to generate primers. Ribozymes were then synthesised using touchdown PCR using the components and conditions described in Section 2.2.5.3.

The PCR products obtained were then run on a 2% agarose gel to verify their presence and size prior to being cloned into a plasmid vector.

3.2.3.2 Generation of DOK7 expression constructs

A DOK7 expression construct was created using the DOK7 expression primers listed in Table 2.6 using the techniques described in Section 2.2.5. The PCR products obtained were then run on a 2% agarose gel to verify their presence and size prior to being cloned into a plasmid vector.

3.2.3.3 TOPO TA cloning of DOK7 transgenes into a pEF6/His TOPO plasmid vector

The verified DOK7 ribozyme/expression inserts were cloned into a pEF6/V5-His-TOPO plasmid (Invitrogen, Paisley, UK) as described in Section 2.2.5.4 and then transformed into chemically competent *E.coli*, as described in Section 2.2.5.5.

3.2.3.4 Orientation checking

Following overnight incubation, orientation checking and selection of correctly oriented colonies was performed as described in Section 2.2.5.6 using T7F and BGHR primers, the details of which are given in Table 2.6.

3.2.3.5 Amplification and purification of correctly oriented colonies

The correctly oriented colonies (DOK7expCol3, DOK7rib1Col4, DOK7rib2Col3) were then amplified and purified using the GenElute™ Plasmid Miniprep Kit (Sigma-Alrich, St.Louis, MO, USA) as described in Section 2.2.5.7. Plasmids were verified using agarose gel electrophoresis as described previously in Section 2.2.2.5. .

3.2.3.6 Transfection of colorectal cancer cells and generation of stable transfectants

Transfection of colorectal cancer cells using electroporation was performed as described in Section 2.2.5.9. An empty pEF plasmid vector was used to transfect colorectal cancer cells using the same technique in order to provide a control cell line. Stable transfected colorectal cancer cell lines were established as described in Section 2.2.5.10.

3.2.3.7 Verification of DOK7 knockdown using RT-PCR and Q-PCR

Verification of transfection was carried out using PCR and qPCR as previously described.

3.2.4 Materials and methods for determination of DOK7 expression in other human cancers

3.2.4.1 Additional cancer cell lines

3.2.4.1.1 Breast cancer cell lines

Three breast cancer cell lines were used in this study: ZR-751, MCF-7 and MDA-MB-231. These cell lines were acquired from the ECACC (Salisbury, UK) or ATCC (Middlesex, UK) and their characteristics are listed in Table 3.2.

Table 3.2 Details of breast cancer cell lines used in this study

	ZR-75-1	MCF-7	MDA-MB-231
Species	Human	Human	Human
Tissue	Breast adenocarcinoma, established from malignant ascites	Breast adenocarcinoma, established from a malignant pleural effusion	Breast adenocarcinoma, established from a malignant pleural effusion
Gender	Female	Female	Female
Age	63 years	69 years	51 years
Morphology	Epithelial	Epithelial	Epithelial
Growth mode	Adherent	Adherent	Adherent
Characteristics	Ductal carcinoma ER+, PR+, HER2+	Ductal carcinoma ER+, PR+, HER2-	ER-, PR-, HER2-
Country		USA	

These breast cancer cell lines were screened for DOK7 expression using the same methods described for colorectal cancer cells in Section 3.2.2.

3.2.4.2 Additional clinical cohort data

3.2.4.2.1 Gastric cancer clinical cohort

3.2.4.2.1.1 Patient selection

Gastric adenocarcinoma and Siewert type III gastro-oesophageal junction adenocarcinoma tissues (n = 245) with matched adjacent background tissues (n = 158) were collected immediately after surgical resection at the Beijing Cancer Hospital from informed, consented patients. All patients underwent surgery without any prior treatment. The tissue samples were stored at -80^{o}C at the Tissue Bank of Peking University Oncology School with a record of the relevant clinical and histopathological data. All protocols were reviewed and approved by the Beijing Cancer Hospital Research Ethics Committee (MTA10062009).

3.2.4.2.1.2. Collection of tissue samples

Tissue was recovered from the operating theatre during the procedure by a researcher and delivered immediately to a Consultant Histopathologist. The surgical specimen was examined by the Consultant Histopathologist, who obtained fresh samples of gastric carcinoma, normal matched gastric tissue and mesenteric tissue. Tissue samples were placed in labelled universal containers, frozen in liquid nitrogen and were stored in the research laboratory at -80°C prior to use. The remaining surgical specimen was fixed and examined by the same Consultant Histopathologist and the subsequent report was obtained for data stratification.

3.2.4.2.1.3 Isolation of RNA and cDNA from tissue samples

Frozen tissue samples were sectioned into 8-10μm sections using a Leica CM1900 Cryostat and homogenized. RNA was isolated from the homogenized tissue using TRI Reagent® as described in Section 2.2.2.1, quantified as described in Section 2.2.2.2 and converted into cDNA by reverse transcription using a High Capacity cDNA Reverse Transcription kit as described in Section 2.2.2.3.

3.2.4.2.1.4 Quantitative PCR

Quantitative PCR to determine the level of DOK7 mRNA expression was simultaneously performed on the cDNA samples obtained from the gastric cancer patient cohort using the Amplifluor™ Universal Detection system (Intergen®, New York, USA) as described in Section 2.2.2.6 using the DOK7F1 and DOK7ZR1 primers, details of which are listed in Table 2.6. The components and conditions used for qPCR are described in Section 2.2.2.6.2.

3.2.4.2.1.5 Statistical analysis

Data obtained from qPCR was analysed using the Mann-Whitney test for non-parametric data and Kruskal-Wallis test. Survival analysis was performed using Kaplan-Meier survival analysis. The threshold for statistical significance was $p<0.05$. Data was normalized by RNA concentration.

3.3 Results

3.3.1 Cohort data

3.3.1.1 Patient demographics

A total of 94 samples were obtained from primary colorectal cancer tissue and 80 samples were obtained from normal background colorectal tissue (See Section 2.2.7.1). Paired cancer and normal samples were available for 68 patients, enabling both overall and paired (within patient) comparisons to be undertaken.

3.3.1.2 Histopathological features of cohort colorectal cancers

The histopathological features of the tumours included in this study are shown in Table 3.3. All tumour samples included in the current study were confirmed adenocarcinomas. Metastatic status of the tumour was defined as the presence of metastases either at the time of surgery or the development of metastases in the follow up period.

Table 3.3 Histopathological features of colorectal cancer tissue samples

			Number (Percentage)
Anatomical location	Colon	Right colon	28 (29.8%)
		Transverse colon	2 (2.1%)
		Left colon	22 (23.4%)
	Rectum		22 (23.4%)
	Location unknown		20 (21.3%)
Tumour grade	1 (well differentiated)		2 (2.1%)
	2 (moderately differentiated)		54 (57.4%)
	3 (poorly differentiated)		14 (14.9%)
	Grade unknown		24 (25.5%)
Dukes' stage	A		7 (7.4%)
	B		33 (35.1%)
	C		32 (34.0%)
	Dukes' stage unknown		22 (23.4%)
T stage	T1		2 (2.1%)
	T2		10 (10.6%)
	T3		40 (42.6%)
	T4		18 (19.1%)
	T stage unknown		24 (25.5%)
Overall tumour stage	I		9 (9.6%)
	II		30 (31.9%)
	III		26 (27.7%)
	IV		6 (6.4%)
	Overall stage unknown		23 (24.5%)
Nodal status	Node negative (N0)		39 (41.5%)
	1-3 lymph nodes positive (N1)		16 (17.0%)
	≥4 lymph nodes positive (N2)		15 (16.0%)
	Nodal status unknown		24 (25.5%)
Metastatic status	Distant metastases		19 (20.2%)
	No distant metastases		50 (53.2%)
	Metastatic status unknown		25 (26.6%)

3.3.1.3 DOK7 expression is significantly reduced in colorectal cancer compared to normal colorectal tissue

The expression of DOK7 is significantly reduced in colorectal cancer compared to normal colorectal tissue. Median DOK7 mRNA expression per 50µg of total cellular RNA was 148.9 copies for colorectal carcinoma tissue samples (n = 94, IQR = 41-525) compared with 342.3 for normal colorectal tissue (n = 80, IQR = 63-1104, p = 0.0199) for the whole cohort and 121.2 (n = 68, IQR = 42-407) vs. 342.3 copies (n = 68, IQR = 73-1104) respectively for the paired tissue samples (p = 0.0090). Data is shown in Figure 3.1.

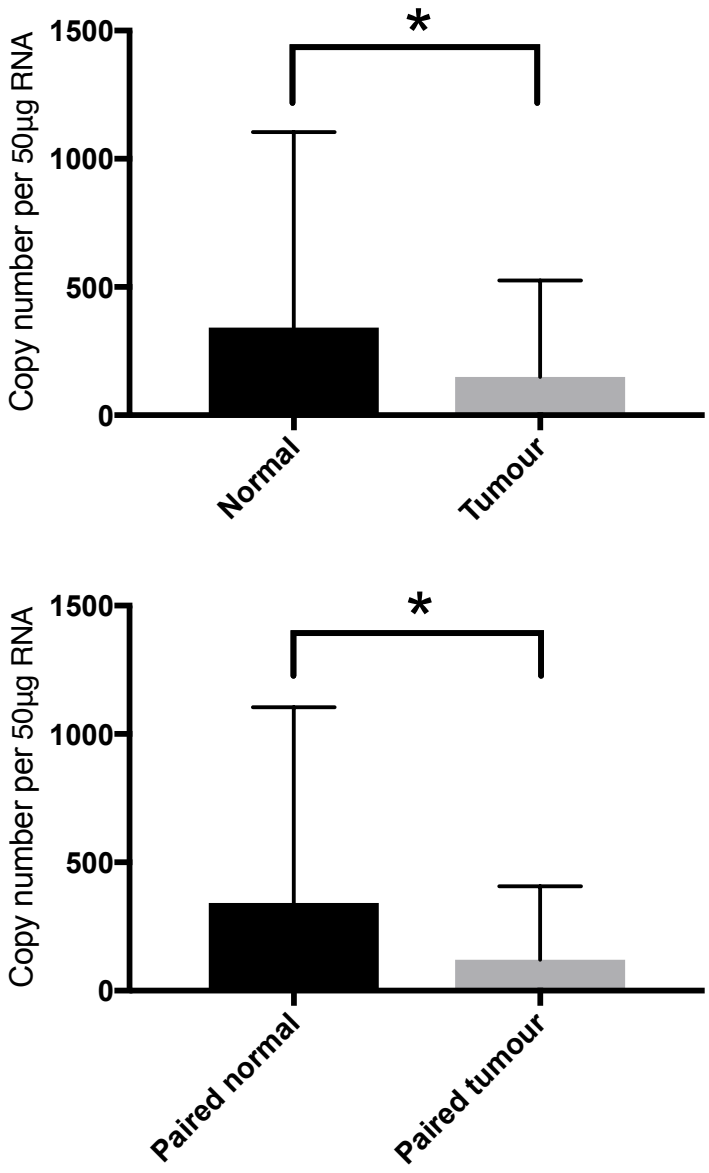

Figure 3.1. DOK7 expression in colorectal cancer and normal colorectal tissue. In this figure and in all subsequent figures in this chapter * indicates $p < 0.05$.

3.3.1.4 DOK7 expression is not related to degree of colorectal tumour differentiation

The expression of DOK7 in relation to the grade of tumour differentiation is shown in Figure 3.2. The median copy number per 50μg of total cellular RNA was reduced in grade 1 (median copy number 106.0, n = 2, IQR not calculated due to sample size), grade 2 (median copy number 138.1, n = 54, IQR = 43-525) and grade 3 colorectal cancer samples (median copy number 140.0, n = 14, IQR = 18.6 – 444.8) compared to normal colorectal tissue (median copy number 342.3, n = 80, IQR = 63-1104). Median copy number was significantly reduced in Grade 2 cancer samples compared to normal colorectal tissue ($p = 0.0312$) and for Grade 2 and Grade 3 samples combined *vs.* normal tissue ($p = 0.0124$) but failed to reach significance for Grade 1 samples *vs.* normal ($p = 0.2859$) and Grade 3 samples *vs.* normal ($p = 0.0639$). Analysis using the Kruskal-Wallis test did not reveal a significant difference in median copy number between different grades of tumour differentiation ($p = 0.714$).

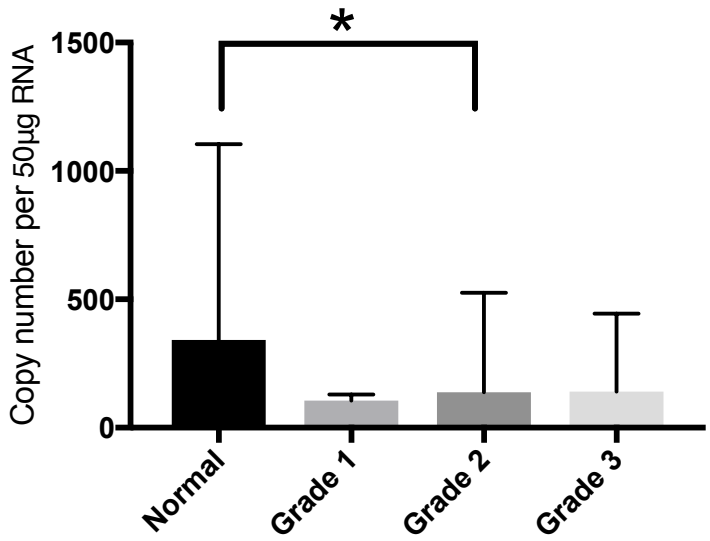

Figure 3.2 DOK7 expression by degree of tumour differentiation

3.3.1.5 DOK7 expression is significantly decreased in node negative colorectal cancer compared with normal colorectal tissue

DOK7 expression was significantly decreased in node negative colorectal cancer samples compared with normal colorectal tissue (median copy number 131.5, n = 39, IQR = 28-451 *vs.* 342.3, n = 80, IQR = 63-1104 respectively, p = 0.0159). By comparison, there was a trend towards increased median copy number in colorectal cancer samples from patients with N1 disease (median copy number 399.8, n = 16, IQR = 123-680). DOK7 expression was decreased in N2 colorectal cancer samples compared to normal (median copy number 74.8, n = 15, IQR = 18-298).

There was no significant difference in median copy number between patients with node negative and node positive disease (131.5 *vs.* 144.6, p = 0.5906). DOK7 expression in relation to nodal status of colorectal cancer tissue samples is shown in Figure 3.3.

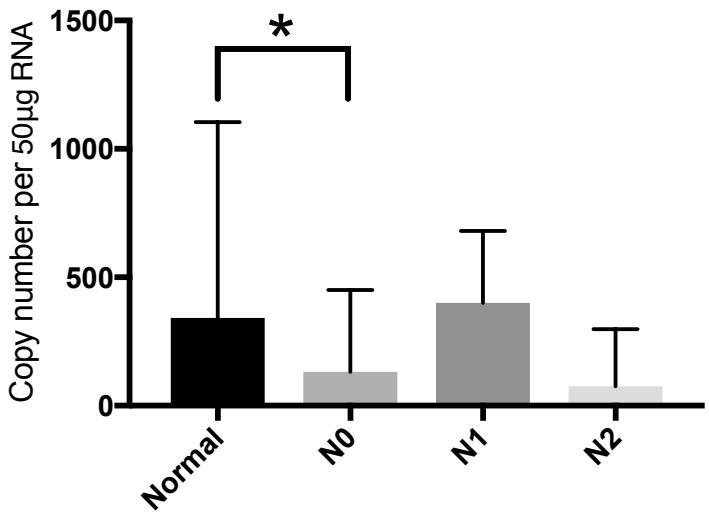

Figure 3.3 DOK7 expression by nodal status of colorectal cancer

3.3.1.6 DOK7 expression is significantly reduced in Dukes' stage B colorectal cancer compared to normal colorectal tissue

DOK7 expression was reduced across all Dukes' stages of colorectal cancer compared to normal colorectal tissue (Dukes' A median copy number 153.2, n = 7, IQR = 59-1308; Dukes' B median copy number 119.6, n = 33, IQR = 27-382; Dukes' C median copy number 168.9, n = 32, IQR = 57-568 vs. median copy number 342.3, n = 80, IQR 63-1104 for normal colorectal tissue) but did not reach statistical significance except for the Dukes' B group ($p = 0.0068$). DOK7 expression in relation to Dukes' stage is shown in Figure 3.4.

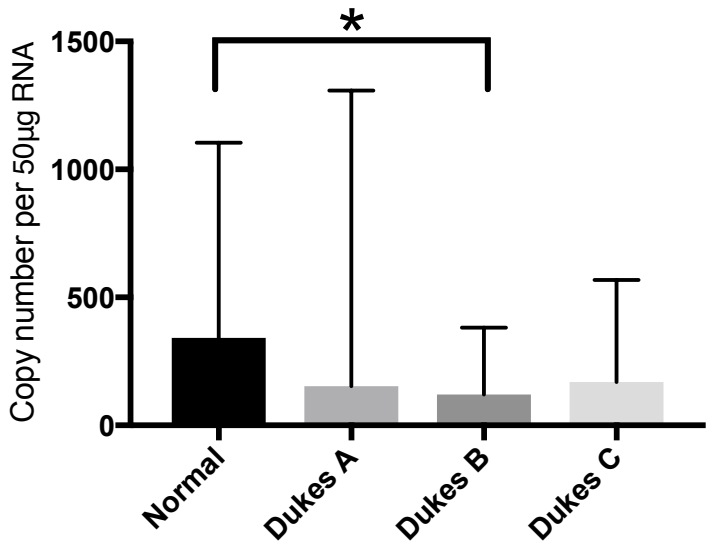

Figure 3.4 DOK7 expression and Dukes' stage of colorectal cancer

3.3.1.7 DOK7 expression is inversely associated with T stage in colorectal cancer

The level of DOK7 expression decreases with increasing T stage. Median DOK7 mRNA expression per 50μg of total cellular RNA was 2560.5 for T1 disease (n = 2, IQR not calculated due to sample size), 466.6 for T2 disease (n = 10, IQR = 111-1248), 120.3 for T3 disease (n = 40, IQR = 30-388) and 134.8 for T4 disease (n = 18, IQR = 25.2-419.1). In comparison with normal colorectal tissue (median copy number 342.3, n = 80, IQR = 63-1104), the median copy number was not significantly different for T1 (p = 0.0952) or T2 disease (p = 0.9693) but was significantly reduced in both T3 (0.0048) and T4 (p = 0.0287) disease.

When T stages were combined, median copy number was significantly reduced in T2/3 cancers (median copy number 130.8, p = 0.0161), T3/4 cancers (median copy number 120.3, p = 0.0013) and T2/3/4 cancers (median copy number 130.8, p = 0.0043) in comparison with normal colorectal tissue.

Further analysis of the colorectal cancer samples using the Kruskal-Wallis test revealed a significant difference in DOK7 expression between T stages (p = 0.038). DOK7 expression in relation to T stage in colorectal cancer is shown in Figure 3.5.

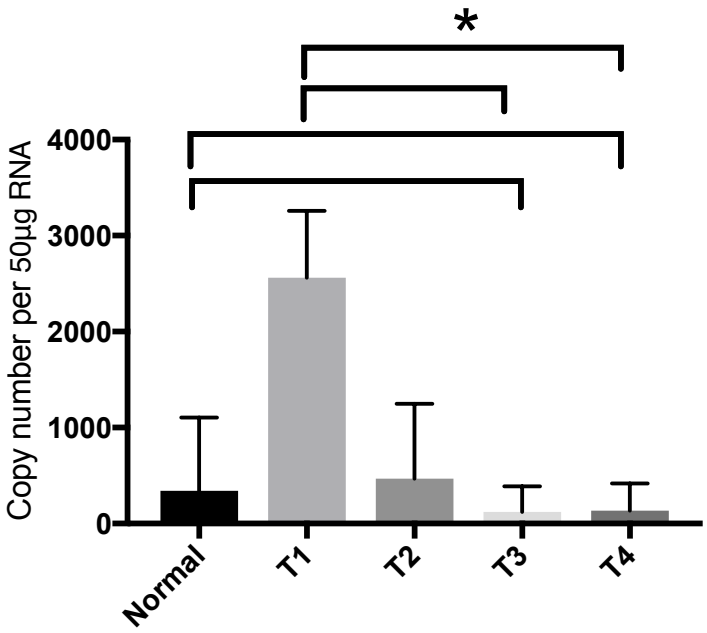

Figure 3.5 DOK7 expression and T stage of colorectal cancer

3.3.1.8 DOK7 expression is significantly reduced in Stage II colorectal cancer

Compared to normal colorectal tissue (median copy number 342.3, n = 80, IQR = 63-1104), DOK7 expression was increased in Stage I disease (median copy number 531.4, n = 9, IQR = 93-1322, p = 0.7133), decreased in Stage II disease (median copy number 113.9, n = 30, IQR = 24-329, p = 0.0023), decreased in Stage III disease (median copy number 137.4, n = 26, IQR = 67.6-566.8, p =0.1778) and decreased in Stage IV disease (median copy number 238.5, n = 6, IQR = 15-1703, p = 0.4924). However, only the difference in DOK7 median copy number between normal colorectal tissue and Stage II disease reached statistical significance. Between-group comparison revealed that there was a significant difference in DOK7 expression between Stage I and Stage II colorectal cancer (p = 0.0404) but not between other stages. Kruskal-Wallis test did not reveal a significant difference between different stages of disease (p = 0.206). DOK7 expression in relation to the overall stage of disease is shown in Figure 3.6.

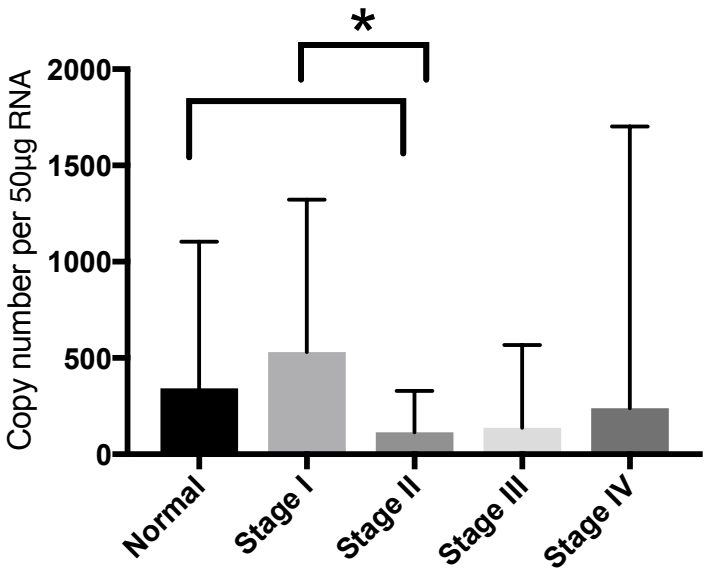

Figure 3.6 DOK7 expression and overall stage of colorectal cancer

3.3.1.9 DOK7 expression is significantly reduced in right sided colonic tumours and in rectal cancers

When analysed by anatomical location, DOK7 expression was significantly reduced in right-sided colonic cancers (median copy number 94.8, n = 28, IQR = 21-381, p = 0.0183) and in rectal cancers (median copy number 157.1, n = 22, IQR = 49.7-411.1, p = 0.0419) when compared with normal colorectal tissue (median copy number 342.3, n = 80, IQR = 63-1104). DOK7 expression in left sided colonic cancers was also reduced compared to normal colorectal tissue but failed to reach statistical significance (median copy number 136.4, n = 22, IQR = 58-557, p = 0.2223). In transverse colonic tumour samples, median copy nmber was 350 (n = 2, IQR not calculated due to sample size). There was no significant difference between median copy number between cancer samples at different sites. DOK7 expression in relation to anatomical location of tumour is shown in Figure 3.7.

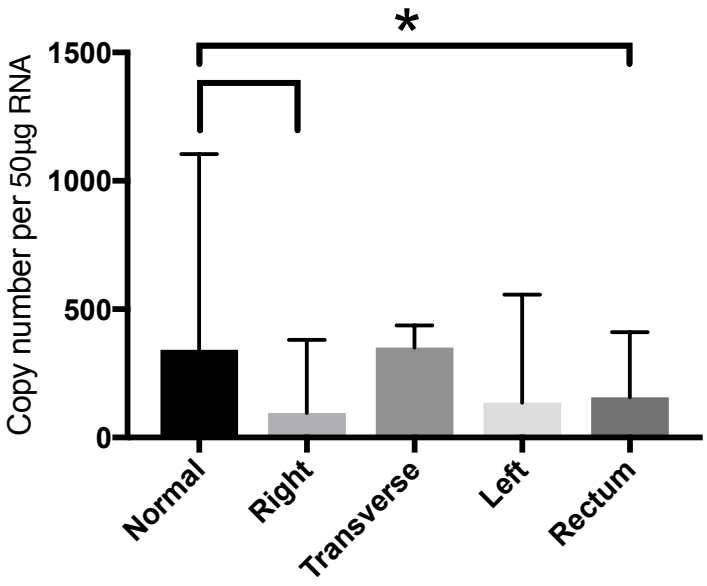

Figure 3.7 DOK7 expression and anatomical location of colorectal cancer

3.3.1.10 DOK7 expression is not associated with neoadjuvant/adjuvant treatment status

DOK7 expression was significantly lower in colorectal cancer tissue obtained from patients who had not undergone, or did not undergo neoadjuvant or adjuvant treatment respectively compared to normal colorectal tissue (median copy number 129.8, n = 42, IQR = 43-495 vs. 342.3, n = 80, IQR = 63-1104 respectively, p = 0.0417). DOK7 expression was also lower in colorectal cancer tissue obtained from patients who underwent adjuvant chemotherapy (median copy number 144.6, n = 13, IQR = 35-636) and neoadjuvant chemoradiotherapy (median copy number 90.0, n = 5, IQR = 50.7-358.2) but this failed to reach statistical significance (p = 0.2086 and p = 0.2247 respectively). In the sole patient who had radiotherapy, the median copy number was 1.2609 (IQR not calculated due to sample size). There was no significant difference in the level of DOK7 expression between those undergoing no additional treatment and those undergoing either adjuvant chemotherapy or neoadjuvant chemoradiotherapy.

3.3.1.11 DOK7 expression is not associated with invasiveness of tumour

Compared to normal colorectal tissue, DOK7 expression in colorectal cancer tissue was significantly reduced in both invasive (median copy number 125.5, $p = 0.0367$) and non-invasive (142.4, $p = 0.0319$) disease. There was no significant difference in level of DOK7 expression found in colorectal cancer samples from patients with invasive and non-invasive disease ($p = 0.7550$).

3.3.1.12 DOK7 expression and disease-free survival

The level of DOK7 expression was significantly reduced in colorectal cancer tissue samples taken from both patients who remained disease-free (median copy number 108.2, $p = 0.0321$) and in those in who did not (median copy number 153.2, $p = 0.0359$). There was no significant difference in level of DOK7 expression between those who remained disease-free and those who did not ($p = 0.6794$).

3.3.1.13 DOK7 expression and survival status

The level of DOK7 expression was significantly lower in colorectal cancer tissue samples obtained from both patients who were alive (median copy number 79.5, $p = 0.0109$) at the end of follow up and those who died (median copy number 165.4, $p = 0.0373$). There was no significant difference in level of DOK7 expression between survivors and those who died ($p = 0.3089$).

3.3.1.14 DOK7 expression and presence of metastatic status

The level of DOK7 expression was observed to be lower in colorectal cancer tissue samples obtained from both patients with distant metastases (median copy number 193.2, $p = 0.0984$), and those without (median copy number 114.8, $p = 0.0526$) compared to normal colorectal tissue but this was not found to be statistically significant. There was no significant difference in level of DOK7 expression between those patients with distant metastases and those without ($p = 0.7625$).

3.3.1.15 DOK7 expression and local recurrence disease

The level of DOK7 expression was significantly lower in colorectal cancer tissue samples obtained from patients who did not subsequently go on to have local recurrence (median copy number 136.4, $p = 0.0435$). Although the level of DOK7 expression was reduced in colorectal cancer tissue samples from patients who did have subsequent disease recurrence, this difference was not statistically different (median copy number 177.6, $p = 0.2119$). The level of DOK7 expression was not significantly different between those patients who had local recurrence of their disease and those who did not ($p = 0.7270$).

3.3.1.16 DOK7 expression and patient survival

The Kaplan-Meier survival curve for DOK7 expression in colorectal cancer (dichotomized according to the median DOK7 transcript number for the whole cohort) is shown below. Low DOK7 expression is associated with significantly reduced survival ($p = 0.011$) when compared with the survival of patients with high levels of DOK7 expression. Data is shown in Figure 3.8.

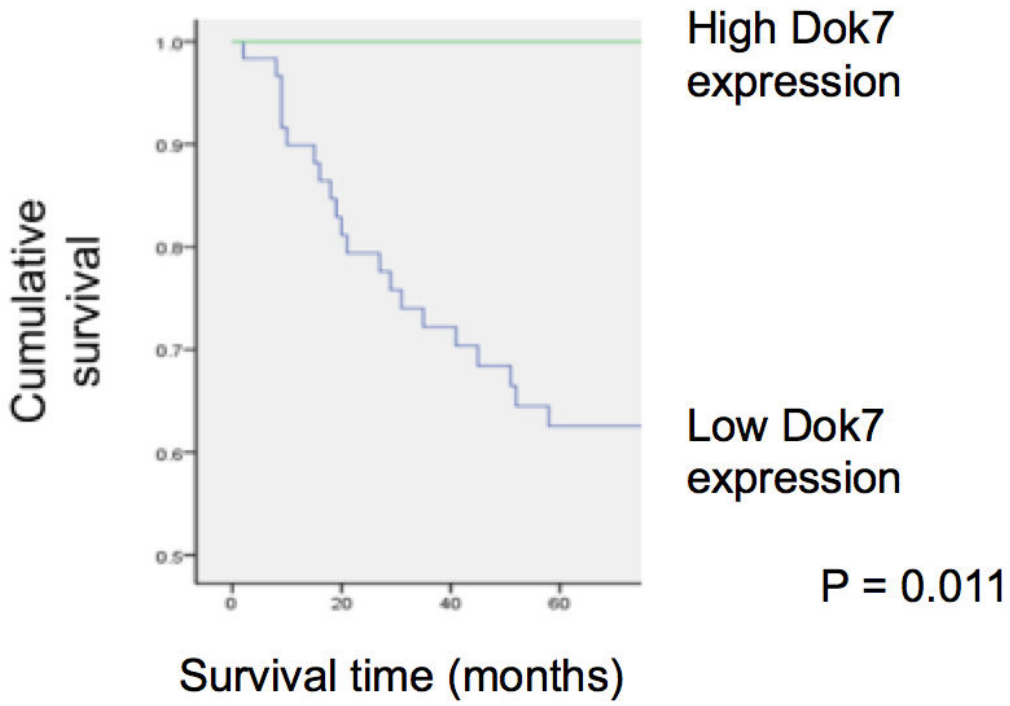

Figure 3.8 Kaplan-Meier survival curve for DOK7 expression in colorectal cancer cohort dichotomized according to the median value of DOK7 expression for the whole cohort. Blue line represents low DOK7 mRNA expression (n = 62); green line represents high DOK7 expression (n = 12).

3.3.2 Colorectal cell line data

3.3.2.1 DOK7 is variably expressed in colorectal cancer cell lines

The expression of DOK7 was examined in four colorectal cancer cell lines: HT-115, RKO, HRT-18 and Caco-2. HECV cell line was used as a control. Screening PCR revealed that DOK7 expression in colorectal cancer cell lines is variable. Expression of DOK7 is highest in HRT-18 cells with weaker expression seen in Caco-2 cells and little or no expression seen in HT-115 and RKO cells. Data is shown in Figure 3.9. Three cell lines were chosen for further analysis: HRT-18, HT-115 and RKO.

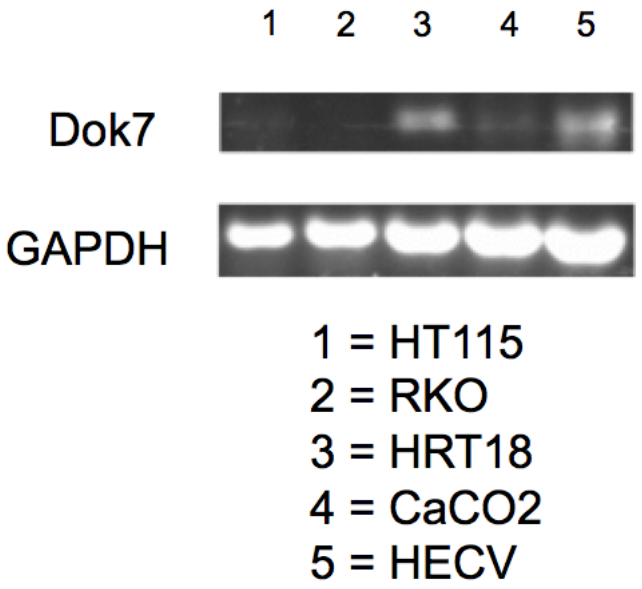

Figure 3.9 DOK7 expression in human colorectal cancer cell lines

3.3.2.2 Expression of DOK7 in HRT-18 ribozyme transgenic cell lines

Two ribozyme transgenes were used to attempt knockdown of DOK7 in HRT-18 cells: rib1 and rib2 which were used singly and in combination to produce three transgenic cell lines: HRT-18rib1, HRT-18rib2 and HRT-18rib1+2. Expression of DOK7 in these transgenic cell lines was examined using PCR. There was no reduction in DOK7 expression in HRT-18rib1 cell line. Expression of DOK7 in HRT-18rib2 and HRT-18rib1+2 appeared to be reduced but was not completely knocked out. Data is shown in Figure 3.10.

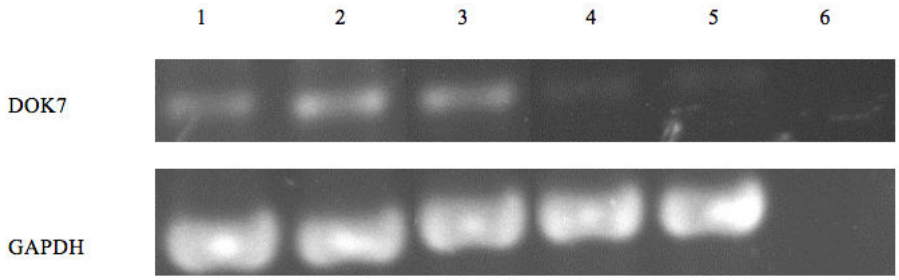

Legend: 1 = HRT18WT, 2 = HRT18pEF, 3 = HRT18rib1, 4 = HRT18rib2, 5 = HRT18rib1+2, 6 = Negative

Figure 3.10 DOK7 expression in HRT-18rib1, HRT-18rib2 and HRT-18rib1+2 transgenic cell lines

3.3.2.3 Attempted DOK7 overexpression in HT-115 and RKO cells

A DOK7 expression insert was used to forcibly overexpress DOK7 in HT-115 and RKO cells to produce two transgenic cell lines: HT115exp and RKOexp.

Expression of DOK7 in these transgenic cell lines was examined using PCR. There was no reduction in DOK7 expression in HRT-18rib1 cell line. DOK7 expression was not convincingly increased in either HT-115exp or RKOexp cells compared to the pEF control. Data is shown in Figure 3.11 and 3.12.

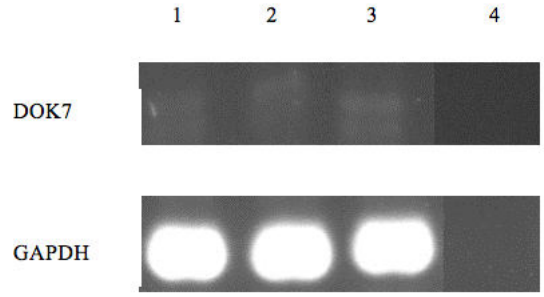

Legend: 1 = HT115WT, 2 = HT115pEF, 3 = HT115exp, 4 = Negative

Figure 3.11 DOK7 expression in HT-115exp cell line

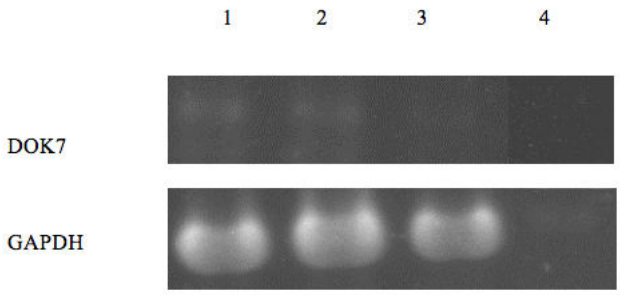

Legend: 1 = RKOWT, 2 = RKOpEF, 3 = RKOexp, 4 = Negative

Figure 3.12 DOK7 expression in RKOexp cell line

3.3.2.4 Analysis of transgenic cell lines using qPCR

Analysis using qPCR showed increased DOK7 expression in RKOexp transfected cells compared to pEF cells but failed to show increased expression in HT115exp or reduced expression in HRT18 knockdown cells.

3.3.3 DOK7 expression in other human cancers

3.3.3.1 Breast cancer cell line data

See Appendix 5.

3.3.3.2 Gastric cancer clinical cohort data

See Appendix 6.

3.4 Discussion

To our knowledge, this is the first study to attempt to characterise the expression of DOK7 in colorectal cancer and our data show a number of interesting findings. DOK7 mRNA expression is significantly reduced in colorectal cancer compared to normal colorectal tissue, both across the whole dataset and when paired data is analysed separately. This is in keeping with previous (unpublished) findings in the host laboratories that show reduced levels of DOK7 expression in breast cancer tissue compared to normal breast tissue, suggesting a potential tumour suppressor role for DOK7.

Furthermore, DOK7 expression is inversely related to colorectal cancer T stage and DOK7 expression is low in T3/T4 and Dukes' B cancers, suggesting a possible role in primary tumour growth and bowel wall invasion. Whilst there was no significant difference in DOK7 expression by nodal status or metastatic status, survival analysis shows that low DOK7 expression is associated with poorer survival compared to high DOK7 mRNA expression, in keeping with a potential tumour suppressor role.

Analysis of DOK7 mRNA expression in human colorectal cancer cell lines revealed that DOK7 is variably expressed in colorectal cancer cells. DOK7 is strongly expressed by HRT-18 colorectal cancer cells with weaker levels of expression seen in Caco-2 and little or no DOK7 expression seen in HT-115 and RKO cells, the more poorly differentiated and highly aggressive colorectal cancer cell lines. In breast cancer cell lines, DOK7 expression was reduced or absent in MDA-MB-231, a poorly differentiated metastatic breast adenocarcinoma. However, analysis of DOK7 mRNA expression in our gastric cancer cohort failed to demonstrate any significant difference in expression between gastric cancer and normal gastric tissue. Furthermore, there was no significant difference in DOK7 mRNA expression between gastric cancer samples when analysed by T stage, nodal status, distant metastases, overall stage, location within the stomach, disease free status and overall survival.

A search of online gene array data identified a cohort of 585 colorectal cancer samples with 19 non-tumour tissues (gene array cohort data shown in Appendix 7). Interestingly, analysis of this cohort revealed that DOK7 mRNA expression was increased in colorectal cancer compared to normal colorectal tissue (median DOK7 value 4.493 vs. 4.358, $p = 0.037$), the opposite to what was found in our dataset. Moreover, when this cohort of colorectal cancers were divided into subgroups representing different molecular subtypes as identified by Marisa *et al* and analysed for level of DOK7 expression there was a significant difference in DOK7 expression in different molecular subtypes ($p = 0.05$) (266).

Again, in contrast to our findings, analysis of this cohort failed to show any association between DOK7 mRNA expression and T stage ($p = 0.616$) but showed that DOK7 mRNA expression was significantly reduced in node positive disease compared to node negative colorectal cancers (median DOK7 value 4.416 vs. 4.525, $p = 0.001$) and was significantly reduced in Stage III tumours compared to Stage II ($p < 0.01$) and Stage IV tumours ($p < 0.05$). In keeping with our findings, DOK7 mRNA expression was not affected by presence of distant metastases ($p = 0.171$). Finally, survival analysis revealed that high DOK7 expression, defined by expression levels over the 75% centile, was associated with significantly poorer overall survival ($p = 0.033$). There are many possible explanations for the differences seen between our own data and that from the online gene array – there were very few non-tumour tissues included in the gene array cohort, there is no information provided as to how the gene array data was collected and it is not possible to check that the primers used were similar to those used in our laboratories, leading to significant limitations in the ability to compare our results with that of the gene array data set.

Aberrations in cell signalling pathways downstream of tyrosine kinases have been associated with many types of human cancer. Previous studies have shown that the Dok proteins act as tumour suppressors in a range of human cancers including leukaemia (142, 143, 255), lung

cancer (90), breast cancer (257) and histiocytic sarcoma (261). Conflicting results have been shown in relation to ovarian cancer (267).

In colorectal cancer, previous studies have shown that Dok-2 expression is reduced in colorectal cancer tissue compared with normal colorectal tissue and that loss of Dok-2 expression is associated with disease recurrence and poorer five-year overall survival (259).

There is currently a lack of information regarding the role of DOK7 in cancer. In 2013, Heyn *et al* investigated DNA methylation in identical twins who were discordant for breast cancer diagnosis (258). They found hypermethylation of the DOK7 promoter region in the peripheral blood of the twins with breast cancer, in primary breast cancer tissue and breast cancer cell lines (258). However, there are, to-date, no published studies on the role of DOK7 in colorectal cancer.

Following verification of DOK7 mRNA expression in the clinical cohort and colorectal cancer cells, we had planned to use gene transfer techniques to create cells with knockdown or overexpression of DOK7. However, PCR failed to show successful DOK7 expression in transfected RKO and HT-115 cells and there was incomplete knockdown of DOK7 in transfected HRT-18 cells despite repeating the PCR several times with freshly prepared primers, running check PCR of expression plasmids and optimizing the conditions of the expression primers.

Further investigation revealed that DOK7 has several different variants, which code for Dok7 isoforms. A diagrammatic representation of the structures of DOK7 variants 1-3 is shown in Figure 3.13.

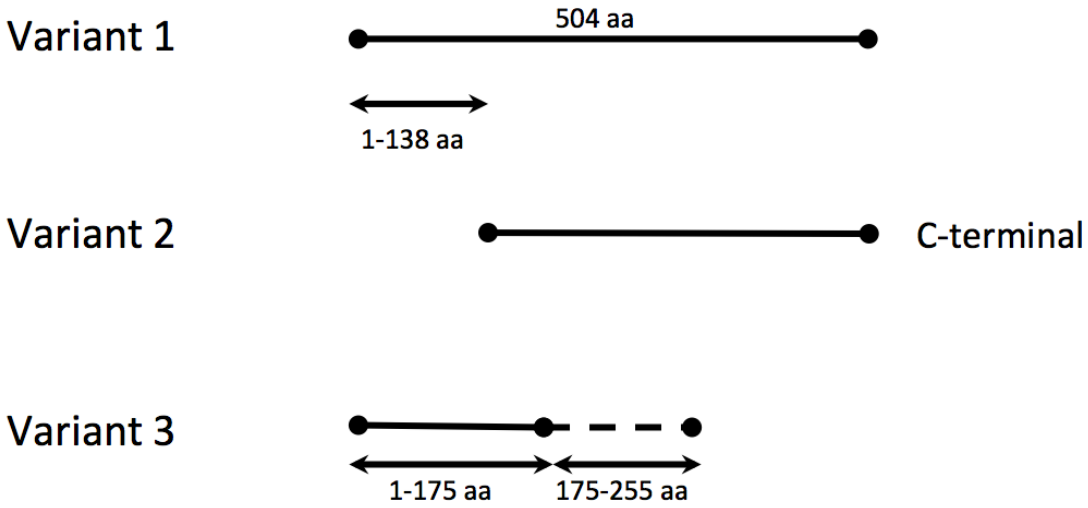

Figure 3.13 Diagrammatic representation of the structure of DOK7 isoforms 1-3 coded for by DOK7 variants 1-3 (DOK7V1-3)

The software programme Primer 3 was used to assess the product sizes that would be produced using the existing DOK7 primers for variants 1-3. This revealed similar/identical product sizes for more than one transcript variant of DOK7 across the range of primers used as shown in Table 3.4. It therefore became apparent that due to overlaps in the structure of these variants, the existing plasmids and primers had not been able to distinguish between these variants resulting in our inability to confirm successful knockdown.

Table 3.4 Product sizes produced with DOK7 primers for DOK7V1, DOK7V2 and DOK7V3 demonstrating lack of specificity of DOK7 primers for DOK7 variants

Primers	DOK7V1	DOK7V2	DOK7V3
Dok7F8R8	409bp	409bp	409bp
Dok7F9R9	479bp	468bp	-
Dok7exF2R4	1512bp	1501bp	-
Dok7F1ZR1	129bp	129bp	-
Dok7F2ZR2	115bp	115bp	115bp

These variants and isoforms present an interesting challenge and may explain the differences in DOK7 mRNA expression seen in our own cohort compared to the cohort of 585 colorectal cancer cases, though this difference may also be due to the limitations already described above. A review of the previous literature did not yield any reference to the existence of these variants and isoforms in previous laboratory studies and thus there is no advice on how these variations should be accommodated for in the design of primers or antibodies nor any preceding data on the expression of these variants or the role of their corresponding isoforms. This discovery led us to develop new DOK7 variant specific qPCR primers and the development of these and the variant specific expression profiles obtained using these are the subject of the next chapter.

In summary, our data suggest that DOK7 expression is reduced in colorectal cancer, particularly in T3/4 disease and that low DOK7 expression is associated with poorer patient survival. These results are consistent with the pattern of DOK protein expression found in relation to other Dok family members in a range of human cancers and to the expression of Dok-2 in relation to colorectal cancer. We therefore suggest that DOK7 may play a potential tumour suppressor role in relation to colorectal cancer.

Chapter 4: Expression of DOK7 variant-1, -2 and -3 (V1, V2 and V3) in colorectal cancer clinical cohort

4.1 Introduction

The downstream of tyrosine kinase (DOK) protein family has seven members, DOK1-7. The precise role of these proteins is not entirely clear although some authors have suggested a potential tumour suppressor role. The aim of this clinically oriented PhD is to determine the role of DOK7 in colorectal cancer and to establish if there is an association between DOK7 expression and clinical outcome.

During initial investigations, analysis of three human colorectal cancer cell lines (HRT18, HT115 and RKO) revealed high DOK7 expression in HRT18 and little or no expression in HT115 and RKO cells. Analysis of tissue obtained from a cohort of patients with colorectal cancer revealed that DOK7 expression was significantly reduced in colorectal cancer tissue compared with normal colorectal tissue ($p=0.0199$) and that DOK7 level was significantly negatively correlated with increasing T stage ($p = 0.038$).

Initial attempts to knockdown DOK7 using ribozyme transgenes in HRT18 colorectal cancer cells were partly successful. However, attempts to overexpress DOK7 in HT115 and RKO cells failed. Further investigations revealed that DOK7 has several isoforms encoded by several transcript variants.

Having established the relative structures of DOK7 variant 1 (DOK7V1), DOK7 variant 2 (DOK7V2) and DOK7 variant 3 (DOK7V3), the aim of the work presented in this chapter was to produce variant specific DOK7 primers and to determine the expression of DOK7V1-3 in both the clinical cohort and the colorectal cancer cell lines. It was hoped that this would potentially allow variant specific *in vitro* cell models to be subsequently developed that would allow the effect of DOK7 variant expression on colorectal cancer cell function to be explored.

4.2 Materials and methods

4.2.1 Materials and methods for determination of DOK7V1/V2/V3 expression in colorectal cancer patient cohort tissue samples

4.2.1.1 Patient selection

The selection of patients has previously been discussed in Section 3.2.1.1.

4.2.1.2 Collection of tissue samples

The collection of tissue samples is described in Section 2.2.7.1.

4.2.1.3 Isolation of RNA and cDNA from tissue samples

Frozen tissue samples were sectioned into 8-10μm sections using a Leica CM1900 Cryostat and homogenized. RNA was isolated from cells using TRI Reagent® (Sigma-Aldrich Inc., Poole. UK), as described in Section 2.2.2.1, and quantified using a spectrophotometer as described in Section 2.2.2.2. Reverse transcription using a High Capacity cDNA Reverse transcription kit was used to synthesis cDNA as described in Section 2.2.2.3.

4.2.1.4 Quantitative PCR

Quantitative PCR to determine the level of DOK7 V1/V2/V3 mRNA expression was simultaneously performed on all of the cDNA samples obtained from the patient cohort using the variant specific primers shown in Table 4.1, which were designed using an online primer design tool (Primer blast, https://www.ncbi.nlm.nih.gov/tools/primer-blast/). The full details of these primers are shown in Table 2.6.

The components and conditions used for qPCR are provided in Section 2.2.2.6.2.

Table 4.1 Variant specific qPCR primers

Gene	Primer
DOK7V1	DOK7V1F1 DOK7V1ZR1
DOK7V2	DOK7V2F1 DOK7V2ZR1
DOK7V3	DOK7V3F1 DOK7V3ZR1

4.2.1.5 Statistical analysis

Data obtained from qPCR was analysed using the Mann-Whitney test for non-parametric data and Kruskal-Wallis test. Survival analysis was performed using Kaplan-Meier survival analysis. The threshold for statistical significance was $p<0.05$. Data was normalized by RNA concentration.

4.2.2 Materials and methods for determination of DOK7V1/V2/V3 expression in colorectal cancer cell lines

4.2.2.1 Colorectal cancer cell lines

The details of the colorectal cancer cell lines used in this study are shown in Section 2.1.1. All cells were maintained according to the supplier's instructions. Details of the media used for cell culture are provided in Section 2.1.6.1 and the methods of cell culture used are described in Section 2.2.1.

4.2.2.2 Primers

The variant specific primers used in this study are shown in Table 4.2. Full details of these primers are shown in Table 2.6.

Table 4.2 Variant specific primers and product sizes

		Product sizes obtained with DOK7 variant (bp)		
Gene	Primer pair	Variant 1	Variant 2	Variant 3
DOK7V1	DOK7V1 F8R8	595	-	-
	DOK7V1 F9R9	609	-	-
DOK7V2	DOK7V2 F8R8	-	597	-
DOK7V3	DOK7V3 F8R8	-	-	229
	DOK7V3 F9R9	-	-	227

4.2.2.3 RNA isolation and cDNA synthesis

RNA was isolated from cells using TRI Reagent® (Sigma-Aldrich Inc., Poole. UK), as described in Section 2.2.2.1, and quantified using a spectrophotometer as described in Section 2.2.2.2. Reverse transcription using a High Capacity cDNA Reverse transcription kit was used to synthesis cDNA as described in Section 2.2.2.3.

4.2.2.4 PCR

The synthesised cDNA was screened for DOK7V1/V2/V3 expression using PCR. The components and conditions used for PCR are described in Section 2.2.2.4.2.

Size separation of the resulting PCR products was performed using 1-2% agarose gel electrophoresis and visualized using SYBR® Safe DNA gel stain (Life Technologies Ltd, Paisley, UK) and UV transillumination as described in Section 2.2.2.5.

4.2.2.5 qPCR

Quantitative PCR to determine the level of DOK7V1/V2/V3 mRNA expression was performed on the cDNA samples obtained from the colorectal cell lines using the Amplifluor™ Universal Detection system (Intergen®, New York, USA) as described in Section 2.2.2.6 and the variant specific qPCR primers listed in Table 4.1.

The components and conditions used for qPCR are described in Section 2.2.2.6.2.

4.3 Results

4.3.1 Cohort data

4.3.1.1 Patient demographics

The patient demographics are shown in Section 3.3.1.1.

4.3.1.2 Tumour histopathological features

The histopathological features of the colorectal tumours of patients included in this study are shown in Table 3.3.

4.3.1.3 DOK7V1 expression

4.3.1.3.1 DOK7V1 expression is significantly reduced in colorectal cancer compared to normal colorectal tissue

The expression of DOK7V1 is significantly reduced in colorectal cancer compared to normal colorectal tissue. Median DOK7V1 mRNA expression per 50μg of total cellular RNA (copy number) was 0.4 (IQR = 0.0-5.8) copies for colorectal carcinoma tissue (n = 94) compared with 18.1 (IQR = 9.3-638.5) for normal colorectal tissue (n = 80) (p = 0.0000) for the whole cohort, and 0.2 (IQR = 0.0-3.4) vs. 17.6 (IQR = 8-768) copies for paired tissue samples (n = 68 in each group) respectively (p = 0.0000). Data is shown in Figure 4.1 below.

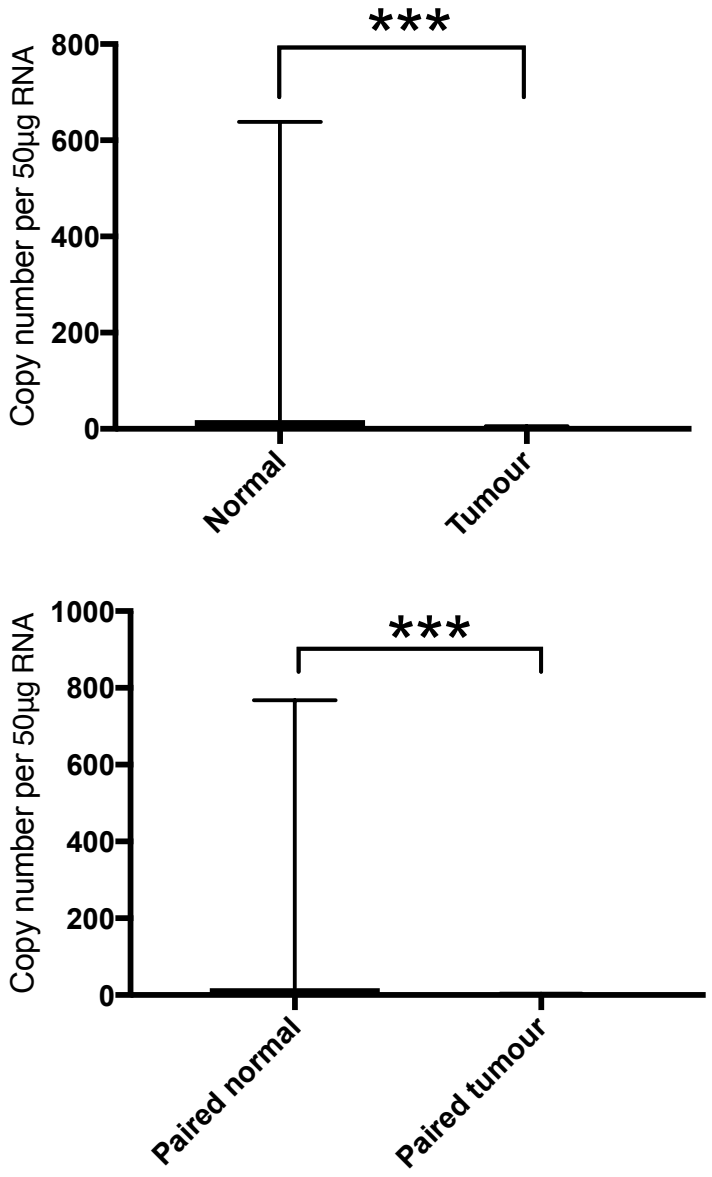

Figure 4.1 DOK7V1 mRNA expression in colorectal cancer and normal colorectal tissue. In this figure and all subsequent figures in this chapter, * indicates $p < 0.05$, ** indicates $p < 0.01$ and *** indicates $p < 0.001$.

4.3.1.3.2 DOK7V1 expression is not related to degree of colorectal tumour differentiation

The expression of DOK7V1 in relation to degree of tumour differentiation is shown in Figure 4.2. The median copy number per 50µg of total cellular RNA was significantly reduced in Grade 1 (1.2 copies, n = 2, IQR not calculated due to sample size, p = 0.0183), Grade 2 (0.2 copies, n = 54, IQR = 0.0-4.8, p = 0.0000) and Grade 3 (2.0 copies, n = 14, IQR = 0-35, p = 0.0004) colorectal cancer tissue compared to normal colorectal tissue (18.1 copies, n = 80, IQR = 9.3-638.5). Analysis using the Kruskal-Wallis test did not reveal a significant difference in median copy number between different grades of tumour differentiation (p = 0.264).

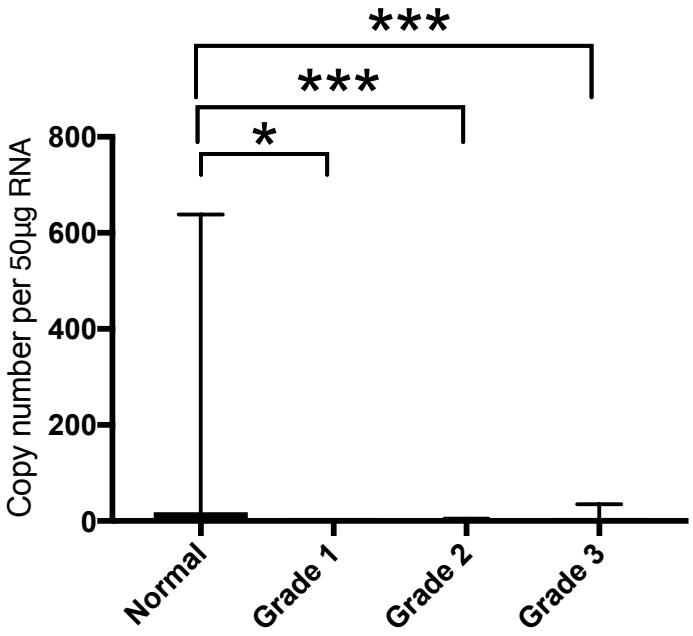

Figure 4.2 DOK7V1 expression by degree of tumour differentiation

4.3.1.3.3 DOK7V1 expression is not related to colorectal cancer nodal status

DOK7V1 expression was significantly decreased in node negative colorectal cancer samples compared with normal colorectal tissue (median copy number 0.5, n = 39, IQR = 0.0-4.7 *vs.* 18.1, n = 80, IQR = 9.3-638.5) respectively, p = 0.0000). Median DOK7V1 mRNA expression per 50μg of total cellular RNA (copy number) was 1.3 (IQR = 0.1-15.2) in colorectal cancer tissue obtained from patients with N1 disease (n = 16) and 0.2 (0-9) in colorectal cancer tissue obtained from patients with N2 disease (n = 15). There was no significant difference in median copy number between patients with node negative and node positive disease (0.5 *vs.* 0.2, p = 0.4854). DOK7V1 expression in relation to colorectal cancer nodal status is shown in Figure 4.3.

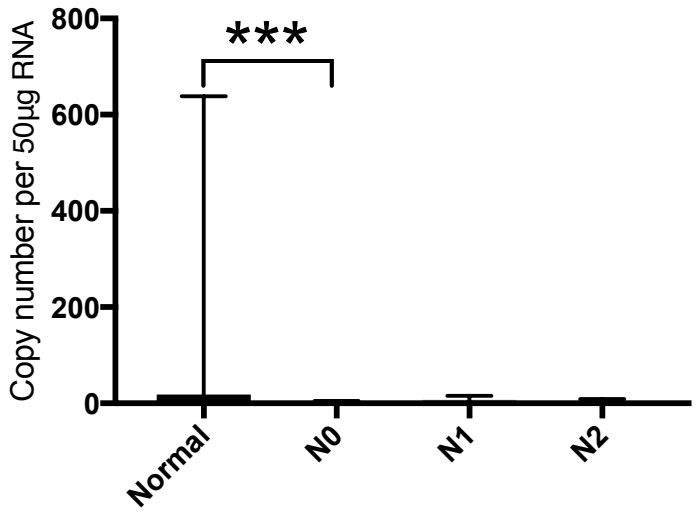

Figure 4.3 DOK7V1 mRNA expression by nodal status of colorectal cancer

4.3.1.3.4 DOK7V1 expression is significantly reduced across all Dukes' stage colorectal cancer

DOK7V1 expression was significantly reduced across all Dukes' stages of colorectal cancer compared to normal colorectal tissue (median copy number 1.7 (IQR = 0.355-3.699), 0.1 (IQR = 0.0-5.9) and 0.2 (IQR = 0.1-15.4) for Dukes' A (n = 7), Dukes' B (n = 33) and Dukes' C (n = 32) tumours respectively compared to 18.1 (IQR = 9.3-638.5) in normal colorectal tissue, p values = 0.0000 for all three comparisons). DOK7V1 expression in relation to Dukes' stage is shown in Figure 4.4.

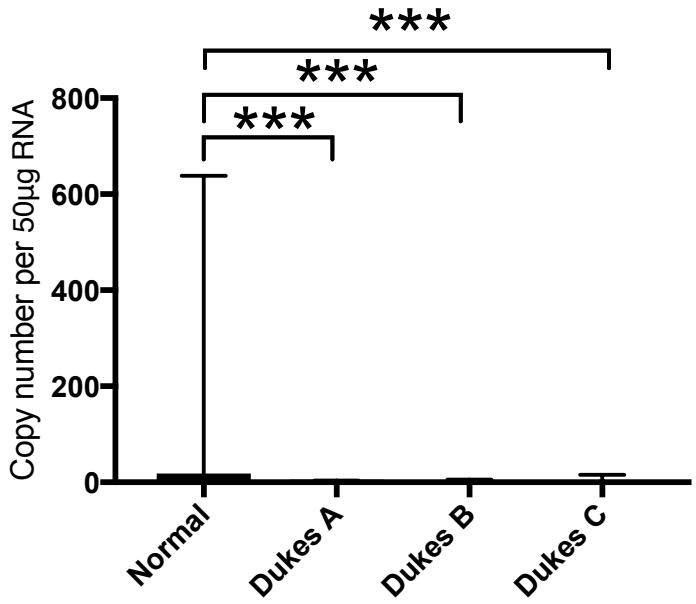

Figure 4.4 DOK7V1 mRNA expression and Dukes' stage of colorectal cancer

4.3.1.3.5 DOK7V1 expression and T stage of colorectal cancer

The level of DOK7V1 expression decreased with increasing T stage, with median copy numbers of 6.8 (n = 2, IQR not calculated due to sample size) for T1 disease, 3.6 (n = 10, IQR = 0-22) for T2 disease, 0.2 (n = 40, IQR = 0.0-2.7) for T3 disease and 0.1 (n = 18, IQR = 0.0-8.5) for T4 disease. In comparison with normal colorectal tissue (n = 80, median DOK7V1 mRNA expression 18.1, IQR = 9.3-638.5), the median copy number was not significantly different for T1 (p = 0.0952) but was significantly reduced in T2 (p = 0.0125), T3 (p = 0.0000) and T4 (p = 0.0000) disease. DOK7V1 expression in relation to T stage is shown in Figure 4.5

When T stages were combined, median copy number was significantly reduced in T2/3 cancers (median copy number 0.5, p = 0.0000), T3/4 cancers (median copy number 0.2, p = 0.0000) and T2/3/4 cancers (median copy number 0.2, p = 0.0000) in comparison with normal colorectal tissue.

Further analysis of the colorectal cancer samples using the Kruskal-Wallis revealed that the difference in DOK7V1 expression between T stages was not significant (p = 0.072).

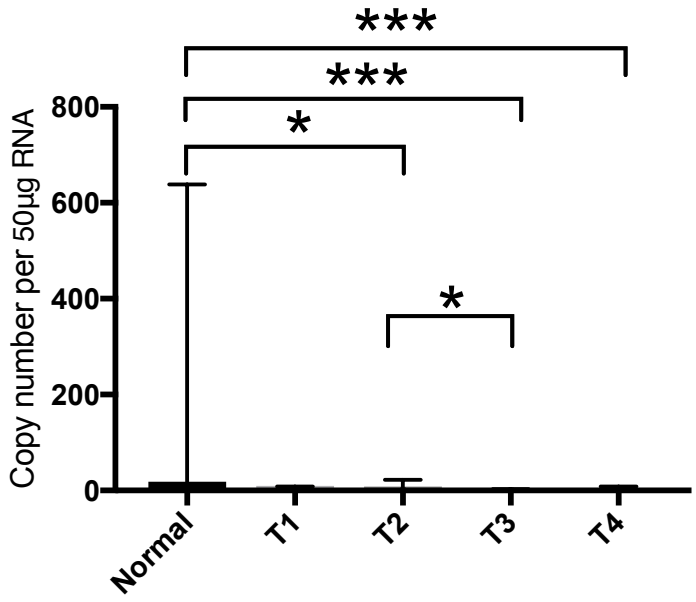

Figure 4.5 DOK7V1 expression and T stage of colorectal cancer

4.3.1.3.6 DOK7V1 expression is significantly associated with overall stage of colorectal cancer

Compared to normal colorectal tissue (median copy number 18.1, n = 80, IQR = 9.3-638.5), DOK7V1 expression was reduced in Stage I disease (median copy number 2.5, n = 9, IQR = 0.44-7.30, p = 0.0001), decreased in Stage II disease (median copy number 0.1, n = 30, IQR = 0.0-3.6, p = 0.0000), decreased in Stage III disease (median copy number 0.2, n = 26, IQR = 0.0-5.7, p =0.0000) and increased in Stage IV disease (median copy number 60.0, n = 6, IQR = 1.6-259.1, p = 0.3827), though the latter failed to reach statistical significance. Between-group comparisons using the Kruskal-Wallis test revealed that there was a significant difference in DOK7V1 expression between different stages of disease (p = 0.041). DOK7V1 expression in relation to overall stage of colorectal cancer is shown in Figure 4.6.

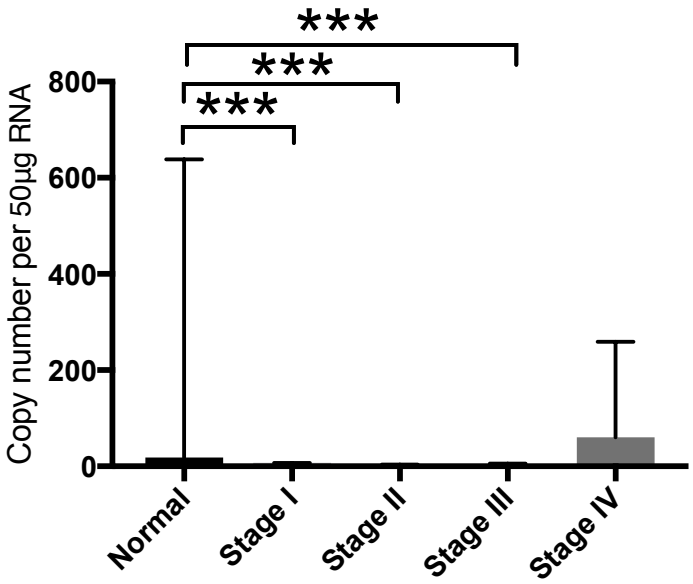

Figure 4.6 DOK7V1 expression and overall stage of colorectal cancer

4.3.1.3.7 DOK7V1 expression and anatomical location of colorectal cancer

When analysed by anatomical location, DOK7V1 expression was significantly reduced in right-sided colonic cancers (median copy number 0.2, n = 28, IQR = 0-6, p = 0.0000), left-sided colonic cancers (median copy number 0.8, n = 22, IQR = 0.1-4.9, p = 0.0000) and transverse colonic cancers (median copy number 0.0, n = 2, IQR not calculated due to sample size, p = 0.0169) when compared with normal colorectal tissue (median copy number 18.1, n = 80, IQR = 9.3-638.5). DOK7V1 expression in rectal cancers was also significantly reduced compared to normal colorectal tissue (median copy number 0.1, n = 22, IQR = 0.0-1.3, p = 0.0000). There was no significant difference in DOK7V1 expression between cancer samples at different sites. DOK7V1 expression in relation to anatomical site of colorectal tumour is shown in Figure 4.7.

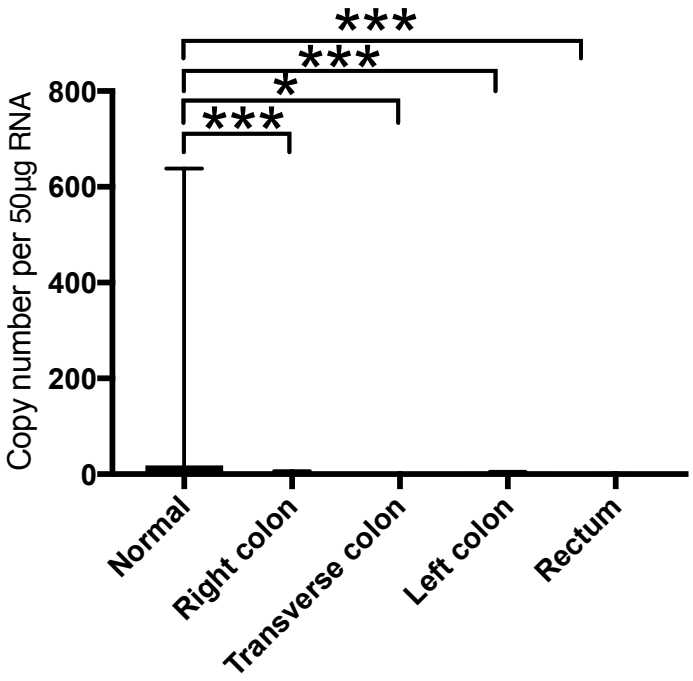

Figure 4.7 DOK7V1 expression and anatomical location of colorectal cancer

4.3.1.3.8 DOK7V1 expression and neoadjuvant/adjuvant treatment status

DOK7V1 expression was significantly lower in colorectal cancer tissue obtained from patients who did not undergo any additional therapy compared to normal colorectal tissue (median copy number 0.3, n = 42, IQR = 0.0-3.0 vs. 18.1, n = 80, IQR = 9.3-638.5 respectively, p = 0.0000). DOK7V1 expression was also significantly lower in colorectal cancer tissue obtained from those patients who underwent adjuvant chemotherapy (median copy number 0.2, n = 13, IQR = 0.02-0.42, p = 0.0000) and neoadjuvant chemoradiotherapy (median copy number 0.0, n = 5, IQR = 0.003 – 0.409, p = 0.0002) compared to normal colorectal tissue. In the one patient who underwent adjuvant radiotherapy, median DOK7V1 expression was 0 (IQR not calculated due to sample size). There was no significant difference in the level of DOK7V1 expression between those who received no additional treatment and those who had either undergone adjuvant chemotherapy or neoadjuvant chemoradiotherapy. DOK7V1 expression in relation to neoadjuvant/adjuvant treatment status is shown in Figure 4.8.

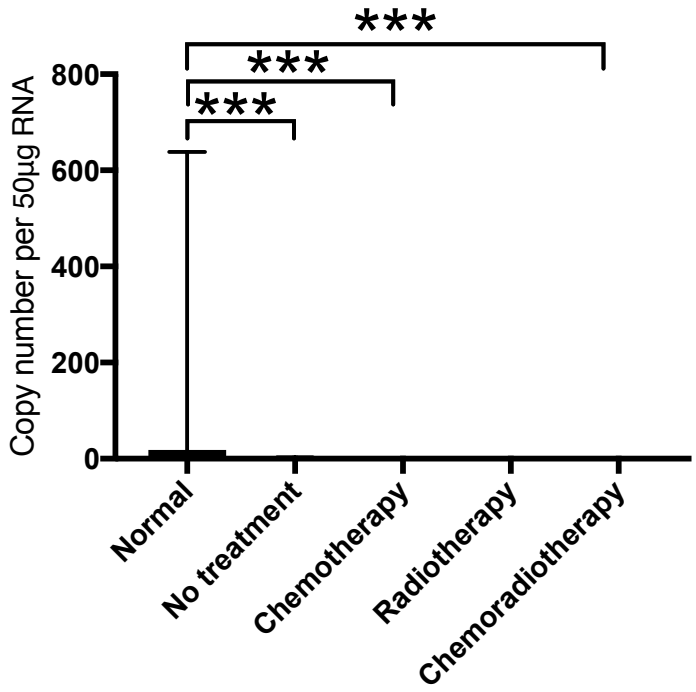

Figure 4.8 DOK7V1 expression and neoadjuvant/adjuvant treatment status

4.3.1.3.9 DOK7V1 expression and tumour invasiveness

Compared to normal colorectal tissue, DOK7V1 expression in colorectal cancer tissue was reduced in both invasive (median copy number 0.2, p = 0.0000) and non-invasive disease (median copy number 0.3, p = 0.0000). There was no significant difference in level of DOK7V1 expression between colorectal cancer samples from those with invasive and those with non-invasive disease (p = 0.7508).

4.3.1.3.10 DOK7V1 expression and disease-free status

The level of DOK7V1 expression was significantly reduced in colorectal cancer tissue samples taken from both patients who remained disease-free (median copy number 0.6, p = 0.0000) and those who did not (median copy number 0.1, p = 0.0000) patients. The level of DOK7V1 expression was significantly lower in colorectal cancer samples from patients did not remain disease-free compared to those who remained disease-free (p = 0.0230).

4.3.1.3.11 DOK7V1 expression and survival status

The level of DOK7V1 expression was significantly lower in colorectal cancer tissue samples obtained from both patients who were alive (median copy number 0.2, p = 0.0000) at the end of follow up and those who died (median copy number 0.1, p = 0.0000). There was no significant difference in the level of DOK7V1 expression in colorectal cancer samples obtained from patients who were alive compared to those who had died (p = 0.1239).

4.3.1.3.12 DOK7V1 expression and metastatic status

The level of DOK7V1 expression was observed to be lower in colorectal cancer tissue samples obtained from both patients with distant metastases (median copy number 0.1, p = 0.0000), and those without (median copy number 0.4, p = 0.0000) compared to normal colorectal tissue. There was no significant difference in the level of DOK7V1 expression in colorectal cancer samples obtained from patients with distant metastases compared to those with without (p = 0.1564).

4.3.1.3.13 DOK7V1 expression and local recurrence of disease

The level of DOK7V1 expression was significantly lower in colorectal cancer tissue samples obtained both from patients who did and did not subsequently go on to have local recurrence (median copy number 0.0 vs. 0.2, p = 0.0000 and p = 0.0000). There was no significant difference in level of DOK7V1 expression between colorectal cancer samples obtained from patients with local recurrence compared to those obtained from patients without (p = 0.1010).

4.3.1.3.14 DOK7V1 expression and overall patient survival

The Kaplan-Meier survival curve for DOK7V1 expression in colorectal cancer (dichotomized according to the median value of DOK7V1 expression for the whole cohort) is shown below in Figure 4.9. Low DOK7V1 expression (n = 26) is associated with reduced overall survival when compared with the overall survival of patients with high levels of DOK7V1 expression (n = 48) but this difference failed to reach statistical significance (p = 0.093).

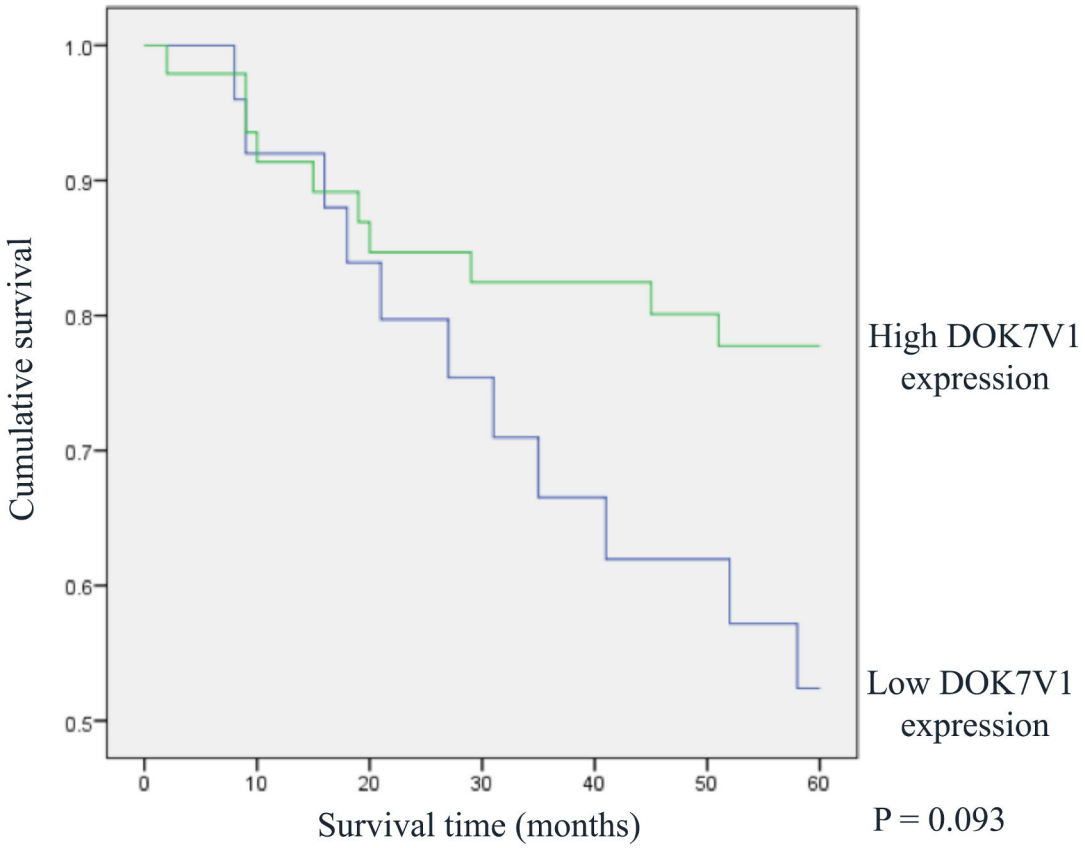

Figure 4.9 Overall patient survival in patients with high (green) DOK7V1 expression (n = 48) compared to those with low (blue) DOK7V1 expression (n = 26)

4.3.1.3.15 DOK7V1 expression and disease-free patient survival

The Kaplan-Meier disease-free survival curve for DOK7V1 expression in colorectal cancer (dichotomized according to the median value of DOK7V1 expression for the whole cohort) is shown below in Figure 4.10. Low DOK7V1 expression (n = 26) is associated with significantly reduced disease-free survival when compared with the disease-free survival of patients with high levels of DOK7V1 expression (n = 48) (p = 0.036).

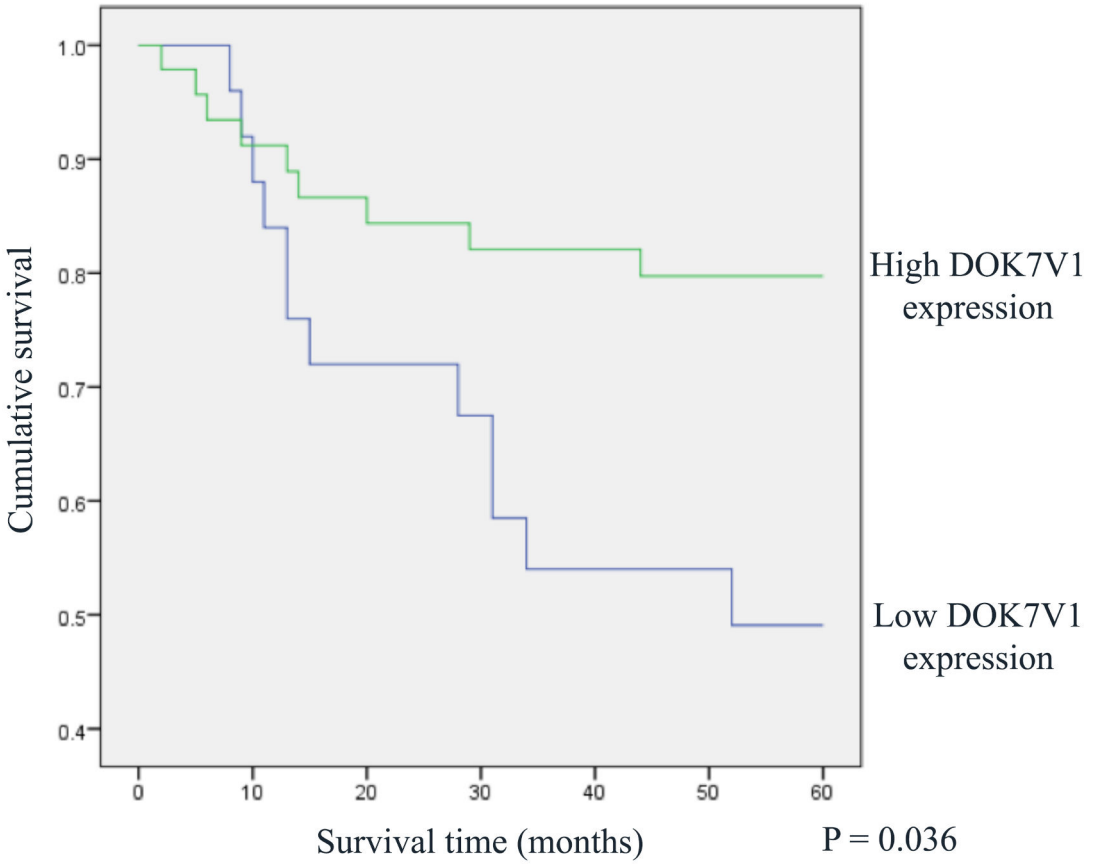

Figure 4.10 Disease-free patient survival in patients with high (green) DOK7V1 expression (n = 48) compared to those with low (blue) DOK7V1 expression (n = 26)

4.3.1.4 DOK7V2 expression

4.3.1.4.1 DOK7V2 expression is significantly increased in colorectal cancer compared to normal colorectal tissue

The expression of DOK7V2 is significantly increased in colorectal cancer compared to normal colorectal tissue. Median DOK7V2 mRNA expression per 50µg of total cellular RNA was 0.9 copies (n = 94, IQR = 0-15) for colorectal carcinoma tissues compared with 0.0 copies (n = 80, IQR = 0.0-3.983) for normal colorectal tissue (p = 0.0000) for the whole cohort, and 0.7 (n = 68, IQR = 0.1-11.7) vs. 0.0 (n = 68, IQR = 0.0-4.846) copies for paired colorectal carcinoma and paired normal colorectal tissue samples respectively (p = 0.0003). Data is shown in Figure 4.11.

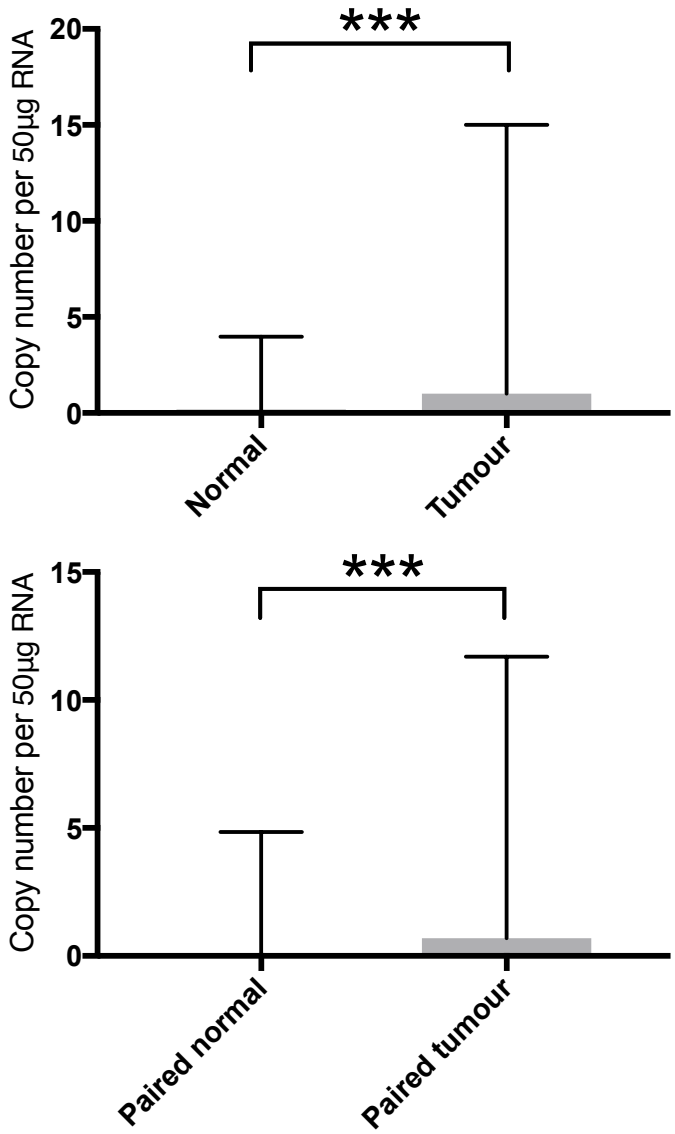

Figure 4.11 DOK7V2 expression in colorectal cancer and normal colorectal tissue

4.3.1.4.2 DOK7V2 expression is not related to degree of colorectal tumour differentiation

The expression of DOK7V2 in relation to degree of tumour differentiation is shown in Figure 4.12. The median copy number of DOK7V2 per 50µg of total cellular RNA was increased in Grade 1 (10.7 copies, n = 2, IQR not calculated due to sample size, p = 0.1910), Grade 2 (median copy number 0.4, n = 54, IQR = 0.1-12.4, p = 0.0020 copies) and Grade 3 (median copy number 8.5, n = 14, IQR = 0.55-18.08, p = 0.0016) colorectal cancers compared to normal colorectal tissue (median copy number 0.0, n = 80, IQR = 0.0-3.983). Analysis using the Kruskal-Wallis test did not reveal a significant difference in DOK7V2 median copy number between different grades of tumour differentiation (p = 0.316).

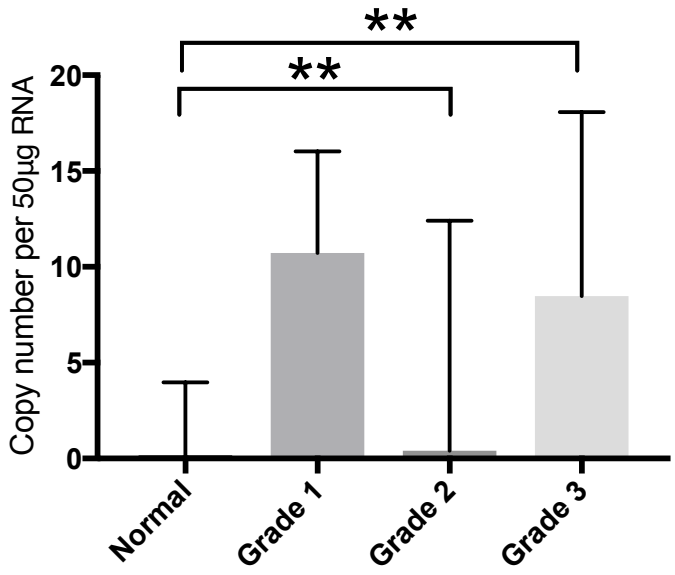

Figure 4.12 DOK7V2 expression by degree of tumour differentiation

4.3.1.4.3 DOK7V2 expression and colorectal cancer nodal status

DOK7V2 expression was significantly increased in node negative colorectal cancer samples compared with normal colorectal tissue (median copy number 0.7, n = 39, IQR 0.1-20.1 *vs.* 0.0, n = 80, IQR = 0.0-3.983 respectively, p = 0.0006). Median DOK7V2 mRNA expression per 50µg of total cellular RNA (copy number) was 4.3 in colorectal cancer samples obtained from patients with N1 disease (n = 16, IQR = 0.2-17.69) and 0.1 in colorectal cancer samples obtained from patients with N2 disease (n = 15, IQR = 0.0-10.61). There was no significant difference in median copy number between patients with node negative and node positive disease (0.7 *vs.* 0.6, p = 0.5704). DOK7V2 expression in relation to colorectal cancer nodal status is shown in Figure 4.13.

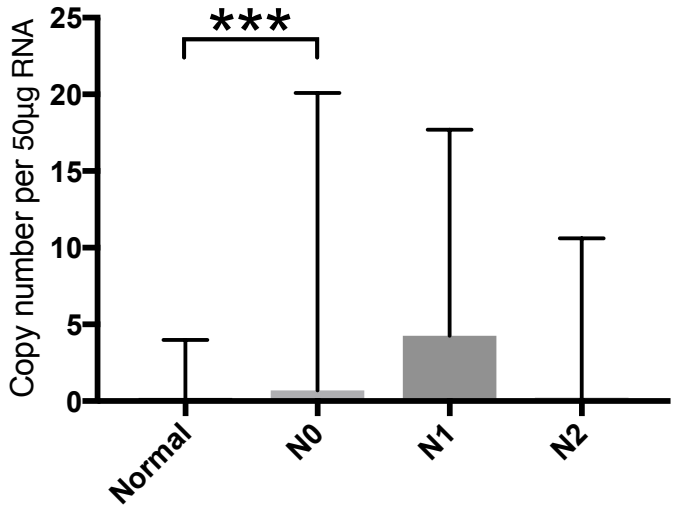

Figure 4.13 DOK7V2 expression by nodal status of colorectal cancer

4.3.1.4.4 DOK7V2 mRNA expression is significantly increased across all Dukes' stages of colorectal cancer

DOK7V2 mRNA expression was significantly increased across all Dukes' stages of colorectal cancer compared to normal colorectal tissue. Median copy number for Dukes' A was 3.4 (n = 7, IQR = 0.23-21.03, p = 0.0272), Dukes' B was 0.6 (n = 33, IQR = 0.1-19.3, p = 0.0029) and Dukes' C was 1.2 (n = 32, IQR = 0.08-15.45, p = 0.0038) compared to 0.0 in normal colorectal tissue (n = 80, IQR = 0.0-3.983). DOK7V2 mRNA expression in relation to Dukes' stage is shown in Figure 4.14.

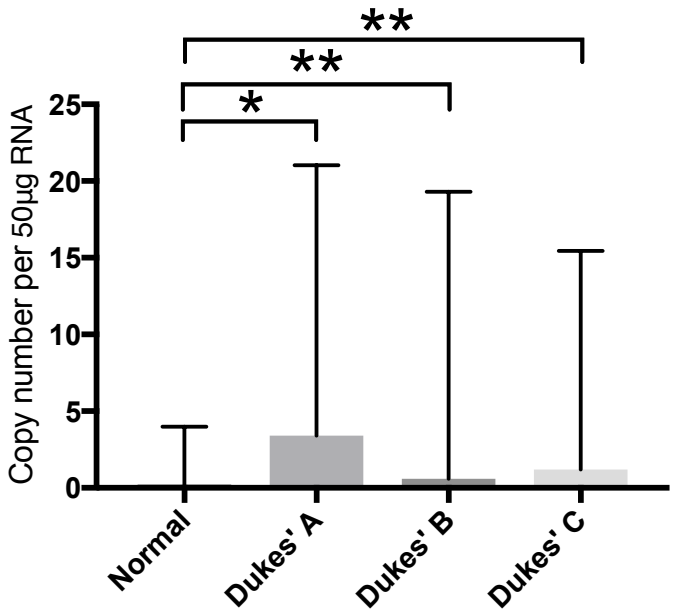

Figure 4.14 DOK7V2 mRNA expression and Dukes' stage of colorectal cancer

4.3.1.4.5 DOK7V2 expression and T stage of colorectal cancer

DOK7V2 expression was significantly increased in T2 (median copy number 8.3, n = 10, IQR = 0.21-26.51, p = 0.0028), T3 (median copy number 0.5, n = 40, IQR = 0.1-11.3, p = 0.0036) and T4 (median copy number 1.1, n = 18, IQR = 0.0-23.6, p = 0.0480) colorectal cancer tissue compared to normal colorectal tissue (median copy number 0.0, n = 80, IQR = 0.0-3.983). DOK7V2 mRNA expression was increased in T1 colorectal cancers compared to normal colorectal tissue (median copy number 9.9 vs. 0.0, p = 0.1216), although this difference was not statistically significant. DOK7V2 mRNA expression in relation to T stage of colorectal cancer is shown in Figure 4.15.

When T stages were combined, median copy number was significantly increased in T2/3 cancers (median copy number 0.6, p = 0.0003), T3/4 cancers (median copy number 0.5, p = 0.0014) and T2/3/4 cancers (median copy number 0.6, p = 0.0002) in comparison with normal colorectal tissue.

Further analysis of the colorectal cancer samples using the Kruskal-Wallis revealed that there was no significant difference in DOK7V2 expression between T stages (p = 0.407).

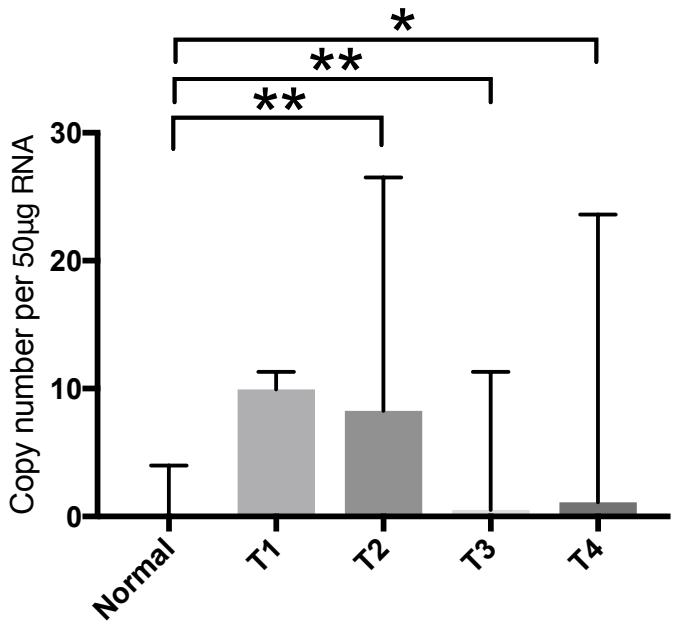

Figure 4.15 DOK7V2 expression and T stage of colorectal cancer

4.3.1.4.6 DOK7V2 expression and overall stage of colorectal cancer

Compared to normal colorectal tissue, DOK7V2 expression was significantly increased in Stage I disease (median copy number 7.1, n = 9, IQR = 0.24-21.15 *vs.* 0.0, n = 80, IQR = 0.0-3.983, p = 0.0042), Stage II disease (median copy number 0.5, n = 30, IQR = 0.0-18.8, p = 0.0083), Stage III disease (median copy number 0.4, n = 26, IQR = 0.05 – 7.21, p =0.0450) and Stage IV disease (median copy number 16.5, n = 6, IQR = 9.06 – 23.56, p = 0.0028). Between-group comparisons using the Kruskal-Wallis test revealed that there was no significant difference in DOK7V2 expression between different stages of disease (p = 0.072). DOK7V2 mRNA expression in relation to overall stage of colorectal cancer is shown in Figure 4.16.

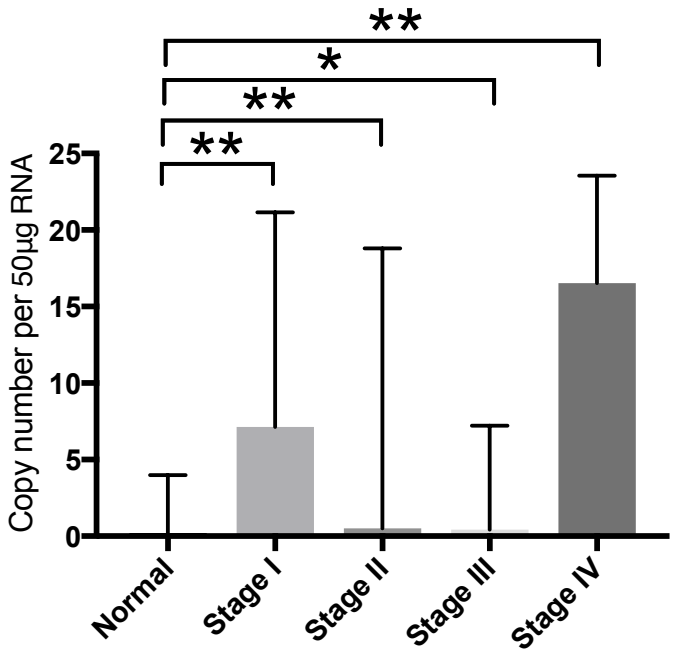

Figure 4.16 DOK7V2 mRNA expression and overall stage of colorectal cancer

4.3.1.4.7 DOK7V2 expression and anatomical location of colorectal cancer

When analysed by anatomical location, DOK7V2 mRNA expression was significantly increased in right-sided colonic cancers (median copy number 0.3, n = 28, IQR = 0.03-12.48, p = 0.0364) and left-sided colonic cancers (median copy number 6.2, n = 22, IQR = 0.4-18.8, p = 0.0001) compared to normal colorectal tissue (median copy number 0.0, n = 80, IQR 0.0-3.983). The level of DOK7V2 expression was also increased in transverse colonic cancers (median copy number 0.2, n = 2, IQR not calculated due to sample size, p = 0.5885) and rectal cancers (median copy number 0.5, n = 22, IQR = 0.07-7.43, p = 0.0678) but this difference did not reach statistical significance. DOK7V2 expression was significantly higher in left colonic cancers compared to right colonic cancers (p = 0.0411) and rectal cancers (p = 0.0378) but was not significantly different to levels found in transverse colonic tumours (p = 0.0848). DOK7V2 mRNA expression in relation to anatomical location of colorectal cancer is shown in Figure 4.17.

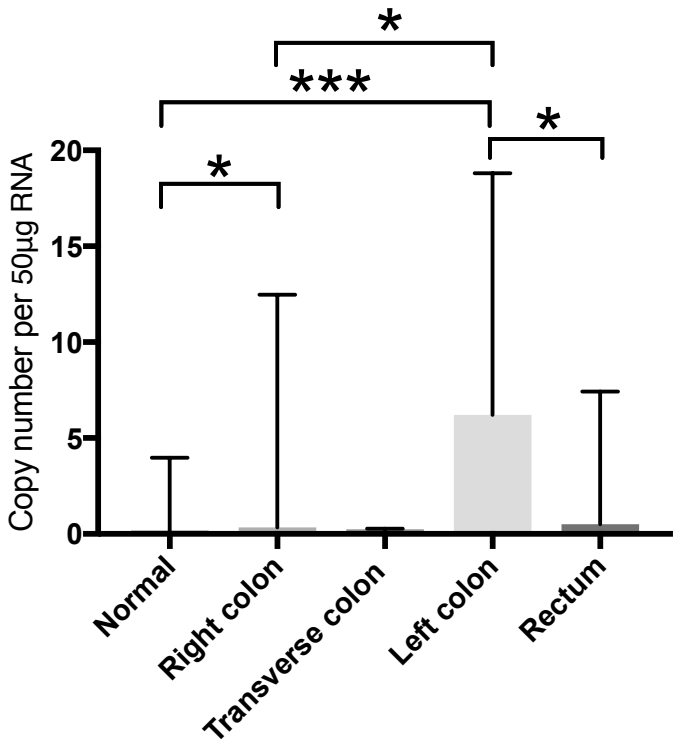

Figure 4.17 DOK7V2 expression and anatomical location of colorectal cancer

4.3.1.4.8 DOK7V2 expression and neoadjuvant/adjuvant treatment status

DOK7V2 mRNA expression was significantly higher in colorectal cancer tissue obtained from patients who underwent no additional therapy compared to normal colorectal tissue (median copy number 0.7, n= 42, IQR = 0.1-16.6 vs. 0.0, n = 80, IQR = 0.0-3.983, p = 0.0007). DOK7V2 expression was also higher in colorectal cancer tissue obtained from patients who had adjuvant chemotherapy (median copy number 0.2, n = 13, IQR = 0.040 – 2.370, p = 0.4218) and neoadjuvant chemoradiotherapy (median copy number 0.1, n = 5, IQR = 0.044-0.515, p = 0.9404) but was not significantly different to the levels in normal colorectal tissue. Median DOK7V2 mRNA expression in the single patient who underwent radiotherapy was 0.0 copies (IQR not calculated due to sample size). There was no significant difference in the level of DOK7V2 expression between patients who underwent no additional therapy and those who underwent either adjuvant chemotherapy or neoadjuvant chemoradiotherapy. The level of DOK7V2 mRNA expression in relation to neoadjuvant/adjuvant treatment status is shown in Figure 4.18.

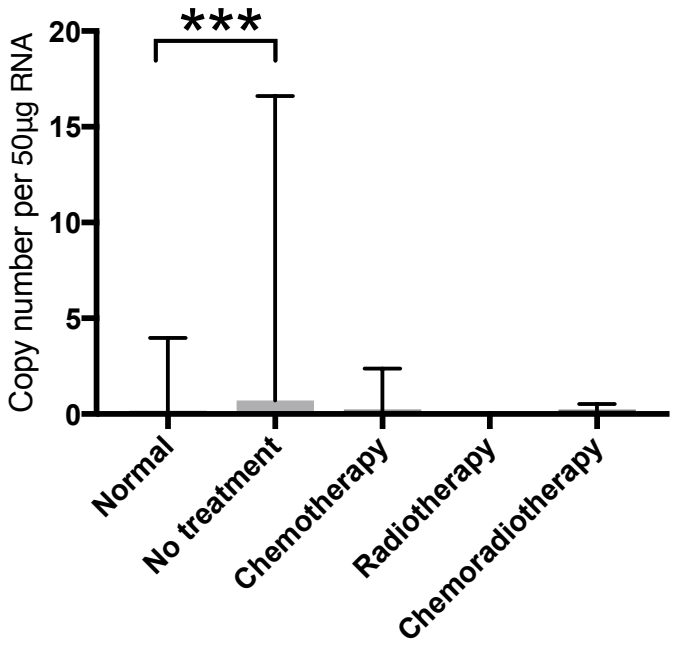

Figure 4.18 DOK7V2 expression and neoadjuvant/adjuvant treatment status

4.3.1.4.9 DOK7V2 expression and tumour invasiveness

Compared to normal colorectal tissue, DOK7V2 mRNA expression in colorectal cancer tissue was significantly increased in both invasive (median copy number 1.2, $p = 0.0045$) and non-invasive (median copy number 0.6, $p = 0.0021$) disease. There was no significant difference in level of DOK7V2 expression between colorectal cancer samples taken from patients with invasive and non-invasive disease ($p = 0.7550$).

4.3.1.4.10 DOK7V2 expression and disease-free status

The level of DOK7V2 mRNA expression was significantly increased in colorectal cancer tissue samples taken from patients who remained disease-free (median copy number 0.6, $p = 0.0008$) compared to normal colorectal tissue. The level of DOK7V2 expression was also increased in patients who suffered further disease but this difference did not reach statistical significance (median copy number 0.2, $p = 0.3320$) patients. The level of DOK7V2 expression was not significantly different between colorectal cancer samples obtained from patients who remained disease free *vs.* those who did not ($p = 0.1119$).

4.3.1.4.11 DOK7V2 expression and survival status

The level of DOK7V2 expression was significantly higher in colorectal cancer tissue samples obtained from patients who were alive (median copy number 0.4, p = 0.0057) compared to normal colorectal tissue. Although DOK7V2 expression levels were higher in patients who died compared to normal colorectal tissue, this difference was not significant (median copy number 0.2 vs. 0.0, p = 0.1271). There was no significant difference in DOK7V2 expression between colorectal cancer samples obtained from patients who were alive at the end of follow-up compared to those who had died (p = 0.4908).

4.3.1.4.12 DOK7V2 expression and metastatic status

The level of DOK7V2 mRNA expression was significantly higher in colorectal cancer samples obtained from patients without distant metastases compared to normal colorectal tissue (median copy number 0.7 vs. 0.0, p = 0.0003). The level of DOK7V2 expression was higher in colorectal cancer samples obtained from patients with distant metastases compared to normal colorectal tissue, but this difference did not reach statistical significance (median copy number 0.2 vs. 0.0, p = 0.2119). There was no significant difference in DOK7V2 expression between colorectal cancer samples obtained from patients with distant metastases and those without (p = 0.1685).

4.3.1.4.13 DOK7V2 expression and local recurrence of disease

The level of DOK7V2 mRNA expression was significantly higher in colorectal cancer patients without local recurrence compared to normal colorectal tissue (median copy number 0.5 vs. 0.0, $p = 0.0009$). The level of DOK7V2 expression was the same in colorectal cancer samples obtained from patients with local recurrence compared to normal colorectal tissue (median copy number 0.0 vs. 0.0, $p = 0.9502$). There was no significant difference in level of DOK7V2 expression between colorectal cancer samples obtained from patients with local recurrence compared to those without ($p = 0.3973$).

4.3.1.4.14 DOK7V2 expression and overall patient survival

The Kaplan-Meier survival curve for DOK7V2 mRNA expression in colorectal cancer (dichotomized according to the median value of DOK7V2 expression for the whole cohort) is shown in Figure 4.19. Low DOK7V2 expression (n = 11) is associated with reduced overall survival when compared with the overall survival of patients with high levels of DOK7V2 expression (n = 63) but this difference failed to reach statistical significance (p = 0.064).

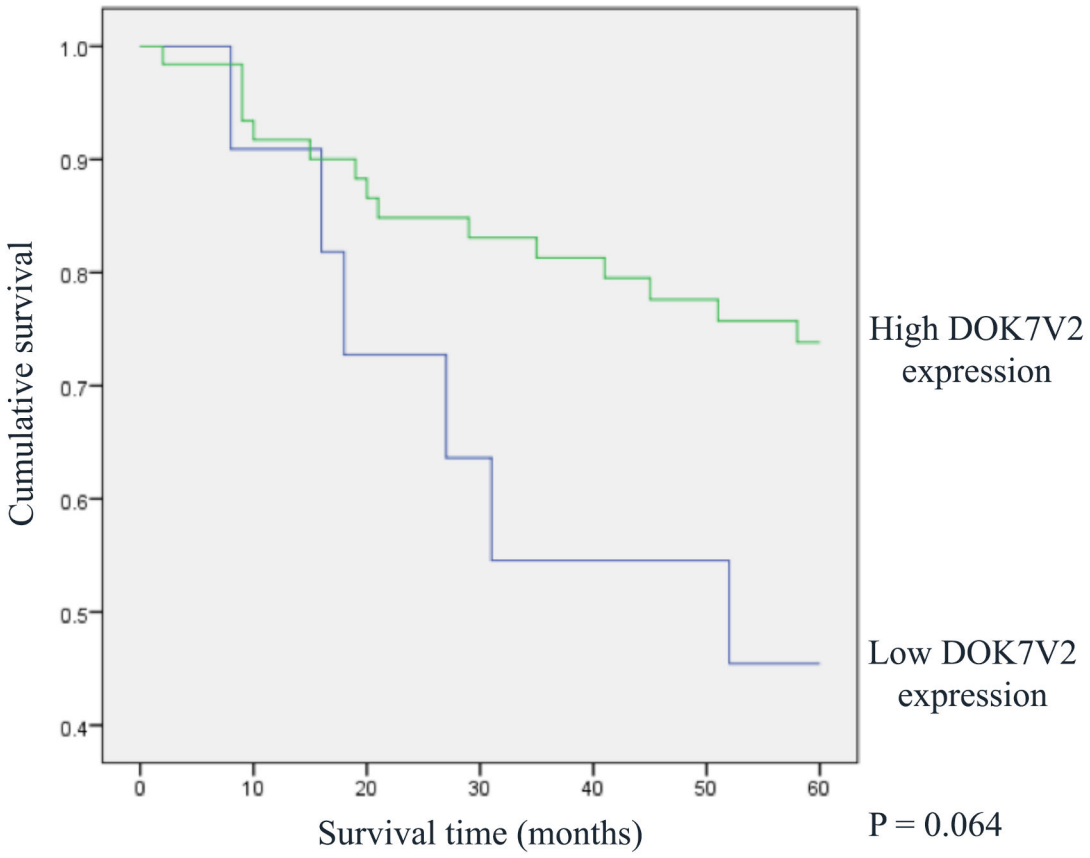

Figure 4.19 Overall patient survival in patients with high (green) DOK7V2 expression (n = 63) compared to those with low (blue) DOK7V2 expression (n = 11)

4.3.1.4.15 DOK7V2 expression and disease-free patient survival

The Kaplan-Meier disease-free survival curve for DOK7V2 expression in colorectal cancer (dichotomized according to the median value of DOK7V2 expression for the whole cohort) is shown below in Figure 4.20. Low DOK7V2 expression (n = 11) is associated with significantly reduced disease-free survival when compared with the disease-free survival of patients with high levels of DOK7V2 expression (n = 63) (p = 0.009).

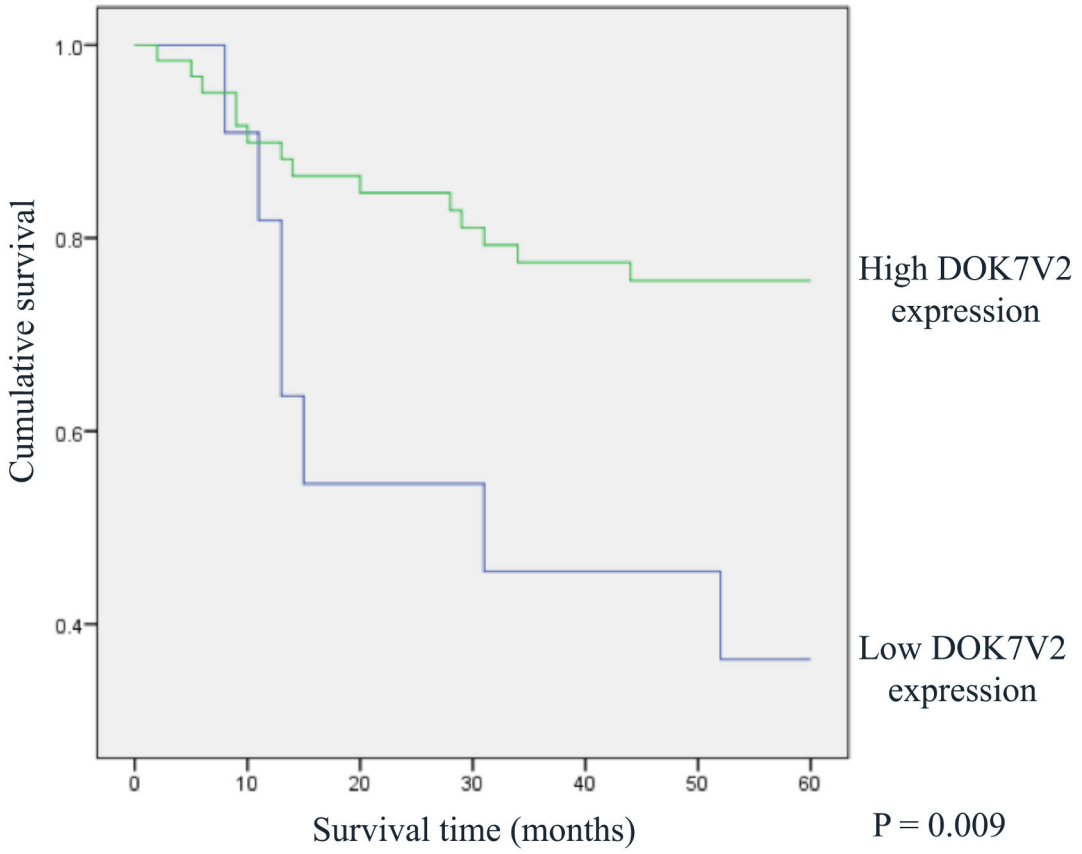

Figure 4.20 Disease-free patient survival in patients with high (green) DOK7V2 expression (n = 63) compared to those with low (blue) DOK7V2 expression (n = 11)

4.3.1.5 DOK7V3 expression

4.3.1.5.1 DOK7V3 mRNA expression is increased in colorectal cancer compared to normal colorectal tissue across the whole cohort but not for paired samples

The level of DOK7V3 expression is increased in colorectal cancer compared to normal colorectal tissue. Median DOK7V3 mRNA expression per 50µg of total cellular RNA was significantly higher in colorectal carcinoma tissues (median copy number 15.1, n = 94, IQR = 1-512) compared with normal colorectal tissue (median copy number 2.4, n = 80, IQR = 0-391, p = 0.0263) for the whole cohort. Paired tumour *vs.* normal comparison (median copy number 8.1, n = 68, IQR = 1-465 *vs.* median copy number 2.1, n = 68, IQR = 0-391 respectively) showed a similarly increased level of DOK7V3 in colorectal cancer, but this difference did not reach statistical significance (p = 0.0765). Data is shown in Figure 4.21.

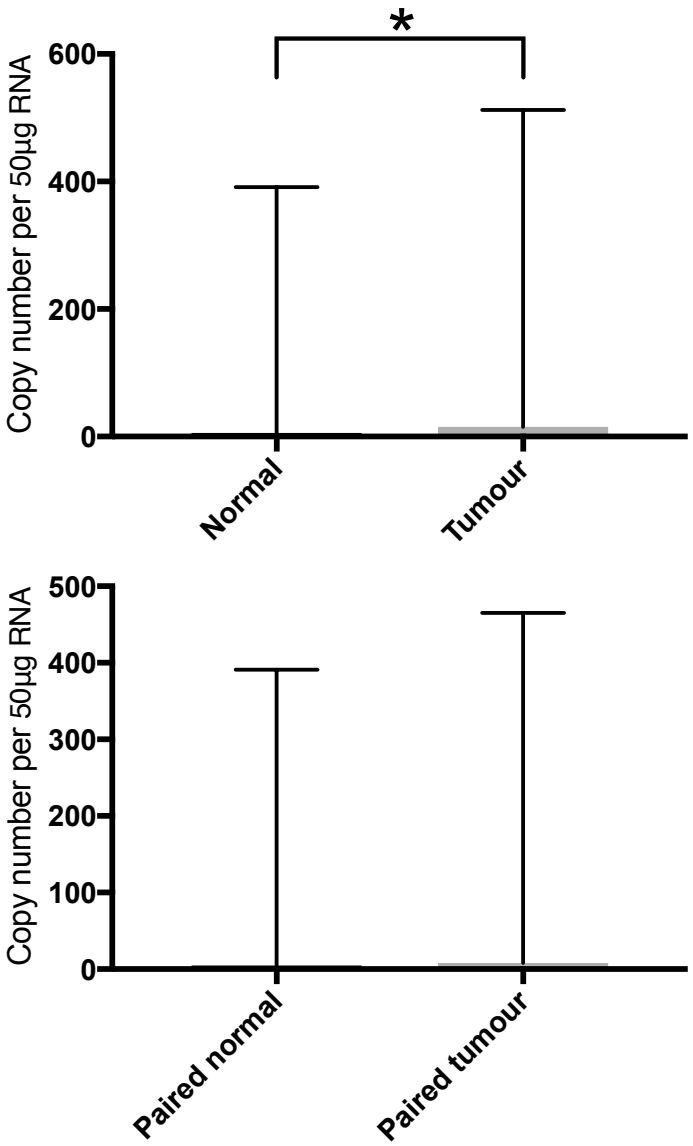

Figure 4.21 DOK7V3 mRNA expression in colorectal cancer and normal colorectal tissue

4.3.1.5.2 DOK7V3 expression is not related to degree of colorectal tumour differentiation

The expression of DOK7V3 mRNA in relation to degree of tumour differentiation is shown in Figure 4.22. The median copy number of DOK7V3 per 50μg of total cellular RNA was increased in well differentiated (median copy number 1520.2, n = 2, IQR not calculated due to sample size vs. 2.4, n = 80, IQR = 0-391, p = 0.5377) and moderately differentiated (median copy number 6.0, n = 54, IQR = 1-252, p = 0.4181 copies) colorectal cancer samples compared to the level in normal colorectal tissue but these differences were not statistically significant. DOK7V3 expression was significantly higher in poorly differentiated colorectal cancer samples compared to normal colorectal tissue (median copy number 211.8, n = 14, IQR = 12-1430, p = 0.0140). Analysis using the Kruskal-Wallis test did not reveal a significant difference in median copy number between different grades of tumour differentiation (p = 0.085).

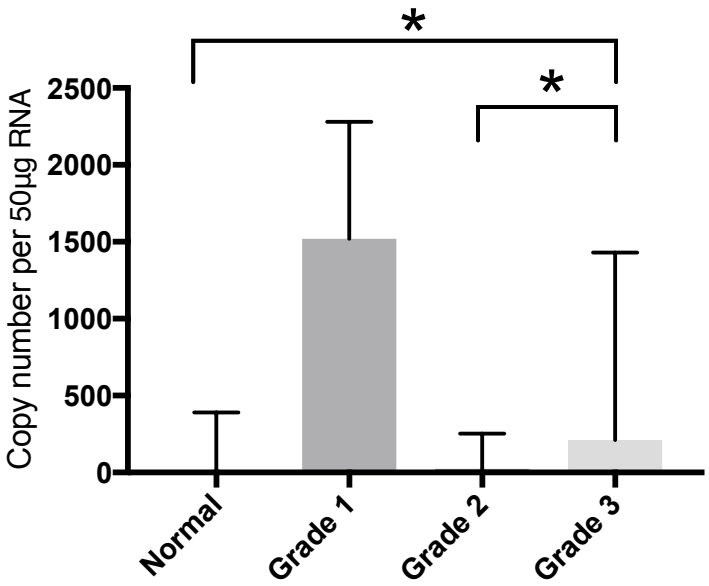

Figure 4.22 DOK7V3 expression by degree of tumour differentiation

4.3.1.5.3 DOK7V3 expression and colorectal cancer nodal status

DOK7V3 expression is increased in node negative colorectal cancer samples compared with normal colorectal tissue but this difference was not statistically significant (median copy number 11.3, n = 39, IQR = 1-366 *vs.* 2.4, n = 80, IQR = 0-391 respectively, p =0.1620). Median DOK7V3 expression was 12.6 copies (n = 16, IQR = 1-944) in colorectal carcinoma tissue obtained from patients with N1 disease and 5.7 copies (n = 15, IQR = 1-55) in colorectal carcinoma tissue obtained from patients with N2 disease. There was no significant difference in level of DOK7V3 expression between colorectal cancer samples obtained from patients with node negative and node positive disease (11.3 *vs.* 8.4, p = 0.8361). The level of DOK7V3 mRNA expression in relation to colorectal cancer nodal status is shown in Figure 4.23.

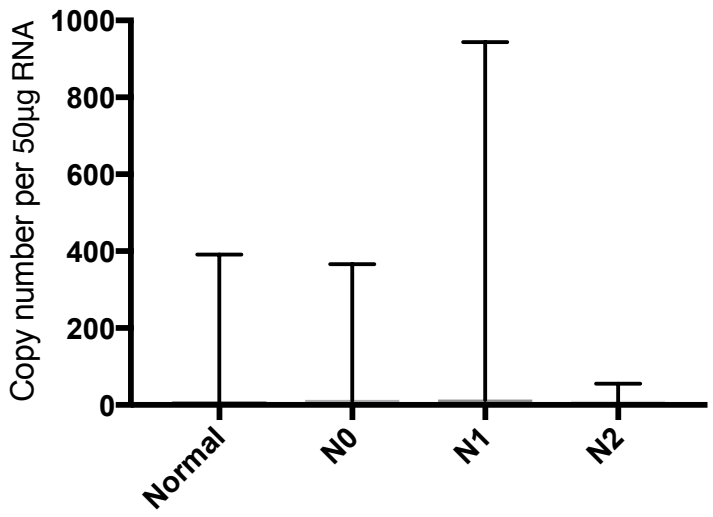

Figure 4.23 DOK7V3 expression by nodal status of colorectal cancer

4.3.1.5.4 DOK7V3 expression and Dukes' stage

DOK7V3 expression was increased across all Dukes' stages of colorectal cancer compared to normal colorectal tissue (Dukes' A median copy number 35.8, n = 7, IQR = 1-279, Dukes' B median copy number 6.3, n = 33, IQR = 1-677 and Dukes' C median copy number 11.7, n = 32, IQR = 1-610 compared to median copy number 2.4, n = 80, IQR = 0-391 in normal colorectal tissue) but these differences were statistically non-significant ($p = 0.2579$, $p = 0.2691$ and $p = 0.1955$ respectively). DOK7V3 mRNA expression in relation to Dukes' stage is shown in Figure 4.24.

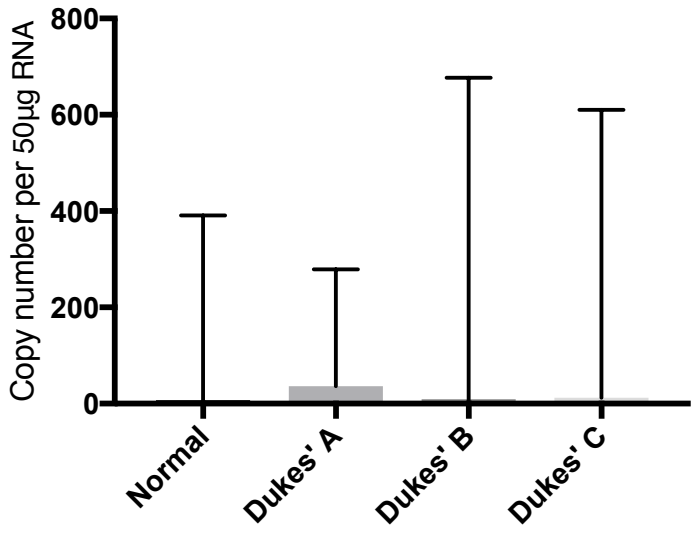

Figure 4.24 DOK7V3 expression and Dukes' stage of colorectal cancer

4.3.1.5.5 DOK7V3 expression and T stage of colorectal cancer

DOK7V3 expression was increased, though not significantly, in T1 (median copy number 712.8, n = 2, IQR not calculated due to sample size, p = 0.1622), T2 (median copy number 157.4, n = 10, IQR = 1-2397, p = 0.0754), T3 (median copy number 7.4, n = 40, IQR = 1-192, p = 0.4796) and T4 (median copy number 4.7, n = 18, IQR = 1-654, p = 0.2810) colorectal cancer tissue compared to normal colorectal tissue (median copy number 2.4, n = 80, IQR = 0-391). There was no significant difference in DOK7V3 expression compared to normal colorectal tissue when T2/3, T3/4 and T2/3/4 were grouped. DOK7V3 expression in relation to T stage of colorectal cancer is shown in Figure 4.25.

Further analysis of the colorectal cancer samples using the Kruskal-Wallis revealed that there was no significant difference in DOK7V3 expression between T stages (p = 0.263).

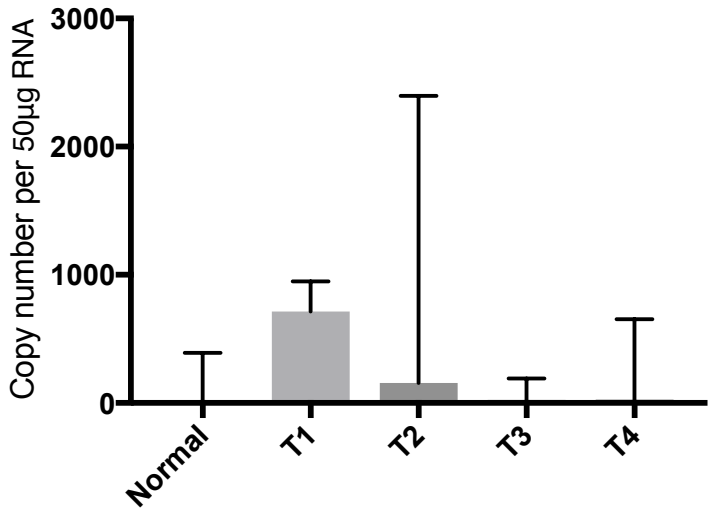

Figure 4.25 DOK7V3 expression and T stage of colorectal cancer

4.3.1.5.6 DOK7V3 expression and overall stage of colorectal cancer

Compared to normal colorectal tissue (median copy number 2.4, n = 80, IQR = 0-391), DOK7V3 expression was increased, though not significantly, in Stage I disease (median copy number 243.5, n = 9, IQR = 14-1816, p = 0.0559), Stage II disease (median copy number 5.0, n = 30, IQR = 1-256, p = 0.4768) and Stage III disease (median copy number 4.4, n = 26, IQR = 1-122, p = 0.6542). The level of DOK7V3 expression was significantly increased in Stage IV disease compared to normal colorectal tissue (median copy number 660.4, n = 6, IQR = 158-1218, p = 0.0180). Between-group comparisons using the Kruskal-Wallis test revealed that there was no significant difference in DOK7V3 expression between different stages of disease (p = 0.143). DOK7V3 expression in relation to overall stage of colorectal cancer is shown in Figure 4.26.

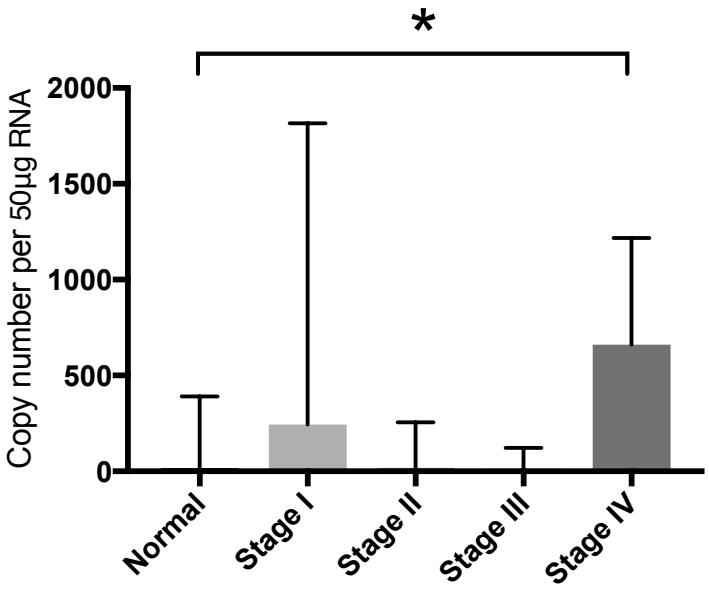

Figure 4.26 DOK7V3 expression and overall stage of colorectal cancer

4.3.1.5.7 DOK7V3 expression and anatomical location of colorectal cancer

When analysed by anatomical location, DOK7V3 expression was significantly increased in left-sided colonic cancers compared to normal colorectal tissue (median copy number 108.6, n = 22, IQR = 2-733 *vs.* 2.4, n = 80, IQR = 0-391, p = 0.0258). Compared to normal colorectal tissue samples, there was no significant difference between the level of DOK7V3 expression in colorectal cancer samples obtained from right colonic cancers (median copy number 12.2, n = 28, IQR = 1-574, p = 0.4061), transverse colonic cancers (median copy number 6.8, n = 2, IQR not calculated due to sample size, p = 0.9401) or rectal cancers (median copy number 1.6, n = 22, IQR = 0-20, p = 0.7852). The level of DOK7V3 expression was significantly higher in left colonic cancer samples compared to those obtained from rectal cancers (p = 0.0089) but comparisons of other tumour sites did not reveal statistically significant differences. DOK7V3 mRNA expression according to anatomical location is shown in Figure 4.27.

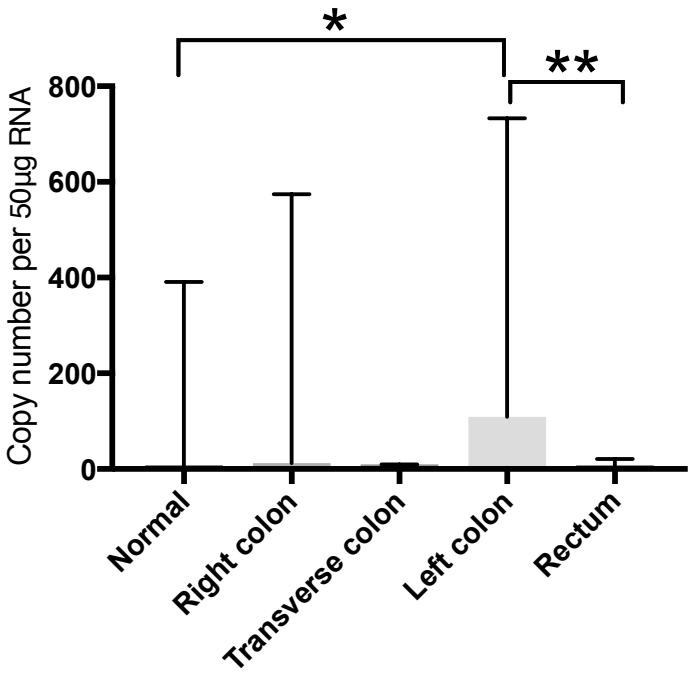

Figure 4.27 DOK7V3 expression and anatomical location of colorectal cancer

4.3.1.5.8 DOK7V3 expression and neoadjuvant/adjuvant treatment status

The level of DOK7V3 mRNA expression was higher in colorectal cancer samples obtained from patients who underwent no additional therapy compared to normal colorectal tissue but this difference was not statistically significant (median copy number 11.6, n = 42, IQR = 1-301 *vs.* 2.4, n = 80, IQR = 0-391, p = 0.1341). By comparison, the level of DOK7V3 expression was decreased in colorectal cancer samples obtained from patients who underwent adjuvant chemotherapy (median copy number 2.3, n = 13, IQR = 0.3-12.5, p = 0.6697) and neoadjuvant chemoradiotherapy (median copy number 1.0, n = 5, IQR = 0.317 – 1.647, p = 0.2913) but was not statistically significant for either comparison. The sole patient who underwent radiotherapy had a DOK7V3 median copy number of 0.3 (IQR not calculated due to sample size). When treatment groups were compared, the level of DOK7V3 expression was significantly higher in colorectal cancer samples obtained from patients who did not undergo additional therapy compared to the neoadjuvant chemoradiotherapy group (p = 0.0324) but did not reach significance when the patients with no additional therapy were compared to patients who underwent adjuvant chemotherapy (p = 0.0714). DOK7V3 expression in relation to neoadjuvant/adjuvant treatment status is shown in Figure 4.28.

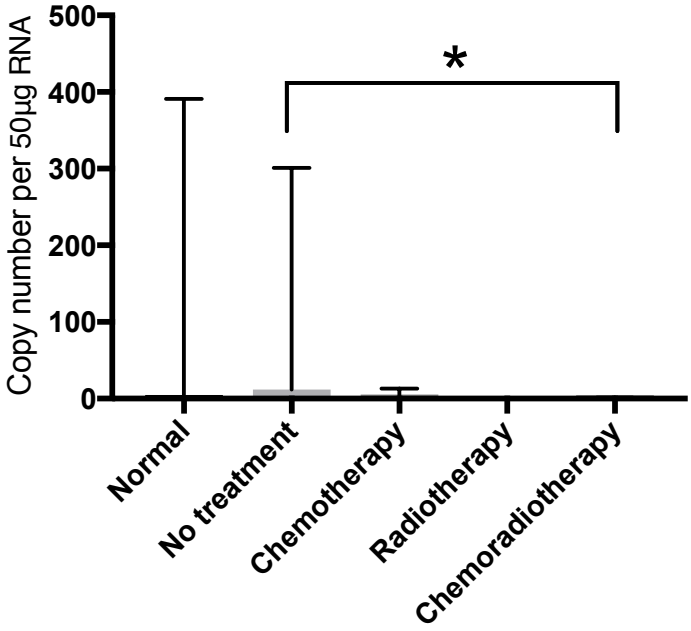

Figure 4.28 DOK7V3 expression and neoadjuvant treatment status

4.3.1.5.9 DOK7V3 expression and tumour invasiveness

The level of DOK7V3 mRNA expression was higher in colorectal cancer samples obtained from patients both with invasive (median copy number 13.5 *vs.* 2.4, p = 0.1686) and non-invasive (median copy number 6.3 *vs.* 2.4, p = 0.2935) disease but the difference did not reach statistical significance for either group. There was no significant difference in the level of DOK7V3 expression in colorectal cancer samples obtained from patients with or without invasive disease (p = 0.5954).

4.3.1.5.10 DOK7V3 expression and disease-free status

The level of DOK7V3 mRNA expression was higher in colorectal cancer samples obtained from patients who remained disease-free (median copy number 8.4 vs. 2.4, p = 0.1872) and those who did not (median copy number 6.3 vs. 2.4, p = 0.7635) but the difference did not reach statistical significance for either group. There was no significant difference in level of DOK7V3 expression between colorectal cancer samples obtained from patients who remained disease-free compared to patients who developed further disease (p = 0.4455).

4.3.1.5.11 DOK7V3 expression and survival status

Compared to normal colorectal tissue, the level of DOK7V3 mRNA expression was higher in colorectal cancer samples obtained from patients both who survived (median copy number 6.3 vs. 2.4, p = 0.2632) and died (median copy number 4.7 vs. 2.4, p = 0.7789) from their disease but these differences did not reach statistical significance. There was no significant difference in DOK7V3 expression between colorectal cancer samples obtained from patients who survived compared to those obtained from those who died of their disease (p = 0.6479).

4.3.1.5.12 DOK7V3 expression and metastatic status

The level of DOK7V3 mRNA expression was higher in colorectal cancer samples obtained from both patients with distant metastases (median copy number 6.3 vs. 2.4, p = 0.4528) and those without (median copy number 8.1 vs. 2.4, p = 0.1532) metastatic disease, compared to normal colorectal tissue but these differences did not reach statistical significance. There was no significant difference in DOK7V3 expression between colorectal cancer samples obtained from patients with distant metastatic disease compared to those obtained from patients without distant metastatic disease (p = 0.7018).

4.3.1.5.13 DOK7V3 expression and local recurrence of disease

The level of DOK7V3 expression was higher in colorectal cancer samples obtained from both patients with (median copy number 6.3 vs. 2.4, p = 0.9440) and without (median copy number 6.3 vs. 2.4, p = 0.1920) local recurrence compared to normal colorectal tissue but these differences did not reach statistical significance. There was no significant difference in DOK7V3 expression between colorectal cancer samples obtained from patients with and without local disease recurrence (p = 0.5606).

4.3.1.5.14 DOK7V3 expression and overall patient survival

The Kaplan-Meier survival curve for DOK7V3 expression in colorectal cancer (dichotomized according to the median value of DOK7V3 expression for the whole cohort) is shown in Figure 4.29. Low DOK7V3 expression (n = 48) is associated with reduced overall survival when compared with the overall survival of patients with high levels of DOK7V3 expression (n = 26) but this difference failed to reach statistical significance (p = 0.228).

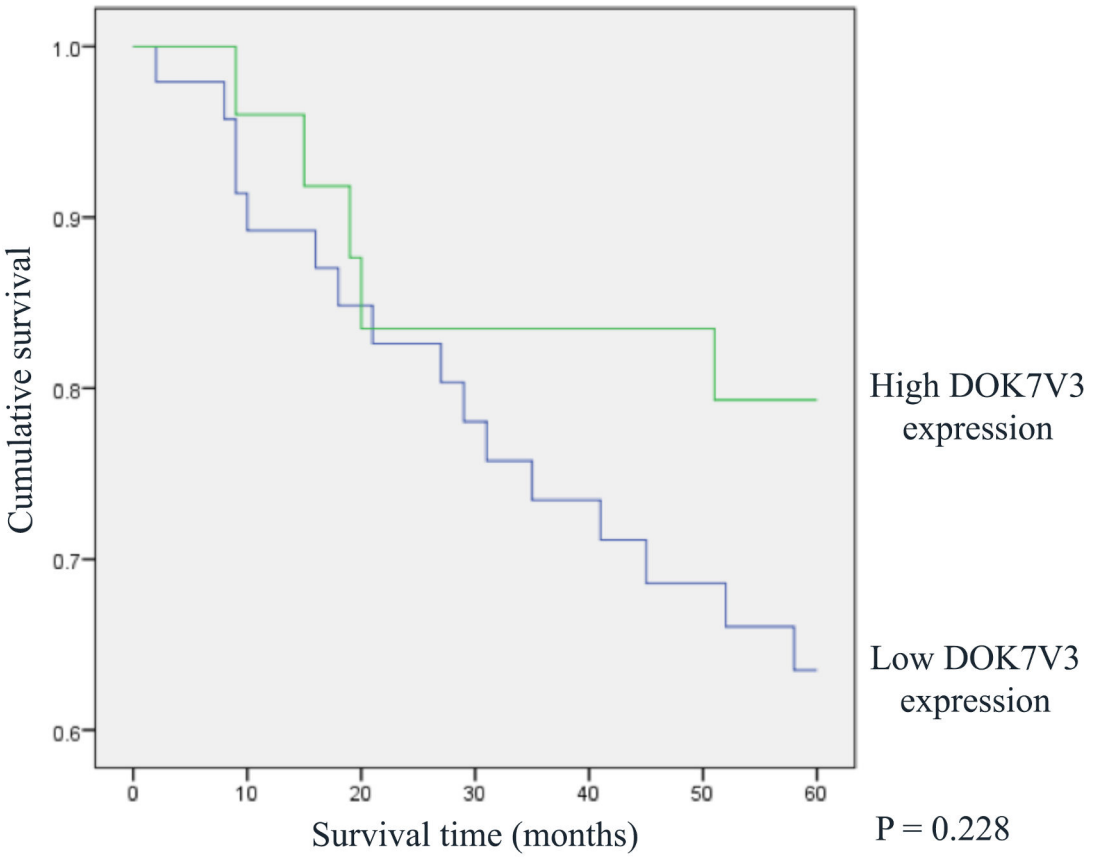

Figure 4.29 Overall patient survival in patients with high (green) DOK7V3 expression (n = 26) compared to those with low (blue) DOK7V3 expression (n = 48)

4.3.1.5.15 DOK7V3 expression and disease-free patient survival

The Kaplan-Meier disease-free survival curve for DOK7V3 expression in colorectal cancer (dichotomized according to the median value of DOK7V3 expression for the whole cohort) is shown in Figure 4.30. Low DOK7V3 expression (n = 48) is associated with reduced disease-free survival when compared with the disease-free survival of patients with high levels of DOK7V3 expression (n = 26) but the difference did not reach statistical significance (p = 0.102).

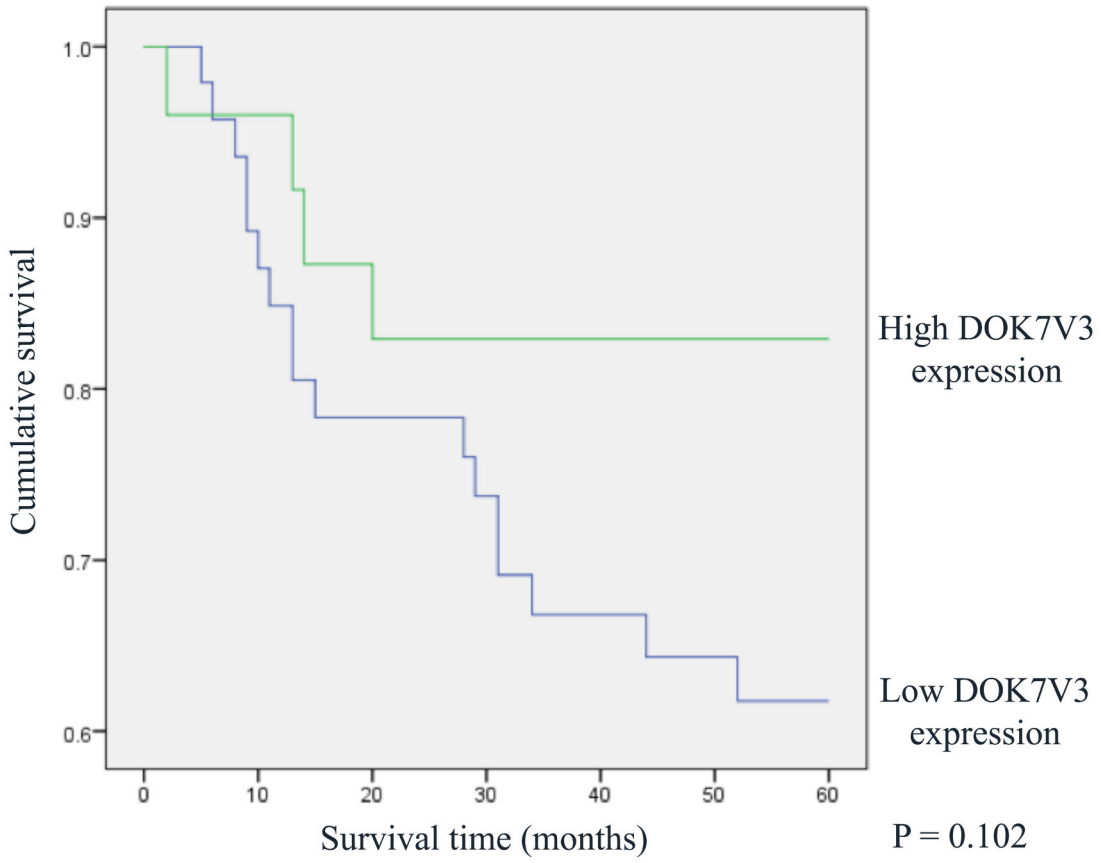

Figure 4.30 Disease-free patient survival in patients with high (green) DOK7V3 expression (n = 26) compared to those with low (blue) DOK7V3 expression (n = 48)

4.3.2 Colorectal cell line data

4.3.2.1 Expression of DOK7V1-3 in colorectal cancer cell lines: PCR data

Data from PCR shows that DOK7V1 is strongly expressed by HRT-18 cells with reduced expression in HT-115 cells and very little expression in RKO cells.

DOK7V2 shows a similar pattern of expression to DOK7V1 with high levels of DOK7V2 expression in HRT-18 cells, lower levels of expression in HT-115 cells and low levels of expression in RKO cells.

The expression of DOK7V1-3 in colorectal cancer cell lines is shown in Figure 4.31.

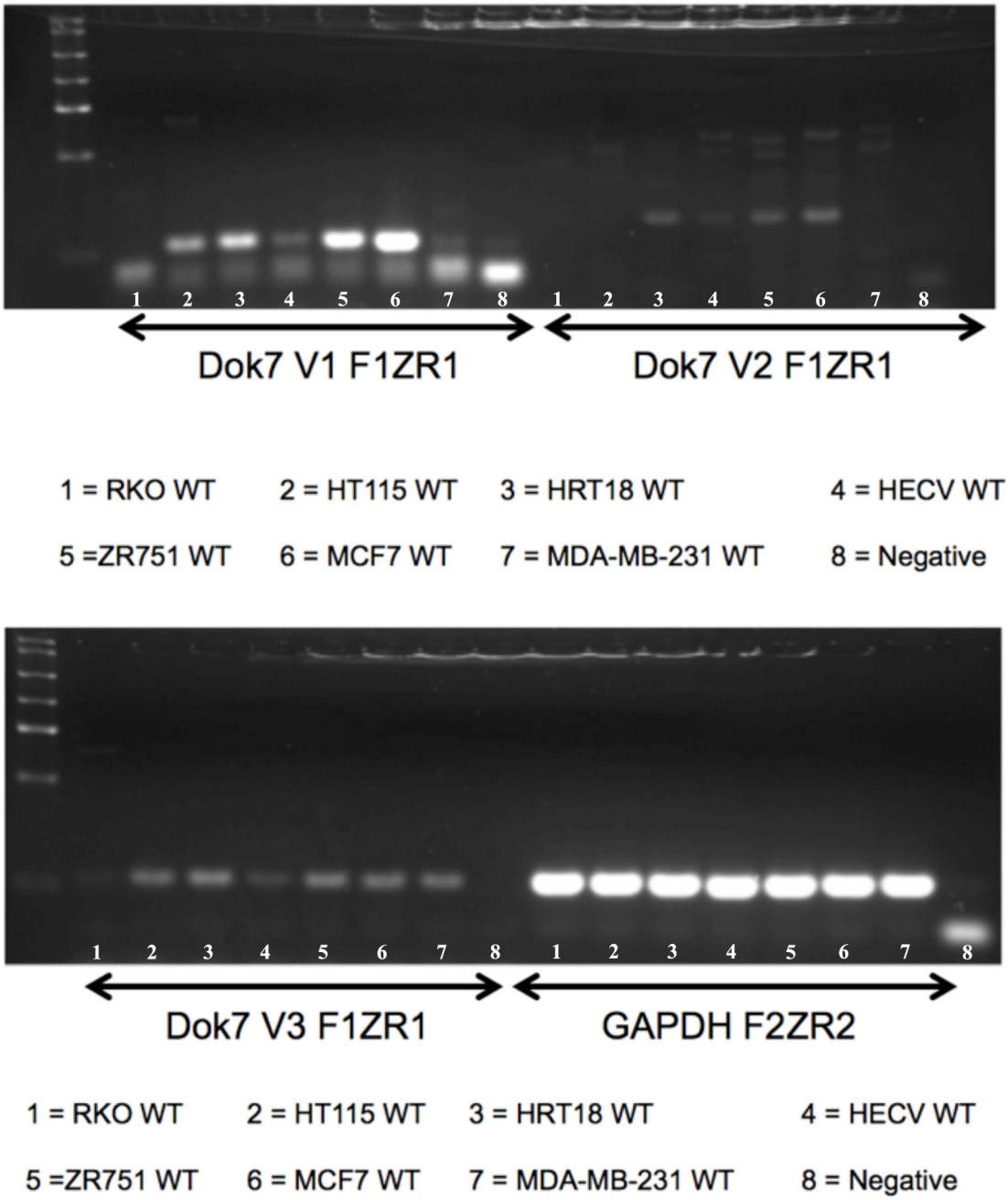

Figure 4.31 Expression of DOK7V1-3 in colorectal cancer cell lines – qPCR results

4.3.2.2 Expression of DOK7V1-3 in colorectal (RKO, HT115 and HRT18), endothelial (HECV) and breast (ZR751, MCF7, MDA-MB-231) cancer cell lines: qPCR data

Focusing on colorectal cancer cell lines, data obtained using qPCR shows a similar pattern of expression to DOK7V1 with high levels of DOK7V2 expression in HRT-18 cells, lower levels of expression in HT-115 cells and low levels of expression in RKO cells. These results suggest that RKO colorectal cancer cell line would be the optimal cell line for creating overexpression models of DOK7V1 and DOK7V2. Data is shown in Figure 4.32.

A.

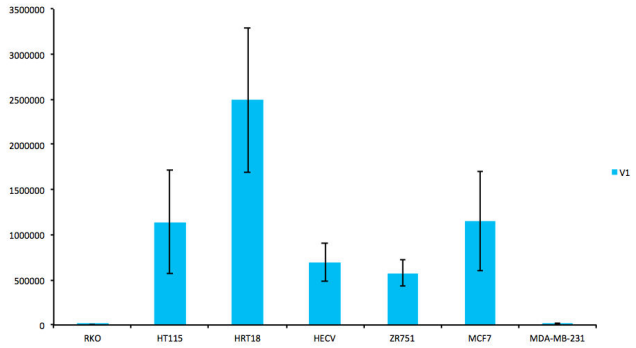

B.

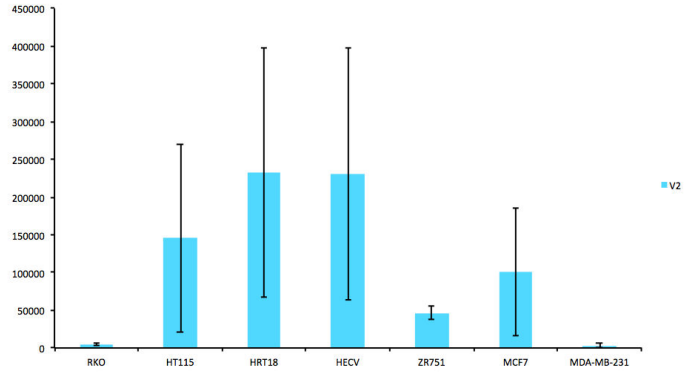

C.

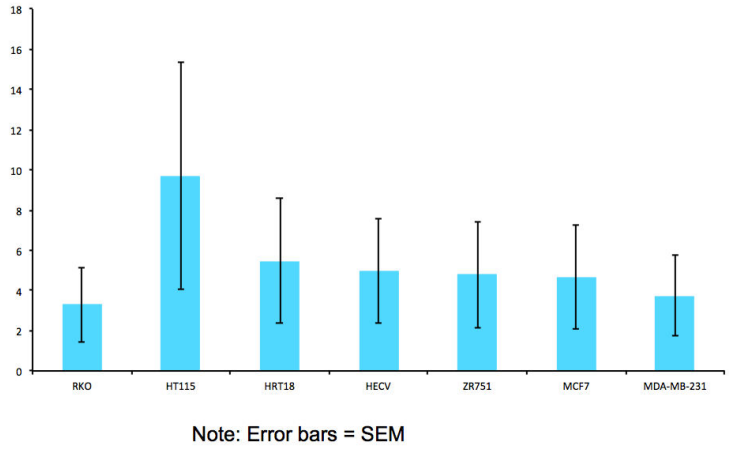

Figure 4.32 Expression of DOK7V1-3 in colorectal (RKO, HT115, HRT18), endothelial (HECV) and breast (ZR751, MCF&, MDA-MB-231) cancer cell lines – qPCR results. A. Expression of DOK7V1 in colorectal, endothelial and breast cancer cell lines. B. Expression of DOK7V2 in colorectal, endothelial and breast cancer cell lines. C. Expression of DOK7V3 in colorectal, endothelial and breast cancer cell lines

4.4 Discussion

To our knowledge, this is the first study to characterise the expression of DOK7 variants 1, 2 and 3 in human cancer and specifically, in a colorectal cancer clinical cohort and cell lines. Our data show a number of interesting findings.

Firstly, the expression of DOK7V1 is significantly reduced in colorectal cancer compared to normal colorectal tissue. Furthermore, DOK7V1 expression is significantly associated with overall stage of disease and is significantly reduced in patients who suffered further disease events compared to those who remained disease free. Low DOK7V1 expression was also associated with significantly reduced length of disease free survival compared to that of patients with high DOK7V1 expression.

We found no association between DOK7V1 expression and degree of colorectal cancer differentiation, Dukes' stage, anatomical location, treatment status or nodal status. DOK7V1 expression was not a significant predictor of local invasion, the development of distant metastases, local recurrence rate or overall survival. DOK7V1 expression decreased with increasing T stage but Kruskal Wallis analysis revealed that the difference in DOK7V1 expression between T stages was not statistically significant.

By comparison, the expression of DOK7V2 is significantly increased in colorectal cancer compared to normal colorectal tissue. The level of DOK7V2 expression is significantly higher in left-sided colonic cancers compared to right-sided colonic cancer and rectal cancers. Low DOK7V2 expression was associated with significantly reduced disease-free survival when compared to that of patients with high DOK7V2 expression.

No association was found between level of DOK7V2 expression and degree of tumour differentiation, nodal status, Dukes' stage, T stage, overall stage, treatment status, tumour invasiveness, disease-free status and overall survival.

DOK7V3 expression was significantly increased in colorectal cancer compared to normal colorectal tissue across the whole cohort data, but not for paired samples. DOK7V3 expression was significantly higher in left-sided colonic cancer samples compared to those obtained from rectal cancers. DOK7V3 expression was also significantly higher in patients who did not require any neoadjuvant/adjuvant treatment compared to those who underwent chemoradiotherapy.

There was no association between DOK7V3 expression and the degree of tumour differentiation, nodal status, Dukes' stage, T stage or overall stage of disease. Dok7V3 was not associated with the likelihood of metastatic disease development, local recurrence, tumour invasiveness, disease-free survival or overall survival.

The expression of DOK7 variants 1,2 and 3 also differed between different colorectal cancer cell liens. DOK7V1 and DOK7V2 are strongly expressed by HRT-18 cells with reduced levels seen in RKO and HT-115 cells. DOK7V3 expression is highest in HT-115 cells with lower levels of expression seen in RKO and HRT-18 cells.

Cossins *et al* investigated the mutations seen in DOK7 congenital myasthenic syndrome in their 2012 publication. In addition to identifying 34 different mutations, they found 27 additional variants, which they believed were non-pathogenic. These are illustrated in Figure 4.33.

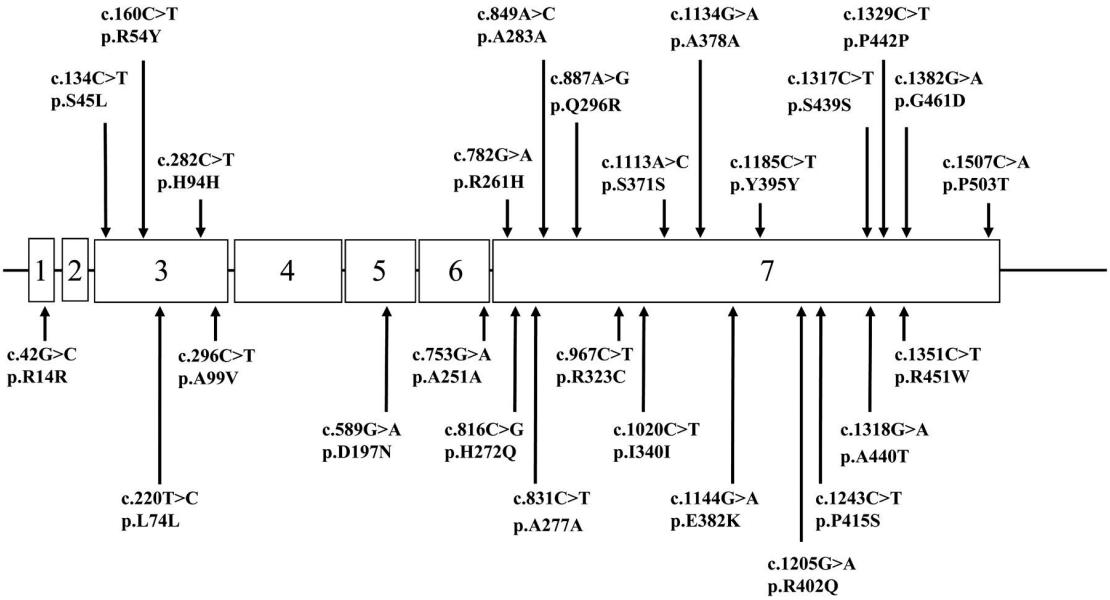

Figure 4.33 Schematic diagram of DOK7 showing the exons and positions of 27 exonic variants identified during routine DNA screening likely to be non-pathogenic. Predicted amino acid changes are indicated. Figure taken from Cossins et al 'The spectrum of mutations that underlie the neuromuscular junction synaptopathy in DOK7 congenital myaesthenic syndrome' Hum Mol Genet 2012 Sep 1;21(17):3765-75.

In their paper, they comment on three additional pathogenic silent nucleotide variants in the N-terminal portion of DOK7 that can alter the splicing of the DOK7 RNA transcript. One of these is in exon 1 (c.48C>T, p.G16G) and the other two are located in exon 4 (c.414C>T, p.L138L and c.513C>T, p. G171G). The first of these variants produces a shorter transcript that misses out exon 1 resulting in an in-frame deletion of 18 amino acid residues MTEAALVEGQVKLRDGKK. The second variant produced two different sized transcripts – a longer correctly spliced transcript and a shorter transcript with a deletion of 94 nucleotides at the 5' end of exon 4 resulting in a frameshift. The last of the variants resulted in a truncated exon 4, which had lost the last 21 nucleotides of the exon. The gel electrophoresis of the amplicons generated by Cossins et al using vector-specific primers and the sequencing data and aberrant splicing due to the variants are shown in Figure 4.34.

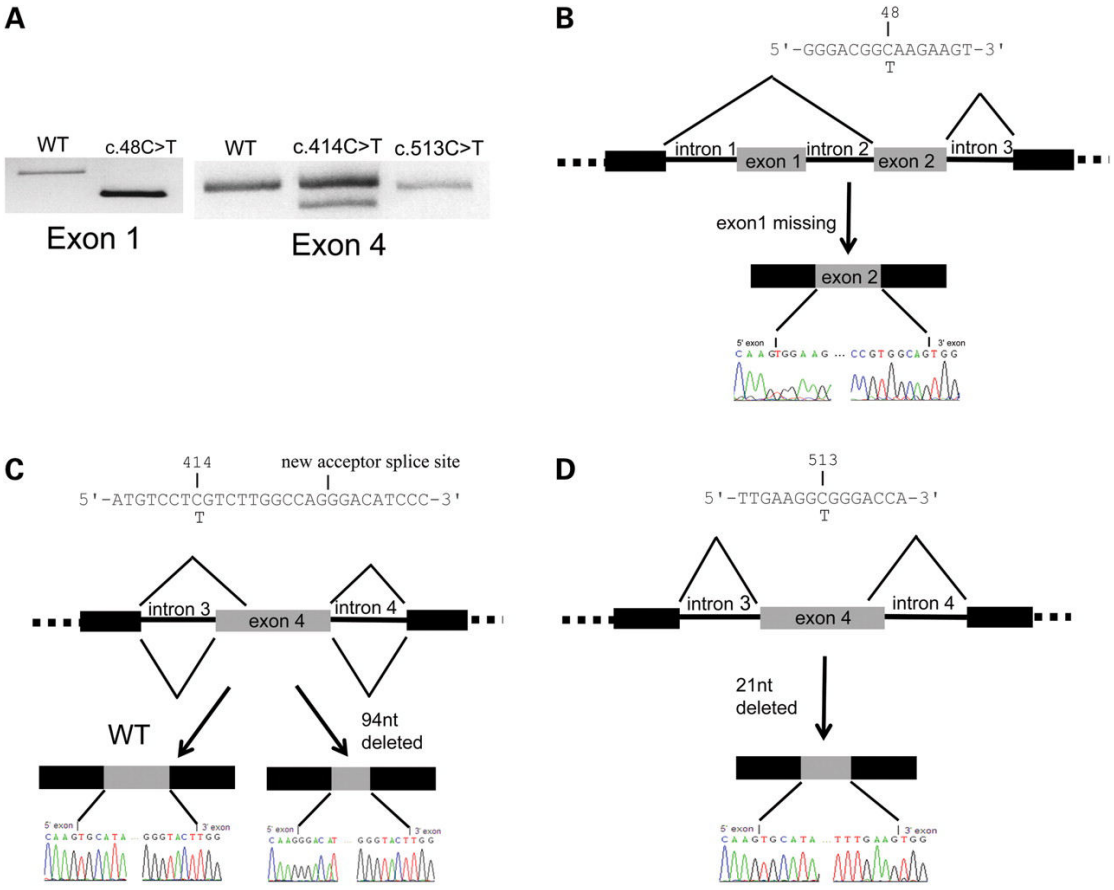

Figure 4.34. Silent nucleotide variants in N-terminal portion of DOK7 resulting in altered splicing of the DOK7 RNA transcript. (A) Gel electrophoresis of amplicons generated using vector-specific primers. All three silent variants produce different sized transcripts compared to wild-type. (B-D) Sequencing data and schematic diagrams showing aberrant splicing arising due to the variants. Figure taken from Cossins et al 'The spectrum of mutations that underlie the neuromuscular junction synaptopathy in DOK7 congenital myaesthenic syndrome' Hum Mol Genet 2012 Sep 1;21(17):3765-75.

Our data show that not only does the expression of different DOK7 variants differ between normal and cancer tissue, but that the expression of DOK7V1 appears to be diametrically opposed to the expression of DOK7V2 and, to a lesser extent, DOK7V3. Specifically, we have shown that the expression of DOK7V1 is significantly reduced in colorectal cancer tissue compared to normal colorectal tissue whilst the expression of DOK7V2 and DOK7V3 are significantly increased in colorectal cancer compared to normal colorectal tissue.

Attempts to confirm Dok7 expression at the protein level failed. The antibodies available and the DOK7 isoforms detected by them are shown in Table 4.3. Despite several attempts to confirm Dok7 Isoform 1, 2 and 3 expression at the protein level we were unable to do so. As demonstrated in the table, this may in part be due to the fact that the antibodies are not specific for different isoforms of Dok7. Owing to the limited time available for the current study and the cost and time required to raise isoform specific antibodies in animals, it was decided to focus on the mRNA expression of DOK7 and its variants and to assess the effects on protein expression and interactions using protein microarray.

Overall, the results discussed in this chapter suggest that the expression of individual DOK7 variants differs in colorectal cancer compared to normal colorectal tissue and that individual DOK7 variants may play different roles in human cancer. Further work is necessary to elucidate the effects of DOK7 variant expression on colorectal cancer cell function.

Table 4.3 DOK7 antibodies available for use in this study and isoforms detected by them

Antibody	Product number	Dok7 Isoform 1 (53kDa)	Dok7 Isoform 2 (37kDa)	Dok7 Isoform 3 (27kDa)
pDok7 (Tyr 395)	SC-68691	✔	✔	✖
Dok7 (N-terminal)	AP-13568a	✔	✖	✔
Dok7	SC-50463	✔	✔	✖

Chapter 5: Creation of DOK7 variant overexpression and knockdown constructs and creation of transgenic cell lines

5.1 Introduction

In the first results chapter, we analysed the expression profiles of DOK7 in a cohort of patients with colorectal cancer and colorectal cancer cell lines and examined the association between DOK7 expression and the clinical and pathological features of colorectal cancer as well as patient outcomes. We found that DOK7 mRNA expression is significantly reduced in colorectal cancer tissue compared with normal colorectal tissue and that DOK7 mRNA expression is inversely associated with T stage. Moreover, we found that DOK7 mRNA expression is significantly associated with overall survival in patients with colorectal cancer. In colorectal cancer cell lines, we found that the expression of DOK7 is variable and that DOK7 is highly expressed in HRT-18 colorectal cancer cells with little or no expression in HT-115 and RKO cells.

In the second results chapter, we analysed the expression profiles of DOK7V1, DOK7V2 and DOK7V3 in the same clinical cohort and colorectal cell lines and once again, examined the association between the expression of these DOK7 variants and clinicopathological features of colorectal cancer and patient outcomes. Our data revealed a number of interesting findings. Firstly, the expression of DOK7V1 is significantly reduced in colorectal cancer compared to normal colorectal tissue and is significantly associated with overall stage of disease and disease-free survival. In contrast, DOK7V2 expression is significantly increased in colorectal cancer compared to normal colorectal tissue, is higher in left-sided colonic cancers compared to right-sided cancers and is significantly associated with disease-free survival. Finally, DOK7V3 expression is also increased in colorectal cancer compared to normal colorectal tissue and is higher in left-sided colonic cancers compared to rectal cancers. Furthermore, DOK7V3 expression is significantly higher in patients who did not require any adjuvant treatment compared to those who underwent chemoradiotherapy.

Therefore, our results suggest that the expression of individual DOK7 variants differs in colorectal cancer compared to normal colorectal tissue and that individual DOK7 variants may play different roles in human cancer. In this chapter, we discuss how DOK7 variant specific transgenic cell lines were created.

5.2 Materials and methods

The manipulation of gene expression was performed using techniques described in Section 2.2.5.

5.2.1 Materials and methods used for the overexpression of DOK7 variants

5.2.1.1 Colorectal cancer cell lines

RKO colorectal cell line was used in this study. Details of this cell line are shown in Section 2.1.1. Cells were maintained according to the supplier's instructions. Wild type cells were maintained in the appropriate media for cell culture as described in Section 2.1.6.1 and the methods of cell culture used are described in Section 2.2.1. Stable transfected cells were maintained in the same media treated with 0.5µg/ml blasticidin as described in Section 2.2.5.10.

5.2.1.2 Primers

The variant specific primers used in this study are listed in Table 4.1.

5.2.1.3 Generation of synthetic DOK7V1-3 sequences

Synthetic DOK7 variant 1 (DOK7V1), DOK7 variant 2 (DOK7V2) and DOK7 variant 3 (DOK7V3) genes were assembled by Life Technologies Ltd (Paisley, UK) using synthetic oligonucleotides and/or PCR products. The sequence of DOK7V1 construct is shown in

Figure 5.1, the sequence of DOK7V2 construct is shown in Figure 5.2 and the sequence of DOK7V3 is shown in Figure 5.3.

The DOK7V1 fragment was cloned into pMK (kanR) vector using PacI and AscI cloning sites, the DOK7V2 fragment was cloned into pMA-T vector using Sfil and Sfil cloning sites and the DOK7V3 fragment was cloned into pMK (kanR) vector. Plasmid DNA was purified from transformed bacteria, quantified using UV spectroscopy and the final construct was verified by sequencing. Sequence congruence within the used restriction sites was 100% for all constructs and sequence identity was confirmed as 100% for all three variants. Life Technologies Ltd supplied 5µg of lyophilized plasmid DNA for each variant. These were dissolved in 50µl of distilled water on receipt and stored at -20°C until use. The plasmid map for DOK7V1 is shown in Figure 5.4, DOKV2 is shown in Figure 5.5 and DOK7V3 is shown in Figure 5.6.

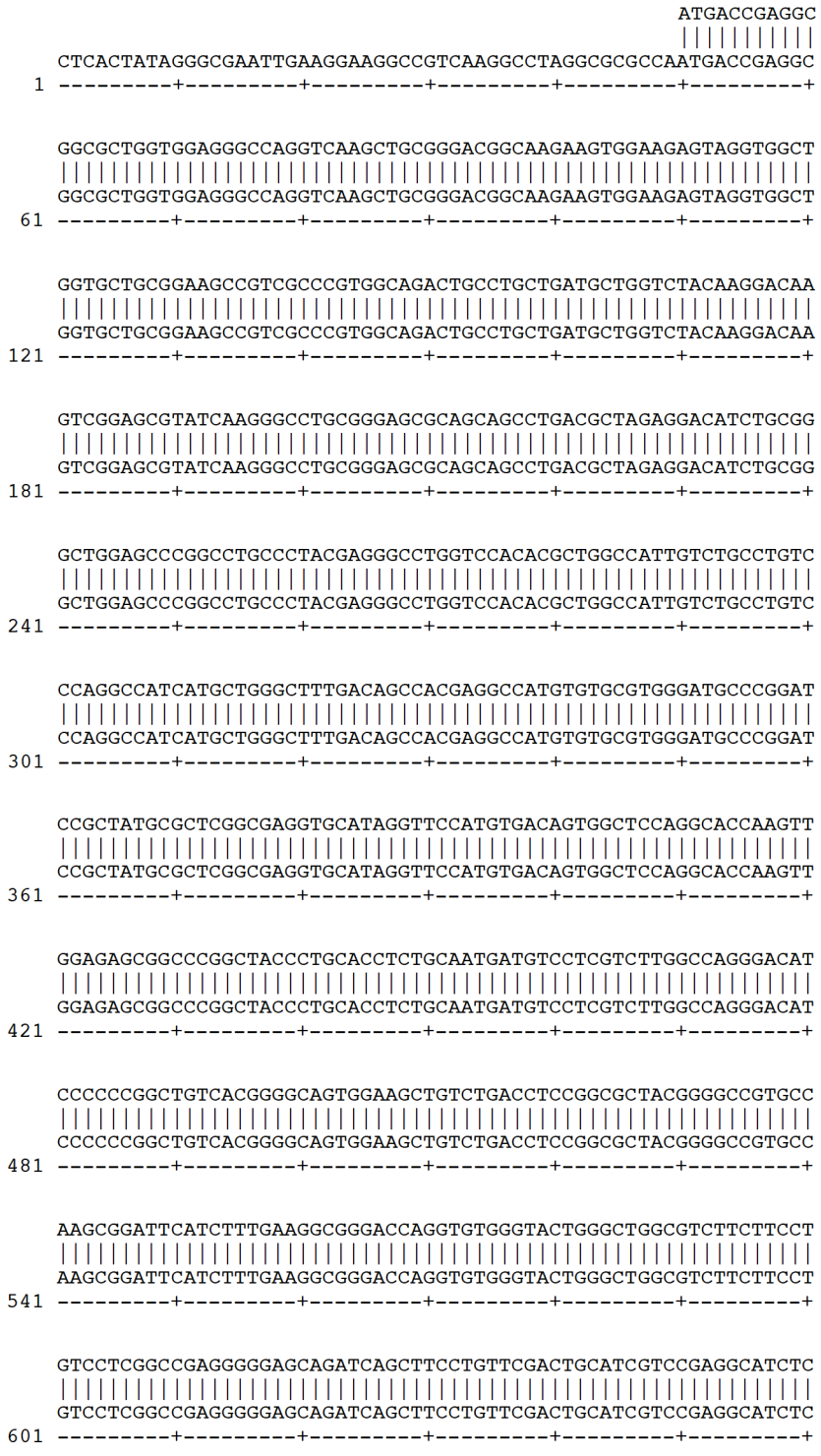
ATGACCGAGGC
CTCACTATAGGGCGAATTGAAGGAAGGCCGTCAAGGCCTAGGCGCGCCAATGACCGAGGC
1
GGCGCTGGTGGAGGGCCAGGTCAAGCTGCGGGACGGCAAGAAGTGGAAGAGTAGGTGGCT
GGCGCTGGTGGAGGGCCAGGTCAAGCTGCGGGACGGCAAGAAGTGGAAGAGTAGGTGGCT
61
GGTGCTGCGGAAGCCGTCGCCCGTGGCAGACTGCCTGCTGATGCTGGTCTACAAGGACAA
GGTGCTGCGGAAGCCGTCGCCCGTGGCAGACTGCCTGCTGATGCTGGTCTACAAGGACAA
121
GTCGGAGCGTATCAAGGGCCTGCGGGAGCGCAGCAGCCTGACGCTAGAGGACATCTGCGG
GTCGGAGCGTATCAAGGGCCTGCGGGAGCGCAGCAGCCTGACGCTAGAGGACATCTGCGG
181
GCTGGAGCCCGGCCTGCCCTACGAGGGCCTGGTCCACACGCTGGCCATTGTCTGCCTGTC
GCTGGAGCCCGGCCTGCCCTACGAGGGCCTGGTCCACACGCTGGCCATTGTCTGCCTGTC
241
CCAGGCCATCATGCTGGGCTTTGACAGCCACGAGGCCATGTGTGCGTGGGATGCCCGGAT
CCAGGCCATCATGCTGGGCTTTGACAGCCACGAGGCCATGTGTGCGTGGGATGCCCGGAT
301
CCGCTATGCGCTCGGCGAGGTGCATAGGTTCCATGTGACAGTGGCTCCAGGCACCAAGTT
CCGCTATGCGCTCGGCGAGGTGCATAGGTTCCATGTGACAGTGGCTCCAGGCACCAAGTT
361
GGAGAGCGGCCCGGCTACCCTGCACCTCTGCAATGATGTCCTCGTCTTGGCCAGGGACAT
GGAGAGCGGCCCGGCTACCCTGCACCTCTGCAATGATGTCCTCGTCTTGGCCAGGGACAT
421
CCCCCCGGCTGTCACGGGGCAGTGGAAGCTGTCTGACCTCCGGCGCTACGGGGCCGTGCC
CCCCCCGGCTGTCACGGGGCAGTGGAAGCTGTCTGACCTCCGGCGCTACGGGGCCGTGCC
481
AAGCGGATTCATCTTTGAAGGCGGGACCAGGTGTGGGTACTGGGCTGGCGTCTTCTTCCT
AAGCGGATTCATCTTTGAAGGCGGGACCAGGTGTGGGTACTGGGCTGGCGTCTTCTTCCT
541
GTCCTCGGCCGAGGGGGAGCAGATCAGCTTCCTGTTCGACTGCATCGTCCGAGGCATCTC
GTCCTCGGCCGAGGGGGAGCAGATCAGCTTCCTGTTCGACTGCATCGTCCGAGGCATCTC
601

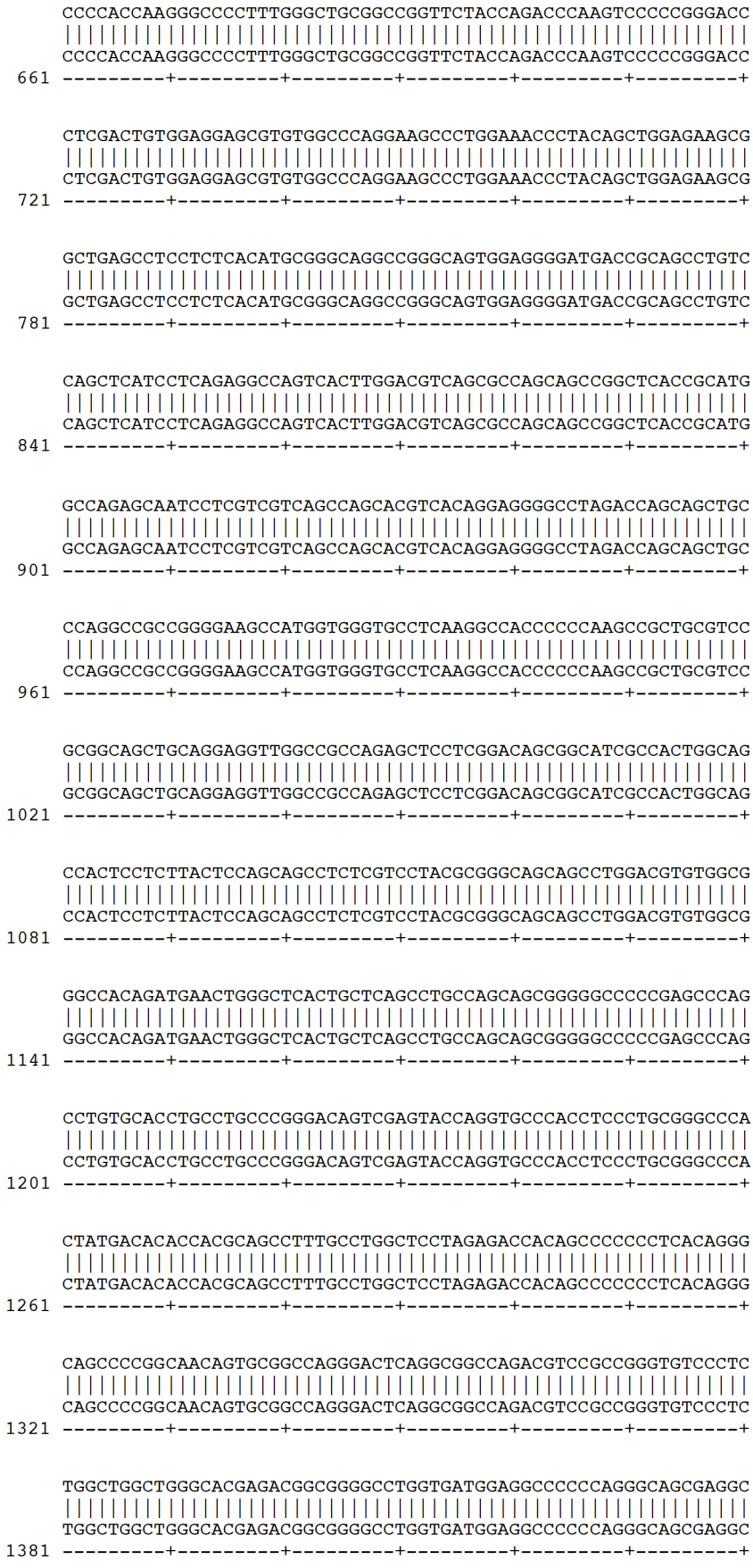
CCCCACCAAGGGCCCCTTTGGGCTGCGGCCGGTTCTACCAGACCCAAGTCCCCCGGGACC
CCCCACCAAGGGCCCCTTTGGGCTGCGGCCGGTTCTACCAGACCCAAGTCCCCCGGGACC
661
CTCGACTGTGGAGGAGCGTGTGGCCCAGGAAGCCCTGGAAACCCTACAGCTGGAGAAGCG
CTCGACTGTGGAGGAGCGTGTGGCCCAGGAAGCCCTGGAAACCCTACAGCTGGAGAAGCG
721
GCTGAGCCTCCTCTCACATGCGGGCAGGCCGGGCAGTGGAGGGGATGACCGCAGCCTGTC
GCTGAGCCTCCTCTCACATGCGGGCAGGCCGGGCAGTGGAGGGGATGACCGCAGCCTGTC
781
CAGCTCATCCTCAGAGGCCAGTCACTTGGACGTCAGCGCCAGCAGCCGGCTCACCGCATG
CAGCTCATCCTCAGAGGCCAGTCACTTGGACGTCAGCGCCAGCAGCCGGCTCACCGCATG
841
GCCAGAGCAATCCTCGTCGTCAGCCAGCACGTCACAGGAGGGGCCTAGACCAGCAGCTGC
GCCAGAGCAATCCTCGTCGTCAGCCAGCACGTCACAGGAGGGGCCTAGACCAGCAGCTGC
901
CCAGGCCGCCGGGGAAGCCATGGTGGGTGCCTCAAGGCCACCCCCCAAGCCGCTGCGTCC
CCAGGCCGCCGGGGAAGCCATGGTGGGTGCCTCAAGGCCACCCCCCAAGCCGCTGCGTCC
961
GCGGCAGCTGCAGGAGGTTGGCCGCCAGAGCTCCTCGGACAGCGGCATCGCCACTGGCAG
GCGGCAGCTGCAGGAGGTTGGCCGCCAGAGCTCCTCGGACAGCGGCATCGCCACTGGCAG
1021
CCACTCCTCTTACTCCAGCAGCCTCTCGTCCTACGCGGGCAGCAGCCTGGACGTGTGGCG
CCACTCCTCTTACTCCAGCAGCCTCTCGTCCTACGCGGGCAGCAGCCTGGACGTGTGGCG
1081
GGCCACAGATGAACTGGGCTCACTGCTCAGCCTGCCAGCAGCGGGGGCCCCCGAGCCCAG
GGCCACAGATGAACTGGGCTCACTGCTCAGCCTGCCAGCAGCGGGGGCCCCCGAGCCCAG
1141
CCTGTGCACCTGCCTGCCCGGGACAGTCGAGTACCAGGTGCCCACCTCCCTGCGGGCCCA
CCTGTGCACCTGCCTGCCCGGGACAGTCGAGTACCAGGTGCCCACCTCCCTGCGGGCCCA
1201
CTATGACACACCACGCAGCCTTTGCCTGGCTCCTAGAGACCACAGCCCCCCCTCACAGGG
CTATGACACACCACGCAGCCTTTGCCTGGCTCCTAGAGACCACAGCCCCCCCTCACAGGG
1261
CAGCCCCGGCAACAGTGCGGCCAGGGACTCAGGCGGCCAGACGTCCGCCGGGTGTCCCTC
CAGCCCCGGCAACAGTGCGGCCAGGGACTCAGGCGGCCAGACGTCCGCCGGGTGTCCCTC
1321
TGGCTGGCTGGGCACGAGACGGCGGGGCCTGGTGATGGAGGCCCCCCAGGGCAGCGAGGC
TGGCTGGCTGGGCACGAGACGGCGGGGCCTGGTGATGGAGGCCCCCCAGGGCAGCGAGGC
1381

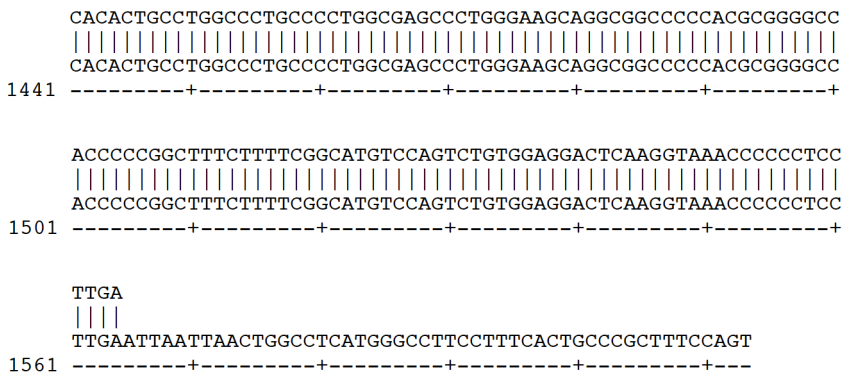

Figure 5.1. Sequence of DOK7V1 (Provided by Life Technologies)

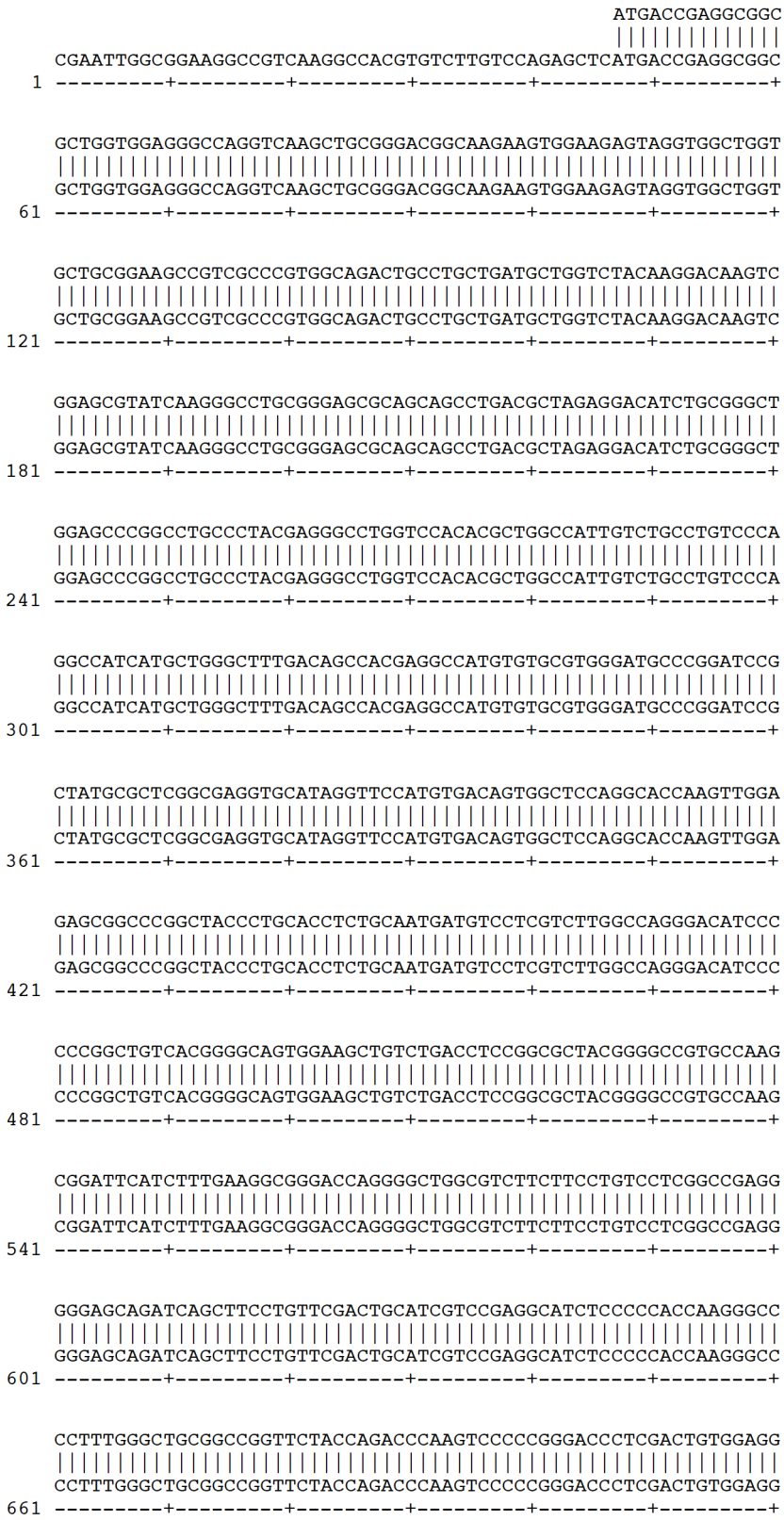
ATGACCGAGGCGGC
CGAATTGGCGGAAGGCCGTCAAGGCCACGTGTCTTGTCCAGAGCTCATGACCGAGGCGGC
1
GCTGGTGGAGGGCCAGGTCAAGCTGCGGGACGGCAAGAAGTGGAAGAGTAGGTGGCTGGT
GCTGGTGGAGGGCCAGGTCAAGCTGCGGGACGGCAAGAAGTGGAAGAGTAGGTGGCTGGT
61
GCTGCGGAAGCCGTCGCCCGTGGCAGACTGCCTGCTGATGCTGGTCTACAAGGACAAGTC
GCTGCGGAAGCCGTCGCCCGTGGCAGACTGCCTGCTGATGCTGGTCTACAAGGACAAGTC
121
GGAGCGTATCAAGGGCCTGCGGGAGCGCAGCAGCCTGACGCTAGAGGACATCTGCGGGCT
GGAGCGTATCAAGGGCCTGCGGGAGCGCAGCAGCCTGACGCTAGAGGACATCTGCGGGCT
181
GGAGCCCGGCCTGCCCTACGAGGGCCTGGTCCACACGCTGGCCATTGTCTGCCTGTCCCA
GGAGCCCGGCCTGCCCTACGAGGGCCTGGTCCACACGCTGGCCATTGTCTGCCTGTCCCA
241
GGCCATCATGCTGGGCTTTGACAGCCACGAGGCCATGTGTGCGTGGGATGCCCGGATCCG
GGCCATCATGCTGGGCTTTGACAGCCACGAGGCCATGTGTGCGTGGGATGCCCGGATCCG
301
CTATGCGCTCGGCGAGGTGCATAGGTTCCATGTGACAGTGGCTCCAGGCACCAAGTTGGA
CTATGCGCTCGGCGAGGTGCATAGGTTCCATGTGACAGTGGCTCCAGGCACCAAGTTGGA
361
GAGCGGCCCGGCTACCCTGCACCTCTGCAATGATGTCCTCGTCTTGGCCAGGGACATCCC
GAGCGGCCCGGCTACCCTGCACCTCTGCAATGATGTCCTCGTCTTGGCCAGGGACATCCC
421
CCCGGCTGTCACGGGGCAGTGGAAGCTGTCTGACCTCCGGCGCTACGGGGCCGTGCCAAG
CCCGGCTGTCACGGGGCAGTGGAAGCTGTCTGACCTCCGGCGCTACGGGGCCGTGCCAAG
481
CGGATTCATCTTTGAAGGCGGGACCAGGGGCTGGCGTCTTCTTCCTGTCCTCGGCCGAGG
CGGATTCATCTTTGAAGGCGGGACCAGGGGCTGGCGTCTTCTTCCTGTCCTCGGCCGAGG
541
GGGAGCAGATCAGCTTCCTGTTCGACTGCATCGTCCGAGGCATCTCCCCCACCAAGGGCC
GGGAGCAGATCAGCTTCCTGTTCGACTGCATCGTCCGAGGCATCTCCCCCACCAAGGGCC
601
CCTTTGGGCTGCGGCCGGTTCTACCAGACCCAAGTCCCCCGGGACCCTCGACTGTGGAGG
CCTTTGGGCTGCGGCCGGTTCTACCAGACCCAAGTCCCCCGGGACCCTCGACTGTGGAGG
661

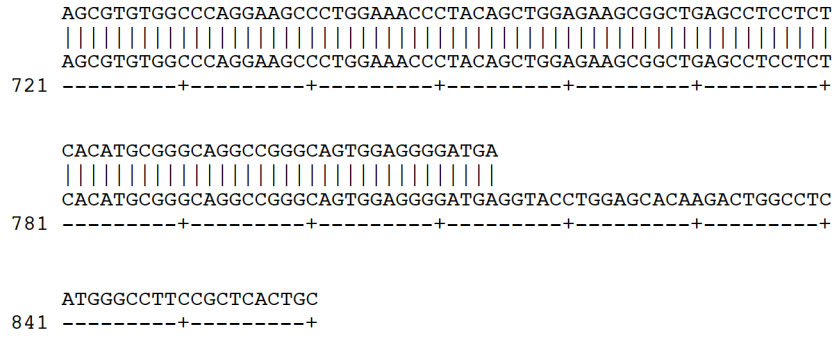

Figure 5.2. Sequence of DOK7V2 (Provided by Life Technologies)

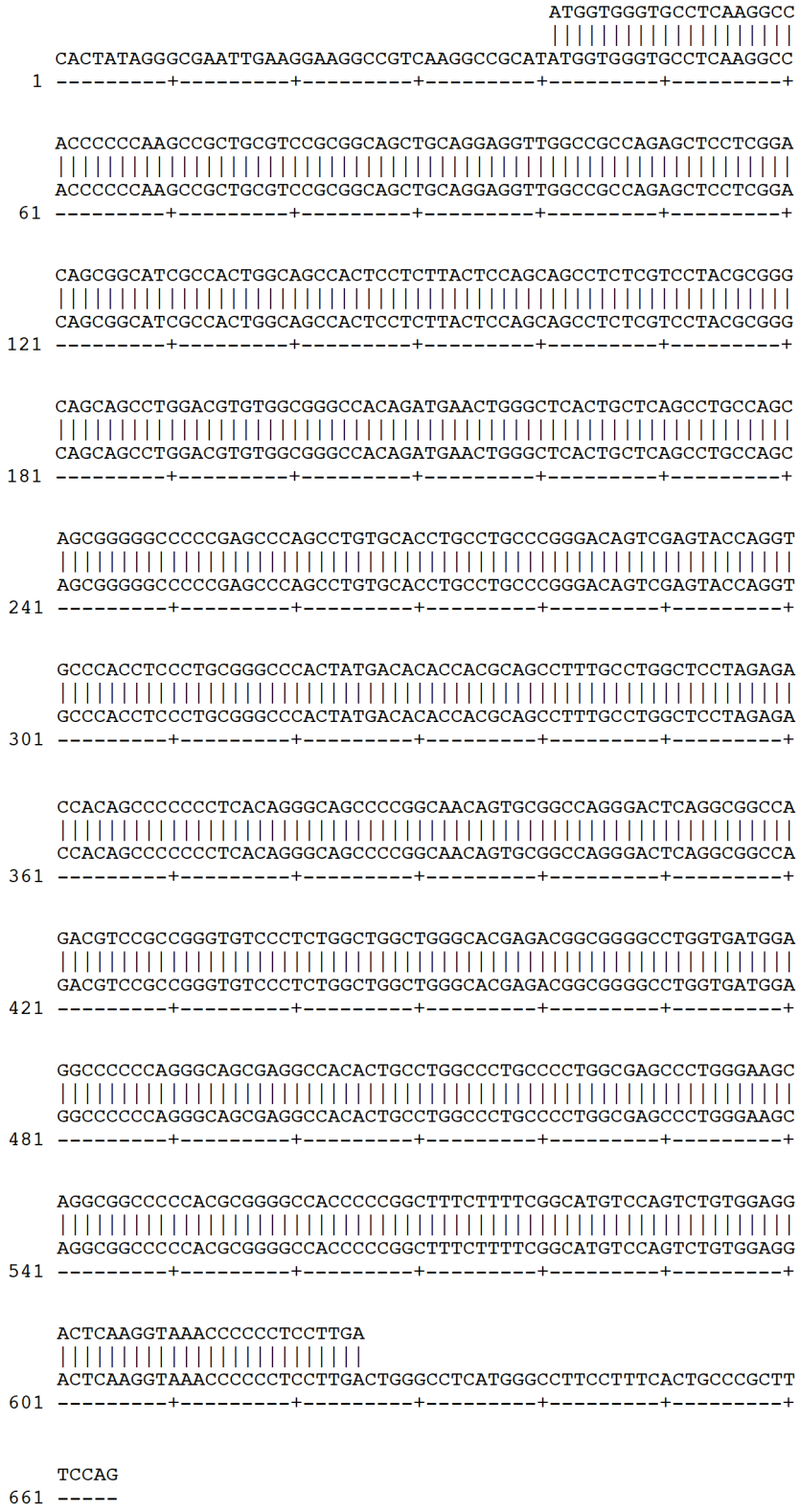

Figure 5.3 Sequence of DOK7V3 (Provided by Life Technologies)

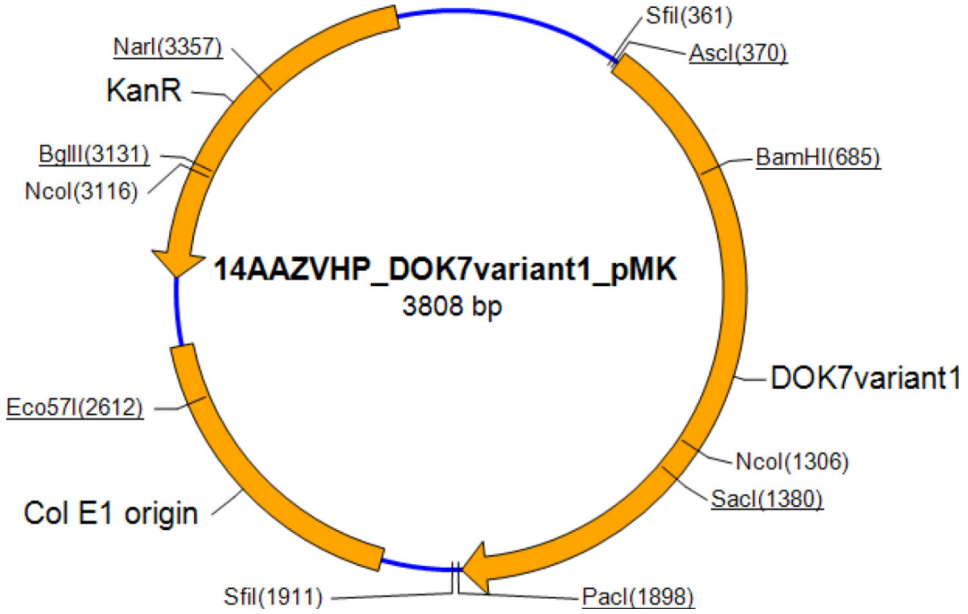

Figure 5.4. Plasmid map for DOK7V1 (Provided by Life Technologies)

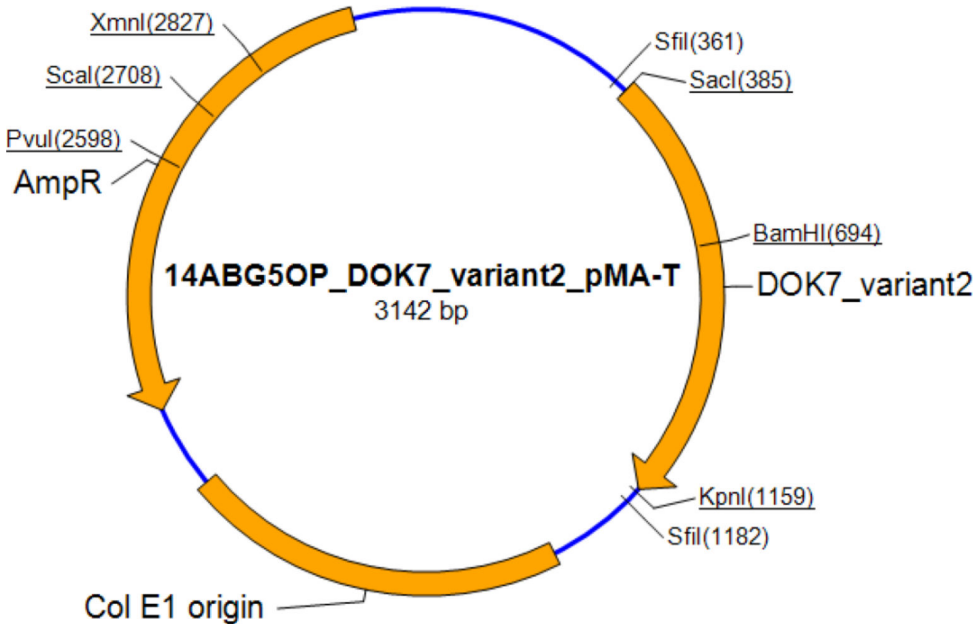

Figure 5.5 Plasmid map for DOK7V2 (Provided by Life Technologies)

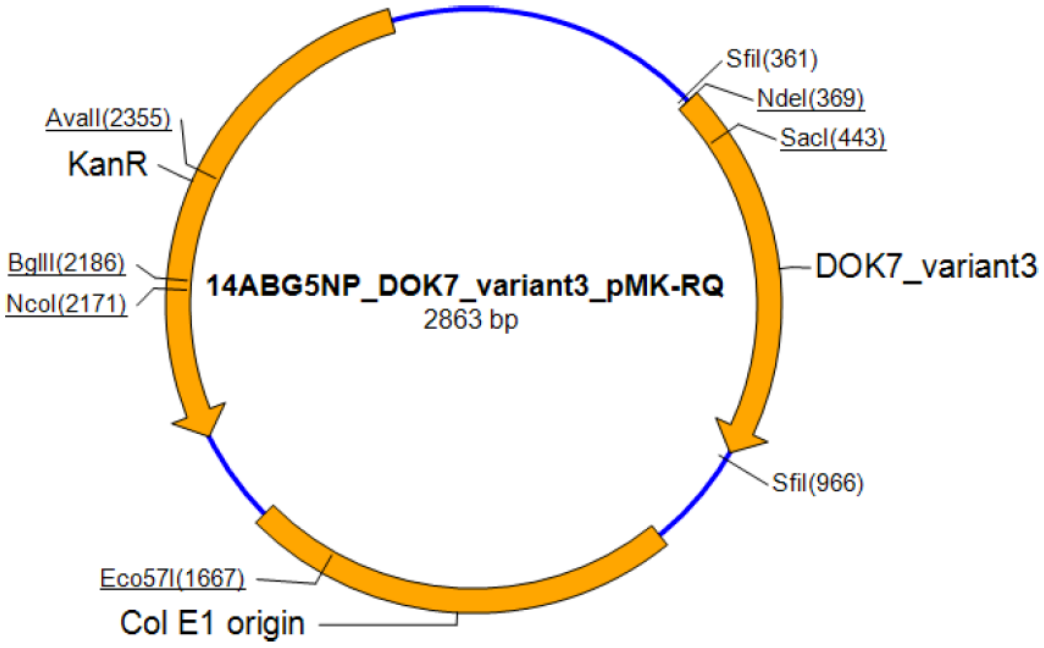

Figure 5.6 Plasmid map for DOK7V3 (Provided by Life Technologies)

5.2.1.4 Extraction and amplification of synthesised sequences

The synthesised plasmids containing DOK7V1, DOK7V2 and DOK7V3 were not suitable for immediate use in mammalian cells owing to the nature and number of antibiotic resistance sites. Primers that would enable the extraction of the synthesised sequences from the plasmids were designed and are shown in Table 5.1.

Table 5.1 Primers used for extraction of synthesised DOK7V1, DOK7V2 and DOK7V3 sequences from plasmids supplied by Life Technologies.

Primer	Primer type	Sequence
DOK7V2exF1	Forward primer	atgaccgaggcggcgctggtgga
DOK7V3exF1	Forward primer	atggtgggtgcctcaaggccac
DOK7V2exR1	Reverse primer	tcatcccctccactgcccggcct
DOK7V2exR1b	Reverse primer	tcccctccactgcccggcct
DOK7V3exR1	Reverse primer	tcaaggaggggggtttaccttga
DOK7V3exR1b	Reverse primer	aggaggggggtttaccttga

Two types of reverse primer were designed: R1 primers which contained a stop codon and no His tag, and R1b primers which did not contain a stop codon but instead contained a His tag. The purpose of the latter was to facilitate potential future targeting of the sequence using His antibodies during protein analysis, Western blot and immunohistochemistry.

The combinations of the primers used to extract each individual variant of DOK7 are shown in Table 5.2 along with their expected product sizes.

Table 5.2 Primer pairs used for extraction of DOK7V1, DOK7V2 and DOK7V3 with product sizes

Target sequence	Primer pair used	PCR product	Product size
DOK7V1	DOK7V2exF1 DOK7V3exR1	DOK7V1Stop	1515bp
	DOK7V2exF1 DOK7V3exR1b	DOK7V1His	
DOK7V2	DOK7V2exF1 DOK7V2exR1	DOK7V2Stop	767bp
	DOK7V2exF1 DOK7V2exR1b	DOK7V2His	
DOK7V3	DOK7V3exF1 DOK7V3exR1	DOK7V3Stop	585bp
	DOK7V3exF1 DOK7V3exR1b	DOK7V3His	

The components used in each PCR reaction undertaken to generate products from the synthesised vectors are shown in Table 5.3 and the conditions used are shown in Table 5.4.

Table 5.3 Components of PCR reactions used to extract synthesised DOK7V1, DOK7V2 and DOK7V3 from synthesised plasmids

Component	Volume
2x High fidelity PCR mix	25µL
Forward primer	2µL
Reverse primer	2µL
Plasmid (0.025ng/ µL 1:100 in PCR H_20)	2µL
PCR H_20	19µL
Total volume per reaction	50µL

Table 5.4 Conditions used for PCR reactions for extraction of synthesised DOK7V1-3 sequences from plasmids

Step	Temperature (°C)	Time (minutes: seconds)	Number of cycles
Initialisation	94	05:00	
Denaturation	94	00:20	30 cycles
Annealing	55	00:20	
Extension/elongation	72	02:00	
Final extension	72	10:00	
Final hold	4	∞	

Following the PCR, 10µL of each sample was mixed with 2µL loading dye . A 1% agarose gel was prepared and 5µL of a PCR ladder was loaded into the first well with 8µL of each sample pipetted into the consecutive remaining wells. The gel was run at 100V, 100mA and 50W for 45 minutes and then visualised using the Syngene U: Genius 3 fluorescence UV transilluminator (Synoptics Ltd, Cambridge, UK) in order to confirm the presence and correct size of the PCR products. The remaining 15µL of the PCR product was mixed with 2µL of Red Mastermix and the final extension step was run again at 72°C for 10 minutes followed by 4°C for infinity. The PCR products were then stored at -20°C until further use.

Bands of the correct size were excised from the agarose gel and elution to obtain the products was performed using GenElute™ Gel Extraction kit as described below.

5.2.1.5 Extraction of bands from agarose gel and product separation using gel elution kit

The GenElute™ Gel Extraction kit was used to purify the DOK7V1, DOK7V2 and DOK7V3 linear DNA fragments from the agarose gel. Briefly, the principles of elution are that DNA fragments are extracted from the agarose gel and solubilised to dissolve the agarose gel. The extracted DNA fragments are then selectively absorbed onto a silica membrane, contaminants are removed and finally, the DNA is eluted in a buffer. This isolated DNA can then be used for PCR, cloning and other purposes. The manufacturers state that typical DNA recovery is 50-55% and can be as high as 80%. Each column can process up to 3.5g agarose and can bind up to 10µg of DNA.

The DNA fragment of interest (DOK7V1/DOK7V2/DOK7V3) was excised from the agarose gel using a sterile, sharp disposable scalpel taking care to trim away any excess agarose gel outside of the band of interest. The gel was then weighed prior to adding 3 gel volumes of the Gel Solubilisation solution to the gel slice. The gel mixture was incubated at 50-60°C for 10

minutes, vortexing briefly every 2-3 minutes, until the gel slice was completely dissolved and the mixture was yellow in colour.

Meanwhile, a binding column was prepared by placing the GenElute™ Binding Column G into a 2ml collection tube. Five hundred microlitres of Column Preparation solution was added to each binding column and the tube was centrifuged for 1 minute. The flow-through liquid was then discarded. One gel volume of 100% isopropanol was added to the gel mixture and mixed until the contents of the tube were homogenous. The solubilised gel solution (up to a maximum of 700µL) was loaded into the binding column and centrifuged for 1 minute. The flow through liquid was discarded. If the solubilised gel solution exceeded 700µL volume this step was repeated until all the solution had been used.

Seven hundred microlitres of wash solution was then added to the binding column and the tube centrifuged for 1 minute. The flow-though liquid was discarded and then the tube containing the binding column was centrifuged again for 1 minute to remove any excess ethanol.

Finally, the binding column was transferred to a new collection tube and 50µL Elution Solution pre-heated to 65°C was added to the centre of the membrane. The tube was incubated for 1 minute and then centrifuged for 1 minute. The eluted solution was then poured off and stored at -20°C.

5.2.1.6 Confirmation of extracted DOK7 variant sequences

The DOK7 variant sequences obtained using the elution kits were verified using PCR. The components used for each reaction are shown in Table 5.5 and the conditions used are shown in Table 5.6.

Table 5.5 Components used in PCR reaction to confirm extracted DOK7 variant sequences

Component	Volume
2x Green GoTaq Mastermix	6µL
Forward primer (1:10)	1µL
Reverse primer (1:10)	1µL
DNA/Vector/Plasmid (1:100)	1µL
PCR H_2O	3µL
Total volume	12µL

Table 5.6 Conditions used in PCR reaction to confirm extracted DOK7 variant sequences

Step	Temperature (°C)	Time (minutes:seconds)	Number of cycles
Initialisation	94	05:00	
Denaturation	94	00:20	25-32 cycles
Annealing	55	00:20	
Extension/elongation	72	00:40	
Final extension	72	10:00	
Final hold	4	∞	

The PCR products were then run on a 1-2% agarose gel at 120V, 100mA and 50W for 45 minutes. The gel was visualised using a UV transilluminator. Following the PCR, the variant

specific plasmids were quantified and 10μL of plasmid at a concentration of 100ng/μL was prepared and submitted for sequencing.

5.2.1.7 TOPO TA cloning of DOK7V expression constructs into a pEF/His TOPO plasmid vector

The PCR products obtained from the previous steps are shown in Table 5.7.

Table 5.7 PCR products used for cloning

Variant	Primers used	PCR fragment cloned
DOK7V1	DOK7V2exF1 DOK7V3exR1	DOK7V1stop
	DOK7V2exF1 DOK7V3exR1b	DOK7V1His
DOK7V2	DOK7V2exF1 DOK7V2exR1	DOK7V2stop
	DOK7V2exF1 DOK7V2exR1b	DOK7V2His
DOK7V3	DOK7V3exF1 DOK7V3exR1	DOK7V3stop
	DOK7V3exF1 DOK7V3exR1b	DOK7V3His

Note: stop = stop codon included in sequence, His = stop codon removed, His tag inserted.

The verified DOK7V1/V2/V3 expression constructs were cloned into a pEF6/V5-His-TOPO plasmid (Invitrogen, Paisley, UK) as described in Section 2.2.5.4 and then transformed into chemically competent *E.coli*, as described in Section 2.2.5.5.

5.2.1.8 Orientation checking

Following overnight incubation, the ampicillin selection agar plates were removed from the incubator and colonies were identified.

Orientation checking was performed using conventional PCR using forward primers paired with either T7F or BGHR primers. The components for the PCR reaction are shown in Table 5.8 and the conditions used are shown in Table 5.9.

Table 5.8 Components used in PCR reaction for orientation checking

Component	Volume
2x Green GoTaq Mastermix	6µL
PCR H2O	4µL
Forward variant specific primer (1:10)	1µL
T7F/BGHR primer	1µL
E.coli colony	Touch with sterile pipette tip
Total volume	12µL

Table 5.9 Conditions used in PCR reaction for orientation checking

Step	Temperature (°C)	Time (minutes:seconds)	Number of cycles
Initialisation	94	10:00	
Denaturation	94	00:30	25-30 cycles
Annealing	55	00:30	
Extension/elongation	72	01:30	
Final extension	72	10:00	
Final hold	4	∞	

Products were visualised using agarose gel electrophoresis and UV transillumination as described in Section 2.2.2.5 and subsequently purified and amplified as described in Section 2.2.5.7.

5.2.1.9 Quantification of plasmid DNA

The plasmids were quantified using a spectrophotometer set to a double stranded DNA setting using PCR water as a blank. Ideal values were determined as being between 0.2-1µg.

5.2.1.10 Confirmation of plasmid DNA using sequencing

The isolated plasmids were submitted for sequencing along with T7F primer (concentration 100pmol/µL). The plasmids and their expected product sizes are shown in Table 5.10.

Table 5.10 Plasmids submitted for sequencing and their expected product sizes

Plasmid	Expected product size	Expected product size with T7F
5.1 (DOK7V2Stop)	768bp	868bp
4.1 (DOK7V2His)	768bp	868bp

Note: Plasmid numbers identify original plate number and colony from which plasmid was extracted, purified and amplified.

5.2.1.11 Transfection of colorectal cancer cells and generation of stable transfectants

Colorectal cancer cells were transfected using electroporation as described in Section 2.2.5.9 and stable transfected cell lines were established as described in Section 2.2.5.10.

5.2.1.12 Isolation of RNA and cDNA synthesis

RNA was isolated from cells using TRI Reagent® (Sigma-Aldrich Inc., Poole. UK), as described in Section 2.2.2.1, and quantified using a spectrophotometer as described in Section 2.2.2.2. Reverse transcription using a High Capacity cDNA Reverse transcription kit was used to synthesis cDNA as described in Section 2.2.2.3.

5.2.1.13 Verification of DOK7 variant overexpression in transfected cells using PCR

Verification of successful DOK7 variant overexpression in stable transfected cells was performed using PCR.

5.3 Results

5.3.1 Extraction of DOK7V2 sequences from synthesised vectors

The DOK7V2 sequences were extracted from the synthesised vectors supplied by Life Technologies Ltd as shown in Figure 5.7. It was decided to focus on DOK7V2 sequences owing to the non-specific bands seen for DOK7V1 and the weaker bands seen for DOK7V3.

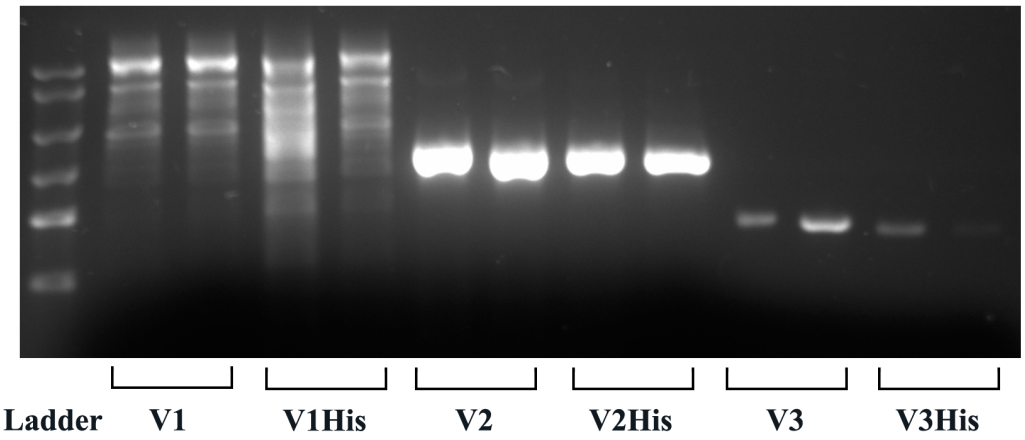

Figure 5.7 Synthesised DOK7V1, DOK7V2 and DOK7V3 sequences visualised following gel electrophoresis. V1 = DOK7V1 with stop codon, V1His = DOK7V1 without stop codon and with His Tag, V2 = DOK7V2 with stop codon, V2His = DOK7V2 without stop codon and with His tag, V3 = DOK7V3 with stop codon, V3His = DOK7V3 without stop codon and with His tag.

5.3.2 Confirmation of extracted DOK7V2 sequences

The extracted DOK7V2 sequences were confirmed using variant specific qPCR primers. Representative confirmation PCR results for DOK7V2 are shown in Figure 5.8.

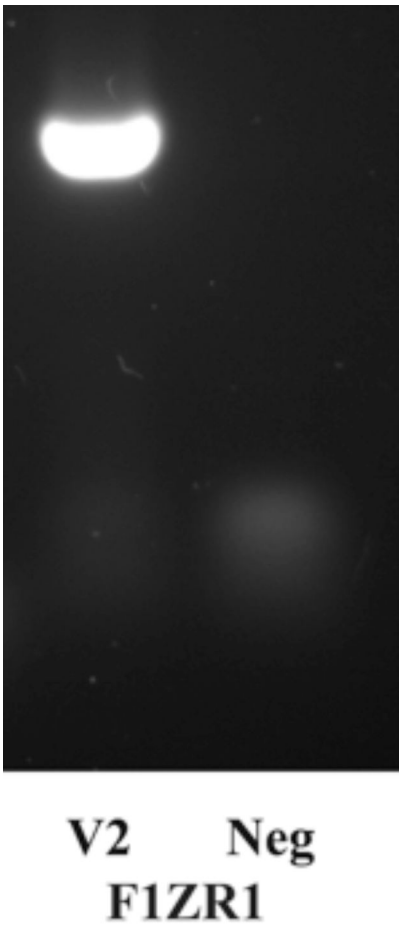

Figure 5.8 Confirmation of DOK7V2 vector shown on agarose gel using UV trans illumination using DOK7V2 F1ZR1 primers. V2 = vector, Neg = negative control.

5.3.3 Confirmation of correct orientation of PCR products

Following transformation of DOK7V2Stop and DOK7V2His plasmids into chemically competent E.coli, each colony was checked using PCR, firstly to verify the orientation of the inserted transgene as shown in Figure 5.9 and secondly to verify the presence and correct size of the products.

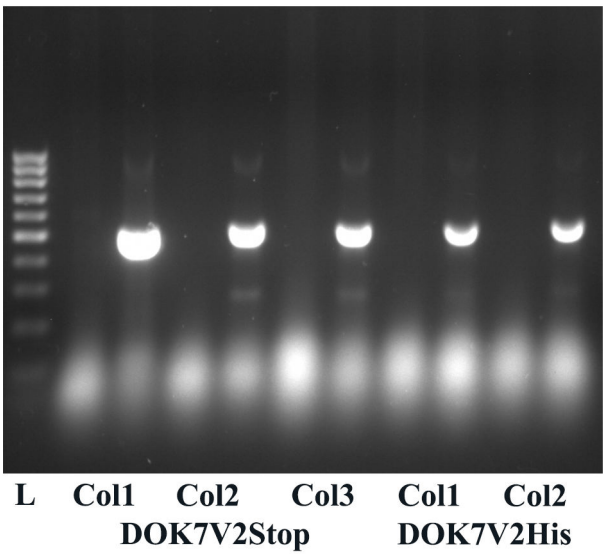

Figure 5.9 Confirmation of correct orientation of PCR products. Following transformation of DOK7V2Stop and DOK7V2His plasmids into chemically competent E.coli, each colony was checked using PCR, firstly to verify the orientation of the inserted transgene and secondly to verify the presence and correct size of the products.

5.3.4 Successfully obtained plasmids following extraction, cloning and orientation checking

A summary of the correctly oriented successfully inserted PCR products following extraction, amplification, cloning and colony orientation checking are shown in Table 5.11.

Table 5.11. Successfully obtained plasmids following extraction, cloning and orientation checking

Plate/colony number (Date grown)	DOK7 variant	Originating primer pair	PCR product
5/1 (04/09/2014)	V2	DOK7V2exF1 DOK7V2exR1	DOK7V2Stop
4/1 (12/06/2014)	V2	DOK7V2exF1 DOK7V2exR1b	DOK7V2His

5.3.5 Confirmation of plasmid DNA using sequencing

Results from formal sequencing analysis were entered into Nucleotide BLAST (https://blast.ncbi.nlm.nih.gov/Blast.cgi?PAGE_TYPE=BlastSearch), which confirmed they matched the known sequences for DOK7 Variant 2 with ≥99% identity of sequence alignment.

5.3.6 Verification of DOK7V2 overexpression in RKO cells

Successful overexpression of DOK7V2 in RKO cells at the mRNA level was confirmed using PCR as shown in Figure 5.10.

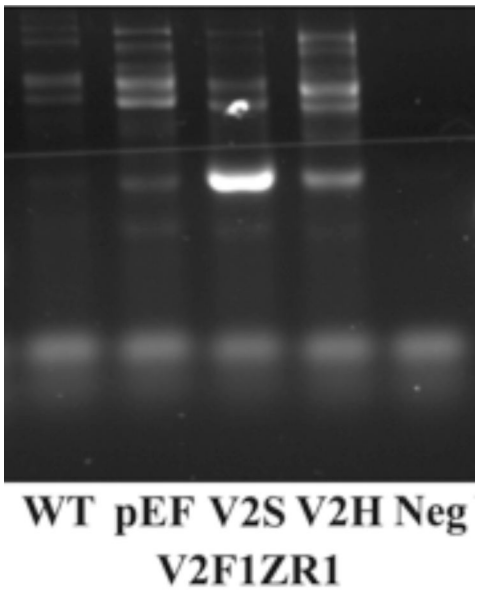

Figure 5.10 Verification of DOK7V2 overexpression in RKO cells. Compared to RKO WT and RKO pEF cells, the expression of DOK7V2 is increased in DOK7V2Stop expression (V2S) and, to a lesser extent, in the DOK7V2His expression (V2H) cells.

5.4 Discussion

In order to create DOK7 variant specific transgenic cell lines we used ribozyme transgenes and overexpression constructs. The latter were created using synthesised DOK7V1-3 obtained from Life Technologies Ltd. Owing to the nature and number of antibiotic resistance sites, the plasmids supplied by Life Technologies Ltd were not suitable for immediate use in mammalian cells. This made using the synthesised sequences somewhat more complicated since the sequences had to be extracted from the plasmids and amplified prior to cloning into the more suitable pEF/His TOPO plasmid vector.

Firstly, primers that would enable the extraction of the synthesised sequences were designed. In addition, two reverse primers were designed; one that contained a stop codon and a second for each variant sequence that contained no stop codon but instead contained a His tag. The purpose of the His tag was to enable potential future targeting of the sequence using His antibodies during protein analysis, Western blot and immunohistochemistry. The products produced using PCR were then separated using gel electrophoresis and bands of the correct sizes were excised from the agarose gel. In order to extract the DNA fragments from the agarose gel a GenElute™ Gel extraction kit was used. The products thereby obtained were then verified by PCR prior to their cloning into a pEF/His TOPO plasmid vector. Following orientation checking, the resulting plasmids were quantified and verified using formal sequencing analysis. These plasmids were then used to transfect colorectal cancer cells and successful overexpression at the mRNA level in the resulting stable transfectants was confirmed using PCR.

One of the limitations of the work discussed in this chapter is that unfortunately, despite good GAPDH bands being seen on protein analysis, no bands were seen using DOK7 antibodies and therefore, manipulation of DOK7 variant expression at the protein level could not be directly verified using Western blot.

The transgenic cell lines produced as a result of the work discussed in this chapter will enable the role of DOK7 variants and their interacting protein partners and interaction with cell signalling pathways to be analysed in the subsequent chapters. Since the DOK7V2 overexpression constructs produced more convincing results than the other constructs created, it was decided to focus the work of the remaining chapters on DOK7V2 overexpression.

Chapter 6: Effect of DOK7V2 overexpression on colorectal cancer cell function

6.1 Introduction

Most, if not all, cancer cells share a number of characteristic acquired capabilities, listed by Hanahan and Weinberg as (i) self-sufficiency in growth signals, (ii) insensitivity to anti-growth signals, (iii) evasion of apoptosis, (iv) limitless replicative potential, (v) sustained angiogenesis and (vi) tissue invasion and metastasis (76). Alterations in oncogenes and tumour suppressor genes may enable cells to acquire these characteristic capabilities resulting in modulation of key cell signalling pathways and ultimately, changes in cell behaviour. Such changes may manifest as alterations in cancer cell proliferation, tumour growth, cell adhesion, invasion, migration and rate of apoptosis.

The DOK7 gene is highly variable in the human population with multiple sequence variants encoding different protein isoforms (268). Our data suggest that the expression of these variants may differ between colorectal cancer tissue and normal colorectal tissue. Moreover, DOK7V1 expression is significantly lower in colorectal cancer tissue compared to normal colorectal tissue whilst DOK7V2 expression is significantly higher, suggesting that the different variants may play opposing roles.

The role of different DOK7 mRNA splice variants and the expression of their corresponding protein isoforms have not previously been investigated in relation to cancer. However, the role of DOK7 gene mutations in congenital myasthenic syndrome has recently been explored by Beeson and his team in Oxford (268, 269). They report that around 18% of genetically diagnosed CMS cases in the UK have mutations in DOK7 and from 72 patients studied, 34 different pathogenic mutations and 27 rare, but non-pathogenic, mutations were identified by examining the number and complexity of AChR clusters in C2C12 mouse myotubes (268, 269). In over 50% of DOK7 CMS patients, the exon 7 frameshift mutation 1124_1127dupTGCC is found in at least one allele resulting in aberrant AChR clustering (268, 269). In several patients there is truncation of, or mutation in, the large 3'exon of DOK7

resulting in the loss of C-terminal region function, though MuSK binding is retained (268). However, mutations may also occur towards the N-terminal region of the protein where the PH and PTB domains are found (268).

Previous studies have identified a key role for Dok-7 in the development of the neuromuscular junction. Yamanashi *et al* found that Dok-7 overexpression in skeletal muscle resulted in an increase in the total area of AChR clustering in the central region of the muscle as well as an increased number of AChR clusters suggesting increased NMJ formation (270). Despite this work investigating the role of Dok-7 in skeletal muscle, there is nothing in the currently published literature regarding the effect of Dok-7 on cancer cell proliferation, tumour growth, cell adhesion, cell invasion, cell motility/migration or apoptosis.

The functional role of the other Dok proteins is somewhat better understood. Several previous authors have shown that Dok-1-4 are negative regulators of cell proliferation (94, 95, 97, 99, 103, 112, 116, 199-202, 216). Negative regulation of cell growth by the Dok proteins may occur due to inhibition of epidermal growth factor (EGF) induced ERK activation or via the inhibition of c-Src induced cell transformation (112, 124, 147). Accordingly, loss of Dok-1-3 has been shown to result in increased cell proliferation (90, 97, 142, 202, 244, 261).

Contrary to these findings, however, other authors have found that Dok-1 plays a positive regulatory role with regard to cell proliferation (77, 251, 262). For example, Inoue *et al* demonstrated in mice that lack of Dok-1 was associated with decreased proliferation of splenic CD4+ T cell and splenic B cells in response to IL-4 (251). Furthermore, IL-4 induced surface expression of CD23 was significantly reduced in B cells prepared from Dok-1-deficient mice (251). Moreover, forced expression of Dok-1 in a myeloid cell line led to increased IL-4 induced proliferation (251). The authors suggest that the increased proliferative response to IL-4 associated with Dok-1 may be due to sustained phosphorylation of Stat6 and IL-4Rα (251). Dok-4, Dok-5 and Dok-6 have all been shown to play a role in

neurite outgrowth in mouse cortical neurons (104, 105, 128, 220). Consequently, knockdown of Dok-6 is associated with an approximate 25% reduction in neurite outgrowth in mouse primary cortical neurons (128)

The Dok proteins have also been implicated in cell adhesion. Noguchi *et al* found that tyrosine phosphorylation of Dok-1 is induced by cell adhesion to extracellular matrix proteins and that this is dependent on Src family kinases and the Dok-1 PH domain (198). Work by Abramson *et al* established that Dok-1 and Dok-2 are associated with CrkL, Cas and Nck, three proteins that are implicated in the regulation of actin-cytoskeletal reorganization, which is known to play a role in cell adhesion and migration (154). Dok-2 has also been found in PMP, which are associated with increased expression of adhesion molecules, angiogenesis and metastasis in cancer (212-214). Deficiency of Dok-2 has been associated with increased platelet-fibrinogen and platelet-platelet adhesion in discoid platelets and was associated with increased thrombus accumulation in vivo (160).

Other studies have suggested a potential role for the Dok proteins in cancer cell invasion and migration. Mashima *et al* found that loss of Dok-1, Dok-2 and Dok-3 in mice was associated with increased tumour invasiveness and multiple organ spread (261). Meanwhile, Dok-1 has been shown to play a positive regulatory role with regard to cell spreading and migration and has been shown to play an important role in SCF-1alpha/CXCL12 induced chemotaxis in T cells (77, 198, 231, 262). Sattler *et al* suggested that Dok-1 might mediate its effect on cell migration via the interaction of its PTB domain with multiple tyrosine residues on SHIP1 (207). Master *et al* found that overexpression of Dok-2 was associated with increased Ang1-mediated migration in endothelial cells via its association with Tek, Nck and Pak/Pak1 and the subsequent activation of Pak kinase (210).

Finally, the evidence regarding the Dok proteins and apoptosis is somewhat conflicting. Di Cristofano *et al* found no association between Dok-1 activation and growth factor

deprivation-induced apoptosis (97). However, Yamakawa *et al* found that overexpression of Dok-1 in B cells resulted in increased activin A-induced apoptotic responses and postulated that this occurs due to Dok-1 acting as an adaptor protein linking activin receptors with Smads (218). Moreover, Van Slyke *et al* found that Dok-2 potentiates anoikis, which is apoptosis induced by cell detachment (103). Consistent with this, Yasuda *et al* and Niki *et al* both found that mice lacking Dok-1 and Dok-2 displayed reduced apoptosis (143, 271). Pan *et al* concluded that Dok-5 is required for the blockade of TrkC-induced apoptosis by NT-3 signalling and that it mediates this action via the regulation of caspase-3 activity (223).

The aim of this chapter was to determine whether DOK7 variant overexpression resulted in altered colorectal cancer cell behaviour focusing on DOK7V2. Plasmids constructed from synthesised DOK7V2 sequences were used to create colorectal cancer cells that overexpressed DOK7V2 respectively. The effect of DOK7V2 expression on colorectal cancer cell behaviour was then investigated using functional assays to assess cell proliferation, adhesion, invasion and migration.

6.2 Materials and methods

6.2.1 Cell lines

RKO wild type (RKOWT), empty plasmid control (RKO pEF) and V2 overexpression cell lines (RKOV2Stop/5.1 and RKOV2His/4.1) were used in this study. The creation of these transgenic cell lines is described in Chapter 5 and the cell line used was the same cell line verified in Section 5.3.6.

6.2.2 Functional assays

6.2.2.1 *In vitro* growth assay

The methodology used for the *in vitro* growth assay has previously been described in Section 2.2.6.1.

6.2.2.2 *In vitro* cell Matrigel® matrix adhesion assay

The methodology used for the *in vitro* Matrigel® adhesion assay has previously been described in Section 2.2.6.2.

6.2.2.3 *In vitro* cell Matrigel® matrix invasion assay

The methodology used for the *in vitro* Matrigel® invasion assay has previously been described in Section 2.2.6.3.

6.2.2.4 *In vitro* cell motility assay

The methodology used for the *in vitro* cell motility assay has previously been described in Section 2.2.6.4.

6.3 Results

6.3.1 Effect of DOK7V2 overexpression on growth of RKO cells

The effect of DOK7V2 overexpression on the growth of RKO cells was analysed using an *in vitro* growth assay comparing the growth of $RKO^{DOK7V2stopexp}$ cells with the growth of RKO^{pEF} control cells. Overexpression of DOK7V2 was associated with a decrease in the growth rate of RKO cells, but this difference failed to reach statistical significance. Data is shown in Figure 6.1.

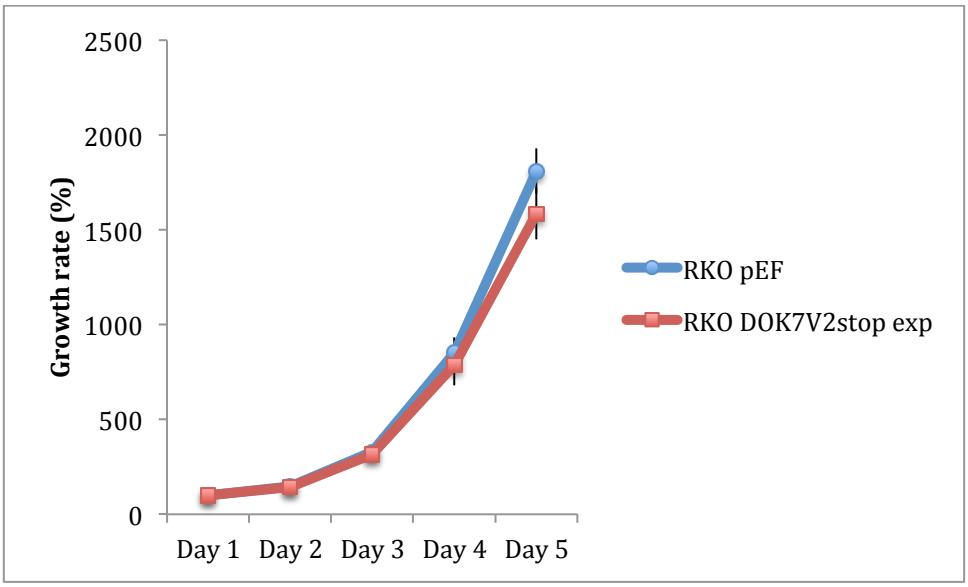

Figure 6.1. Effect of DOK7V2 overexpression on colorectal cancer cell growth. Growth rate was decreased in the RKO DOK7V2stopexp cells compared to RKO pEF control cells. Growth rate was measured by recording absorbance measured after fixing and staining cells with crystal violet after 1-4 days of incubation and is shown as a percentage of Day 1 growth. Data shown is representative of at least three independent repeats and was normalised by using the day 1 growth plate as a baseline. Lines correspond to growth rate (%) and error bars represent the standard error of the mean (SEM).

6.3.2 Effect of DOK7V2 overexpression on in vitro cell-matrix adhesion

The effect of DOK7V2 overexpression on the adhesive capacity of RKO cells was analysed using an *in vitro* Matrigel® matrix adhesion assay comparing the adhesion of $RKO^{DOK7V2exp}$ cells and $RKO^{DOK7V2stopexp}$ cells with the adhesion of RKO^{pEF} control cells. Overexpression of DOK7V2 was associated with a decrease in the adhesive capacity of RKO cells but this difference failed to reach statistical significance (average absorbance 1.95 vs. 1.88, $p = 0.745$). Data is shown in Figure 6.2.

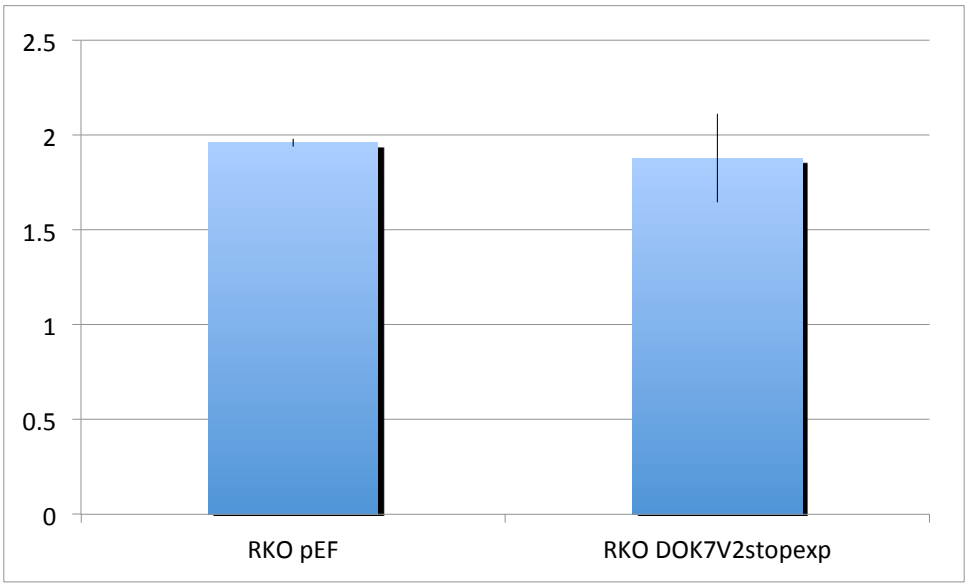

Figure 6.2 Effect of DOK7V2 overexpression on colorectal cancer cell adhesion. Cell adhesion to the Matrigel® matrix was decreased in the $RKO^{DOK7V2stopexp}$ cells compared to RKO^{pEF} control cells after 45 minutes incubation. Graph illustrates absorbance measured after fixing and staining cells after 45 minutes incubation. There was a decrease in the adhesiveness of RKO DOK7V2stopexp cells (mean ± SEM = 1.88 ± 0.23) compared to RKO pEF control cells (1.96 ± 0.02), but this difference was not statistically significant ($p = 0.745$). Data shown is representative of at least three independent repeats and was normalized by using the corresponding day 1 growth plate as a baseline. Bar corresponds with mean absorbance and error bars represent SEM.

6.3.3 Effect of DOK7V2 overexpression on invasion by RKO cells

The effect of DOK7V2 overexpression on the invasive capacity of RKO cells was analysed using an *in vitro* Matrigel® matrix invasion assay comparing the invasion through a Matrigel® layer of $RKO^{DOK7V2stopexp}$ cell compared with RKO^{pEF} control cells. Overexpression of DOK7V2 was associated with an increase in the invasiveness of RKO cells but this difference failed to reach statistical significance (mean absorbance 0.48 vs. 0.49, $p = 0.938$). Data is shown in Figure 6.3.

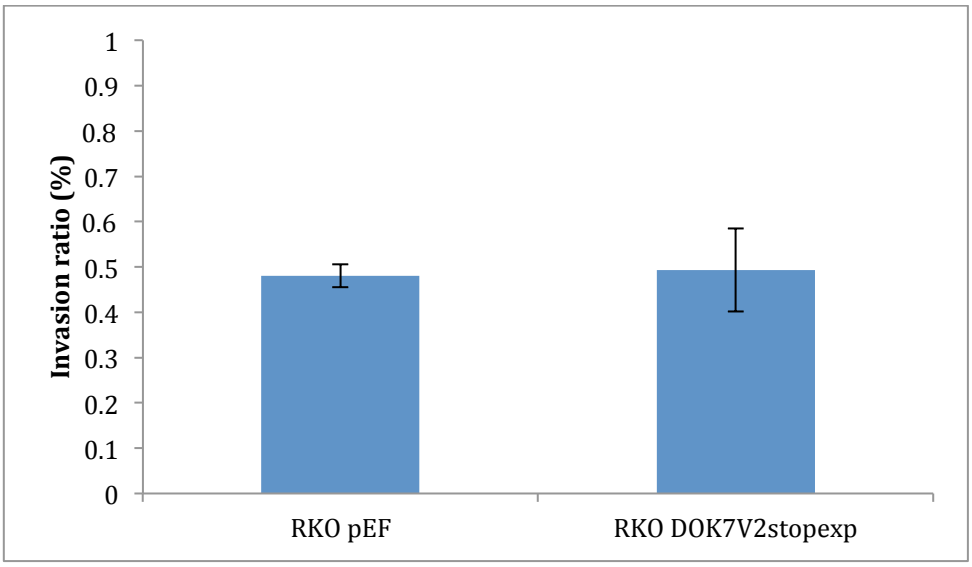

Figure 6.3 Effect of DOK7V2 overexpression on colorectal cancer cell invasion. Cell invasion through the Matrigel® matrix was slightly increased in the RKO DOK7V2expstop cells compared to RKO pEF control cells after 3 days incubation. Graph illustrates the absorbance measured from fixed and stained cells on the well side of the well insert and the bottom of the well combined. There was a slight increase in the invasiveness of RKO DOK7V2expstop cells (mean ± SEM = 0.49 ± 0.09) compared to RKO pEF control cells (0.48 ± 0.03) but this difference was not statistically significant ($p = 0.938$). Data shown is representative of at least three independent repeats and was normalized by seeding density in a control well without insert. Bar corresponds with mean number of adhered cells and error bars represent standard error of the mean.

6.3.4 Effect of DOK7V2 overexpression on cell motility analysed by scratch assay

Attempts to determine the effect of DOK7V2 overexpression on RKO cell motility using a scratch assay failed due to the fact that the monolayer of all RKO experimental cell lines became detached from the well base when the media was changed or when the scratch was made with the pipette tip.

6.4 Discussion

The current study utilized verified overexpression DOK7V2 constructs to investigate the effect of DOK7V2 on colorectal cancer cell function.

Our data demonstrate no significant effect of DOK7V2 overexpression on colorectal cancer cell growth. Although there was a trend towards reduced colorectal cancer cell adhesion and towards increased colorectal cancer cell invasion with DOK7V2 overexpression, the differences did not reach statistical significance. Despite several attempts to analyse the effect of DOK7V2 overexpression on colorectal cancer cell migration using a scratch assay, technical difficulties resulted in failure of the experiments.

Overall, despite the differences observed in DOK7V2 expression between colorectal cancer cells and normal colorectal tissue, we did not find any significant differences in colorectal cancer cell function with modulation of DOK7V2 expression at the mRNA level. One explanation for these findings is the limited capability of a simplified functional assay and culture media to replicate the complexity of the tumour *in vivo*.

Chapter 7: Identification of potential interacting proteins and signalling pathways associated with DOK7V2

7.1 Introduction

The results discussed in the previous chapters suggest that DOK7V2 may be implicated in the development of colorectal cancer and may be associated with the survival of patients with colorectal cancer.

Dok-7 is a cytoplasmic adapter protein involved in the formation of the neuromuscular junction and it is required for MuSK localization and activation as well as AChR clustering. Adaptor proteins typically contain protein binding sites that mediate protein-protein interactions resulting in the formation of signalling complexes and although previous studies have shed light on how Dok-7 functions in relation to NMJ formation, there is little information available regarding its role in cancer cell signalling.

STRING analysis identifies a number of predicted functional partners of Dok-7 but it is interesting to note that, of these, experimental evidence exists only for its predicted interaction with MuSK, with other predicted interactions based on textmining data. The top 10 predicted functional partners of Dok-7, as identified by STRING are shown in Table 7.1 and the top 50 predicted functional partners of Dok-7 are illustrated in Figure 7.1.

Table 7.1 Top 10 predicted functional partners of Dok-7 according to STRING

Name		Length (aa)	Evidence	Confidence score
Muscle, skeletal, receptor tyrosine kinase	MUSK	869	Experimental Textmining	Highest
Receptor-associated protein of the synapse	RAPSN	412	Textmining	High
Agrin	AGRN	2045	Textmining	High
FAD1 flavin adenine dinucleotide synthetase homolog	FLAD1	587	Textmining	High
Dolichyl-phosphate (UDP-N-acetylglucosamine) N-acetylglucosaminephosphotransferase 1	DPAGT1	408	Textmining	High
Feline leukaemia virus subgroup C cellular receptor family, member 2	FLVCR2	526	Textmining	High
Neurotrophic tyrosine kinase, receptor, type 3	NTRK3	839	Textmining	Medium
Neurotrophic tyrosine kinase, receptor, type 2	NTRK2	838	Textmining	Medium
Ribosomal RNA processing 7 homolog A	RRP7A	280	Textmining	Medium
Acetylcholinesterase	ACHE	617	Textmining	Medium

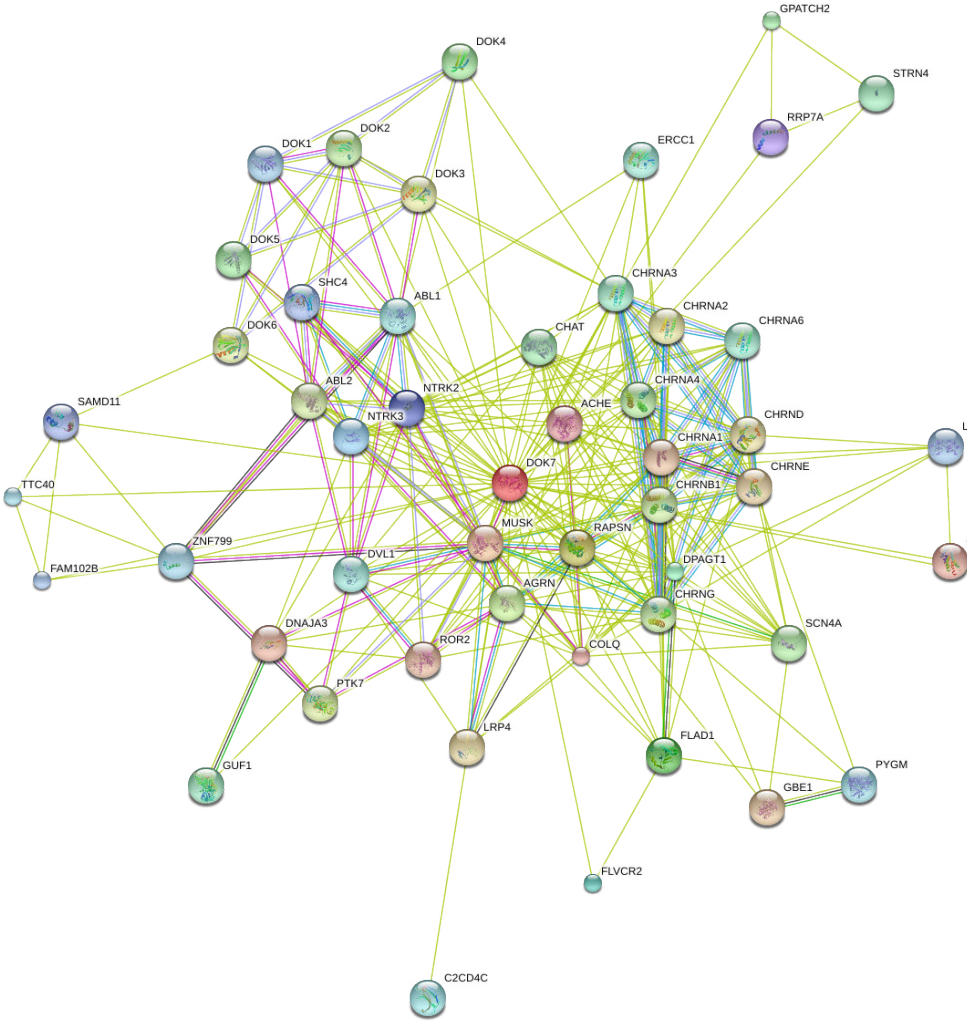

Figure 7.1 Top 50 predicted functional partners of Dok-7 according to STRING anal
illustrating links between proteins

Dok-7 forms a dimer and interacts with the cytoplasmic portion of MuSK, resulting in its phosphorylation and activation. The interaction of Dok-7 with MuSK is mediated via the PTB domain, although the PH domain is also required for MuSK activation. The C-terminal of Dok-7 contains a nuclear export signal necessary for the cytoplasmic localisation of Dok-7, SH2 target motifs required for MuSK activation and tyrosine residues, which are phosphorylated by agrin, resulting in the recruitment of the adapter proteins Crk and Crk-L. Meanwhile, the PH domain in the N-terminal of Dok-7 enables the nuclear import of Dok-7.

There is currently no published literature on the protein interactions of Dok-7, or indeed its isoforms, in relation to human cancer. Our hypothesis for the experimental work discussed in this chapter is that DOK7V2 interacts with other cell signalling proteins implicated in the development and progression of colorectal cancer. Therefore, the aim of the experimental studies described in this chapter was to investigate protein expression in RKOpEF and RKODOK7V2 overexpression cells to determine whether DOK7V2 expression is associated with changes in downstream protein expression and to establish potential interacting proteins and signalling pathways associated with DOK7V2. In order to address these questions, we used an established antibody based protein microarray to firstly, identify changes in protein expression associated with DOK7V2 expression and secondly, identify changes in phosphorylation of proteins involved in key cell signalling pathways.

One of the potential benefits of identifying signalling pathways involved in Dok signalling is the possibility of identifying targets for therapy. Although there have been no reports of therapeutic interventions in relation to Dok-7 in cancer, it is notable that in CMS associated with DOK7 mutation, treatment with ephedrine or salbutamol is effective (268). Currently, the mechanism of action of these drugs is not fully understood but it has been suggested that the β2-agonsts compensate for the destabilized postsynaptic apparatus via second messenger pathways (268).

7.2 Materials and methods

7.2.1 Cell lines

The following cell lines were used in the experiments discussed in this chapter: RKO pEF, containing an empty plasmid control, and RKO DOK7V2Stop/5.1 cell line, containing DOK7V2 full coding sequence. These cell lines were established as previously detailed in Chapter 5.

7.2.2 Preparation of lysis buffer for protein microarray

The preparation of the lysis buffer has previously been described in Section 2.2.4.2.

7.2.3 Preparation and quantification of protein samples for protein microarray

Protein samples were prepared for protein microarray and quantified as described in Section 2.2.4.2.2.

7.2.4 Protein microarray technique

The principles of the Kinex™ KAM-880 antibody microarray used in this study are discussed in Section 2.2.4.1.

7.2.5 Statistical analysis of protein microarray data

The results of the protein microarray were provided in an Excel spreadsheet containing the following data:

Target protein name/full target protein name

Phospho Site

Flag (Control/Treated)

Globally normalized median (Control/Treated)

% error range (Control/Treated)

Log2 (Intensity Corrected) (Control/Treated)

% CFC (Treated from Control)

Z score (Control/Treated): Measures the relationship of the signal intensity to the mean, indicates its positive or negative relationship to the mean and its variation from the mean in terms of standard deviation.

Z-score difference (Treated-Control): Calculated as the difference between Z scores for the control vs. treated group.

Z-ratio (Treated, Control): Potential candidate proteins affected by Dok7V2 expression were identified by the following criteria: z ratio ≥ 1.96 or ≤ -1.96.

Antibodies with good read were defined as those with flag = 0 in both of the physical replicates and these were included in analysis. Antibodies with poor reads (flag = 1 for either or both of the physical replicates) were excluded from further analysis.

7.3 Results

7.3.1 Analysis of protein microarray data

The microarray chip is shown in Figure 7.2

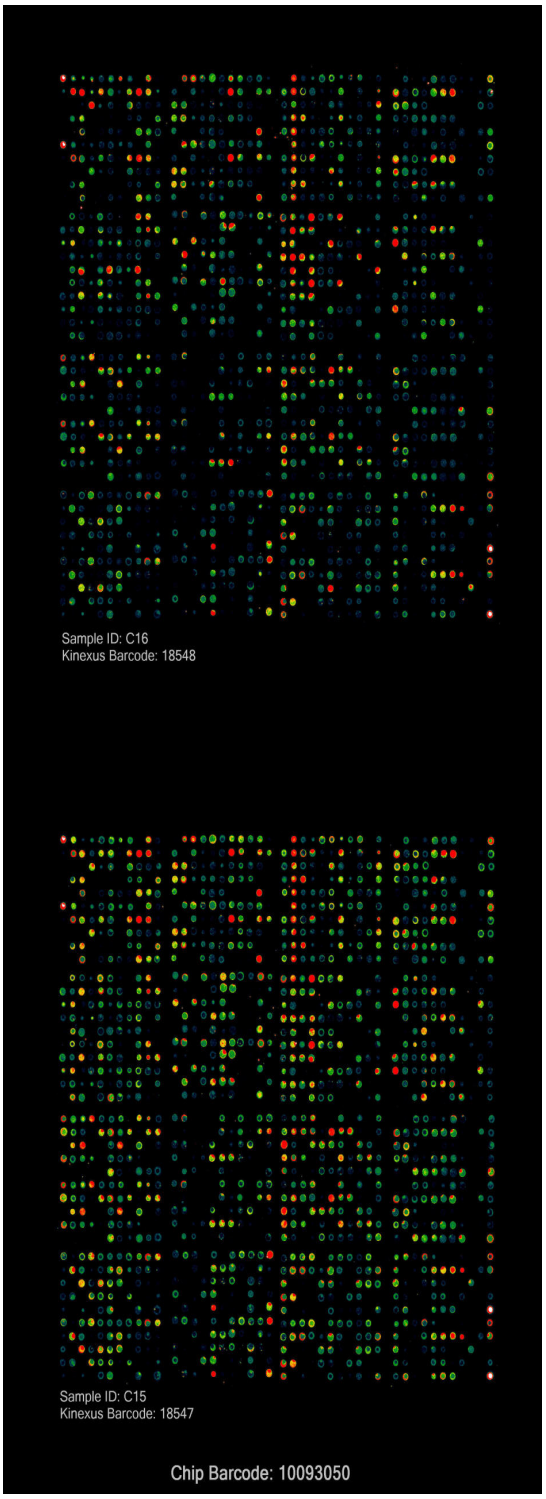

Figure 7.2 Image of microarray chip. Sample ID C15 = RKO pEF control cell protein lysate, Sample ID C16 = RKO DOK7V2stopexp cell protein lysate.

Of the 877 antibodies tested, 874 had good reads (Flag = 0). The three antibodies with poor reads (flag = 1) shown in Table 7.2 below were excluded from further analysis.

Table 7.2 Antibodies with poor read (flag = 1) excluded from analysis

Antibody code	Target protein	Full target protein name	Phospho Site
NN042	FAS	Tumour necrosis factor superfamily member 6 (Apo1, CD95)	Pan-specific
NK117-3	Nek2	NIMA (never-in-mitosis)-related protein-serine kinase 2	Pan-specific
PN070	Rb	Retinoblastoma-associated protein 1	T821

7.3.2 Expression/activation of predicted functional partners in RKO^{pEF} and RKO^{DOK7V2exp} cells

The STRING output data for predicted functional partners of Dok-7 was compared with the list of antibodies analysed by protein microarray. The top 50 predicted functional partners identified using STRING analysis are shown in Figure 7.1. Of these, the evidence for the predicted association was obtained from experimental evidence for 1 of the predicted partners and by textmining for 50 of the predicted functional partners.

Of the 50 predicted functional partners identified using STRING analysis, 14 were included in the microarray analysis. The relative expression/activation of these proteins in RKO DOK7V2pEF and RKO DOK7V2 overexpression cells is shown in Table 7.3.

Table 7.3 Expression/phosphorylation of STRING predicted functional partners in control *vs.* DOK7V2 overexpressing RKO cells as determined by protein microarray analysis.

Target protein	Panspecific/ Phosphosite	RKO pEF median	RKODOK7V2 median	%CFC	Z-ratio
AAK1	S637	4612	3667	-21	-0.70
Abl	Pan	895	687	-23	-0.91
Abl	Pan	6300	5438	-14	-0.39
Abl	Y393	438	347	-21	-0.84
CDK5	Pan	6907	8557	24	0.93
CDK5	Pan	6946	6180	-11	-0.27
CDK5	Pan	4395	4215	-4	-0.02
DOK2	Y142	6362	3567	-44	-1.96
DOK2	Y142	5263	3301	-37	-1.56
EGFR	Pan	7861	6891	-12	-0.32
EGFR	Pan	11848	9236	-22	-0.73
EGFR	Pan	17331	20287	17	0.77
EGFR	Pan	8839	8865	0	0.17
EGFR	T693	684	784	14	0.53
EGFR	Y1068	224	280	25	0.80
EGFR	Y1110	1679	2018	20	0.75
EGFR	Y1148	1063	945	-11	-0.37
EGFR	Y1148	716	1016	42	1.31
EGFR	Y1197	133	206	55	1.55
EGFR	Y998	4420	3197	-28	-1.05
ErbB2	Pan	2860	3082	8	0.38
ErbB2	Pan	12100	11309	-7	-0.07

ErbB2	Pan	4028	6209	54	1.70
ErbB2	T686	7892	7127	-10	-0.21
ErbB2	Y1248	7194	4545	-37	-1.52
JAK2	Pan	739	726	-2	-0.02
JAK2	Pan	9212	7945	-14	-0.37
JAK2	Pan	6853	6471	-6	-0.06
JAK2	Pan	7665	8432	10	0.50
JAK2	Y1007 & Y1008	106	80	-24	-1.08
JAK2	Y1007/ Y1008	1105	1085	-2	-0.01
SG2NA	Pan	4857	3900	-20	-0.67
Shc1	Y239/Y240	4619	3507	-24	-0.87
Shc1	Y349	143	172	20	0.63
Src	Pan	6008	4839	-20	-0.64
Src	Pan	3312	3529	6	0.35
Src	Pan	1053	1204	14	0.55
Src	Y418	283	410	45	1.34
Src	Y529	410	562	37	1.16
Striatin	Pan	13257	18531	40	1.41
TEC	Y519	10404	8890	-15	-0.40
TrkA	Pan	1805	1315	-27	-1.07
TrkB	Pan	3573	5067	42	1.39
TrkB	Y705	160	369	131	3.02

7.3.3 Effect of DOK7V2 manipulation on protein expression

7.3.3.1 Proteins overexpressed in $RKO^{DOK7V2exp}$ cells compared to RKO^{pEF} cells

Proteins overexpressed in $RKO^{DOK7V2exp}$ cells compared to RKO^{pEF} cells were found by identifying pan-specific antibodies with increased normalized median values in $RKO^{DOK7V2exp}$ cells compared to RKO^{pEF} cells (z-ratios exceeding 1.96). There were a total of 20 proteins that were overexpressed in $RKO^{DOK7V2exp}$ cells compared to RKO^{pEF} cells and these are shown, in order of decreasing Z-ratio, in Table 7.4.

Table 7.4 Overexpressed proteins in $RKO^{DOK7V2exp}$ cells compared to RKO^{pEF} cells identified by protein antibody-based microarray, organised in order of decreasing Z-ratio.

Target protein	Phospho site	RKO^{pEF} normalized median	$RKO^{DOK7V2exp}$ normalised median	%CFC	Z-ratio
VGFR2	Pan	4477	12035	168	3.73
JAK3	Pan	5649	13305	135	3.26
PRKDC	Pan	6476	14894	130	3.18
MEK5	Pan	3972	8490	113	2.89
mTOR	Pan	7981	16629	108	2.83
Catenin b	Pan	2003	4172	108	2.76
WNK2	Pan	5831	11889	104	2.74
DUSP4	Pan	9349	18193	94	2.59
Cdc25C	Pan	9139	17120	87	2.45
ERK1	Pan	10495	19478	85	2.43
MKK4	Pan	10073	18180	80	2.32
Grp94	Pan	4583	8310	81	2.30
PDGFRB	Pan	4003	7208	80	2.27
PDK4	Pan	8092	14416	78	2.26
4E-BP1	Pan	151	282	87	2.24
Ros	Pan	7024	12404	76	2.22
MKK6	Pan	6945	12037	73	2.16
ErbB4	Pan	10178	17237	69	2.09
DUSP3	Pan	12805	21521	68	2.07
PTEN	Pan	83	146	76	1.99

7.3.3.2 Proteins underexpressed in RKO^{DOK7V2exp} cells compared to RKO^{pEF} cells

Proteins underexpressed in RKO^{DOK7V2exp} cells compared to RKO^{pEF} cells were found by identifying pan-specific antibodies with decreased normalized median values in RKO^{DOK7V2exp} cells compared to RKO^{pEF} cells (z-ratios below -1.96). There were a total of 12 proteins that were underexpressed in RKO^{DOK7V2exp} cells compared to RKO^{pEF} cells and these are shown, in order of increasing Z-ratio, in Table 7.5 below.

Table 7.5 Underexpressed proteins in $RKO^{DOK7V2exp}$ cells compared to RKO^{pEF} cells identified by protein antibody-based microarray, organised in order of increasing Z-ratio.

Target protein	Phospho site	RKO pEF normalized median	RKODOK7V2 normalised median	%CFC	Z-ratio
PTP1D/SHP2	Pan	299	102	-66	-3.92
PDK3	Pan	334	145	-57	-3.04
GNB2L1	Pan	3015	1502	-50	-2.43
Haspin	Pan	1659	839	-50	-2.40
STI1	Pan	252	131	-48	-2.38
Smad2/3	Pan	335	176	-48	-2.34
PCTK1	Pan	1966	1013	-49	-2.33
ROCK-I/ROKb	Pan	304	165	-46	-2.23
MEK1	Pan	305	167	-45	-2.20
PTP-PEST	Pan	73	42	-42	-2.06
DRAK2	Pan	4425	2456	-45	-2.02
BMX (Etk)	Pan	537	311	-42	-1.97

7.3.4 Effect of DOK7V2 manipulation on protein phosphorylation

7.3.4.1 Proteins activated in $RKO^{DOK7V2exp}$ cells compared to RKO^{pEF} cells

Proteins activated in $RKO^{DOK7V2exp}$ cells compared to RKO^{pEF} cells were found by identifying phosphosite-specific antibodies with increased normalized median values in $RKO^{DOK7V2exp}$ cells compared to RKO^{pEF} cells (z-ratio exceeding 1.96, $p = 0.05$). There were a total of 12 proteins that were activated in $RKO^{DOK7V2exp}$ cells compared to RKO^{pEF} cells detected by 13 phosphosite-specific antibodies. There are shown in order of decreasing Z-ratio in Table 7.6.

Table 7.6 Activated proteins in $RKO^{DOK7V2exp}$ cells compared to RKO^{pEF} cells identified by protein antibody-based microarray, organised in order of decreasing Z-ratio.

Target protein	Phospho site	RKO pEF normalized median	RKODOK7V2 normalised median	%CFC	Z-ratio
TrkB	Y705	160	369	131	3.02
CREB1	S133	5376	11217	108	2.82
Cyclin B1	S147	535	1139	113	2.78
BRCA1	S1497	960	2007	109	2.74
CDK1/2	Y15	191	388	103	2.55
IKKa	T23	287	572	99	2.50
4E-BP1	T45	158	316	99	2.47
ATF2	S94/S112	257	502	95	2.42
PLCg1	Y783	80	152	90	2.27
PLCg1	Y771	354	636	79	2.13
Connexin 43	S367	797	1409	76	2.12
ERK5	T218+Y220	630	1091	73	2.03
Cofilin 2	S3	3236	5402	67	1.98

7.3.4.2 Proteins functionally suppressed in RKO^{DOK7V2exp} cells compared to RKO^{pEF} cells

Proteins functionally suppressed in RKO^{DOK7V2exp} cells compared to RKO^{pEF} cells were found by identifying phosphosite-specific antibodies with decreased normalized median values in RKO^{DOK7V2exp} cells compared to RKO^{pEF} cells (z-ratio below -1.96). There were a total of 5 proteins that were inhibited in RKO^{DOK7V2exp} cells compared to RKO^{pEF} cells. There are shown in order of increasing Z-ratio in Table 7.7.

Table 7.7 Inhibited proteins in $RKO^{DOK7V2exp}$ cells compared to RKO^{pEF} cells identified by protein antibody-based microarray, organised in order of increasing Z-ratio.

Target protein	Phospho site	RKO pEF normalized median	RKODOK7V2 normalised median	%CFC	Z-ratio
IRAK4	T345+S346	75	37	-51	-2.67
Met	Y1003	4405	2210	-50	-2.38
CDK1	Y19	3652	2032	-44	-2.02
Dok2	Y142	6362	3567	-44	-1.96
VAV1	Y826	1432	820	-43	-1.96

7.3.5 Analysis of interacting proteins to determine related signalling pathways

7.3.5.1 Analysis of proteins overexpressed in RKO^{DOK7V2exp} cells compared to RKO^{pEF} cells

In order to determine the role of proteins overexpressed in RKO^{DOK7V2exp} cells compared to RKO^{pEF} cells, a literature review was undertaken. The summarized results are shown in Table 7.8.

Table 7.8 Role of proteins overexpressed in $RKO^{DOK7V2exp}$ cells compared to RKO^{pEF} cells and their related signalling pathways

Target protein	Type of protein	Related signalling pathway(s)	Role	Ref
VGFR2	Type III receptor tyrosine kinase	PI3K-Akt MAPK1/ERK2 MAPK3/ERK1 MAPK AKT1 Phosphorylates PLCG1	When activated VGFR2 recruits Shc, GRB2, PI3K, Nck, SHP-1 and SHP-2. Promotes VEGF-induced endothelial proliferation, survival, migration and differentiation. Negatively regulates apoptosis. Promotes cytoskeletal reorganization. Key role in regulation of angiogenesis.	(272) (273)
JAK3	Non-receptor tyrosine kinase	JAK-STAT PI3K-Akt GPCR	Involved in cell growth, migration and differentiation. Activating mutations are found in acute megakaryoblastic leukaemia	(274) (275) (276)
PRKDC	Catalytic subunit of DNA-dependent serine/threonine protein kinase of PI3/PI4-kinase family	Akt ERK ErbB/HER G2/M DNA damage checkpoint	Sensor for DNA damage. Required for double strand DNA break repair and recombination. Implicated in cell proliferation	(277) (278) (276) (279)
MEK5	Dual specificity	ErbB/HER,	Activates ERK5 and MAPK.	(280)

	protein kinase, member of MAP kinase family	MAPK, IL6	Inhibits NF-κB. Involved in growth factor stimulated cell proliferation and muscle cell differentiation	
mTOR	Atypical serine/threonine kinases	Downstream of PI3K/Akt pathway, mTOR	Promotes cell growth. Central regulator of cellular metabolism, growth and survival. Directly or indirectly regulates the phosphorylation of >800 proteins	(276)
Catenin b	Part of protein complex that constitute adherens junctions (AJs)	Wnt/Beta-catenin, ErbB/HER	Involved in the regulation of cell adhesion and growth between cells. May play a role in contact inhibition. Mutations are associated with colorectal adenomatous polyposis	(281)
WNK2	Serine-threonine kinase belonging to protein kinase superfamily	MEK ERK 1/2	Regulated electrolyte homeostasis, cell signalling survival and proliferation. Negatively regulates EGF-induced activation of ERK/MAPK pathway	(282)
DUSP4	Dual specificity protein phosphatase	Negatively regulates MAPK, SAPK/JNK	Negatively regulate MAP kinase superfamily (MAP/ERK, SAPK/JNK, p38)	(283)

Cdc25C	Tyrosine phosphatase belonging to the Cdc25 phosphatase family	G2/M DNA damage checkpoint, MAPK	Regulation of cell division, suppresses p53-induced growth arrest	(284)
ERK1	Serine/threonine kinase	Angiogenesis, apoptosis regulation, ErbB/HER, MAPK, IL6, mTOR, TGF-beta	Involved in the regulation of cell growth and differentiation. Plays a key role in MAPK cascades.	(285)
MKK4	Dual specificity kinase of the STE7 family	B cell receptor, ErbB/HER, IL6, MAPK, SAPK/JNK, T cell receptor, TGF-beta	Phosphorylates and activates JNK1, JNK2 and p38. Mediates cell responses to stress and inflammatory cytokines. Inactivated or deleted in approximately of 5% tumours	(276) (286)
Grp94	Chaperone protein	Akt	Regulation of innate and adaptive immunity. Promotion of tumour proliferation and metastasis	(287)

PDGFRB	Receptor tyrosine kinase	Angiogenesis	Recruits SH2-containing proteins such as Grb2, Src, GAP, PTPN11, PI3K PLC-gamma and Nck. Regulates cell proliferation, survival, differentiation, chemotaxis and migration. Overexpressed in metastatic medulloblastoma. Activating translocations found in myeloproliferative disorders and cancers	(276) (288)
PDK4	Atypical protein kinase	Insulin receptor, regulation of fatty acid biosynthesis and oxidation	Regulation of glucose metabolism. Involved in cell response to starvation, insulin receptor signalling, regulation of fatty acid biosynthetic process and oxidation, pH regulation	(289) (289)
4E-BP1	Translation, translation initiation	Angiogenesis, Insulin receptor, mTOR, PI3K/Akt	Sequesters eIF4E repressing the initiation of translation of proteins involved in cell proliferation, survival, angiogenesis, EMT and metastatic progression (290). Underexpressed or phosphorylated in most tumours, loss of 4E-BP1 function is associated with increased EMT and metastatic capability (290).	(290) (291)

Ros	Proto-oncogenic receptor tyrosine kinase	TOR	Aberrant expression in CNS tumours. Upregulated in human glioma. Plays a role in differentiation, growth, proliferation.	(276)
MKK6	Dual specificity protein kinase of the STE7 family	TGFβ, B cell receptor, ErbB/HER, IL6, MAPK	Activates p38 MAPK activity, involved in cell cycle arrest and DNA damage induced protein phosphorylation	(292)
ErbB4	Receptor tyrosine kinase, member of the epidermal growth factor receptor subfamily	Akt, ErbB/HER	Involved in mitogenesis and differentiation May function as a tumour suppressor but expression varies between tumours from different locations.	(276) (293)
DUSP3	Non receptor, dual specificity protein phosphatase	Negatively regulates MAPK, JNK cascade, T cell receptor, T cell activation. Positively regulates mitotic cell cycle	Phosphorylated by ZAP-70.	(294)

PTEN	Phosphoinositide 3-phosphatase	Negatively regulates PI3K/Akt. Key modulator of AKT-mTOR. Also involved in T cell receptor signalling, Wnt, B cell receptor and insulin receptor signalling	Tumour suppressor. Plays a role in negative regulation of migration, proliferation, cell size, focal adhesion formation, organ growth, Implicated in many cancers.	(295)

7.3.5.2 Analysis of proteins activated in RKO^{DOK7V2exp} cells compared to RKO^{pEF} cells

In order to determine the role of proteins upregulated in RKO^{DOK7V2exp} cells compared to RKO^{pEF} cells, a literature review was undertaken. The summarized results are shown in Table 7.9.

Table 7.9 Role of proteins activated in $RKO^{DOK7V2exp}$ cells compared to RKO^{pEF} cells and their related signalling pathways

Target protein	Type of protein	Signalling pathway	Role	Ref
TrkB	Transmembrane Receptor with intracellular tyrosine receptor activity. Acts as a receptor for brain-derived neurotrophic factor (BDNF), neurotrophin-4 (NT4) and neurotrophin-3 (NT3) (296).	MAPK, Ras-PI3K-AKT1 pathway, PLCG1 and protein kinase C, NF-κB	Cell differentiation Growth and survival Synaptic plasticity Suppresses anoikis Two point mutations found in colon tumours and cell lines Enhances metastases in rats Associated with poor prognosis in neuroblastoma and may play a role in chemoresistance	(297) (276)
CREB1	Transcription factor of the leucine zipper family	cAMP, PI3K-AKT , B cell receptor, ErbB/HER, T cell receptor, MAPK	Phosphorylated by several protein kinases. Involved in cell differentiation. Positively regulates transcription.	(298, 299)
Cyclin B1	Cyclin family protein	AMPK, G2/M DNA damage checkpoint	Activator protein involved in cell cycle regulation. Regulates CDK kinases. Involved in mitosis.	(300) (301)
BRCA1	Nuclear phosphoprotein	Negatively	Involved in transcription,	(302)

	with E3 ubiquitin-protein ligase activity	regulates oestrogen receptor signalling pathway, G2/M DNA damage checkpoint	DNA repair, ubiquitination, transcriptional regulation and maintains genomic stability. Required for normal cell cycle progression from G2 to mitosis Acts as a tumour suppressor. Plays a role in apoptosis, angiogenesis and proliferation. Mutations are associated with breast and ovarian cancers	(303)
CDK1/2	Serine/Threonine protein kinases	MAPK, PI3K-AKT, ErbB/HER, G2/M DNA damage checkpoint, apoptosis, Rb, G1/S checkpoint, Ras signal transduction	Involved in cell cycle regulation. CDK1 is involved in cell migration, DNA damage response, epithelial cell differentiation, negative regulation of apoptosis. CDK2 is involved in DNA damage response, positive regulation of cell proliferation and cell cycle regulation.	(304) (305) (276) (306) (307)

IKKa	Serine/threonine protein kinase	PI3K/AKT and PI-3K cascade, NF-κB , T and B cell receptor, TNF	Phosphorylates inhibitors of NF-κB. Involved in inflammatory and immune responses and the regulation of apoptosis.	(308) (309)
4E-BP1	Translation initiation	MAPK, mTOR, PI3K/AKT, AMPK, angiogenesis, insulin receptor, Signalling by GPCR	Negatively regulates translation. Positively regulates mitotic cell cycle at G1/S transition.	(310) (311) (291)
ATF2	Transcription factor, member of leucine zipper family of DNA binding proteins	PI3K-AKT, MAPK, SAPK/JNK, B cell receptor	Transcriptional activator of genes involved in anti-apoptosis, cell growth and DNA damage. Evokes oncogenic or tumour suppressor events depending on the tissue.	(312) (313) (314)
PLCg1	Calcium dependent phosphatidylinositol-specific phospholipase C	PI-3K cascade, FGFR, MAPKK, calcium signalling,	Regulation of intracellular signalling cascades. Involved in reorganization of actin and cell migration. Involved in activation of	(315) (316)

		EGFR, T cell receptor, angiogenesis, ErbB/HER	MAPKK activity, positive regulation of angiogenesis and cell migration	
Connexin 43	Gap junction protein	I-κB kinase/NF-κB cascade	Negative regulation of cell growth, positively regulates I-κB kinase/NF-κB cascade	(317) (318)
ERK5	Protein kinase of the MAPK family	ErbB/HER signalling, GPCR signalling to MAPKs, IL6 signalling, mTOR	Involved in angiogenesis. May block apoptosis in endothelial cells. Transduces EGF growth signal. Activated in ErbB2 overexpressing breast cancer and downstream of MEK5 in metastatic prostate cancer. Negatively regulates cell-cell adhesion.	(276) (319)
Cofilin 2	Cytoskeletal protein	Actin and microtubule dynamics, TGF-β signalling	Regulation of actin-filament dynamics. Mutations are associated with congenital myopathy	(320) (321)

7.3.5.3 Analysis of proteins underexpressed in RKO^{DOK7V2exp} cells compared to RKO^{pEF} cells

In order to determine the role of proteins underexpressed in RKO^{DOK7V2exp} cells compared to RKO^{pEF} cells, a literature review was undertaken. The summarized results are shown in Table 7.10.

Table 7.10 Role of proteins underexpressed in RKO^{DOK7V2exp} cells compared to RKO^{pEF} cells and their related signalling pathways

Target protein	Type of protein	Signalling pathway	Role	Ref
PTP1D/ SHP2	SH2-containing tyrosine-specific protein phosphatase	GPCR, PAK, EGFR, ephrin receptor, B cell receptor, ErbB/HER, FGFR, IL-6, insulin, receptor, phosphoinositide -mediated and PI3K signalling pathways	Involved in the regulation of cell growth, differentiation, migration and death. Also involved in the regulation of integrin-mediated cell adhesion	(322) (323) (324)
PDK3	Atypical protein kinase	Pyruvate dehydrogenase pathway	Regulates glucose metabolism and aerobic respiration	(325) (326)
GNB2L1	G-beta like scaffold protein that links protein kinase C to its substrates	ERK, CREB pathway. Negatively regulates protein kinase B and Wnt signalling	Regulates calcium release and IGF-1-mediated Akt activation. Involved in repression of translation. Negatively regulates cell growth, phagocytosis, and translation. Positively regulates apoptosis and cell migration.	(327) (328)

Haspin	Serine/threonine protein kinase		Cell cycle regulation	(329)
STI1	Chaperone protein		Involves in stress response. Interacts with Hsp70 and Hsp90.	(330) (331)
Smad2	Transcription factor	Activin receptor, TGF-β, BMP and angiogenesis signalling pathways	Mediates TGF-beta signalling. Regulates proliferation, morphogenesis, apoptosis and differentiation	(332) (333) (334)
Smad3	Transcription factor	Activin receptor, angiogenesis, G1/S checkpoint and TGF-β signalling pathways	Mediates TGF-beta signalling. Negatively regulates cell growth, mitotic cell cycle Inhibits wound healing	(332) (333) (335)
PCTK1/ PCTAIRE-1 protein-serine kinase/CDK16	Member of cdc2/cdkx subfamily of serine/threonine family of protein kinases		Signal transduction in terminally differentiated cells, exocytosis, transport of secretory cargo from endoplasmic reticulum	(336) (337)
ROCK-I/ROKb	Serine/threonine kinase	RhoGDI, ephrin receptor, NF-κB, PI3K/AKT, TGF-β, VEGFR	Regulates actin cytoskeleton and cell polarity. Regulate smooth muscle contractility, stress	(276) (338) (339)

		and death receptor signalling pathways	fibre and focal adhesion, cell adhesion and motility. Negatively regulates inflammatory cell migration and VEGF-induced angiogenic endothelial cell activation Regulates PTEN phosphorylation and stability	
MEK1	Dual specificity protein kinase of STE7 kinase family	MAPK/ERK, angiogenesis, B cell receptor, ErbB/HER, IL6, insulin receptor, T cell receptor, PI3K-AKT and PI3K signalling cascades	Induces MAPK activity. Regulates proliferation, differentiation, transcription, motility and chemotaxis. Overexpressed/overactivated in many tumour types. Involved in colon cell growth and motility	(276) (340) (341)
PTP-PEST/PTPN12	Protein tyrosine phosphatase	GPCR, PAK and EGFR signalling pathways	May regulate protein intracellular half-life, oncogenesis, cell shape and motility	(342) (343)
DRAK2/STK17B	Calmodulin-dependent serine/threonine kinase of the		Positive regulator of apoptosis	(344) (345)

	DAPK family			
BMX (Etk)	Non-receptor tyrosine kinase of the Tec family	AKT, STAT	Involved in IL-6-induced differentiation and the growth and differentiation of haematopoietic cells. Involved in TNF-induced angiogenesis and signalling of TEK and FLT1 receptors Required for phosphorylation and activation of Stat3-induced cell differentiation. Also involved in IL-6 induced differentiation Involved in adaptive cellular response to extracellular stress	(346) (347)

7.3.5.4 Analysis of proteins functionally suppressed in RKO^{DOK7V2exp} cells compared to RKO^{pEF} cells

In order to determine the role of proteins functionally suppressed in RKO^{DOK7V2exp} cells compared to RKO^{pEF} cells, a literature review was undertaken. The summarized results are shown in Table 7.11.

Table 7.11 Role of proteins downregulated in RKO^{DOK7V2exp} cells compared to RKO^{pEF} cells and their related signalling pathways

Target protein	Type of protein	Signalling pathway	Role	Ref
IRAK4	Serine/threonine protein kinase	Toll-like receptor (TLR), T-cell receptor (TCR), NF-κB, and IL1R signalling pathways	Activates NF-kappaB Initiates innate immune response	(348) (349)
Met/ Hepatocyte growth factor receptor	Proto-oncogenic receptor tyrosine kinase	PI3K-AKT, RAS-ERK, PLCgamma-PKC signalling pathways	Regulates proliferation, chemotaxis, morphogenesis and survival. Involved in embryonic development, wound healing and tissue remodelling. Necessary for invasive growth and EMT. Mutations seen in renal carcinoma and hepatocellular carcinoma. Upregulation in carcinomas correlates with metastases and poor outcome	(350) (276) (351)
CDK1	Cyclin-dependent	MAPK, PI-3K, apoptosis,	Involved in cell cycle control, essential for G1/S and G2/M	(352) (304)

	kinase, member of serine/threonine protein kinase family	ErbB/HER and G2/M DNA damage checkpoint cascades	phase transitions and cell migration. Activated in many cancers. Negatively regulates apoptosis.	(306)
Dok2	Adaptor protein	ErbB/HER	Attenuates EGF-induced MAPK activation Constitutively tyrosine phosphorylated in haematopoietic progenitors from CML patients in the chronic phase Substrate for p210(bcr/abl) Attenuates EGF-stimulated MAP kinase activation	(353) (354)
Vav 1 guanine nucleotide exchange factor 1	Proto-oncogenic guanine nucleotide exchange factor (GEF) of the Dbl family	Actin dynamics, B cell and T cell receptor, ErbB/HER, VEGFR and PI-3K cascades	Involved in cell differentiation, proliferation, actin cytoskeletal rearrangement and transcriptional alteration. Involved in T-cell and B-cell development and activation. Positively regulates apoptosis,	(355) (356)

7.3.6 Analysis of interacting proteins for a potential role in colorectal cancer

7.3.6.1 Analysis of proteins overexpressed in RKO^{DOK7V2exp} cells compared to RKO^{pEF} cells: review of the literature for role in cancer

In order to determine the role of proteins overexpressed in RKO^{DOK7V2exp} cells compared to RKO^{pEF} cells, a literature review was undertaken. The summarized results are shown in Table 7.12.

Table 7.12 Role of proteins overexpressed in $RKO^{DOK7V2exp}$ cells compared to RKO^{pEF} cells in cancer

Target protein	Role in Cancer
VGFR2	Expressed by endothelial cells and in the malignant epithelium of colorectal cancers with strongest expression at the invasive tumour edge (357). Expressed to a lesser degree in colorectal lymph node and liver metastases (357). Phosphorylated VEGFR2/KDR expression in colorectal cancer cells is associated with larger tumour size and poor differentiation (358). VEGFR2 tyrosine kinase inhibitors inhibit tumour growth in vivo, have an anti-angiogenic effect and inhibit the development of hepatic metastases (359, 360).
JAK3	JAK3 mRNA is expressed in colon cancer cell lines and primary tumours (361). Inhibition of JAK3 in SW480 and HT29 colorectal cancer cell lines downregulates phosphorylated pSTAT3 and reduces colon cancer cell viability as a result of apoptosis and cell cycle arrest (361). STAT3 and JAK3 are frequently expressed in stage II and stage IV colon cancer (361). The intensity of JAK3 immunostaining is significantly associated with tumour differentiation, pT stage and TNM stage (362).
PRKDC/DNAPK	DNA-PK activity is significantly upregulated in colorectal cancer tissue compared with adjacent normal colorectal tissue (363). Increased expression of DNA-PK catalytic subunit is associated with clinical stage, lymphatic invasion and distant metastases and adverse survival outcomes in colorectal cancer patients (364). Plays a role in cellular resistance to oxidative stress and may influence the responsiveness of cells to radiotherapy (365, 366).
MEK5	Expression of phosphorylated MEK5 is significantly higher in colorectal

	cancer tissues compared to normal colorectal tissue and is significantly correlated with depth of tumour invasion, lymph node metastases, distant metastases, high pre-operative CEA level, stage of disease and poorer survival outcomes (367).
mTOR	Inhibition of mTOR reduces the growth of colon cancer cells but increases the transformation and invasiveness of intestinal epithelial cells (368).
Catenin b	The β-catenin gene (CTNNB1) gene is frequently mutated in colorectal cancer and is more highly expressed in left-sided colorectal tumours (369-372). Its expression is associated with increased tumour proliferation, invasion and metastases and may be a marker of improved response to neo-adjuvant chemoradiotherapy in rectal cancer (369-371).
WNK2	No literature relating to the role of WNK2 in colorectal cancer but WNK1 is activated in colon cancer cell lines (373). However, studies investigating WNK2 expression in meningioma and cervical cancer cells have suggested that WNK2 may act as a tumour suppressor (374, 375).
DUSP4	In colorectal cancer, high DUSP4 expression is associated with poorer overall survival and the presence of BRAF mutations (376).
Cdc25C	General studies of Cdc25C function suggest a mitotic function (377).
ERK1	Although ERK1 levels are similar in colorectal cancer tissues and pared normal tissue, activity of ERK1 is downregulated in most colorectal cancer and in colorectal adenomas (378, 379). Another study has shown that constitutive phosphorylation of Erk1/2 is dependent on Kirsten-ras (380). In the human colon cancer cell line HT-29, activation of ERK1/2 results in macroautophagy (381). Stimulation of ERK1/2 activation however has been demonstrated in response to GSNO, a nitric oxide donor, and is thought to play a role in NO-induced apoptosis (382). The

	phosphorylation of ERK1/2 along with that of c-Met and AKT has been shown to be induced by HGF which also upregulates VEGF mRNA and protein levels (383). The main activator of ERK1 is MEK1, which is involved in the regulation of tumour cell proliferation and cell transformation (384). Activation of ERK1/2 is also thought to play a role in the stimulation of colon cancer cell invasion and migration (385).
MKK4	In colorectal cancer cells, MKK4 has been shown to mediate the ROS-stimulated phosphorylation of JNK (386). Immunohistochemical studies have shown that phosphorylated MKK4 is present in colorectal cancer tissue, and that its expression correlates with depth of tumour invasion, differentiation, TNM stage and the presence of metastases but was also associated with improved survival outcomes (387). Certain polymorphisms in the promoter of MKK4 have been associated with a reduced risk of colorectal cancer development (388).
Grp94	Grp94 expression is associated with the expression of c-myc oncogene in colorectal cancer cell lines (389). The expression of Grp94 is significantly higher in colon cancer tissue than in adjacent background colonic tissue and high Grp94 expression is associated with poorer tumour differentiation and presence of metastases (390).
PDGFRB	The majority of human colorectal cancers express PDGFRB in the stroma (but not the epithelium) of colorectal cancer tissue with strongest IHC staining seen in vascular cells (391, 392). However, it is not associated with tumour characteristics or prognosis (391).
PDK4	Conflicting evidence regarding expression in human colorectal cancer (393, 394).
4E-BP1	Expression of 4E-BP1 is upregulated in colorectal cancer cells compared to normal colon cells and is also upregulated in colorectal cancer tissue

	compared to non-cancerous tissue (395). Furthermore, 4E-BP1 expression in the liver is higher in in patients with CRC liver metastases compared to those without liver metastases (395). 4E-BP1 expression is significantly correlated with nodal status and is more frequently expressed in patients with an advanced stage of presentation (395). Moreover, 4E-BP1 expression is associated with significantly shorter survival time and reduced time to disease recurrence (395). Another study by Diab-Assaf *et al* found that overall 4E-BP1 expression as determined by immunohistochemical staining was increased in colorectal adenoma tissue compared to normal colorectal tissue but was decreased in colorectal adenocarcinoma tissue (396). Furthermore, when 4E-BP1 was present in colorectal adenocarcinoma, it was highly phosphorylated or inactivated (396). A study of patients with stage II colon cancer found that expression of phosphorylated-4E-BP1 was inversely associated with disease-free survival (397).
Ros	Mutated in non-small cell lung cancer and gastric cancer (398).
MKK6	Upregulated in human colon cancers (399).
ErbB4	Overexpressed in human colorectal cancer (400). Mutated in 0.6% of CRC (401). Genetic variations of ErbB4 are associated with increased colorectal cancer risk (402, 403). Phosphorylated ERbB4 is associated with poorer prognosis in colorectal cancer (404). ErbB4 membranous protein expression predicts for CRC lymph node positivity (405).
DUSP3	Implicated in several human cancers, found to be both tumour-suppressing and tumour-promoting (406). Upregulated in cervical cancer but downregulated in NSCLC (407, 408). Pro-angiogenic (409).
PTEN	Reduced PTEN expression may play a role in colorectal carcinogenesis and loss of PTEN is associated with shorter survival (410, 411). PTEN

	expression correlates with differentiation, lymph node metastases, infiltration of the serosa and Dukes' stage in colorectal cancers but is not associated with tumour size (412). Loss of function or PTEN mutation is a predictor of poor colorectal tumour response to anti-EGFR treatment as well as being a predictor of shorter progression free survival and overall survival (413).

7.3.6.2 Analysis of proteins activated in RKO^{DOK7V2exp} cells compared to RKO^{pEF} cells: review of the literature for role in cancer

In order to determine the role of proteins activated in RKO^{DOK7V2exp} cells compared to RKO^{pEF} cells, a literature review was undertaken. The summarized results are shown in Table 7.13.

Table 7.13 Role of proteins activated in $RKO^{DOK7V2exp}$ cells compared to RKO^{pEF} cells in cancer

Target protein	Role in Cancer
TrkB	TrkB is necessary for CRC cell growth and survival (414). High TrkB is associated with poor prognosis in CRC and enhanced malignant potential with regard to proliferation, migration, invasion and anoikis (415-417). Tissue TrkB mRNA expression is associated with lymph node metastases and TrkB expression is associated with poorer prognosis (418).
CREB1	Promotes colorectal cancer tumour aggressiveness (419).
Cyclin B1	High levels expressed in human colorectal cancer (420).
BRCA1	Risk of CRC is increased in female carriers of BRCA1 mutations below the age of 50 (421).
CDK1/2	CDK1 is activated in many cancers including colon cancer (306).
IKKa	Nuclear IKKa is associated with malignancy (422). In murine models, elevated levels in the skin increase the malignant potential of skin cancers (423).
4E-BP1	4E-BP1 has been shown to be highly activated in colorectal cancers and colorectal adenomas with high-grade intraepithelial neoplasia and intensity of IHC staining correlates with depth of tumour invasion (424).
ATF2	Plays an important role in colorectal cancer (425). Contributes to cisplatin resistance in non-small cell lung cancer (426). Increases pancreatic cancer cell invasiveness by inducing EMT (427). Associated with poor prognosis in renal cell carcinoma (428). Conflicting data on role in skin cancers (429, 430).
PLCg1	Promotes tumour cell growth and migration (431).
Connexin 43	Conflicting results; some studies show connexin 43 is overexpressed in human colorectal cancer cells (432) whilst others have shown that connexin 43 is downregulated and that loss of expression is associated with shorter disease-

	free and overall survival (433).
ERK5	Overexpressed in human adenomas and adenocarcinomas, expression correlates with greater invasive and metastatic potential (434). ERK5 expression correlates with NF-κB activation in CRC (434). Overactivation of ERK5 is associated with increased cell cycle progression and cell migration (434).
Cofilin 2	Reduced expression has been found in pancreatic cancer (435).

7.3.6.3 Analysis of proteins underexpressed in RKO^{DOK7V2exp} cells compared to RKO^{pEF} cells: review of the literature for role in cancer

In order to determine the role of proteins underexpressed in RKO^{DOK7V2exp} cells compared to RKO^{pEF} cells, a literature review was undertaken. The summarized results are shown in Table 7.14.

Table 7.14 Role of proteins underexpressed in $RKO^{DOK7V2exp}$ cells compared to RKO^{pEF} cells in cancer

Target protein	Role in cancer
PTP1D/SHP2	Downregulation of SHP2 in colorectal cancer may promote cancer metastases and invasion via the negative regulation of c-Src and consequently villin-induced cell migration and invasion (436).
PDK3	Previous studies have shown levels of PDK3 are increased in colorectal cancer compared to adjacent normal tissues and are positively associated with severity of cancer and negatively associated with disease-free survival (437).
GNB2L1	Tumour suppressor in gastric cancer (438). Expression is correlated with differentiation level and lymph node metastasis in colorectal cancer (439). Inhibits growth and induces apoptosis of colon cells and promotes cell-cell adhesion and reduces the invasive potential of colon cancer cells (440, 441).
Haspin	Highly expressed during cell proliferation and in several cancers (442).
STI1	Promotes proliferation in glioma cells via MAPK and PI3K pathways (443). Increases glioblastoma cell migration (444).
Smad2/3	Smad2 mutations are implicated in colorectal and lung cancers (445). Smad2 may act as tumour suppressor in colorectal cancer and is inactivated in LOH colorectal cancers (446). C-terminally phosphorylated Smad 3 (pSmad3C) and linter phosphorylated Smad 3 (pSmad3L) are potential biomarkers in colorectal cancer (447).
PCTK1	Implicated in cancer cell proliferation and anti-apoptosis (448). siRNA treatment targeting PCTAIRE1 reduces tumour volume and weight and results in increased apoptosis in human colorectal cancer cells (448).

ROCK-I/ROKb	ROCK1 genetic polymorphisms may modify susceptibility to colorectal cancer (449).
MEK1	Deregulation of the MEK pathway is implicated in melanoma, pancreatic, lung, colorectal and breast cancers (450). MEK is recognized as a potential therapeutic target in colorectal cancer and several MEK inhibitors are under evaluation by clinical trials (451).
PTP-PEST	Downregulation of PTP-PEST in colorectal cancer may promote cancer metastases and invasion via the negative regulation of c-Src and consequently villin-induced cell migration and invasion (436).
DRAK2	Implicated in the regulation of apoptosis in colorectal cancer cells (452).
BMX (Etk)	Implicated in prostate cancer (453). Contributes to tumour angiogenesis and growth in colon, lung and melanoma tumour deposits (454).

7.3.6.4 Analysis of proteins functionally suppressed in RKO^{DOK7V2exp} cells compared to RKO^{pEF} cells: review of the literature for role in cancer

In order to determine the role of proteins functionally suppressed in RKO^{DOK7V2exp} cells compared to RKO^{pEF} cells, a literature review was undertaken. The summarized results are shown in Table 7.15.

Table 7.15 Role of proteins functionally suppressed in $RKO^{DOK7V2exp}$ cells compared to RKO^{pEF} cells in cancer

Target protein	Role in cancer
IRAK4	Increased phosphorylation state found in melanoma patients (455). Inhibition of IRAK4 inhibits tumour growth and increases cell death (455).
Met/ Hepatocyte growth factor receptor	HGFR activation promotes colorectal cancer cell survival, invasion and resistance to apoptosis and its expression in colon cancer correlates with depth of tumour invasion and is a marker of metastatic disease (456-458).
CDK1	High nuclear/cytoplasmic ratio of Cdk1 expression predicts poor prognosis in colorectal cancer patients (459). High level of phosphorylated CDK1 is associated with prolonged disease-free survival in colorectal cancer patients (460).
Dok2	Loss of DOK2 found in 1/3 of CRC specimens (259). Loss of DOK2 is associated with CRC recurrence and poorer 5-year overall survival rate (259).
Vav 1	Overexpression is associated with advanced cancer stage or lymph node metastases (461).

7.4 Discussion

Data obtained from qPCR analysis of our cohort tissues demonstrates that DOK7V2 expression is increased in colorectal cancer tissue compared with normal colorectal tissue.

Here, we have shown that, overexpression of DOK7V2 in colorectal cancer cells is associated with changes in the expression and phosphorylation (activation) of numerous proteins in RKO cells.

Of the predicted functional partners identified using STRING analysis, two proteins were found to be differently phosphorylated in DOK7V2 overexpression RKO cells. Firstly, functional suppression of DOK2 at phosphosite Y142 was observed in RKO DOK7V2 cells compared to RKO pEF control cells. Secondly, increased activation of TrkB at phosphosite Y705 was observed in RKO DOK7V2 cells compared to RKO pEF control cells.

The microarray data reveals a number of interesting findings. Notable proteins overexpressed in DOK7V2 overexpression cells include the receptor tyrosine kinase VGFR2, the non-receptor tyrosine kinase JAK3 and the atypical serine/threonine kinase mTOR. VGFR2 is a receptor tyrosine kinase which plays a key role in the regulation of angiogenesis and which has been shown to promote endothelial proliferation, survival, migration and differentiation whilst negatively regulating apoptosis (272, 273). mTOR is an atypical serine/threonine kinase, which promotes cell growth and is a key regulator of cell metabolism and survival. It regulates the phosphorylation of hundreds of proteins (276).

JAK3 is involved in cell growth, migration and differentiation and has been found to be activated in acute megakaryoblastic leukaemia (274-276). Other proteins overexpressed in RKO DOK7V2 overexpression cells that have been implicated in cell proliferation are PRKDC, MEK5, WNK2, ERK1, Grp94 and PDGFRB. PRKDC, MEK5, catenin b, DUSP4,

Grp94 and 4E-BP1 have previously been linked with colorectal tumour aggressiveness and poorer clinical outcomes. Cell signalling pathways associated with these proteins include the PI-3K-Akt, MAPK, JAK-STAT, mTOR, ErbB/HER, Wnt/β-catenin and angiogenesis signalling pathways

Notable proteins activated in the DOK7V2 overexpression cells include the transmembrane receptor tyrosine kinase TrkB, transcription factor CREB1, Cyclin B1, translational protein 4E-BP1 and protein kinase ERK5, the expression of all of which have previously been linked with increased colorectal cancer malignant potential and poorer clinical outcomes. TrkB is a transmembrane receptor with intracellular tyrosine receptor activity which has been previously associated with cell differentiation, growth, survival and suppressed anoikis as well as poor prognosis and increased metastases (276, 297). CREB1 is also known to play a role in cell differentiation and a number of the other proteins activated in RKODOK7V2 overexpression cells are known to play a role in cell cycle progression, including Cyclin B1, BRCA1 and CDK1/2 (298) (300-302). Cell signalling pathways associated with the activated proteins include the PI-3K-Akt, MAPK, mTOR, ErbB/HER and angiogenesis signalling pathways

Of the proteins exhibiting reduced expression in RKO DOK7V2 overexpression cells, PTP1D/SHP2 and PTP-PEST are notable in that their downregulated in colorectal cancer has previously been associated with cancer metastasis, cell migration and invasion (436). We also found that there was reduced levels of phosphorylation of CDK1, a proteins whose level of phosphorylation has previously been associated with the length of disease-free survival of colorectal cancer patients (460). Reduced phosphorylation of Dok-2 was also observed, consistent with previous findings that Dok-2 acts as a tumour suppressor in colorectal cancer (259). By comparison, the hepatocyte growth factor receptor, Met, was observed to be downregulated in RKO DOK7V2 overexpression cells. Previous studies have linked Met

activation with increased colorectal cancer cell survival, invasion and evasion of apoptosis (458).

A number of the proteins modulated by DOK7V2 expression participate in the mTOR signalling pathway. This important pathway regulates cell growth, proliferation and survival (462). Activation of the mTOR pathway is associated with tumour formation and angiogenesis and also occurs in insulin resistance and T-lymphocyte activation (462). This has led to the development of mTOR inhibitors, which are used in a variety of pathological conditions including cancer (462). The impact of DOK7V2 overexpression on the mTOR pathway is illustrated in Figure 7.3 and the impact on the Jak/STAT and angiogenesis pathways are illustrated in Figure 7.4 and Figure 7.5 respectively. In these diagrams, over- or under-expression of a protein is indicated by an arrow and an asterisk indicates protein activation. Where there is more than one member of a protein family, for example ERK1 and ETK5, the number of the protein affected is indicated in brackets.

In summary, analysis of DOK7V2 overexpression in a colorectal cancer cell line compared with a control cell line has revealed a number of differences in the expression and activation of other proteins. These findings provide a useful starting point for future work to elucidate how DOK7 isoforms interact with other cell signalling proteins.

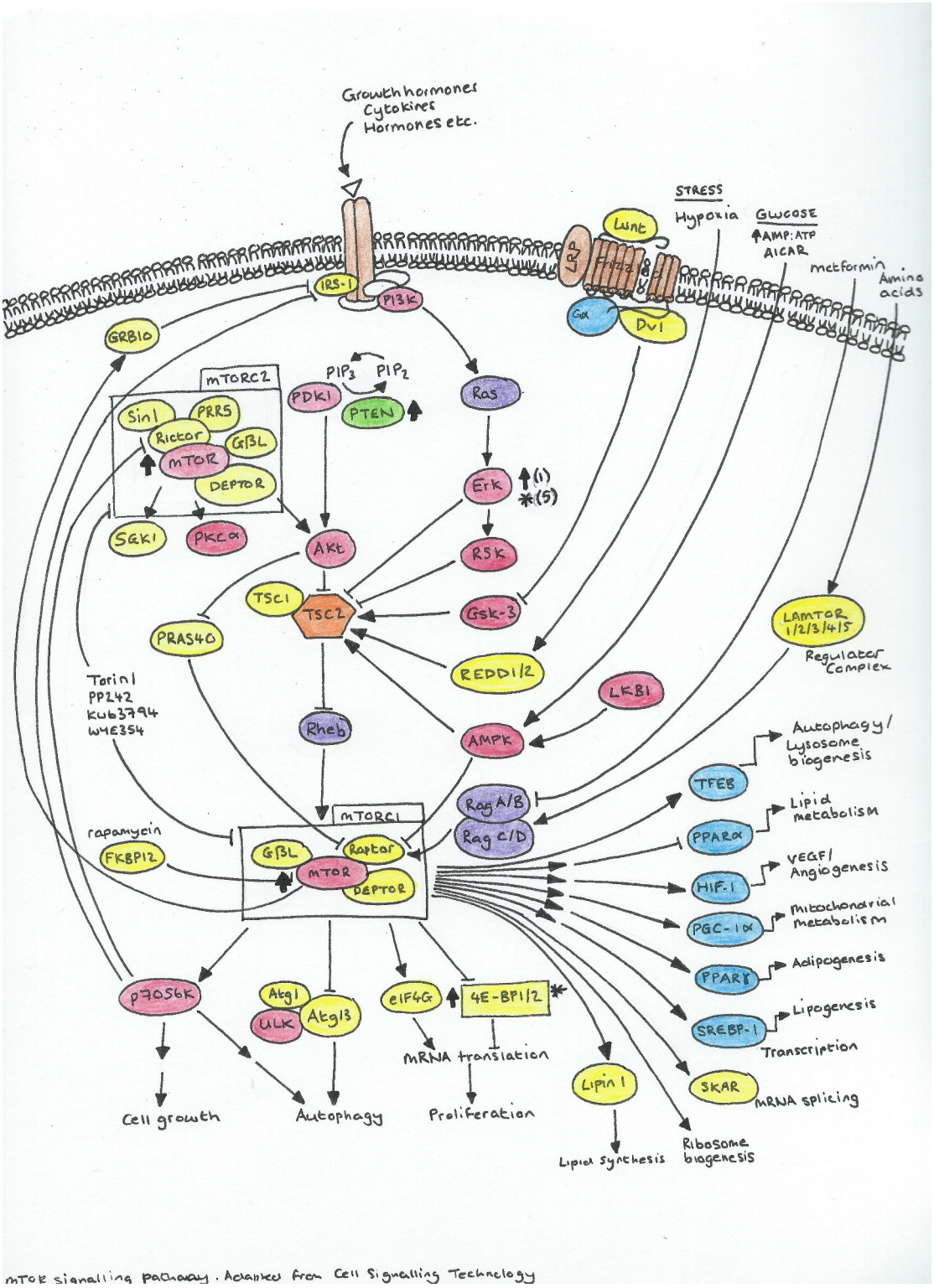

Figure 7.3 Impact of DOK7V2 overexpression on the mTOR pathway. Diagram adapted from Cell Signalling Technology.

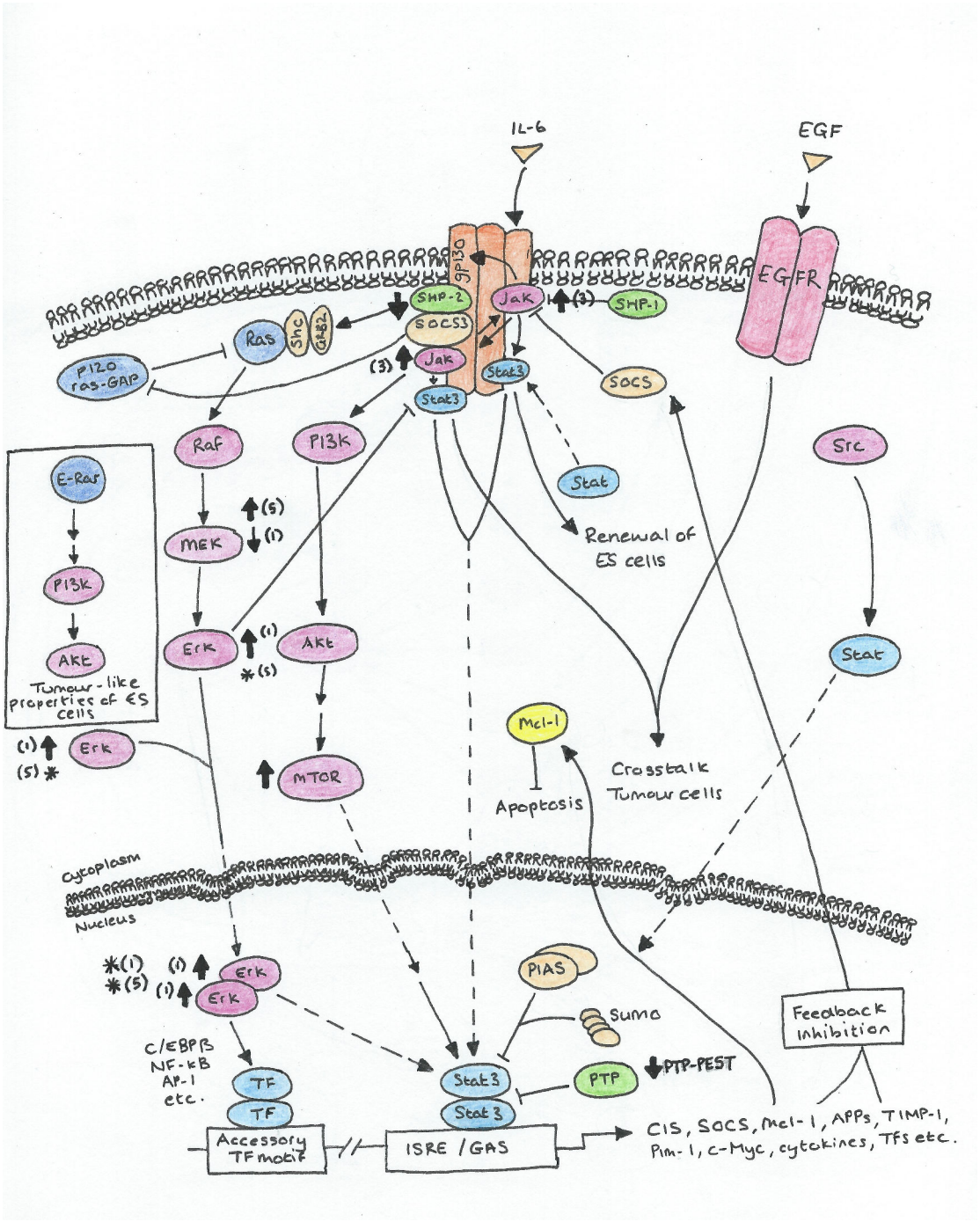

Figure 7.4 Impact of DOK7V2 overexpression on Jak/STAT pathway. Diagram adapted from Cell Signalling Technology.

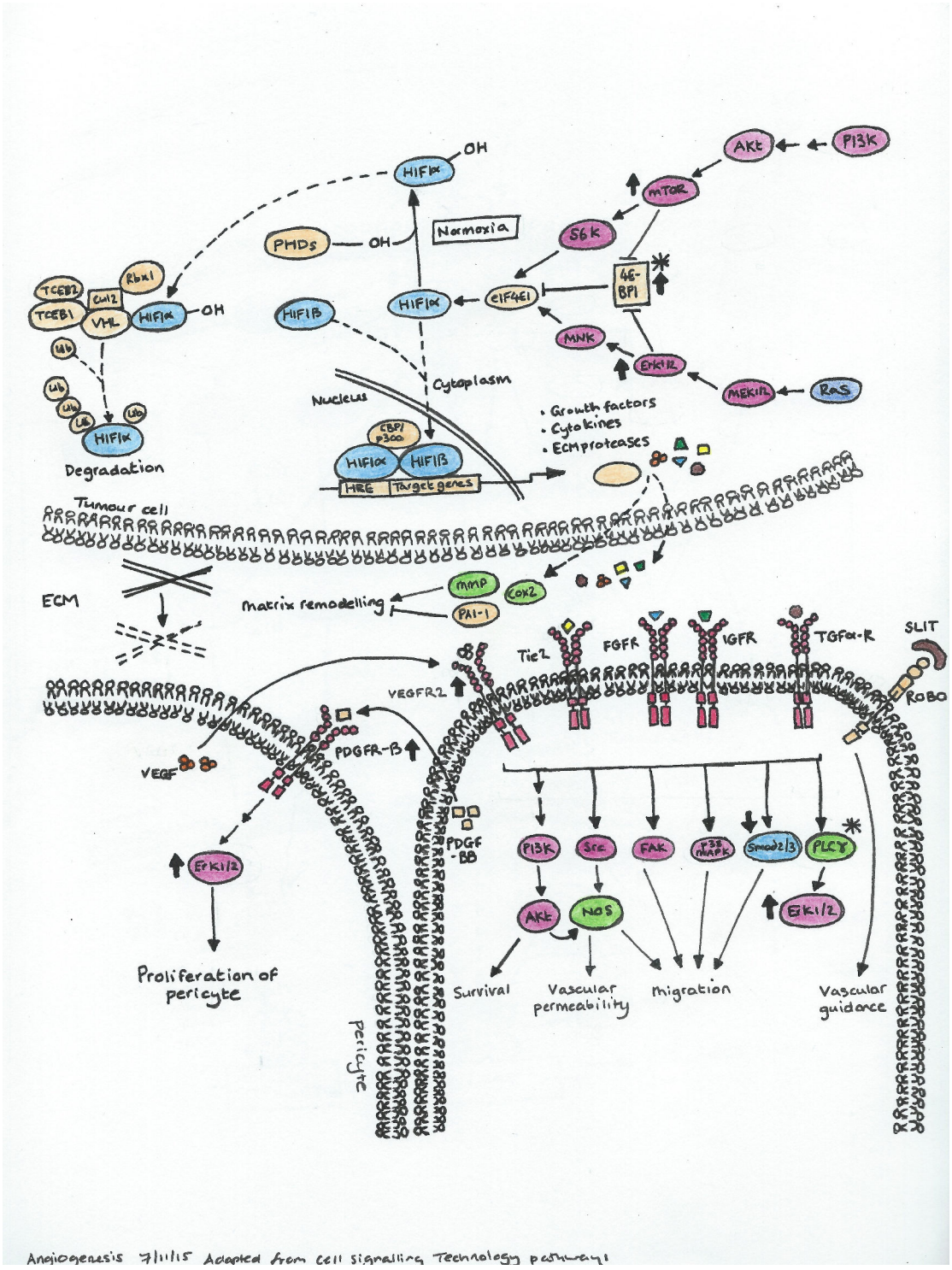

Figure 7.5 Impact of DOK7V2 overexpression on the angiogenesis pathway. Diagram adapted from Cell Signalling Technology.

Chapter 8: General Discussion

8.1 Dok proteins in colorectal cancer

The Dok proteins are a family of cytoplasmic adaptor proteins involved in signalling pathways downstream of tyrosine kinase. Tyrosine phosphorylation of proteins by protein tyrosine kinases (PTKs) is a reversible process that plays an important role in the regulation of a variety of cellular functions including cell growth, differentiation and cell motility. Activation of PTKs by extracellular stimuli results in the phosphorylation of both the PTK as well as other substrates including trans-membrane receptors and the adaptor proteins. The latter then either recruit or inhibit further downstream molecules, thereby regulating tyrosine kinase signalling pathways. Aberrations in this process of tyrosine phosphorylation and downstream signal transduction are associated with many types of cancer. Consequently, there has been an effort to investigate and understand this complex process in order to evaluate its potential as a target for therapeutic intervention. The Dok proteins possess structural characteristics typical of adapter proteins and, like other adapter molecules, they associate with activated cell-surface receptors and aid in the docking of downstream signalling molecules, facilitating intracellular signal transduction. Their precise role is unclear but they are thought to play a possible tumour suppressor role in relation to human malignancies. Dok-7, the most recently identified member of this family, has mostly been investigated with regard to its role in musculoskeletal diseases and little is currently known about its role in cancer. A recently published paper looking at twin pairs discordant for breast cancer suggested hypermethylation of the Dok-7 promoter occurs in breast cancer and may occur prior to cancer diagnosis, raising the possibility that Dok-7 may have a potential role as a cancer biomarker. However, there has been no research to date investigating the role of Dok-7 in colorectal cancer, one of the commonest cancers in the UK and a significant cause of cancer related death.

8.2 Main conclusions of this study

8.2.1 Expression of DOK7 in human colorectal cell lines

Initial studies of DOK7 mRNA expression revealed that DOK7 is variably expressed in colorectal cancer cells. Interestingly, lower levels of DOK7 expression were seen in HT-115 and RKO cell lines, which are the more poorly differentiated and highly aggressive colorectal cancer cell lines and this trend was also observed in breast cancer cell lines, with lowest levels of expression seen in MDA-MB-231, a poorly differentiated metastatic breast adenocarcinoma.

8.2.2 Expression of DOK7 in colorectal clinical cohort and association with tumour pathology and clinical outcome data

Preliminary results found that DOK7 mRNA expression is significantly reduced in colorectal cancer compared to normal colorectal tissue in keeping with a potential tumour suppressor role for DOK7. Our data also revealed that DOK7 expression was inversely related to colorectal cancer T stage and that low DOK7 expression was associated with poorer survival compared to high DOK7 expression, suggesting a tumour suppressive effect that may be of clinical importance. These results correlate with our previous (unpublished) findings in the host laboratories that found reduced levels of DOK7 expression in breast cancer tissue compared to normal breast tissue.

However, our analysis of gene array data obtained from a cohort of 585 colorectal cancer samples found conflicting results. We found that in this cohort, DOK7 mRNA expression was increased in colorectal cancer compared to normal colorectal tissue and that, contrary to our cohort data, poor survival outcomes were associated with high DOK7 expression.

Although DOK7 expression has not previously been examined in relation to colorectal cancer, previous studies have generally suggested a tumour suppressor role for the Dok proteins in a range of human cancers. In relation to colorectal cancer, DOK2 expression has been shown to be reduced in colorectal cancer compared to normal colorectal tissue and low DOK2 expression is associated with poorer survival (259). A recently published study by Friedrich *et al* investigating DOK1 in a large cohort (n = 1492) of colorectal cancer patients found that loss of DOK1 protein was associated with poor prognosis in early stage tumours (463). Furthermore, they found that cytoplasmic expression of DOK1 was associated with better survival outcome whilst nuclear localisation of DOK1 was associated with poorer survival outcomes suggesting that the subcellular compartmentalization of DOK1 played a role in colorectal cancer progression (463).

Difficulties encountered in creating cell models for DOK7 expression along with the conflicting results found between the two sets of cohort data led us to realise the existence of DOK7 variants which code for different protein isoforms.

8.2.3 Expression of DOK7 variants in human colorectal cell lines

The expression of DOK7 variants differed between colorectal cancer cell lines. DOK7V1 and DOK7V2 were both strongly expressed by HRT-18 cells with reduced levels of expression seen in RKO and HT-115 cells. Meanwhile, DOK7V3 expression was highest in HT-115 cells with lower levels of expression seen in RKO and HRT-18 cells. There is no previously published data regarding the expression of DOK7 variants in colorectal cell lines but DOK7 splice variants are acknowledged in research investigating DOK7 congenital myasthenic syndrome.

8.2.4 Expression of DOK7 variants in colorectal clinical cohort and association with tumour pathology and clinical outcome data

Analysis of variant expression in our cohort revealed that the expression of DOK7V1 is significantly reduced in colorectal cancer compared to normal colorectal tissue. By comparison, the expression of DOK7V2 and DOK7V3 is significantly increased in colorectal cancer compared to normal colorectal tissue.

In addition, we found that DOK7V1 expression is significantly associated with overall stage of disease and that low DOK7V1 expression is associated with reduced length of disease free survival. Interestingly, although the level of DOK7V2 expression was increased in colorectal cancer compared to normal colorectal tissue, low DOK7V2 expression was associated with reduced disease-free survival compared to high DOK7V2 expression.

8.2.5 Functional role of DOK7 in colorectal cancer

It took almost a year to develop overexpression cell models using DOK7 variant synthesised sequences. These enabled us to investigate the impact of DOK7V2 overexpression on some of the important functions of colorectal cancer cells, namely cell growth, adhesion and invasion. Despite the differences observed at a cohort level, *in vitro* functional assays revealed no significant differences in colorectal cancer cell growth, adhesion or invasion. This may be due to the inherent limitations of functional assays and culture media in replicating the complexity of the tumour *in vivo*.

8.2.6 Evaluation of DOK7 coordinated cell signalling in colorectal cancer

Although we were unable to pursue protein analysis using Western blot due to difficulties with Dok-7 antibodies and a lack of isoform specific antibodies, we investigated the effect of DOK7V2 overexpression on protein expression and activation using an antibody based protein microarray.

We found that DOK7V2 overexpression is associated with significant changes in the expression and phosphorylation (activation) of numerous proteins in RKO cells.

Notable proteins significantly overexpressed in DOK7V2 overexpression cells include the receptor tyrosine kinase VGFR2, the non-receptor tyrosine kinase JAK3 and the atypical serine/threonine kinase mTOR. These and other overexpressed proteins including PRKDC, MEK5, catenin b, DUSP4, Grp94 and 4E-BP1 have previously been linked with colorectal tumour aggressiveness and poorer clinical outcomes. Cell signalling pathways associated with these proteins include the PI-3K-Akt, MAPK, JAK-STAT, mTOR, ErbB/HER, Wnt/β-catenin and angiogenesis signalling pathways.

Notable proteins significantly activated in the DOK7V2 overexpression cells include the transmembrane receptor tyrosine kinase TrkB, transcription factor CREB1, Cyclin B1, translational protein 4E-BP1 and protein kinase ERK5, the expression of all of which have previously been linked with increased colorectal cancer malignant potential and poorer clinical outcomes. Cell signalling pathways associated with these proteins include the PI-3K-Akt, MAPK, mTOR, ErbB/HER and angiogenesis signalling pathways.

We have been able to illustrate the effect of DOK7V2 overexpression on the mTOR, Jak/STAT and angiogenesis signalling pathways, which all play an important role in colorectal carcinogenesis. Our findings provide a useful starting point for future work to

elucidate how Dok 7 isoforms interact with other cell signalling proteins and to determine whether Dok 7 itself has the potential to be a useful therapeutic target.

8.2.7 Summary of thesis findings

Overall, our results suggest that DOK7 plays a role in colorectal cancer and that different DOK7 variants coding for different protein isoforms may be differentially expressed in colorectal cancer compared to normal colorectal tissue.

8.3 Limitations

There are a number of limitations regarding the data discussed in this thesis. Firstly, the numbers of samples available in some subgroups of the cohort were small and therefore, the results should be treated with some caution. Secondly, our cohort samples were all obtained from patients undergoing surgery for operable colorectal cancer. Consequently, the majority of samples available for analysis were Dukes' B (n=33) and Duke's C (n = 32) cancers with relatively fewer Dukes' A (n = 7). Whilst the data is representative of patients with surgically resectable disease, it may not necessarily be applicable to patients with early, undetected cancer, those undergoing endoscopic removal for early cancers or those with advanced, inoperable disease. Furthermore, the recent introduction of bowel screening in Wales may result in a change in the pathological profile of patients undergoing surgery for bowel cancer in Wales over the next few years towards the detection and treatment of earlier cancers.

A further limitation is that the tissue samples obtained for the current study were obtained from a cohort of patients undergoing treatment for bowel cancer over a 1-year period from 2005-2006. As such, the neo-adjuvant or adjuvant oncological therapy given to some of the patients in this study may have been superseded by newer therapies and therefore, the application of results relating to oncological therapies should be treated with some caution.

In order to address these limitations, ethical approval is currently being sought to collect further operative samples to obtain a larger cohort, to enable analysis of tissue from patients undergoing contemporary oncological treatment and also to include lymph node tissue for analysis. Biopsy material from colonoscopies would also provide useful tissue from early cancers, and also from patients without cancer with normal and adenomatous colorectal mucosa. This would potentially enable more detailed analysis of DOK7 expression during the normal-adenoma-carcinoma sequence but limitations to this include the size of biopsy obtained relative to the quantity of tissue required for diagnosis and also the risks and ethical

considerations involved in obtaining additional biopsies for research study, particularly in patients who are asymptomatic or do not have proven pathology.

One of the main limitations of this thesis is that we were unable to confirm our findings at the protein level despite multiple attempts at Western blot owing to problems with Dok-7 antibodies. Ideally, we would have developed our own variant-specific antibodies but this was not practical given the time restraints of a PhD project as well as the cost and practical difficulties this would have posed.

8.4 Future perspectives

This study has demonstrated that the expression of DOK7 variants may differ in colorectal cancer compared to normal colorectal tissue and that changes in the expression of these variants may impact not only at a cellular level on cell function, but also at a clinical level by affecting tumour pathology and patient outcomes.

This clinically oriented PhD seeks to bridge the gap between what is observed at the cellular level and what is seen clinically. We have identified several interesting novel findings in relation to DOK7 but have generated many questions and avenues for further investigation. Further work is now required to better our understanding of how DOK7 and its variants interact with other proteins, how it modulates cell signalling, how it impacts on colorectal cancer cell function and ultimately, how this information may be usefully applied in the clinical context either as a predictive or diagnostic tool, as a means of prognostication or treatment stratification or as a potential target for molecular therapies.
Specific areas for future work are as follows.

8.4.1 Correlation of findings at the protein level

Unfortunately, attempts to confirm our findings at the protein level using SDS-PAGE and Western blot failed due to difficulties with antibodies. Given more time, we would like to develop isoform specific Dok-7 antibodies that would enable us to confirm our findings at the protein level.

8.4.2 Generation of additional cell models

Owing to the time constraints of a PhD study, work was focused on DOK7V2 overexpression cell models in two colorectal cell lines. With more time, additional cell models would be helpful to correlate this study's findings, investigate the impact of DOK7V1 and DOK7V3 overexpression and to investigate the effects of DOK7V1-3 knockdown on colorectal cancer cell function.

8.4.3 Investigation of additional cell functions

Although this study has shed some light on the effect of DOK7V2 expression on cell growth, adhesion and invasion, attempts to investigate the effect on cell migration using a scratch assay and ECIS failed due to disruption of the RKO cell monolayer. Potential solutions to overcome this particular challenge may include the establishment of cell models using an alternative colorectal cell line or the use of alternative migration assays.

Alternative migration assays include scatter assays, which monitor cell movement from clustered cells by adding a motogen such as HGF or FGF or alternatively, motility assays using a cell carrier bead, which co-culture cells with beads in a universal container overnight allowing cells to attach to the beads. Non-attached cells are washed off using low speed (500-

700 rpm for 5 min) centrifuge and PBS. The beads are resuspended in a medium, added to a culture plate and fixed after a period of 2-4 hours incubation.

8.4.4 Further elucidation of cell signalling pathways

Based on the results of the functional assays and antibody-based protein microarray, some preliminary work has been undertaken to identify potential interacting proteins for DOK7 and to try to establish which cell signalling pathways are implicated.

Further work is necessary firstly to localise DOK7 variants in normal and colorectal cancer cells and secondly, to confirm the role of DOK7V2 in the cell signalling pathways discussed in Figure 7.3-7.5.

A recently published paper by Friedrich *et al* investigating the role of DOK1 in colorectal cancer found that cytoplasmic DOK1 activated peroxisome-proliferator-activated-receptor-gamma (PPARγ) leading to inhibition of the c-FOS promoter and cell proliferation (463). By comparison, nuclear DOK1 was inactive (463). The same authors found that use of a PPARγ-agonist increased the expression of endogenous DOK1 and its interaction with PPARγ, leading them to suggest that DOK1 may be a potential therapeutic target (463).

8.4.5 *In vivo* models

Finally, we plan to correlate our findings using *in vivo* DOK7 variant overexpression mouse models to further explore the impact of DOK7 variant expression on tumour growth and survival. Hopefully this will help us to overcome some of the limitations of cell line based single functional assays.

Appendices

Appendix 1: General compounds used in this study

Table 2.2 General compounds used in this study and their sources

Material/Reagent	**Supplier**
Acetic acid	Fisher Scientific, Leicestershire, UK
Acrylamide mix (30%)	Sigma-Aldrich, Poole, Dorset, UK
Agar	Melford Laboratories Ltd, Suffolk, UK
Ammonium persulphate (APS)	Sigma-Aldrich, Poole, Dorset, UK
Amphotericin B	Sigma-Aldrich, Poole, Dorset, UK
Ampicillin	Sigma-Aldrich, Poole, Dorset, UK
Amplifluor™ UniPrimer™	Intergen Inc., Oxford, United Kingdom
Aprotinin	Sigma-Aldrich, Poole, Dorset, UK
β-glycerophosphate	Sigma-Aldrich, Poole, Dorset, UK
Benzamidine	Sigma-Aldrich, Poole, Dorset, UK
Bio-Rad DC™ Protein Assay	Bio-Rad Laboratories, Hercules, CA, USA
Blasticidin S	Melford laboratories Ltd, Suffolk, UK
Boric acid	Duchefa Biochemie, Haarlem, Netherlands
Bovine serum albumin (BSA)	Sigma-Aldrich, Poole, Dorset, UK
Bromophenol Blue	Sigma-Aldrich, Poole, Dorset, UK
Calcium chloride ($CaCl_2$)	Sigma-Aldrich, Poole, Dorset, UK
Chloroform	Sigma-Aldrich, Poole, Dorset, UK
Coomassie blue	Sigma-Aldrich, Poole, Dorset, UK
Crystal violet	Sigma-Aldrich, Poole, Dorset, UK
Diethylpyrocarbonate (DEPC)	Sigma-Aldrich, Poole, Dorset, UK
Dimethylsulphoxide (DMSO)	Fisons Scientific Equipment, Loughborough, UK
Disodium phosphate (Na_2HPO_4)	BDH Chemicals Ltd, Poole, Dorset, UK
Dithiothreitol	Sigma-Aldrich Ltd, Dorset, UK

Dulbecco's Modified Eagles' Medium/Nutrient mixture F12 Ham (DMEM/F-12) with 2mM L-glutamine	PAA Laboratories, Coelbe, Germany
Ethylenediaminetetraacetic acid (EDTA)	Duchefa Biochemie, Haarlem, Netherlands
Ethanol	Fisher Scientific, Leicestershire, UK
Foetal calf serum (FCS)	PAA Laboratories, Coelbe, Germany
Formalin	Sigma-Aldrich Ltd, Dorset, UK
GenElute™ Plasmid Miniprep kit	Sigma-Aldrich Ltd, Dorset, UK
GenScript® PCR DNA ladder	Qiagen Ltd, Manchester, UK
Glycine	Melford Laboratories Ltd, Suffolk, UK
GoTaq® Green Master Mix	Promega
High capacity cDNA reverse transcription kit	Applied Biosciences
Hydrochloric acid (HCl)	Sigma-Aldrich, Poole, Dorset, UK
Isopropyl alcohol/isopropanol/2-propanol	Sigma-Aldrich, Poole, Dorset, UK
Leupeptin	Sigma-Aldrich, Poole, Dorset, UK
Luminata(TM0 Forte Western HRP chemiluminescence substrate	Millipore, MA, USA
Matrigel®	BD Biosciences, Oxford, UK
Mayer HTX solution	Sigma-Aldrich, Poole, Dorset, UK
Methanol	Fisher Scientific, Leicestershire, UK
Monopotassium phosphate (KH_2PO_4)	BDH Chemicals Ltd, Poole, Dorset, UK
3-(N-morpholino)propanesulfonic	Sigma-Aldrich, Poole, Dorset, UK

acid (MOPS)	
Nitrocellulose membrane	Ammersham, Cardiff, UK
OneShot® TOP10 chemically competent E.coli	Life Technologies, Paisley, UK
pEF6/V5-His TOPO® TA Expression kit	Invitrogen, CA, USA
Penicillin	Sigma-Aldrich, Poole, Dorset, UK
Pepstatin A	Sigma-Aldrich, Poole, Dorset, UK
Peroxidase conjugated goat anti-rabbit IgG	Sigma-Aldrich, Poole, Dorset, UK
Peroxidase conjugated rabbit anti-mouse IgG	Sigma-Aldrich, Poole, Dorset, UK
Phenylmethylsulfonyl fluoride (PMSF)	Sigma-Aldrich, Poole, Dorset, UK
Ponceau S	Sigma-Aldrich, Poole, Dorset, UK
Precision qScript™ RT PCR kit	Primerdesign Ltd, Southampton, UK
Potassium chloride (KCl)	Fisons Scientific Equipment, Loughborough, UK
REDTaq® ReadyMix™ PCR Reaction Mix	Sigma-Aldrich, Poole, Dorset, UK
RPMI	Sigma-Aldrich, Poole, Dorset, UK
Serum bovine albumin	Sigma-Aldrich, Poole, Dorset, UK
SOC medium	Invitrogen, CA, USA
Sodium dodecyl sulphate (SDS)	Melford Laboratories Ltd, Suffolk, UK
Sodium chloride (NaCl)	Sigma-Aldrich, Poole, Dorset, UK
Sodium fluoride	Sigma-Aldrich, Poole, Dorset, UK
Sodium hydroxide (NaOH)	Sigma-Aldrich, Poole, Dorset, UK
Sodium nitrate	Sigma-Aldrich, Poole, Dorset, UK

Sodium orthovanadate (NA_2VO_4)	Sigma-Aldrich, Poole, Dorset, UK
Sodium pyrophosphate	Sigma-Aldrich, Poole, Dorset, UK
Streptomycin	Sigma-Aldrich, Poole, Dorset, UK
Sucrose	Fisons Scientific Equipment, Loughborough, UK
SYBR®Safe DNA gel stain	Life Technologies Ltd, Paisley, UK
Tetramethylethylenediamine (TEMED)	Sigma-Aldrich, Poole, Dorset, UK
TRI Reagent®	Sigma-Aldrich, Poole, Dorset, UK
Tris	Sigma-Aldrich, Poole, Dorset, UK
Tris-Cl	Melford Laboratories Ltd, Suffolk, UK
Triton X-100	Sigma-Aldrich, Poole, Dorset, UK
Trypsin	Sigma-Aldrich, Poole, Dorset, UK
Tryptone	Duchefa Biochemie, Haarlem, Netherlands
Tween 20	Melford Laboratories Ltd, Suffolk, UK
Vectastain Universal ABC kit	Vector Laboratories Inc, Burlingame, CA, USA
Yeast extract	Duchefa Biochemie, Haarlem, Netherlands
Zinc chloride (ZnCl)	Sigma-Aldrich, Poole, Dorset, UK

Appendix 2: General plastic consumables used in this study

Table 2.3 General plastic consumables, hardware and software used in this study and their sources

Plastic consumable/Hardware/Software	**Supplier**
24 well plate	Nunc™, ThermoFisher Scientific, Loughborough, UK
96 well plate	Nunc™, ThermoFisher Scientific
Amplifluor™ detection system	Intergen, England, UK
Applied Biosystems® 2720 PCR Thermal cycler	ThermoFisher Scientific
Cell scraper	ThermoFisher Scientific
Centrifuge	Woolf Laboratories, York, UK
Class II Laminar Flow Cabinet	Woolf Laboratories, York, UK
Cryotube	Woolf Laboratories, York, UK
Drying oven	Woolf Laboratories, York, UK
Electrophoresis gel tray	Scie-Plas Ltd, Cambridge, UK
Electrophoresis unit	Woolf Laboratories, York, UK
Electroporation cuvette (4mm)	Euro Gentech, Southampton, UK
Electroporator	Woolf Laboratories, York, UK
ELx800 plate reading spectrophotometer	Bio-Tek, Wolf Laboratories, York, UK
Eppendorf tube (1.8ml)	Greiner Bio-one GmbH, Bristol, UK
Falcon tube	Greiner Bio-one GmbH, Bristol, UK
Filter paper	Sigma-Aldrich, Poole, Dorset, UK
Filtration unit (0.4µm)	Sigma-Aldrich, Poole, Dorset, UK
Gibco BRL Electrophoresis power supply (model 250EX)	Life Technologies, Paisley, UK
Glass pipette	ThermoFisher Scientific

Glass plates for SDS-PAGE	Woolf Laboratories, York, UK
Hybond nitrocellulose membrane	Amersham Biosciences Ltd, Bucks, UK
iCycler iQ system	Bio Rad, Hercules, CA, USA
Image J	https://imagej.nih.gov/ij/
Incubator	Sanyo Electric, Japan
Labinco rotating wheel	Woolf Laboratories, York, UK
Leica DM IRB microscope	Leica GmbH, Bristol, UK
MicroAmp® Optical Adhesive film	ThermoFisher Scientific, Paisley, UK
Microscope heated plate	Leica, GmbH, Bristol, UK
Microsoft Excel	Microsoft Inc, Redmond, WA, USA
Mini start filter (0.2µm)	Sartorius, Epsom, UK
Mr Frosty™ Freezing Container	Thermo Scientific, Waltham, MA, USA
Neubauer haemocytometer counting chamber	Reichert, Austria
Nitrocellulose membrane	Hybond C, Ammersham, Cardiff
Partec CyFlow® FloMax software	Partec GmbH, Munster, Germany
Partec CyFlow® SL flow cytometer	Partec GmbH, Munster, Germany
PCR tube (200µL)	ABgene, Surrey, UK
Petri dishes (10cm^2)	BibbySterilin Ltd, Staffs, UK
Protein spectrophotometer	BIO-TEK, Wolf Laboratories, York, UK
RNA spectrophotometer	BIO-TEK, Wolf Laboratories, York, UK
SD20 SemiDry Maxi System blotting unit	SemiDRY, Wolf Laboratories, York, UK
Tali® cellular analysis slide	Life Technologies, Paisley, UK
Tali® Image Cytometer	Life Technologies, Paisley, UK
Techne Hybridiser HB-1D drying oven	Wolf Laboratories, York, UK
T-Cy Thermocycler	Creacon Technologies Ltd, Netherlands
Tissue culture flasks (25cm^2 and 75cm^2)	Greiner Labortechnik, Germany

Trans-well inserts 8µm pore size	Corning™ Falcon™, Loughborough, UK
Ultra-Turrax T8 homogeniser	IKA Labortechnik, Staufen, Germany
Universal container (30ml)	Greiner Bio-One Ltd, Gloucestershire, UK
UV1101 Biotech Photometer	WPA, Cambridge, UK
UV light chamber	Germix
UVI band software	UVITEC, Cambridge, UK
UVI-doc system	UVI-Tech Inc., Cambridge, England, UK
UVITEC imager	UVITEC, Cambridge, England, UK

Appendix 3: Antibodies used in this study

Table 2.4 Primary antibodies

Antibody against	Species	Supplier	Catalogue number
C-terminal Dok7 (cDok7)	Rabbit polyclonal	Santa Cruz Biotechnology Inc.	SC-50463
N-terminal Dok7 (nDok7)	Rabbit	Abgene	AP13568a
DOK7 (p-19)	Goat polyclonal	Santa Cruz Biotechnology Inc	SC-55168
Phosphorylated Dok7 (pDok)	Rabbit polyclonal	Santa Cruz Biotechnology	SC-68691
His-probe	Mouse monoclonal	Santa Cruz Biotechnology Inc	SC-53073
His-probe	Mouse monoclonal	Santa Cruz Biotechnology Inc	SC-8036
GAPDH	Mouse monoclonal	Santa Cruz Biotechnology Inc	SC-47724
GAPDH	Mouse monoclonal	Santa Cruz Biotechnology Inc	SC-32233

Table 2.5 Secondary antibodies

Antibody	Supplier	Catalogue number
Peroxidase conjugated Anti-mouse IgG	Sigma-Aldrich, Poole, Dorset, UK	A9044-2ML
Peroxidase conjugated Anti-rabbit IgG	Sigma-Aldrich, Poole, Dorset, UK	A9169

Appendix 4: Primers used in this study

Table 2.6. Sequences of primers used in this study

Gene	Primer	Sequence	Product size (bp)
DOK7	DOK7F1	5'-GAGTAGGTGGCTGGTGCT	129
	DOK7ZR1	5'-ACTGAACCTGACCGTACACAGATGTCCTCTAGCGTCA	
DOK7	DOK7F8	5'-TTCTACCAGACCCAAGTCC	409 (V1, V2, V3 and V4)
	DOK7R8	5'-CTGCTGGAGTAAGAGGAGTG	
DOK7	DOK7F9	5'-GCTGGTCTACAAGGACAAGT	479 (V1, V2 and V4)
	DOK7R9	5'-AGTCGAACAGGAAGCTGAT	
DOK7 Exp	DOK7exF2	5'-ATGACCGAGGCGGCGCTGGT	1512 (V1) 1501 (V2)
	DOK7exR4	5'-AGGAGGGGGGTTTACCTT	
DOK7 Rib 1	DOK7rib1F	5'-CTGCAGCTCCCCCTCGGCCGAGCTGATGAGTCCGTGAGG	74
	DOK7rib1R	5'ACTAGTACTGGGCTGGCGTCTTCTTCCTGTTTCGTCCTCACGGACT	
DOK7 Rib 2	DOK7rib2F	5'CTGCAGGCCCCTCCTGTGACGTGCTGGCTCTGATGAGTCCGTGAGGA	87
	DOK7rib	5'ACTAGTCACCGCATGGCCAGAGCAATCCTCGTCG	

	2R	TTTCGTCCTCACGGACT	
DOK7 V1	DOK7V1 F1	5’-CAGTGGAAGCTGTCTGACCT	90
	DOK7V1 ZR1	5’-ACTGAACCTGACCGTACAGCCAGCCCAGTACCCACA	
DOK7 V2	DOK7V2 F1	5’-ATGATGTCCTCGTCTTGGCC	132
	DOK7V2 ZR1	5’-ACTGAACCTGACCGTACAGAAGACGCCAGCCCCTGGT	
DOK7 V3	DOK7V3 F1	5’-AGGGCTTCATTCACCCCTG	95
	DOK7V3 ZR1	5’-ACTGAACCTGACCGTACAGTCACTGGCAGAGCGATG	
DOK7 V1	DOK7V1 F8	5’-AAAGTGACCCTGGGCTGG	595
	DOK7V1 R8	5’-GCCCAGTACCCACACCTG	
DOK7 V1	DOK7V1 F9	5’-GAGCTATTTTGAAAGTGACCCTG	609
	DOK7V1 R9	5’-CCAGCCCAGTACCCACAC	
DOK7 V2	DOK7V2 F8	5’-TTGAAAGTGACCCTGGGCTG	597
	DOK7V2	5’-GAAGACGCCAGCCCCTGGT	

	R8		
DOK7 V3	DOK7V3 F8	5’-AGGGCTTCATTCACCCCTG	229
	DOK7V3 R8	5’-CTCGGTCATCTTTCAGGGGA	
DOK7 V3	DOK7V3 F9	5’-TTCATTCACCCCTGGCCG	227
	DOK7V3 R9	5’-CTCCTCGGTCATCTTTCAGG	
pEF/His TOPO TA plasmid vector	T7F	TAATACGACTCACTATAGGG	
	BGHR	TAGAAGGCAGTCGAGG	
GAPDH	GAPDH F10	5’AGCTTGTCATCAATGGAAAT	593
	GAPDH R10	5’CTTCACCACCTTCTTGATGT	

Appendix 5: Breast cancer cell line data

The expression of DOK7 was examined in three breast cancer cell lines – MCF7, MDA-MB-231 and ZR751. DOK7 expression was seen in MCF7 and ZR751 cells but was not seen in MDA-MB-231, a poorly differentiated metastatic breast adenocarcinoma. DOK7 mRNA expression in breast cancer cell lines is shown in Figure a5.1 below.

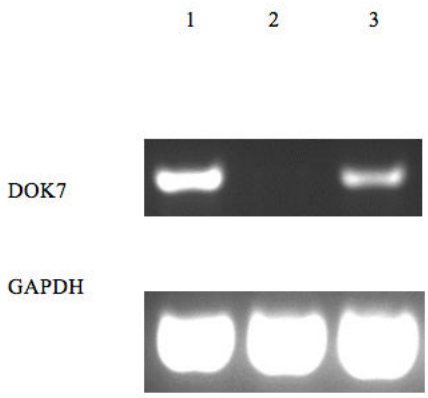

Legend: 1 = MCF7 WT, 2 = MDA-MB-231 WT, 3 = ZR751 WT

Figure a5.1 DOK7 mRNA expression in breast cancer cell lines

Appendix 6: Gastric clinical cohort data

A total of 322 samples were obtained from primary gastric cancer tissue and 183 samples were obtained from normal background gastric tissue. Two hundred and thirty of the patients were male and 92 were female. The median follow up period was 120 months.

The histopathological details of the gastric tumours included in this study are shown in Table a6.1.

Table a6.1. Histopathological details of the gastric tumours included in this study

			Number (%)
Histological type			
	Adenocarcinoma	Non-junctional	256 (79.5%)
		Junctional	51 (15.8%)
	Interstitial/GIST		5 (1.6%)
	Type/location unknown		10 (3.1%)
Grade	High		1 (0.3%)
	High-medium		6 (1.9%)
	Medium		62 (19.3%)
	Medium-low		82 (25.5%)
	Low		136 (42.2%)
	Grade unknown		35 (10.9%)
T stage	T1		16 (5.0%)
	T2		26 (8.1%)
	T3		41 (12.7%)
	T4		231 (71.7%)
	T stage unknown		8 (2.5%)
Overall stage	Stage I		25 (7.8%)
	Stage II		60 (18.6%)
	Stage III		219 (68.0%)
	Stage IV		9 (2.8%)
	Overall stage unknown		9 (2.8%)
Nodal status	Node negative (N0)		70 (21.7%)
	N1		48 (14.9%)
	N2		65 (20.2%)
	N3		133 (41.3%)
	Nodal status unknown		6 (1.9%)
Metastatic status	Distant metastases present		41 (12.7%)
	No distant metastases		280 (87.0%)
	Metastatic status unknown		1 (0.3%)

The expression of DOK7 is not significantly different in gastric tumours compared to normal gastric tissue (median DOK7 mRNA expression per 50μg of total cellular RNA was 2438 vs. 2126 respectively, $p = 0.6397$). Data is shown in Table a6.2.

Table a6.2. DOK7 expression in gastric cancer and normal gastric tissue

Tissue	Number of samples analysed	Median DOK7 mRNA expression per 50μg of total cellular RNA (copy number)
Normal gastric tissue	183	2126
Gastric tumours	322	2438

There was no significant difference in DOK7 mRNA expression between gastric cancer samples when analysed by T stage, nodal status, distant metastases, overall stage, location within the stomach, disease free status and overall survival.

Appendix 7: Colorectal gene array data

A search of gene array data identified a cohort of 585 colorectal cancer samples with 19 non-tumour tissues. Interestingly, analysis of this cohort revealed that DOK7 mRNA expression was increased in colorectal cancer compared to normal colorectal tissue (median DOK7 value 4.493 vs. 4.358, $p = 0.037$), the opposite to what was found in our dataset. Data is shown in Figure a7.1.

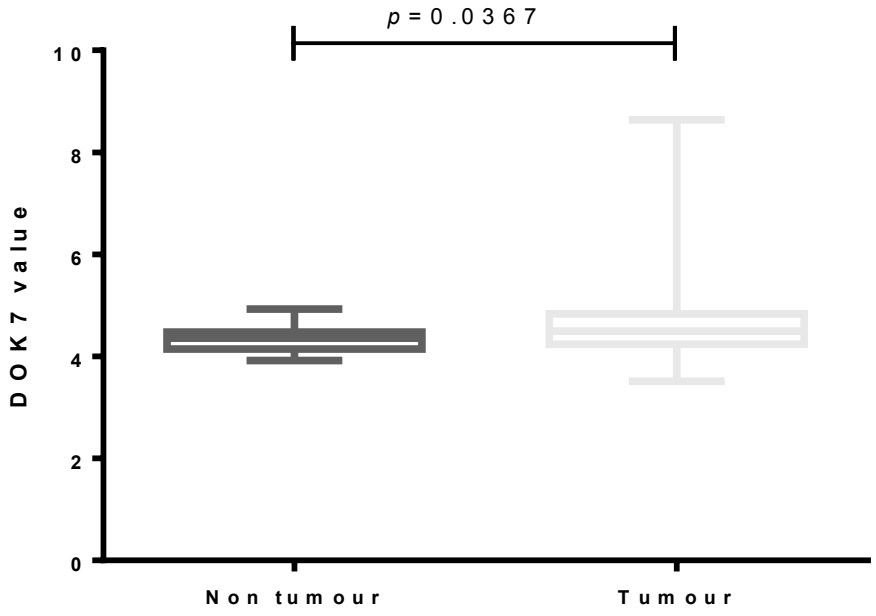

Figure a7.1 DOK7mRNA expression in colorectal cancer and normal colorectal tissue in a cohort of 585 colorectal cancer samples and 19 non-tumour tissues

Moreover, when this cohort of colorectal cancers were divided into subgroups representing different molecular subtypes as identified by Marisa *et al* and analysed for level of DOK7 expression there was a significant difference in DOK7 expression in different molecular subtypes ($p = 0.05$) (266). Data is shown in Figure a7.2.

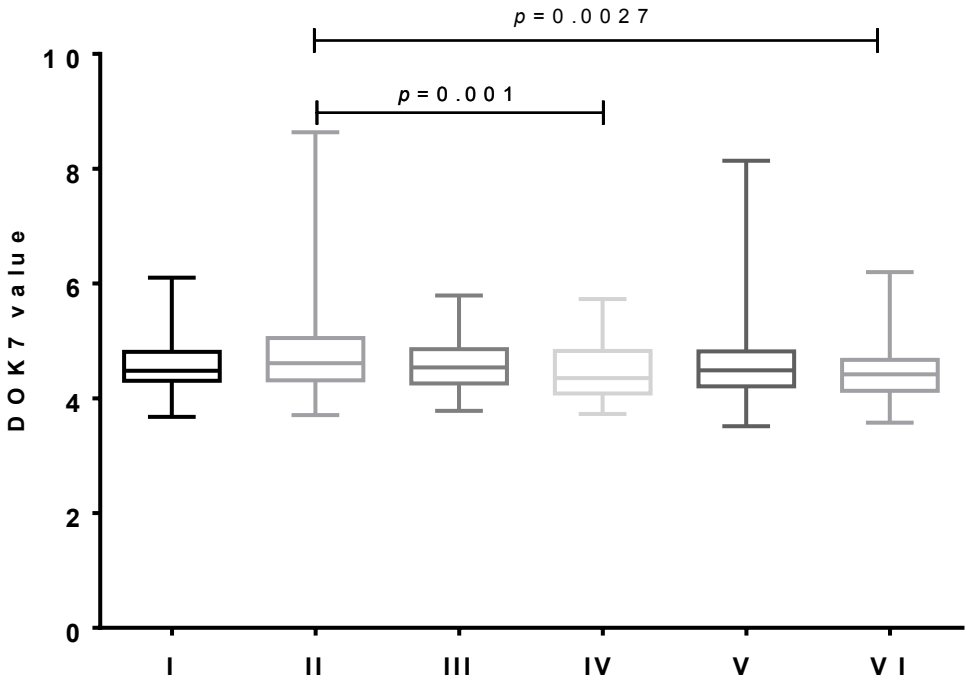

Figure a7.2 DOK7 mRNA expression in colorectal cancer in a cohort of 585 colorectal cancer samples analysed according to molecular subtypes

Again, in contrast to our findings, analysis of this cohort failed to show any association between DOK7 mRNA expression and T stage ($p = 0.616$) but showed that DOK7 mRNA expression was significantly reduced in node positive disease compared to node negative colorectal cancers (median DOK7 value 4.416 vs. 4.525, $p = 0.001$) and was significantly reduced in Stage III tumours compared to Stage II ($p < 0.01$) and Stage IV tumours ($p < 0.05$). In keeping with our findings, DOK7 mRNA expression was not affected by presence of distant metastases ($p = 0.171$). Finally, Kaplan-Meier survival analysis revealed that high DOK7 expression, defined by expression levels over the 75% centile, was associated with significantly poorer overall survival ($p = 0.033$). Data is shown in Figure a7.3.

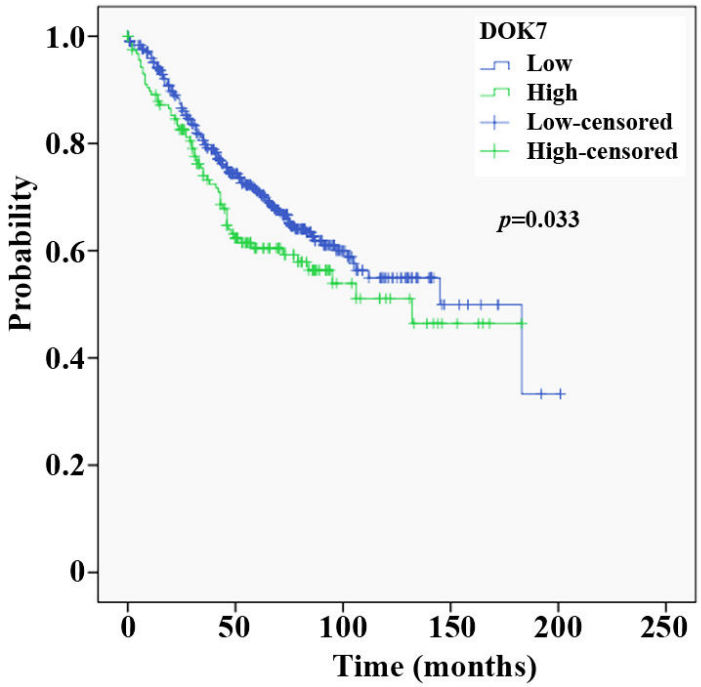

Figure a7.3 Kaplan-Meier survival curve showing overall survival time in months in high (over 75% centile) *vs.* low DOK7 expression in a cohort of 585 colorectal cancer samples.

References

1. Organisation WH. GLOBOCAN 2012 - cancer incidence and mortality worldwide 2014 [Available from: http://globocan.iarc.fr.
2. Ognjanovic S YJ, Maskarinec G, Le Marchand L. NAT2, meat consumption and colorectal cancer incidence: an ecological study among 27 countries. Cancer Causes Control. 2006;17(9):1175-82.
3. Parkin DM BF, Ferlay J, Pisani P. Global cancer statistics, 2002. CA Cancer J Clin. 2005;55(2):74-108.
4. UK CR. Bowel cancer incidence statistics [Available from: http://www.cancerresearchuk.org/health-professional/cancer-statistics/statistics-by-cancer-type/bowel-cancer/incidence - ref-2.
5. UK CR. Bowel cancer survival statistics 2015 [Available from: http://www.cancerresearchuk.org/health-professional/cancer-statistics/statistics-by-cancer-type/bowel-cancer/survival - heading-Three.
6. Uk CR. Bowel cancer statistics 2017 [Available from: http://www.cancerresearchuk.org/health-professional/cancer-statistics/statistics-by-cancer-type/bowel-cancer - collapseOne.
7. Brenner H BA, Foschi R, Hackl M, Larsen IK, Lemmens V, Mangone L, Francisci S and The EUROCARE Working Group. Progress in colorectal cancer survival in Europe from the late 1980s to the early 21st century: the EUROCARE study. Int J Cancer. 2012;131(7):1649-58.
8. Gatta G CR, Sant M, Bell CM, Coebergh JW, Damhuis RA, Faivre J, Martinez-Garcia C, Pawlega J, Ponz de Leon M, Pottier D, Raverdy N, Williams EM, Berrino F. Understanding variations in survival for colorectal cancer in Europe: a EUROCARE high resolution study. Gut. 2000;47(4):533-8.
9. Woodman CB GA, Scott N, Haboubi NY, Collins S. Are differences in stage at presentation a credible explanation for reported differences in the survival of patients with colorectal cancer in Europe? Br J Cancer. 2001;85(6):787-90.
10. Schreuders EH RA, Rabeneck L, Schoen RE, Sung JJY, Young GP, Kuipers EJ. Colorectal cancer screening: a global overview of existing programmes. Gut. 2015;64(10):1637-49.
11. Sunkara V HJ. The colorectal cancer mortality-to-incidence ratio as an indicator of global cancer screening and care. Cancer. 2015;121(10):1563-9.
12. England PH. Routes to Diagnosis 2006-2013 workbook. Public Health England; 2015.
13. Harris GJ SJ. Causes of late diagnosis in cases of colorectal cancer seen in a district general hospital over a 2-year period. Ann R Coll Surg Engl. 1998;80(4):246-8.
14. Mitchell ED P-SB, Macleod U. Risk factors for emergency presentation with lung and colorectal cancers: a systematic review. BMJ Open. 2015(5):e006965 doi:10.1136/bmjopen-2014-.
15. Foot C HT. How to improve cancer survival: Explaining England's relatively poor rates: Cancer Research UK/The King's Fund; 2011 [
16. Drake RL VA, Mitchell AWM. Gray's anatomy for students. 2nd ed. Philadelphia, USA: Elsevier; 2010.
17. Visovan II TM, Ciobanu L, Pascu O, Tantau A. Increasing prevalence of right-sided colonic adenomas in a high-volume endoscopy department in Romania: implications for colorectal cancer screening. J Gastrointestin Liver Dis. 2014;23(2):147-51.

18. Caldarella A CE, Messerini L, Paci E. Trends in colorectal incidence by anatomic subsite from 1985 to 2005: a population-based study. Int J Colorectal Dis. 2013;28(5):637-41.
19. Larsen IK BF. Trends in colorectal cancer incidence in Norway 1962-2006: an interpretation of the temporal patterns by anatomic subsite. International journal of cancer Journal international du cancer. 2010;126(3):721-32.
20. Park SY KB, Shin SJ, Lee SK, Kim TI, Kim WH. Proximal shift in the distribution of adenomatous polyps in Korea over the past ten years. Hepatogastroenterology. 2009;56(91-92):677-81.
21. Distler P HP. Are right- and left-sided colon neoplasms distinct tumours? Dig Dis. 1997;15(4-5):302-11.
22. Gervaz P BP, Morel P. Two colons-two cancers: paradigm shift and clinical implications. J Surg Oncol. 2004;88(4):261-6.
23. Li FY LM. Colorectal cancer, one entity or three. J Zhejiang Univ Sci B. 2009;10(3):219-29.
24. Midgley R KD. Colorectal cancer. Lancet. 1999;353(9150):391-9.
25. UK CR. Types of bowel cancer 2015 [Available from: http://www.cancerresearchuk.org/about-cancer/type/bowel-cancer/about/types-of-bowel-cancer.
26. Negri FV WA, Cunningham D, Normal AR, Chong G, Ross PJ. Mucinous histology predicts for reduced fluorouracil responsiveness and survival in advanced colorectal cancer. Annals of Oncology. 2005;16(8):1305-10.
27. (IARC) IAfRoC. Pathology and Genetics of Tumours of the Digestive System. In: Hamilton SR AL, editor. World Health Organisation Classification of Tumours. Lyon: IARC Press; 2000.
28. Peto R, Roe FJ, Lee PN, Levy L, Clack J. Cancer and ageing in mice and men. British journal of cancer. 1975;32(4):411-26.
29. Fearon ER, Vogelstein B. A genetic model for colorectal tumorigenesis. Cell. 1990;61(5):759-67.
30. van Es JH, Giles RH, Clevers HC. The many faces of the tumor suppressor gene APC. Experimental cell research. 2001;264(1):126-34.
31. Sorich MJ, Wiese MD, Rowland A, Kichenadasse G, McKinnon RA, Karapetis CS. Extended RAS mutations and anti-EGFR monoclonal antibody survival benefit in metastatic colorectal cancer: a meta-analysis of randomized controlled trials. Annals of oncology : official journal of the European Society for Medical Oncology / ESMO. 2014.
32. Finkel T, Cooper GM. Detection of a molecular complex between ras proteins and transferrin receptor. Cell. 1984;36(4):1115-21.
33. Bos JL. ras oncogenes in human cancer: a review. Cancer Res. 1989;49(17):4682-9.
34. Harvey JJ. AN UNIDENTIFIED VIRUS WHICH CAUSES THE RAPID PRODUCTION OF TUMOURS IN MICE. Nature. 1964;204:1104-5.
35. Almoguera C, Shibata D, Forrester K, Martin J, Arnheim N, Perucho M. Most human carcinomas of the exocrine pancreas contain mutant c-K-ras genes. Cell. 1988;53(4):549-54.
36. Rodenhuis S, Slebos RJ, Boot AJ, Evers SG, Mooi WJ, Wagenaar SS, et al. Incidence and possible clinical significance of K-ras oncogene activation in adenocarcinoma of the human lung. Cancer Res. 1988;48(20):5738-41.

37. Feinberg AP, Vogelstein B. Hypomethylation of ras oncogenes in primary human cancers. Biochemical and biophysical research communications. 1983;111(1):47-54.
38. Spandidos DA, Kerr IB. Elevated expression of the human ras oncogene family in premalignant and malignant tumours of the colorectum. British journal of cancer. 1984;49(6):681-8.
39. Bos JL, Fearon ER, Hamilton SR, Verlaan-de Vries M, van Boom JH, van der Eb AJ, et al. Prevalence of ras gene mutations in human colorectal cancers. Nature. 1987;327(6120):293-7.
40. Vogelstein B, Fearon ER, Hamilton SR, Kern SE, Preisinger AC, Leppert M, et al. Genetic alterations during colorectal-tumor development. The New England journal of medicine. 1988;319(9):525-32.
41. Galiatsatos P, Foulkes WD. Familial adenomatous polyposis. The American journal of gastroenterology. 2006;101(2):385-98.
42. Kern SE, Fearon ER, Tersmette KW, Enterline JP, Leppert M, Nakamura Y, et al. Clinical and pathological associations with allelic loss in colorectal carcinoma [corrected]. JAMA : the journal of the American Medical Association. 1989;261(21):3099-103.
43. Jacob S PF. DNA mismatch repair defects: role in colorectal carcinogenesis. Biochimie. 2002;84(1):27-47.
44. Fearnhead NS, Wilding JL, Bodmer WF. Genetics of colorectal cancer: hereditary aspects and overview of colorectal tumorigenesis. British medical bulletin. 2002;64:27-43.
45. Jasperson KW TT, Neklason DW, Burt RW. Hereditary and familial colon cancer. Gastroenterology. 2010;138(6):2044-58.
46. Fearnhead NS WJ, Bodmer WF. Genetics of colorectal cancer: hereditary aspects and overview of colorectal tumourigenesis. Brit Med Bull. 2002;64(1):27-43.
47. Gala M CD. Hereditary colon cancer syndromes. Semin Oncol. 2011;38(4):490-9.
48. Wehbi M CJ, Yang VW, Obideen K, Nam JW, Dacha S. Familial Adenomatous Polyposis: Medscape, WebMD; 2016 [Available from: http://emedicine.medscape.com/article/175377-overview - a6.
49. Support MC. Lynch syndrome 2015 [Available from: http://www.macmillan.org.uk/information-and-support/diagnosing/causes-and-risk-factors/genetic-testing-and-counselling/lynch-syndrome.html - tcm:9-20318.
50. Centre NNGEaD. Predisposition to Inherited Bowel Cancer. In: NHS, editor. 2012.
51. Munoz JC LL, Talavera F. Hereditary colorectal cancer: Medscape; 2016 [Available from: http://emedicine.medscape.com/article/188613-overview.
52. Parkin DM BL, Walker LC. The fraction of cancer attributable to lifestyle and environmental factors in the UK in 2010. Br J Cancer. 2011;105(S2):S77-S81.
53. Lutgens MW, van Oijen MG, van der Heijden GJ, Vleggaar FP, Siersema PD, Oldenburg B. Declining risk of colorectal cancer in inflammatory bowel disease: an updated meta-analysis of population-based cohort studies. Inflammatory bowel diseases. 2013;19(4):789-99.
54. Results of the first round of a demonstration pilot of screening for colorectal cancer in the United Kingdom. BMJ (Clinical research ed). 2004;329(7458):133.

55. Wales PH. Bowel Screening Wales Annual Statistical Report 2015-2016. Cardiff: Public Health Wales; 2017 January 2017.
56. Association of Coloproctology of Great Britain and Ireland CEUaTRCoS, The Health and Social Care Information Centre. National Bowel Cancer Audit Report 2014. Health & Social Care Information Centre; 2014.
57. Ireland TAoCoGBa. 2013 Bowel Cancer Audit Report 2013 [Available from: http://jcp.bmj.com/content/67/9/751.full.pdf+html.
58. (NICE) NIfHaCE. Colorectal cancer: diagnosis and management. 2014.
59. Mark-Christensen A BS, Iversen LH. Magnetic endoscopic imaging as an adjuvant to elective colonoscopy: a systematic review and meta-analysis of randomised controlled trials. Endoscopy. 2015;47(3):251-61.
60. von Wagner C GA, Halligan S, Smith S, Dadswell E, Lilford RJ, Morton D, Atkin W, Wardle J, SIGGAR Investigators. Patient acceptability and psychologic consequences of CT colonography compared with those of colonoscopy: results from a multicenter randomized controlled trial of symptomatic patients. Radiology. 2012;263(3):723-31.
61. Ng CS, Doyle TC, Pinto EM, Courtney HM, Bull RK, Prevost AT, et al. Evaluation of CT in identifying colorectal carcinoma in the frail and disabled patient. European radiology. 2002;12(12):2988-97.
62. Halligan S WK, Dadswell E, Kralj-Hans I, von Wagner C, Edwards R, Yao G, Kay C, Burling D, Faiz O, Teare J, Lilford RJ, Morton D, Wardle J, Atkin W, SIGGAR investigators. Computed tomographic colonography versus barium enema for diagnosis of colorectal cancer or large polyps in symptomatic patients (SIGGAR): a multicentre randomised trial. Lancet. 2013;381(9873):1185-93.
63. Radiologists BSoGaARBaTRCo. Guidance on the use of CT colonography for suspected colorectal cancer. London: The Royal College of Radiologists; 2014.
64. Morson BC. Cuthbert E Dukes OBE MD MSc FRCS FRCPath DPH -1890-1977. Annals of the Royal College of Surgeons of England. 1985;67(6):354.
65. Dukes CE, Bussey HJ. The spread of rectal cancer and its effect on prognosis. British journal of cancer. 1958;12(3):309-20.
66. Cancer AJCo. Colon and Rectum Cancer Staging 7th Edition [Available from: https://cancerstaging.org/references-tools/quickreferences/Documents/ColonMedium.pdf.
67. Excellence NIfHaC. Colorectal cancer: The diagnosis and management of colorectal cancer 2011 [Available from: http://www.nice.org.uk/guidance/CG131.
68. Radiology RCo. Recommendations for cross-sectional imaging in cancer management, 2nd Edition: Colon, rectum and anal canal cancer. London: Royal College of Radiologists; 2014 2014.
69. Xia Q LJ, Wu C, Song S, Tong L, Huang G, Feng Y, Jiang Y, Liu Y, Yin T, Ni Y. Prognostic significance of 18FDG PET/CT in colorectal cancer patients with liver metastases: a meta-analysis. Cancer Imaging. 2015;15(19).
70. Patkar V AD, Davidson T, Jones A, Fox J, Keshtgar M. Cancer multidisciplinary team meetings: Evidence, challenges, and the role of clinical decision support technology. International Journal of Breast Cancer. 2011;2011.
71. Dillman RO CS. Cancer patient survival improvement is correlated with the opening of a community cancer centre: comparisons with intramural and extramural benchmarks. Journal of Oncology Practice. 2005;1(3):84-92.

72. Bouvier AM BE, Danzon A et al. Place of multidisciplinary consulting meetings and clinical trials in the management of colorectal cancer in France in 2000. Gastroenterologie Clinique et Biologique. 2007;31(3):286-91.
73. (HSCIC) HaSCIC. National Bowel Cancer Audit Report 2015. 2015.
74. Excellence NIfHaC. Cetuximab for the first-ine treatment of metastatic colorectal cancer 2009 [Available from: http://www.nice.org.uk/Guidance/TA176.
75. Goldman R, Shields PG. Molecular epidemiology of breast cancer. In vivo (Athens, Greece). 1998;12(1):43-8.
76. Hanahan D, Weinberg RA. The hallmarks of cancer. Cell. 2000;100(1):57-70.
77. Hosooka T, Noguchi T, Nagai H, Horikawa T, Matozaki T, Ichihashi M, et al. Inhibition of the motility and growth of B16F10 mouse melanoma cells by dominant negative mutants of Dok-1. Molecular and cellular biology. 2001;21(16):5437-46.
78. Thiery JP AH, Huang RYJ, Nieto MA. Epithelial-mesenchymal transitions in development and disease. Cell. 2009;139(5):871-90.
79. Gentner B WA, Croner RS, Zeittraeger I, Wirtz RM, Roedel F, Dimmler A, Dorlaque L, Hohenberger W, Hahn EG, Brueckl WM. Differences in the gene expression profile of matrix metalloproteinases (MMPs) and their inhibitors (TIMPs) in primary colorectal tumours and their synchronous liver metastases. Anticancer Res. 2009;29(1):67-74.
80. Nakamura T. Structure and function of hepatocyte growth factor. Progress in growth factor research. 1991;3(1):67-85.
81. Tanigawa N AH, Matsumura M, Lu C, Kitaoka A, Matsuyama K, Muraoka R. Tumour angiogenesis and mode of metastasis in patients with colorectal cancer. Cancer Res. 1997;57(6):1043-6.
82. P C. Mechanisms of angiogenesis and arteriogenesis. Nat Med. 2000;6(4):389-95.
83. Ferrara N CH, Davis-Smyth T, Gerber HP, Nguyen TN, Peers D, Chisholm V, Hillan KJ, Schwall RH. Vascular endothelial growth factor is essential for corpus luteum angiogenesis. Nat Med. 1998;4(3):336-40.
84. Nissen NN PP, Koch AE, Volin MV, Gemelli RL, DiPietro LA. Vascular endothelial growth factor mediates angiogenic activity during the proliferative phase of wound healing. The American journal of pathology. 1998;152(6):1445-52.
85. D R. The crucial role of vascular permeability factor/vascular endothelial growth factor in angiogenesis: a historical review. Br J Haematol. 2005;128(3):303-9.
86. Roy H BS, Yla-Herttuala S. Biology of vascular endothelial growth factors. FEBS Lett. 2006;580(12):2879-87.
87. Risau W FI. Vasculogenesis. Annu Rev Cell Dev Biol. 1995;11:73-91.
88. Institute NC. FDA Approval for Bevacizumab 2017 [Available from: https://www.cancer.gov/about-cancer/treatment/drugs/fda-bevacizumab.
89. Yamanashi Y HO, Beeson D. Dok-7/MuSK signaling and a congenital myasthenic syndrome. Acta Myologica. 2008;27:25-9.
90. Berger AH, Niki M, Morotti A, Taylor BS, Socci ND, Viale A, et al. Identification of DOK genes as lung tumor suppressors. Nature genetics. 2010;42(3):216-23.

91. Ellis C, Moran M, McCormick F, Pawson T. Phosphorylation of GAP and GAP-associated proteins by transforming and mitogenic tyrosine kinases. Nature. 1990;343(6256):377-81.
92. PC Simister SF. Order and disorder in large multi-site docking proteins of the Gab family - implications for signaling complex formation and inhibitor design strategies. Mol Biosyst. 2012;8(1):33-46.
93. Jones N, Dumont DJ. Recruitment of Dok-R to the EGF receptor through its PTB domain is required for attenuation of Erk MAP kinase activation. Current biology : CB. 1999;9(18):1057-60.
94. Carpino N, Wisniewski D, Strife A, Marshak D, Kobayashi R, Stillman B, et al. p62(dok): a constitutively tyrosine-phosphorylated, GAP-associated protein in chronic myelogenous leukemia progenitor cells. Cell. 1997;88(2):197-204.
95. Yamanashi Y, Baltimore D. Identification of the Abl- and rasGAP-associated 62 kDa protein as a docking protein, Dok. Cell. 1997;88(2):205-11.
96. Turhan AG, Solary E, Vainchenker W, Dusanter-Fourt I. Molecular pathophysiology of chronic myelogenous leukemia. Hematology and cell therapy. 1998;40(5):217-21.
97. Di Cristofano A, Niki, M., Zhao, M., Karnell, FG., Clarkson, B., Pear, WS., Van Aelst, L., Pandolfi, PP. . p62(dok), a neagtive regulator of Ras and mitogen-activated protein kinase (MAPK) activity, opposes leukemogenesis by p210(bcr-abl). J Exp Med. 2001;194(3):275-84.
98. LE Marengere TP. Identification of residues in GTPase-activating protein Src homology 2 domains that control binding to tyrosine phosphorylated growth factor receptors and p62. The Journal of biological chemistry. 1992;267(32):22779-86.
99. K Shah KS. A chemical genetic screen for direct v-Src substrates reveals ordered assembly of a retrograde signaling pathway. Chem Biol. 2002;9(1):35-47.
100. R Hemming RA, K Badiani, K Wyant, G Arthur, RD Gietz, B Triggs-Raine. Human growth factor receptor bound 14 binds the activated insulin receptor and alters the insulin-stimulated tyrosine phosphorylation levels of multiple proteins. Biochem Cell Biol. 2001;79(1):21-32.
101. Di Cristofano A, Carpino N, Dunant N, Friedland G, Kobayashi R, Strife A, et al. Molecular cloning and characterization of p56dok-2 defines a new family of RasGAP-binding proteins. The Journal of biological chemistry. 1998;273(9):4827-30.
102. Cong F, Yuan B, Goff SP. Characterization of a novel member of the DOK family that binds and modulates Abl signaling. Molecular and cellular biology. 1999;19(12):8314-25.
103. Van Slyke P CM, Master Z, Kim H, Filmus J, Dumont DJ. Dok-R mediates attenuation of epidermal growth factor-dependent mitogen-activated protein kinase and Akt activation through processive recruitment of c-Src and Csk. Molecular and cellular biology. 2005;25(9):3831-41.
104. Grimm J, Sachs M, Britsch S, Di Cesare S, Schwarz-Romond T, Alitalo K, et al. Novel p62dok family members, dok-4 and dok-5, are substrates of the c-Ret receptor tyrosine kinase and mediate neuronal differentiation. The Journal of cell biology. 2001;154(2):345-54.

105. RJ Crowder HE, M Yang, EM Jr Johnson, J Milbrandt Dok-6, a novel p62 Dok family member, promotes Ret-mediated neurite outgrowth. The Journal of biological chemistry. 2004;279(40):42072-81.
106. Okada K IA, Okada M, Murata Y, Kakuta S, Jigami T, Kubo S, Shiraishi H, Eguchi K, Motomura M, Akiyama T, Iwakura Y, Higuchi O, Yamanashi Y. The muscle protein Dok-7 is essential for neuromuscular synaptogenesis. Science 2006;312(5781):1802-5.
107. A Inoue KS, Y Matsubara, K Okada, N Sato, Y Iwakura, O Higuchi, Y Yamanashi. Dok-7 activates the muscle receptor kinase MuSK and shapes synapse formation. Science Signalling. 2009;2(59):7.
108. Bergamin E HP, Burden SJ, Hubbard SR. The cytoplasmic adaptor protein Dok7 activates the receptor tyrosine kinase MuSK via dimerization. Mol Cell. 2010;39(1):100-9.
109. Tezuka T IA, Hoshi T, Weatherbee SD, Burgess RW, Ueta R, Yamanashi Y. The MuSK activator agrin has a separate role essential for postnatal maintenance of neuromuscular synapse. Proc Natl Acad Sci USA. 2014;111(46):16556-61.
110. Ohkawara B C-SM, Nakata T, Milone M, Asai N, Ito K, Ito M, Masuda A, Ito Y, Engel AG, Ohno K. LRP4 third beta-propeller domain mutations cause novel congenital myasthenia by compromising agrin-mediated MuSK signaling in a position-specific manner. Hum Mol Genet. 2014;23(7):1856-68.
111. Ingham RJ, Holgado-Madruga M, Siu C, Wong AJ, Gold MR. The Gab1 protein is a docking site for multiple proteins involved in signaling by the B cell antigen receptor. The Journal of biological chemistry. 1998;273(46):30630-7.
112. Songyang Z, Yamanashi Y, Liu D, Baltimore D. Domain-dependent function of the rasGAP-binding protein p62Dok in cell signaling. The Journal of biological chemistry. 2001;276(4):2459-65.
113. M Hirata TK, H Takeuchi, H Yagisawa. Pleckstrin homology domain as an inositol compound binding module. Jpn J Pharmacol. 1998;76(3):255-63.
114. Kobayashi R PR, Ashizawa S, Vykoukal J. Targeted mass spectrometric analysis of N-terminally truncated isoforms generated via alternative translation initiation. FEBS Lett. 2009;583(14):2441-5.
115. Bedirian A, Baldwin C, Abe J, Takano T, Lemay S. Pleckstrin homology and phosphotyrosine-binding domain-dependent membrane association and tyrosine phosphorylation of Dok-4, an inhibitory adapter molecule expressed in epithelial cells. The Journal of biological chemistry. 2004;279(18):19335-49.
116. Gerard A GM, Fos C, Guittard G, Compagno D, Galy A, Lemay S, Olive D, Nunes JA. Dok-4 is a novel negative regulator of T cell activation. Journal of immunology. 2009;182(12):7681-9.
117. A Kurotsuchi YM, M Jijiwa, K Kurokawa, Y Itoh, Y Kodama, T Kato, A Enomoto, N Asai, H Terasaki, M Takahashi. Analysis of DOK-6 function in downstream signaling of RET in human neuroblastoma cells. Cancer Science. 2010;101(5):1147-55.
118. Itoh S LS, Osawa M, Che W, Duan Y, Tompkins A, Brookes PS, Sheu SS, Abe J. Mitochondrial Dok-4 recruits Src kinase and regulates NF-kappaB activation in endothelial cells. The Journal of biological chemistry. 2005;280(28):26383-96.
119. Hamuro J HO, Okada K, Ueno M, Iemura S, Natsume T, Spearman H, Beeson D, Yamanashi Y. Mutations causing DOK7 congenital myasthenia ablate functional motifs in Dok-7. The Journal of biological chemistry. 2008;283(9):5518-24.

120. DA Calderwood YF, JM de Pereda, B Garcia-Alvarez, T Nakamoto, B Margolis, CJ McGlade, RC Liddington, MH Ginsberg. Integrin beta cytoplasmic domain interactions with phosphotyrosine-binding domains: a structural prototype for diversity in integrin signaling. Proceedings of the National Academy of Sciences of the United States of America. 2003;100(5):2272-7.
121. Y Zhang ZY, A Farooq, X Liu, C Lu, MM Zhou, C He. Molecular basis of distinct interactions between Dok1PTB domain and tyrosine-phosphorylated EGF receptor. J Mol Biol. 2004;343(4):1147-55.
122. Boulay I NJ, Duplay P. Phosphotyrosine binding-mediated oligomerization of downstream of tyrosine kinase (Dok)-1 and Dok-2 is involved in CD2-induced Dok phosphorylation. Journal of immunology. 2005;175(7):4483-9.
123. Dankort D JN, Jones N, Dumont DJ, Muller WJ. Multiple ErbB-2/Neu Phosphorylation Sites Mediate Transformation through Distinct Effector Proteins. The Journal of biological chemistry. 2001;276(42):38921-8.
124. Jones N, Dumont DJ. The Tek/Tie2 receptor signals through a novel Dok-related docking protein, Dok-R. Oncogene. 1998;17(9):1097-108.
125. Hooker E BC, Lemay S. New insights into Dok-4 PTB domain structure and function. Biochemical and biophysical research communications. 2012;427(1):67-72.
126. Zhang F FG, Wang C, Cao L, Yang HY, Wang GY, Chen YZ, He C. Detection of homo- or hetero-association of Doks by fluorescence resonance energy transfer in living cells. Mol Imaging Biol. 2009;11(3):188-94.
127. Shi L YJ, You Y, Yin B, Gong Y, Xu C, Qiang B, Yuan J, Liu Y, Peng X. Dok5 is substrate of TrkB and TrkC receptors and involved in neurotrophin induced MAPK activation. Cell Signal. 2006;18(11):1995-2003.
128. Li Wq SL, You Yg, Gong Yh, Yin B, Yuan Jg, Peng Xz. Downstream of tyrosine kinase/docking protein 6, as a novel substrate of tropomyosin-related kinase C receptor, is involved in neurotrophin 3-mediated neurite outgrowth in mouse cortex neurons. BMC Biol. 2010;18(8):86.
129. Hallock PT XC, Park TJ, Neubert TA, Curran T, Burden SJ. Dok-7 regulates neuromuscular synapse formation by recruiting Crk and Crk-L. Genes Dev. 2010;24(21):2451-61.
130. Lemay S, Davidson D, Latour S, Veillette A. Dok-3, a novel adapter molecule involved in the negative regulation of immunoreceptor signaling. Molecular and cellular biology. 2000;20(8):2743-54.
131. Kashige N, Carpino N, Kobayashi R. Tyrosine phosphorylation of p62dok by p210bcr-abl inhibits RasGAP activity. Proceedings of the National Academy of Sciences of the United States of America. 2000;97(5):2093-8.
132. MJ Wick LD, D Hu, P Langlais, F Liu. Insulin receptor-mediated p62dok tyrosine phosphorylation at residues 362 and 398 plays distinct roles for binding GTPase-activating protein and Nck and is essential for inhibiting insulin-stimulated activation of Ras and Akt. The Journal of biological chemistry. 2001;276(46):42843-50.
133. H Shinohara TY, Y Yamanashi. Dok-1 tyrosine residues at 336 and 340 are essential for the negative regulation of Ras-Erk signaling, but dispensible for rasGAP-binding. Genes Cells. 2004;9(6):601-7.
134. Z Master JT, A Bishnoi, SH Chen, JM Ebos, P Van Slyke, RS Kerbel, DJ Dumont. Dok-R binds c-Abl and regulates Abl kinase activity and mediates

cytoskeletal reorganization. The Journal of biological chemistry. 2003;278(32):30170-9.
135. NCBI. CRK v-crk avian sarcoma virus CT10 oncogene homolog [Homo sapiens (human)] Gene2015 [Available from: http://www.ncbi.nlm.nih.gov/gene?Db=gene&Cmd=ShowDetailView&TermToSearch=1398.
136. Mertens F HS, Mandahl N, Johansson B, Rydholm A, Biorklund A, Wennerberg J, Jonsson N, Mitelman F. Clonal chromosome aberrations in a keratoacanthoma and a basal cell papilloma. Cancer Genet Cytogenet. 1989;39(2):227-32.
137. Inaba T ON, Gotoh H, Murakami S, Oku N, Itoh K, Ura Y, Nakanishi S, Shimazaki C, Nakagawa M et al. Philadelphia chromosome positive precursor B-cell acute lymphoblastic leukemia with a translocation t(2;14)(p13;q32). Leukemia. 1991;5(8):719-22.
138. Nelms K, Snow AJ, Noben-Trauth K. Dok1 encoding p62(dok) maps to mouse chromosome 6 and human chromosome 2 in a region of translocation in chronic lymphocytic leukemia. Genomics. 1998;53(2):243-5.
139. Sonnier JA BG, Howard-Peebles PN, Rutledge J, Smith RG. Chromosomal translocation involving the immunoglobulin kappa-chain and heavy-chain loci in a child with chronic lymphocytic leukemia. N Engl J Med. 1983;8(309):590-4.
140. Kim DK KJ, Kim HT, Han KH, Shon DG. A specific chromosome aberration in a keratoacanthoma. Cancer Genet Cytogenet. 2003;142(1):70-2.
141. Okada K, Inoue A, Okada M, Murata Y, Kakuta S, Jigami T, et al. The muscle protein Dok-7 is essential for neuromuscular synaptogenesis. Science (New York, NY). 2006;312(5781):1802-5.
142. Niki M DCA, Zhao M, Honda H, Hirai H, Van Aelst L, Cordon-Cardo C, Pandolfi PP. Role of Dok-1 and Dok-2 in leukaemia suppression. J Exp Med. 2004;200(12):1689-95.
143. Yasuda T SM, Iwama A, Ishii A, Ebihara Y, Osawa M, Honda K, Shinohara H, Sudo K, Tsuji K, Nakauchi H, Iwakura Y, Hirai H, Oda H, Yamamoto T, Yamanashi Y. Role of Dok-1 and Dok-2 in myeloid homeostasis and suppression of leukaemia. J Exp Med. 2004;200(12):1681-7.
144. Mashima R HY, Tezuka T, Yamanashi Y. The roles of Dok family adapters in immunoreceptor signaling. Immunol Rev. 2009;232(1):273-85.
145. A Smith JW, CM Cheng, J Zhou, CS Weickert, CA Bondy. High-level expression of Dok-1 in neurons of the primate prefrontal cortex and hippocampus. J Neurosci Res. 2004;75(2):218-24.
146. Panzenbock B, Bartunek P, Mapara MY, Zenke M. Growth and differentiation of human stem cell factor/erythropoietin-dependent erythroid progenitor cells in vitro. Blood. 1998;92(10):3658-68.
147. Lock P, Casagranda F, Dunn AR. Independent SH2-binding sites mediate interaction of Dok-related protein with RasGTPase-activating protein and Nck. The Journal of biological chemistry. 1999;274(32):22775-84.
148. Favre C, Gerard A, Clauzier E, Pontarotti P, Olive D, Nunes JA. DOK4 and DOK5: new Dok-related genes expressed in human T cells. Genes and immunity. 2003;4(1):40-5.
149. Kurokawa K KK, Hasimoto M, Ito Y, Takahashi M. Cell signalling and gene expression mediated by RET tyrosine kinase. J Int Med. 2003;253:627-33.

150. D Cai SD-P, PA Melendez, J Lee, SE Shoelson. Two new substrates in insulin signaling, IRS/DOK4 and IRS6/DOK5. The Journal of biological chemistry. 2003;278(28):25323-30.
151. Lee CM JI, Noh KT, Lee JS, Park JW, Heo DR, Park JH, Chang JH, Choi IW, Kim JS, Shin YK, Park SJ, Han MK, Lee CG, Cho WK, Park YM. An essential regulatory role of downstream of kinase-1 in the ovalbumin-induced murine model of asthma. PLoS One. 2012;7(4):e34554.
152. Mashima R AS, Kajikawa S, Oda H, Nakae S, Yamanashi Y. Dok adaptors play anti-inflammatory roles in pulmonary homeostasis. Genes Cells. 2013;18(1):56-65.
153. T Hiragun ZP, MA Beaven. Dexamethasone up-regulates the inhibitory adaptor protein Dok-1 and suppresses downstream activation of the mitogen-activated protein kinase pathway in antigen-stimulated RBL-2H3 mast cells. Mol Pharmacol. 2005;67(3):598-603.
154. J Abramson GR, I Pecht. Dok protein family members are involved in signaling mediated by the type 1 Fcepsilon receptor. European journal of immunology. 2003;33(1):85-91.
155. Saxon A ZD, Zhang K, Allen LC, Kepley CL. Genetically engineered negative signaling molecules in the immunomodulation of allergic diseases. Curr Opin Allergy Clin Immunol. 2004;4(6):563-8.
156. Kawamata A IA, Miyajima D, Hemmi H, Mashima R, Hayata T, Ezura Y, Amagasa T, Yamanashi Y. Dok-1 and Dok-2 deficiency induces osteopenia via activation of osteoclasts. J Cell Physiol. 2011;226(12):3087-93.
157. Garcia A SY, Antrobus R, Hughes CE, Dwek RA, Watson SP, Zitzmann N. A global proteomics approach identifies novel phosphorylated signaling proteins in GPVI-activated platelets: involvement of G6f, a novel platelet Grb2-binding membrane adapter. Proteomics. 2006;6(19):5332-43.
158. Senis YA AR, Severin S, Parguina AF, Rosa I , Zitzmann N, Watson SP, Garcia A. Proteomic analysis of integrin alphaIIbbeta3 outside-in signaling reveals Src-kinase-independent phosphorylation of Dok-1 and Dok-3 leading to SHIP-1 interactions. J Thromb Haemost. 2009;7(10):1718-26.
159. Parguina AF AJ, Rosa I, Velez P, Gonzalez-Lopez MJ, Guitian E, Eble JA, Loza MI, Garcia A. A detailed proteomic analysis of rhodocytin-activated platelets reveals novel clues on the CLEC-2 signalosome: implications for CLEC-2 signaling regulation. Blood. 2012;120(26):e117-26.
160. Hughan SC SC, Schoenwaelder SM, Sturgeon S, Alwis I, Yuan Y, McFadyen JD, Westein E, Goddard D, Ono A, Yamanashi Y, Nesbitt WS, Jackson SP. Dok-2 adaptor protein regulates the shear-dependent adhesive function of platelet integrin alphaIIbbeta3 in mice. The Journal of biological chemistry. 2014;289(8):5051-60.
161. Biswas R SD, Stanley ER. Drosophila Dok is required for embryonic dorsal closure. Development. 2006;133(2):217-27.
162. Igarashi T, Osuga U, Tsutsumi O, Momoeda M, Ando K, Matsumi H, et al. Expression of Ah receptor and dioxin-related genes in human uterine endometrium in women with or without endometriosis. Endocrine journal. 1999;46(6):765-72.
163. Ohno K. Genetic defects and disorders at the neuromuscular junction. 2011. 2011;63(7):669-78.

164. K O. Congenital myasthenic syndromes. Rinsho Shinkeigaku. 2012;52(11):1159-61.
165. Abicht A MJ, Lochmuller H. Congenital Myasthenic Syndromes Seattle, WA: University of Washington; 1993-2015 [
166. Beeson D HO, Palace J, Cossins J, Spearman H, Maxwell S, Newsom-Davis J, Burke G, Fawcett P, Motomura M, Muller JS, Lochmuller H, Slater C, Vincent A, Yamanashi Y. Dok-7 mutations underlie a neuromuscular junction synaptopathy. Science. 2006;313(5795):1975-8.
167. Palace J LD, Newsom-Davis J, Cossins J, Maxwell S, Kennett R, Jayawant S, Yamanashi Y, Beeson D. Clinical features of the DOK7 neuromuscular junction synaptopathy. Brain. 2007;130(Pt 6):1507-15.
168. Muller JS HA, Vilchez JJ, Colomer J, Bachinski LL, Mihaylova V, Santos M, Schara U, Deschauer M, Shevell M, Poulin C, Dias A, Soudo A, Hietala M, Aarimaa T, Krahe R, Karcagi V, Huebner A, Beeson D, Abicht A, Lochmuller H. Phenotypical spectrum of DOK7 mutations in congenital myasthenic syndromes. Brain 2007;130(Pt 6):1497-506.
169. Anderson JA NJ, Bowe C, McDonald C, Richman DP, Wollmann RL, Maselli RA. Variable phenotypes associated with mutations in DOK7. Muscle Nerve. 2008;37(4):448-56.
170. Selcen D MM, Shen XM, Harper CM, Stans AA, Wieben ED, Engel AG. Dok-7 myasthenia: phenotyic and molecular genetic studies in 16 patients. Ann Neurol. 2008;64(1):71-87.
171. CR S. Structural factors influencing the efficacy of neuromuscular transmission. Ann N Y Acad Sci. 2008;1132:1-12.
172. Lashley D PJ, Jayawant S, Robb S, Beeson D. Ephedrine treatment in congenital myasthenic syndrome due to mutations in DOK7. Neurology. 2010;74(19):1517-23.
173. Lorenzoni PJ SR, Kay CS, Filla L, Miranda AP, Pinheiro JM, Chaouch A, Lochmuller H, Werneck LC. Salbutamol therapy in congenital myasthenic syndrome due to DOK7 mutation. J Neurol Sci. 2013;331(1-2):155-7.
174. Liewluck T SD, Engel AG. Beneficial effects of albuterol in congenital endplate acetylcholinesterase deficiency and Dok-7 myasthenia. Muscle Nerve. 2011;44(5):789-94.
175. Arimura S OT, Tezuka T, Chiyo T, Kasahara Y, Yoshimura T, Motomura M, Yoshida N, Beeson D, Takeda S, Yamanashi Y. Neuromuscular disease. DOK7 gene therapy benefits mouse models of diseases characterized by defects in the neuromuscular junction. Science. 2014;345(6203):1505-8.
176. Jang W, Hua A, Spilson SV, Miller W, Roe BA, Meisler MH. Comparative sequence of human and mouse BAC clones from the mnd2 region of chromosome 2p13. Genome research. 1999;9(1):53-61.
177. Liang X HM, Veach D, Wisniewski D, Clarkson B, Resh MD, Pope RM. Quantification of change in phosphorylation of BCR-ABl kinase and its substrates in response to Imatinib treatment in human chronic myelogenous leukaemia cells. Proteomics. 2006;6(16):4554-64.
178. T H. The Croonian Lecture 1997. The phosporylation of proteins on tyrosine: its role in cell growth and disease. Philos Trans R Soc Lond B Biol Sci. 1998;353(1368):583-605.
179. Fiorini M AM, Fiorentino L, Sala G, Segatto O. Negative regulation of receptor tyrosine kinase signals. FEBS Lett. 2001;490(3):132-41.

180. Lemmon MA SJ. Cell signaling by receptor-tyrosine kinases. Cell. 2010;141(7):1117-34.
181. Blume-Jensen P HT. Oncogenic kinase signalling. Nature. 2001;411(6835):355-65.
182. Ullrich A SJ. Signal transduction by receptors with tyrosine kinase activity. Cell. 1990;61(2):203-12.
183. Robinson DR WY, Lin SF. The protein tyrosine kinase family of the human genome. Oncogene. 2000;19(49):5548-57.
184. Hlavacek WS FJ, Blinov ML, Perelson AS, Goldstein B. The complexity of complexes in signal transduction. Biotechnol Bioeng. 2003;84(7):783-94.
185. Pawson T SJ. Signaling through scaffold, anchoring, and adaptor proteins. Science. 1997;278(5346):2075-80.
186. Mirone G SA, Marfe G. Signaling mechanisms of resistance to EGFR- and Anti-Angiogenic Inhibitors cancer. Crit Rev Oncol Haematol. 2015;S1040-8428(15):30027-5.
187. CL A. The epidermal growth factor receptor: from mutant oncogene in nonhuman cancers to therapeutic target in human neoplasia. J Clin Oncol. 2001;19(18 Suppl):32S-40S.
188. Pritchard CC GW. Colorectal cancer molecular biology moves into clinical practice. Gut. 2011;60(1):116-29.
189. J D. Targeting RAS signalling pathways in cancer therapy. Nat Rev Cancer. 2003;3(1):11-22.
190. JA E. Targeting PI3K signalling in cancer: opportunities, challenges and limitations. Nat Rev Cancer. 2009;9(8):550-62.
191. Parsons DW WT, Samuels Y, Bardelli A, Cummins JM, DeLong L, Silliman N, Ptak J, Szabo S, Willson JK, Markowitz S, Kinzler KW, Vogelstein B, Lengauer C, Velculescu VE. Colorectal cancer: mutations in a signalling pathway. Nature. 2005;436(7052):792.
192. Samuels Y WZ, Bardelli A, Silliman N, Ptak J, Szabo S, Yan H, Gazdar A, Powell SM, Riggins GJ, Willson JK, Markowitz S, Kinzler KW, Vogelstein B, Velculescu VE. High frequency of mutations of the PIK3CA gene in human cancers. Science. 2004;304(5670):554.
193. Danielsen SA LG, Bjornslett M, Meling GI, Rognum TO, Heim S, Lothe RA. Novel mutations of the suppressor gene PTEN in colorectal carcinomas stratified by microsatellite instability- and TP53 mutation- status. Hum Mutat. 2008;29(11):E252-62.
194. Celis-Gutierrez J BM, Walzer T, Pandolfi PP, Jonjic S, Olive D, Dalod M, Vivier E, Nunes JA. Dok1 and Dok2 proteins regulate natural killer cell development and function. The EMBO journal. 2014;33(17):1928-40.
195. S Suzu MT-D, K Nomaguchi, M Yamada, H Hayasawa, F Kimura, K Motoyoshi. p56(dok-2) as a cytokine-inducible inhibitor of cell proliferation and signal transduction. The EMBO journal. 2000;19(19):5114-22.
196. Holland SJ, Gale NW, Gish GD, Roth RA, Songyang Z, Cantley LC, et al. Juxtamembrane tyrosine residues couple the Eph family receptor EphB2/Nuk to specific SH2 domain proteins in neuronal cells. The EMBO journal. 1997;16(13):3877-88.
197. Bhat A, Johnson KJ, Oda T, Corbin AS, Druker BJ. Interactions of p62(dok) with p210(bcr-abl) and Bcr-Abl-associated proteins. The Journal of biological chemistry. 1998;273(48):32360-8.

198. Noguchi T, Matozaki T, Inagaki K, Tsuda M, Fukunaga K, Kitamura Y, et al. Tyrosine phosphorylation of p62(Dok) induced by cell adhesion and insulin: possible role in cell migration. The EMBO journal. 1999;18(7):1748-60.
199. MS Boguski FM. Proteins regulating Ras and its relatives. Nature. 1993;366(6456):643-54.
200. Downward J. Control of ras activation. Cancer Surv. 1996;27:87-100.
201. M Zhao AS, Y Qin, A Di Cristofano, PP Pandolfi, L Van Aelst. Phosphoinositide 3-kinase-dependent membrane recruitment of p62(dok) is essential for its negative effect on mitogen-activated protein (MAP) kinase activation. J Exp Med. 2001;194(3):265-74.
202. JA Janas LVA. Oncogenic tyrosine kinases target Dok-1 for ubiquitin-mediated proteasomal degradation to promote cell transformation. Molecular and cellular biology. 2011;31(13):2552-65.
203. Honma M HO, Shirakata M, Yasuda T, Shibuya H, Iemura S, Natsume T, Yamanashi Y. Dok-3 sequesters Grb2 and inhibits the Ras-Erk pathway downstream of protein-tyrosine kinases. Genes Cells. 2006;11(2):143-51.
204. Latour S GG, Helgason CD, Humphries RK, Pawson T, Veillette A. Regulation of SLAM-mediated signal transduction by SAP, the X-linked lymphoproliferative gene product. Nature immunology. 2001;2(8):681-90.
205. Lemay S DD, Latour S, Veillette A. Dok-3, a novel adapter molecule involved in the negative regulation of immunoreceptor signalling. Molecular and cellular biology. 2000;20(8):2743-54.
206. Ott VL TI, Niki M, Pandolfi PP, Cambier JC. Downstream of kinase, p62(dok), is a mediator of Fc gamma IIB inhibition of Fc epsilon RI signalling. Journal of immunology. 2002;168(9):4430-9.
207. Sattler M, Verma S, Pride YB, Salgia R, Rohrschneider LR, Griffin JD. SHIP1, an SH2 domain containing polyinositol-5-phosphatase, regulates migration through two critical tyrosine residues and forms a novel signaling complex with DOK1 and CRKL. The Journal of biological chemistry. 2001;276(4):2451-8.
208. Downer EJ JD, Lynch MA. Differential role of Dok1 and Dok2 in TLR2-induced inflammatory signaling in glia. Mol Cell Neurosci. 2013;56:148-58.
209. Rijkers ES dRT, Buitenhuis M, Veninga H, Hoek RM, Meyaard L. Ligation of CD200R by CD200 is not required for normal murine myelopoiesis. Eur J Haematol. 2007;79(5):410-6.
210. Z Master NJ, J Tran, J Jones, RS Kerbel, DJ Dumont. Dok-R plays a pivotal role in angiopoietin-1-dependent cell migration through recruitment and activation of Pak. The EMBO journal. 2001;20(21):5919-28.
211. N Jones SC, C Sturk, Z Master, J Tran, RS Kerbel, DJ Dumont. A unique autophosphorylation site on Tie2/Tek mediates Dok-R phosphotyrosine binding domain binding and function. Molecular and cellular biology. 2003;23(8):2658-68.
212. A Garcia SP, S Hughan, TW Anderson, CJ Brock, AC Pearce, RA Dwek, SP Watson, HF Hebestreit, N Zitzmann. Differential proteome analysis of TRAP-activated platelets: involvement of DOK-2 and phosphorylation of RGS proteins. Blood. 2004;103(6):2088-95.
213. Ela Shai IR, Andres F Parguina, Sarah Motahedeh, David Varon, Angel Garcia. Comparative analysis of platelet-derived microparticles reveals differences in their amount and proteome depending on the platelet stimulus. Journal of Proteomics. 2012;76:287-96.

214. Varon D SE. Role of platelet-derived microparticles in angiogenesisand tumour progression. Discov Med. 2009;8(43):237-41.
215. NCBI. Myc myelocytomatosis ongogene [Mus musculus (house mouse)] 2015 [Available from: http://www.ncbi.nlm.nih.gov/gene/17869.
216. Zhao M JJ, Niki M, Pandolfi PP, Van Aelst L. Dok-1 independently attenuates Ras/mitogen-activated protein kinase and Src/c-myc pathways to inhibit platelet-derived growth factor-induced mitogenesis. Molecular and cellular biology. 2006;26(7):2479-89.
217. Yoshida K, Yamashita Y, Miyazato A, Ohya K, Kitanaka A, Ikeda U, et al. Mediation by the protein-tyrosine kinase Tec of signaling between the B cell antigen receptor and Dok-1. The Journal of biological chemistry. 2000;275(32):24945-52.
218. N Yamakawa KT, H Sugino. The rasGAP-binding protein, Dok-1, mediates activin signaling via serine/threonine kinase receptors. The EMBO journal. 2002;21(7):1684-94.
219. Titz B LT, Komisopoulou E, Chen SS, Rubbi L, Graeber TG. The proximal signaling network of the BCR-ABL1 oncogene shows a modular organisation. Oncogene. 2010;29(44):5895-910.
220. Uchida M EA, Fukuda T, Kurokawa K, Maeda K, Kodama Y, Asai N, Hasegawa T, Shimono Y, Jijiwa M, Ichihara M, Murakumo Y, Takahashi M. Dok-4 regulates GDNF-dependent neurite outgrowth through downstream activation of Rap1 and mitogen-activated protein kinase. J Cell Sci. 2006;119(Pt 15):3067-77.
221. Baldwin C BA, Li H, Takano T, Lemay S. Identification of Dok-4b, a Dok-4 splice variant with enhanced inhibitory properties. Biochemical and biophysical research communications. 2007;354(3):783-8.
222. Wen J XQ, Wang C, Liu W, Chen Y, Gao Y, Gong Y, Yin B, Ke Y, Qiang B, Yuan J, Peng X. Dok-5 is involved in cardiomyocyte differentiation through PKB/FOXO3a pathway. J Mol Cell Cardiol. 2009;47(6):761-9.
223. Pan Y ZJ, Liu W, Shu P, Yin B, Yuan J, Qiang B, Peng X. Dok5 is involved in the signaling pathway of neurotrophin-3 against TrkC-induced apoptosis. Neurosci Lett. 2013;553(46-51).
224. Losing M GI, Manno B, Oellerich T, Schnyder T, Bohnenberger H, Stork B, Urlaub H, Batista FD, Wienands J, Engelke M. The Dok-3/Grb2 protein signal module attenuates Lyn kinase-dependent activation of Syk kinase in B cell antigen receptor microclusters. The Journal of biological chemistry. 2013;288(4):2303-13.
225. Nishizumi H TI, Yamanashi Y, Kitamura D, Ilic D, Mori S, Watanabe T, Yamamoto T. Impaired proliferation of peripheral B cells and indication of autoimmune disease in lyn-deficient mice. Immunity. 1995;3(5):549-60.
226. Hibbs ML TD, Armes J, Grail D, Hodgson G, Maglitto R, Stacker SA, Dunn AR. Multiple defects in the immune system of Lyn-deficient mice, culminating in autoimmune disease. Cell. 1995;83(2):301-11.
227. Chan VW MF, Soriano P, DeFranco AL, Lowell CA. Characterisation of the B lymphocyte populations in Lyn-deficient mice and the role of Lyn in signal initiation and down-regulation. Immunity. 1997;7(1):69-81.
228. AM Brauweiler IT, JC Cambier. Bilevel control of B-cell activation by the inositol 5-phosphatase SHIP. Immunol Rev. 2000;176:69-74.

229. Yang WC, Ghiotto M, Barbarat B, Olive D. The role of Tec protein-tyrosine kinase in T cell signaling. The Journal of biological chemistry. 1999;274(2):607-17.
230. Wu L BK, Shen SH. CD45 recruits adapter protein DOK-1 and negatively regulates JAK-STAT signaling in hematopoietic cells. Mol Immunol. 2009;46(11-12):2167-77.
231. S Okabe SF, YJ Kim, M Niki, LM Pelus, K Ohyashiki, PP Pandolfi, HE Broxmeyer. Stromal cell-derived factor-1alpha/CXCL12-induced chemotaxis of T cells involves activation of the RasGAP-associated docking protein p62Dok-1. Blood. 2005;105(2):474-80.
232. Kashiwada M CG, McKeag L, Rouse T, Showalter BM, Al-Alem U, Niki M, Pandolfi PP, Field EH, Rothman PB. Downstream of tyrosine kinases-1 and Src homology 2-containing inositol 5'-phosphatase are required for regulation of CD4+CD25+ T cell development. Journal of immunology. 2006;176(7):3958-65.
233. Stork B NK, Goldbeck I, Alers S, Kahne T, Naumann M, Engelke M, Wienands J. Subcellular localization of Grb2 by the adapter protein Dok-3 restricts the intensity of Ca2+ signaling in B cells. The EMBO journal. 2007;26(4):1140-9.
234. JD Robson DD, A Veillette. Inhibition of the Jun N-terminal protein kinase pathway by SHIP-1, a lipid phosphatase that interacts with the adaptor molecule Dok-3. Molecular and cellular biology. 2004;24(6):2332-43.
235. Neumann K OT, Heine I, Urlaub H, Engelke M. Fc gamma receptor IIb modulates the molecular Grb2 interaction network in activated B cells. Cell Signal. 2011;23(5):893-900.
236. Ou X XS, Li YF, Lam KP. Adaptor protein DOK3 promotoes plasma cell differentiation by regulating the expression of programmed cell death 1 ligands. Proceedings of the National Academy of Sciences of the United States of America. 2014;111(31):11431-6.
237. Engelke M EN, Dittmann K, Stork B, Wienands J. Ca(2+) signalling in antigen receptor-activated B lymphocytes. Immunol Rev. 2007;218:235-46.
238. Niiro H MA, Kurosaki T, Clark EA. The B lymphocyte adaptor molecule of 32kD (Bam32) regulates B cell antigen receptor signalling and cell survival. J Exp Med. 2002;195(1):143-9.
239. T Schnyder AC, C Feest, NE Harwood, T Oellerich, H Urlaub, M Engelke, J Wienands, A Bruckbauer, FD Batista. B cell receptor-mediated antigen gathering requires ubiquitin ligase Cbl and adaptors Grb2 and Dok-3 to recruit dynein to the signaling microcluster. Immunity. 2011;34(6):905-18.
240. Ng CH XS, Lam KP. Dok-3 plays a nonredundant role in negative regulation of B-cell activation. Blood. 2007;110(1):259-66.
241. JG Nemorin PL, G Berube, P Duplay. p62dok negatively regulates CD2 signaling in Jurkat cells. Journal of immunology. 2001;166(7):4408-15.
242. MP Martelli JB, M Bu, BE Bierer. T cell regulation of p62(dok) (DOK-1) association with Crk-L. The Journal of biological chemistry. 2001;276(49):45654-61.
243. Dong S CB, Foulon E, Dufour E, Veillette A, Acuto O, Michel F. T cell receptor for antigen induces linker for activation of T cell-dependent activation of a negative signaling complex involving Dok-2, SHIP-1, and Grb-2. J Exp Med. 2006;203(11):2509-18.

244. Yasuda T BK, Hino A, Honda K, Inoue A, Shirakata M, Osawa M, Tamura T, Nariuchi H, Oda H, Yamamoto T, Yamanashi Y. Dok-1 and Dok-2 are negative regulators of T cell receptor signaling. Int Immunol. 2007;19(4):487-95.
245. R Gugasyan CQ, ST I, D Grail, AM Verhagen, A Roberts, T Kitamura, AR Dunn, P Lock. Dok-related protein negatively regulates T cell development via its RasGTPase-activating protein and Nck docking sites. The Journal of cell biology. 2002;158(1):115-25.
246. A Gerard CF, F Garcon, JG Nemorin, P Duplay, S Pastor, Y Collette, D Olive, JA Nunes. Functional interaction of RasGAP-binding proteins Dok-1 and Dok-2 with the Tec protein tyrosine kinase. Oncogene. 2004;23(8):1594-8.
247. TB van Dijk EvDA, MP Amelsvoort, H Mano, B Lowenberg, M von Lindern. Stem cell factor induces phosphatidylinositol 3'-kinase-dependent Lyn/Tec/Dok-1 complex formation in haematopoietic cells. Blood. 2000;96(10):3406-13.
248. Liang X WD, Strife A, Shivakrupa, Clarkson B, Resh MD. Phosphatidylinositol 3-kinase and Src family kinases are required for phosphorylation and membrane recruitment of Dok-1 in c-Kit signalling. The Journal of biological chemistry. 2002;277(16):13732-8.
249. Guittard G GA, Dupuis-Coronas S, Tronchere H, Mortier E, Favre C, Olive D, Zimmermann P, Payrastre B, Nunes JA. Cutting edge: Dok-1 and Dok-2 adaptor molecules are regulated by phosphatidylinositol 5-phosphate production in T cells. Journal of immunology. 2009;182(7):3974-8.
250. Rider DA HC, de Ridder R, Schuurman J, Favre C, Cooper JC, Walker S, Baadsgaard O, Marschner S, vandeWinkel JG, Cambier J, Parren PW, Alexander DR A human CD4 monoclonal antibody for the treatment of T-cell lymphoma combines inhibition of T-cell signaling by a dual mechanism with potent Fc-dependent effector activity. Cancer Res. 2007;67(20):9945-53.
251. Inoue A YT, Yamamoto T, Yamanashi Y. Dok-1 is a positive regulator of IL-4 signaling and IgE response. J Biochem. 2007;142(2):257-63.
252. H Alvarez de Celis CG, A Descoteaux, P Duplay. Dok proteins are recruited to the phagosome and degraded in a GP63-dependent manner during Leishmania major infection. Microbes Infect. 2015;17(4):285-94.
253. Shinohara H IA, Toyama-Sorimachi N, Nagai Y, Yasuda T, Suzuki H, Horai R, Iwakura Y, Yamamoto T, Karasuyama H, Miyake K, Yamanashi Y. Dok-1 and Dok-2 are negative regulators of lipopolysaccharide-induced signaling. J Exp Med. 2005;201(3):333-9.
254. Kim SS LK, Chin CS, Ng SK, Pereira NA, Xu S, Lam KP. DOK3 is required for IFN-beta production by enabling TRAF3/TBK1 complex formation and IRF3 activation. Journal of immunology. 2014;193(2):840-8.
255. MO Nowicki PP, T Fischer, G Hess, T Pawlowski, T Skorski. Chronic myelogenous leukaemia molecular signature. Oncogene. 2003;22:3952-63.
256. Chitale D GY, Taylor BS, Broderick S, Brennan C, Somwar R, Golas B, Wang L, Motoi N, Szoke J, Reinersman JM, Major J, Sander C, Seshan VE, Zakowski MF, Rusch V, Pao W, Gerald W, Ladanyi M. An integrated genomic analysis of lung cancer reveals loss of DUSP4 in EGFR-mutant tumours. Oncogene. 2009;28(31):2773-83.
257. Ghanem T, Bracken J, Kasem A, Jiang WG, Mokbel K. mRNA expression of DOK1-6 in human breast cancer. World journal of clinical oncology. 2014;5(2):156-63.

258. Heyn H CF, Gomez A, Ferreira HJ, Bell JT, Sayols S, Ward K, Stefansson OA, Moran S, Sandoval J, Eyfjord JE, Spector TD, Esteller M. DNA methylation profiling in breast cancer discordant identical twins identifies DOK7 as novel epigenetic biomarker. Carcinogenesis. 2013;34(1):102-8.
259. Wen X ZM, Guo Y, Zhu Y, Li H, Zhang L, Yu L, Wang X, Peng X. Expression and significance of DOK2 in colorectal cancer. Oncol Lett. 2015;9(1):241-4.
260. C Huang YS, J Jia, L Chen. Identification of melanoma biomarkers based on network modules by integrating the human signalling network with microarrays. J Cancer Res Ther. 2014;10 Suppl:C114-24.
261. Mashima R HK, Yang Y, Morita Y, Inoue A, Arimura S, Nishina H, Ema H, Nakauchi H, Seed B, Oda H, Yamanashi Y. Mice lacking Dok-1, Dok-2, and Dok-3 succumb to aggressive histiocytic sarcoma. Lab Invest. 2010;90(9):1357-64.
262. PL Mercier MB, M Plante, J Gregoire, MC Renaud, K Ghani, B Tetu, I Bairati, D Bachvarov. Characterisation of DOK1, a candidate tumour suppressor gene, in epithelial ovarian cancer. Mol Oncol. 2011;5(5):438-53.
263. Jiang WG, Davies G, Martin TA, Parr C, Watkins G, Mason MD, et al. Targeting matrilysin and its impact on tumor growth in vivo: the potential implications in breast cancer therapy. Clin Cancer Res. 2005;11(16):6012-9.
264. Jiang WG, Hiscox S, Hallett MB, Scott C, Horrobin DF, Puntis MC. Inhibition of hepatocyte growth factor-induced motility and in vitro invasion of human colon cancer cells by gamma-linolenic acid. Br J Cancer. 1995;71(4):744-52.
265. Heyn H, Carmona FJ, Gomez A, Ferreira HJ, Bell JT, Sayols S, et al. DNA methylation profiling in breast cancer discordant identical twins identifies DOK7 as novel epigenetic biomarker. Carcinogenesis. 2013;34(1):102-8.
266. Laetitia Marisa AdR, Alex Duval, Janick Selves, Marie Pierre Gaub, Laure Vescovo, Marie-Christine Etienne-Grimaldi, Renaud Schiappa, Dominique Guenot, Mira Ayadi, Sylvain Kirzin, Maurice Chazal, Jean-Francois Flejou, Daniel Benchimol, Anne Berger, Arnaud Legarde, Erwan Pencreach, Francoise Piard, Dominique Elias, Yann Parc, Slyviane Olschwang, Gerard Milano, Pierre Laurent-Puig, Valerie Boige. Gene expression classification of colon cancer into molecular subtypes: characterisation, validation, and prognostic value. PLOS Medicine. 2013;10(5):e1001453.
267. Mercier PL, Bachvarova M, Plante M, Gregoire J, Renaud MC, Ghani K, et al. Characterization of DOK1, a candidate tumor suppressor gene, in epithelial ovarian cancer. Mol Oncol. 2011;5(5):438-53.
268. D B. Synaptic dysfunction in congenital myasthenic syndromes. Ann N Y Acad Sci. 2012;1275:63-9.
269. Cossins J LW, Belaya K, Maxwell S, Oldridge M, Lester T, Robb S, Beeson D. The spectrum of mutations that underlie the neuromuscular junction synaptopathy in DOK7 congenital myasthenic syndrome. Hum Mol Genet. 2012;21(17):3765-75.
270. Y Yamanashi TT, K Yokoyama. Activation of receptor protein-tyrosine kinases from the cytoplasmic compartment. J Biochem. 2012;151(4):353-9.
271. M Niki ADC, M Zhao, H Honda, H Hirai, L Van Aelst, C Cordon-Cardo, PP Pandolfi. Role of Dok-1 and Dok-2 in leukaemia suppression. J Exp Med. 2004;200(12):1689-95.
272. UniProt. P35968 (VGFR2_HUMAN) 2015 [Available from: http://www.uniprot.org/uniprot/P35968.
273. Technology CS. PhosphoSitePlus Protein Page: VEGFR2 (human) 2016 [

274. UniProt. P52333 (JAK3_HUMAN) 2015 [Available from: http://www.uniprot.org/uniprot/P52333.
275. Gene J. 2015 [Available from: http://www.genecards.org/cgi-bin/carddisp.pl?gene=JAK3.
276. Technology CS. Kinase-Disease Associations 2015 [Available from: http://www.cellsignal.com/contents/resources-reference-tables/kinase-disease-associations/science-tables-kinase-disease?Ntk=Content&N=4294956305&Ntt=VEGFR2&fromPage=plp.
277. UniProt. P78527 (PRKDC_HUMAN) 2015 [Available from: http://www.uniprot.org/uniprot/P78527.
278. GeneCards. PRKDC Gene 2015 [Available from: http://www.genecards.org/cgi-bin/carddisp.pl?gene=PRKDC.
279. Technology CS. PhosphoSitePlus Protein Page: DNAPK 2016 [Available from: http://www.phosphosite.org/proteinAction.action?id=2072&showAllSites=true.
280. PhosphoSitePlus. Protein Page: MEK5 (human) 2016 [Available from: http://www.phosphosite.org/proteinAction.action?id=720&showAllSites=true.
281. PhosphoSitePlus. Protein Page: CTNNB1 (human) 2016 [Available from: http://www.phosphosite.org/proteinAction.action?id=454&showAllSites=true.
282. PhosphoSitePlus. Protein Page: WNK2 (human) 2016 [Available from: http://www.phosphosite.org/proteinAction.action?id=2242&showAllSites=true.
283. PhosphoSitePlus. Protein Page: MKP-2 (human) 2016 [Available from: http://www.phosphosite.org/proteinAction.action?id=1337&showAllSites=true.
284. PhosphoSitePlus. Protein Page: CDC25C (human) 2016 [Available from: http://www.phosphosite.org/proteinAction.action?id=938&showAllSites=true.
285. PhosphoSitePlus. ERK1 2016 [Available from: http://www.phosphosite.org/proteinAction.action?id=595&showAllSites=true.
286. PhosphoSitePlus. Protein Page: MKK4 (human) 2016 [Available from: http://www.phosphosite.org/proteinAction.action?id=659&showAllSites=true.
287. Fu Z ZH, Zou F, Wang X, Chen Y, Liu L. Involvement of the Akt signaling pathway in ER-α36/GRP94-mediated signaling in gastric cancer. Oncol Lett. 2014;8(5):2077-80.
288. PhosphoSitePlus. Protein Page: PDGFRB (human) 2016 [Available from: http://www.phosphosite.org/proteinAction.action?id=634&showAllSites=true.
289. PhosphoSitePlus. Protein Page: PDHK4 (human) 2016 [Available from: http://www.phosphosite.org/proteinAction.action?id=2344&showAllSites=true.
290. Wang J YQ, She QB. New insights into 4E-BP1-regulated translation in cancer progression and metastasis. Cancer Cell Microenviron. 2014;1(5):pii: e331.
291. PhosphoSitePlus. Protein Page: 4E-BP1 (human) 2016 [Available from: http://www.phosphosite.org/proteinAction.action?id=555&showAllSites=true.
292. PhosphoSitePlus. Protein Page: MKK6 (human) 2016 [Available from: http://www.phosphosite.org/proteinAction.action?id=894&showAllSites=true.
293. PhosphoSitePlus. Protein Page: HER4 (human) 2016 [Available from: http://www.phosphosite.org/proteinAction.action?id=594&showAllSites=true.
294. PhosphoSitePlus. Protein Page: DUSP3 (human) 2016 [Available from: http://www.phosphosite.org/proteinAction.action?id=2082&showAllSites=true.
295. PhosphoSitePlus. Protein Page: PTEN (human) 2016 [Available from: http://www.phosphosite.org/proteinAction.action?id=1035&showAllSites=true.

296. Gupta VK YY, Gupta VB, Klistorner A, Graham SL. TrkB Receptor Signalling: Implications in Neurodegenerative,
Psychiatric and Proliferative Disorders. International Journal of Moleculare Sciences. 2013;14:10122-42.
297. GeneCards. NTRK2 Gene 2015 [Available from: http://www.genecards.org/cgi-bin/carddisp.pl?gene=NTRK2.
298. UniProtKB. P16220 (CREB1_HUMAN) 2015 [Available from: http://www.uniprot.org/uniprot/P16220.
299. PhosphoSitePlus. Protein Page: CREB (human) 2016 [Available from: http://www.phosphosite.org/proteinAction.action?id=1489&showAllSites=true.
300. UniProt. P14635 (CCNB1_HUMAN) 2015 [Available from: http://www.uniprot.org/uniprot/P14635.
301. Wang A YN, Ino N, Tanaka T, Mori H. Overexpression of cyclin B1 in human colorectal cancers. Journal of cancer research and clinical oncology. 1997;123(2):124-7.
302. GeneCards. BRCA1 Gene 2015 [Available from: http://www.genecards.org/cgi-bin/carddisp.pl?gene=BRCA1.
303. PhosphoSitePlus. Protein Page: BRCA1 (human) 2016 [Available from: http://www.phosphosite.org/proteinAction.action?id=929&showAllSites=true.
304. GeneCards. CDK1 Gene 2015 [Available from: http://www.genecards.org/cgi-bin/carddisp.pl?gene=CDK1.
305. GeneCards. CDK2 Gene 2015 [Available from: http://www.genecards.org/cgi-bin/carddisp.pl?gene=CDK2.
306. PhosphoSitePlus. Protein Page: CDK1 (human) 2016 [Available from: http://www.phosphosite.org/proteinAction.action?id=582&showAllSites=true.
307. PhosphoSitePlus. Protein Page: CDK2 (human) 2016 [Available from: http://www.phosphosite.org/proteinAction.action?id=583&showAllSites=true.
308. GeneCards. CHUK Gene 2015 [Available from: http://www.genecards.org/cgi-bin/carddisp.pl?gene=CHUK.
309. PhosphoSitePlus. Protein Page: IKKA (human) 2016 [Available from: http://www.phosphosite.org/proteinAction.action?id=461&showAllSites=true.
310. UniProtKB. Q13541 (4EBP1_HUMAN) 2015 [Available from: http://www.uniprot.org/uniprot/Q13541.
311. GeneCards. EIF4EBP1 Gene 2015 [Available from: http://www.genecards.org/cgi-bin/carddisp.pl?gene=EIF4EBP1.
312. UniProtKB. P15336 (ATF2_HUMAN) 2015 [Available from: http://www.uniprot.org/uniprot/P15336.
313. GeneCards. ATF2 Gene 2015 [Available from: http://www.genecards.org/cgi-bin/carddisp.pl?gene=ATF2.
314. PhosphoSitePlus. Protein Page: ATF-2 (human) 2016 [Available from: http://www.phosphosite.org/proteinAction.action?id=922&showAllSites=true.
315. GeneCards. PLCG1 Gene 2015 [Available from: http://www.genecards.org/cgi-bin/carddisp.pl?gene=PLCG1.
316. PhosphoSitePlus. Protein Page: PLCG1 (human) 2016 [Available from: http://www.phosphosite.org/proteinAction.action?id=1029&showAllSites=true.
317. UniProtKB. P17302 (CXA1_HUMAN) 2015 [Available from: http://www.uniprot.org/uniprot/P17302.
318. PhosphoSitePlus. Protein Page: GJA1 (human) 2016 [Available from: http://www.phosphosite.org/proteinAction.action?id=949&showAllSites=true.

319. PhosphoSitePlus. Protein Page: ERK5 (human) 2016 [Available from: http://www.phosphosite.org/proteinAction.action?id=7570&showAllSites=true.
320. GeneCards. CFL2 Gene 2015 [Available from: http://www.genecards.org/cgi-bin/carddisp.pl?gene=CFL2.
321. PhosphoSitePlus. Protein Page: Cofilin-2 (human) 2016 [Available from: http://www.phosphosite.org/proteinAction.action?id=3665&showAllSites=true.
322. UniProt. Q06124 (PTN11_HUMAN) 2015 [Available from: http://www.uniprot.org/uniprot/Q06124.
323. GeneCards. PTPN1 Gene 2015 [Available from: http://www.genecards.org/cgi-bin/carddisp.pl?gene=PTPN1.
324. PhosphoSitePlus. Protein Page: SHP-2 (human) 2016 [Available from: http://www.phosphosite.org/proteinAction.action?id=1103&showAllSites=true.
325. GeneCards. PDK3 Gene 2015 [Available from: http://www.genecards.org/cgi-bin/carddisp.pl?gene=PDK3.
326. PhosphoSitePlus. Protein Page: PDHK3 (human) 2016 [Available from: http://www.phosphosite.org/proteinAction.action?id=2347&showAllSites=true.
327. GeneCards. GNB2L1 Gene 2015 [Available from: http://www.genecards.org/cgi-bin/carddisp.pl?gene=GNB2L1.
328. PhosphoSitePlus. Protein Page: RACK1 (human) 2016 [Available from: http://www.phosphosite.org/proteinAction.action?id=4139&showAllSites=true.
329. GeneCards. GSG2 Gene 2015 [Available from: http://www.genecards.org/cgi-bin/carddisp.pl?gene=GSG2.
330. UniProtKB. P31948 (STIP1_HUMAN) 2015 [Available from: http://www.uniprot.org/uniprot/P31948.
331. PhosphoSitePlus. Protein Page: STI1 (human) 2016 [Available from: http://www.phosphosite.org/proteinAction.action?id=2638&showAllSites=true.
332. GeneCards. SMAD2 Gene 2015 [Available from: http://www.genecards.org/cgi-bin/carddisp.pl?gene=SMAD2.
333. UniProtKB. Q15796 (SMAD2_HUMAN) 2015 [Available from: http://www.uniprot.org/uniprot/Q15796.
334. PhosphoSitePlus. Protein Page: SMAD2 (human) 2016 [Available from: http://www.phosphosite.org/proteinAction.action?id=540&showAllSites=true.
335. PhosphoSitePlus. Protein Page: SMAD3 (human) 2016 [Available from: http://www.phosphosite.org/proteinAction.action?id=1045&showAllSites=true.
336. UniProtKB. Q00536 (CDK16_HUMAN) 2015 [Available from: http://www.uniprot.org/uniprot/Q00536.
337. GeneCards. CDK16 Gene 2015 [Available from: http://www.genecards.org/cgi-bin/carddisp.pl?gene=CDK16.
338. GeneCards. ROCK1 Gene 2015 [Available from: http://www.genecards.org/cgi-bin/carddisp.pl?gene=ROCK1.
339. PhosphoSitePlus. Protein Page: ROCK1 (human) 2016 [Available from: http://www.phosphosite.org/proteinAction.action?id=754&showAllSites=true.
340. GeneCards. MAP2K1 Gene 2015 [Available from: http://www.genecards.org/cgi-bin/carddisp.pl?gene=MAP2K1.
341. PhosphoSitePlus. Protein Page: MEK1 (human) 2016 [Available from: http://www.phosphosite.org/proteinAction.action?id=619&showAllSites=true.
342. GeneCards. PTPN12 Gene 2015 [Available from: http://www.genecards.org/cgi-bin/carddisp.pl?gene=PTPN12.

343. PhosphoSitePlus. Protein Page: PTP-PEST (human) 2016 [Available from: http://www.phosphosite.org/proteinAction.action?id=4997&showAllSites=true.
344. GeneCards. STK17B Gene 2015 [Available from: http://www.genecards.org/cgi-bin/carddisp.pl?gene=STK17B.
345. PhosphoSitePlus. Protein Page: DRAK2 (human) 2016 [Available from: http://www.phosphosite.org/proteinAction.action?id=764&showAllSites=true.
346. GeneCards. BMX Gene 2015 [Available from: http://www.genecards.org/cgi-bin/carddisp.pl?gene=BMX.
347. PhosphoSitePlus. Protein Page: Etk (human) 2016 [Available from: http://www.phosphosite.org/proteinAction.action?id=843&showAllSites=true.
348. UniProt. Q9NWZ3 (IRAK4_HUMAN) 2015 [Available from: http://www.uniprot.org/uniprot/Q9NWZ3.
349. PhosphoSitePlus. Protein Page: IRAK4 (human) 2016 [Available from: http://www.phosphosite.org/proteinAction.action?id=1998&showAllSites=true.
350. GeneCards. MET Gene 2015 [Available from: http://www.genecards.org/cgi-bin/carddisp.pl?gene=MET.
351. PhosphoSitePlus. Protein Page: Met (human) 2016 [Available from: http://www.phosphosite.org/proteinAction.action?id=620&showAllSites=true.
352. UniProt. P06493 (CDK1_HUMAN) 2015 [Available from: http://www.uniprot.org/uniprot/P06493.
353. UniProt. O60496 (DOK2_HUMAN) 2015 [Available from: http://www.uniprot.org/uniprot/O60496.
354. GeneCards. DOK2 2015 [Available from: http://www.genecards.org/cgi-bin/carddisp.pl?gene=DOK2&keywords=dok2.
355. GeneCards. VAV1 Gene 2015 [Available from: http://www.genecards.org/cgi-bin/carddisp.pl?gene=VAV1.
356. PhosphoSitePlus. Protein Page: VAV1 (human) 2016 [Available from: http://www.phosphosite.org/proteinAction.action?id=1065&showAllSites=true.
357. Duff SE JM, Rosa DD, Kumar S, Haboubi N, Sherlock D, O'Dwyer ST, Jayson GC. Vascular endothelial growth factors and receptors in colorectal cancer: implications for anti-angiogenic therapy. Eur J Cancer. 2006;42(1):112-7.
358. Giatromanolaki A KM, Sivridis E, Chlouverakis G, Vourvouhaki E, Turley H, Harris AL, Gatter KC. Activated VEGFR2/KDR pathway in tumour cells and tumour associated vessels of colorectal cancer. Eur J Clin Invest. 2007;37(11):878-86.
359. Kim YR YA, Figueiredo J, Reichardt W, Hu-Lowe D, Petrovsky A, Kang HW, Torres D, Mahmood U, Weissleder R, Bogdanov AA Jr. Detection of early antiangiogenic effects in human colon adenocarcinoma xenografts: in vivo changes of tumor blood volume in response to experimental VEGFR tyrosine kinase inhibitor. Cancer Res. 2005;65(20):9253-60.
360. Sakurai K YN, Yashiro M, Matsuzaki T, Komatsu M, Ohira M, Miwa A, Hirakawa K. A novel angiogenesis inhibitor, Ki23057, is useful for preventing the progression of colon cancer and the spreading of cancer cells to the liver. Eur J Cancer. 2007;43(17):2612-20.
361. Lin Q LR, Chirieac LR, Li C, Thomazy VA, Grammatikakis I, Rassidakis GZ, Zhang W, Fujio Y, Kunisada K, Hamilton SR, Amin HM. Constitutive activation of JAK3/STAT3 in colon carcinoma tumors and cell lines: inhibition of JAK3/STAT3 signaling induces apoptosis and cell cycle arrest of colon carcinoma cells. The American journal of pathology. 2005;167(4):969-80.

362. Mori D NY, Miyazaki K, Tokunaga O. Differential expression of Janus kinase 3 (JAK3), matrix metalloproteinase 13 (MMP13), heat shock protein 60 (HSP60), and mouse double minute 2 (MDM2) in human colorectal cancer progression using human cancer cDNA microarrays. Pathol Res Pract. 2005;201(12):777-89.
363. Hosoi Y WT, Nakagawa K, Matsumoto Y, Enomoto A, Morita A, Nagawa H, Suzuki N. Up-regulation of DNA-dependent protein kinase activity and Sp1 in colorectal cancer. International journal of oncology. 2004;25(2):461-8.
364. Lu Y ZH, Li YZ, Zhao P. [Clinicopathological significance of expressions of DNA dependent protein kinase catalytic subunit and P16 in colorectal carcinoma]. Zhonghua Yi Xue Za Zhi. 2008;88(29):2025-9.
365. Li M LY, Palchik GA, Matsunaga S, Wang D, Chen BP. The catalytic subunit of DNA-dependent protein kinase is required for cellular resistance to oxidative stress independent of DNA double-strand break repair. Free Radic Biol Med. 2014;76:278-85.
366. Huerta S GX, Dineen S, Kapur P, Saha D, Meyer J. Role of p53, Bax, p21, and DNA-PKcs in radiation sensitivity of HCT-116 cells and xenografts. Surgery. 2013;154(2):143-51.
367. Hu B RD, Su D, Lin H, Xian Z, Wan X, Zhang J, Fu X, Jiang L, Diao D, Fan X, Wang L, Wang J. Expression of the phosphorylated MEK5 protein is associated with TNM staging of colorectal cancer. BMC cancer. 2012;12:127.
368. Shao J EB, Sheng H. Roles of phosphatidylinositol 3'-kinase and mammalian target of rapamycin/p70 ribosomal protein S6 kinase in K-Ras-mediated transformation of intestinal epithelial cells. Cancer Res. 2004;64(1):229-35.
369. Sawa M MM, Yamada T. Targeting the Wnt signaling pathway in colorectal cancer. Expert Opin Ther Targets. 2015;6:1-11.
370. Garcia-Florez LJ G-AG, Frunza AM, Barneo-Serra L, Martinez-Alonso C, Fresno-Forcelledo MF. Predictive markers of response to neoadjuvant therapy in rectal cancer. J Surg Res. 2015;194(1):120-6.
371. Zhou J ZM, Huang Y, Feng L, Chen H, Hu Y, Chen H, Zhang K, Zheng L, Zheng S. MicroRNA-320b promotes colorectal cancer proliferation and invasion by competing with its homologous microRNA-320a. Cancer Lett. 2015;356(2 Pt B):669-75.
372. Minoo P ZI, Peterson M, Terracciano L, Lugli A. Characterization of rectal, proximal and distal colon cancers based on clinicopathological, molecular and protein profiles. International journal of oncology. 2010;37(3):707-18.
373. Lenertz LY LB, Min X, Xu BE, Wedin K, Earnest S, Goldsmith EJ, Cobb MH. Properties of WNK1 and implications for other family members. The Journal of biological chemistry. 2005;280(29):26653-8.
374. Moniz S VF, Matos P, Brazao R, Silva E, Kotelevets L, Chastre E, Gespach C, Jordan P. Protein kinase WNK2 inhibits cell proliferation by negatively modulating the activation of MEK1/ERK1/2. Oncogene. 2007;26(41):6071-81.
375. Jun P HC, Lal A, Wong JM, McDermott MW, Bollen AW, Plass C, Held WA, Smiraglia DJ, Costello JF. Epigenetic silencing of the kinase tumor suppressor WNK2 is tumor-type and tumor-grade specific. Neuro Oncol. 2009;11(4):414-22.
376. De Vriendt V DRW, Di Narzo AF, Tian S, Biesmans B, Jacobs B, Budinska E, Sagaert X, Rossi S, D'Ario G, Delorenzi M, Simon I, Vecchione L, Tejpar S. DUSP 4

expression identifies a subset of colorectal cancer tumors that differ in MAPK activation, regardless of the genotype. Biomarkers. 2013;18(6):516-24.
377. Lee G OS, White LS, Sun J, Stappenbeck TS, Piwnica-Worms H. Contributions made by CDC25 phosphatases to proliferation of intestinal epithelial stem and progenitor cells. PLoS One. 2011;6(1):e15561.
378. Park KS KN, Kim JJ, Kim H, Ahn YH, Choi KY. Differential regulation of MAP kinase cascade in human colorectal tumorigenesis. Br J Cancer. 1999;81(7):1116-21.
379. Wang Q DQ, Dong Z, Ehlers RA, Evers BM. Downregulation of mitogen-activated protein kinases in human colon cancers. Anticancer Res. 2000;20(1A):75-83.
380. Ross PJ GM, Cunningham D, DiStefano F, Andreyev HJ, Workman P, Clarke PA. Inhibition of Kirsten-ras expression in human colorectal cancer using rationally selected Kirsten-ras antisense oligonucleotides. Molecular cancer therapeutics. 2001;1(1):29-41.
381. Pattingre S BC, Codogno P. Amino acids interfere with the ERK1/2-dependent control of macroautophagy by controlling the activation of Raf-1 in human colon cancer HT-29 cells. The Journal of biological chemistry. 2003;278(19):16667-74.
382. Jeon HK CS, JUng NP. Association of the ERK1/2 and p38 kinase pathways with nitric oxide-induced apoptosis and cell cycle arrest in colon cancer cells. Cell Biol Toxicol. 2005;21(2):115-25.
383. Zhang YH WW, Xu H, Wang YY, Wu WX. Inducing effects of hepatocyte growth factor on the expression of vascular endothelial growth factor in human colorectal carcinoma cells through MEK and PI3K signaling pathways. Chin Med J. 2007;120(9):743-8.
384. Shama J G-MR, Pouyssegur J, Vial E. Major contribution of MEK1 to the activation of ERK1/ERK2 and to the growth of LS174T colon carcinoma cells. Biochemical and biophysical research communications. 2008;372(4):845-9.
385. Peng L XX, Li W, Qu L, Meng L, Lian S, Jiang B, Wu J, Shou C. PRL-3 promotes the motility, invasion, and metastasis of LoVo colon cancer cells through PRL-3-integrin beta1-ERK1/2 and-MMP2 signaling. Mol Cancer. 2009;8:110.
386. Thuong PT KN, Ohta S, Shiota S, Kanta H, Takeuchi K, Ito F. ent-kaurane diterpenoids from Croton tonkinensis induce apoptosis in colorectal cancer cells through the phosphorylation of JNK mediated by reactive oxygen species and dual-specificity JNK kinase MKK4. Anticancer Agents Med Chem. 2014;14(7):1051-61.
387. Huang MJ WP, Huang J, Zhang XW, Wang L, Liu HL, Wang JP. [Expression and clinicopathological significance of serine-257/threonine-261 phosphorylated MKK4 in colorectal carcinoma]. Zhonghua Yi Xue Za Zhi. 2013;93(10):746-50.
388. Wei Y WL, Lan P, Zhao H, Pan Z, Huang J, Lu J, Wang J. The association between -1304T>G polymorphism in the promoter of MKK4 gene and the risk of sporadic colorectal cancer in southern Chinese population. International journal of cancer Journal international du cancer. 2009;125(8):1876-83.
389. Chen Y SJ. [Closely relationship between expression of endoplasmic reticulum molecular chaperone Grp94 and c-myc oncogene in human colorectal carcinoma cell lines]. Zhonghua Zhong Liu Za Zhi. 1997;19(2):81-4.

390. Wang XP QF, Liu GZ, Chen RF. Correlation between clinicopathology and expression of heat shock protein 70 and glucose-regulated protein 94 in human colonic adenocarcinoma. World J Gastroenterol. 2005;11(7):1056-9.
391. Lindmark G SC, Glimelius B, Pahlman L, Rubin K, Gerdin B. Stromal expression of platelet-derived growth factor beta-receptor and platelet-derived growth factor B-chain in colorectal cancer. Lab Invest. 1993;69(6):682-9.
392. Wehler TC FK, Graf C, Drescher D, Schimanski K, Biesterfeld S, Berger MR, Kanzler S, Junginger T, Galle PR, Moehler M, Gockel I, Schimanski CC. PDGFRalpha/beta expression correlates with the metastatic behavior of human colorectal cancer: a possible rationale for a molecular targeting strategy. Oncol Rep. 2008;19(3):697-704.
393. Blouin JM PG, Collinet M, Nacfer M, Forest C, Laurent-Puig P, Coumoul X, Barouki R, Benelli C, Bortoli S. Butyrate elicits a metabolic switch in human colon cancer cells by targeting the pyruvate dehydrogenase complex. International journal of cancer Journal international du cancer. 2011;128(11):2591-601.
394. Leclerc D LN, Cao Y, Deng L, Wu Q, Powell J, Sapienza C, Rozen R. Genes with aberrant expression in murine preneoplastic intestine show epigenetic and expression changes in normal mucosa of colon cancer patients. Cancer Prev Res (Phila). 2013;6(11):1171-81.
395. Chao MW WL, Lai CY, Yang XM, Cheng YW, Lee KH, Pan SL, Teng CM. eIF4E binding protein 1 expression is associated with clinical survival outcomes in colorectal cancer. Oncotarget. 2015;6(27):24092-104.
396. Diab-Assaf M A-KR, Saadallah-Zeidan N, Habib K, Bitar N, Karam W, Liagre B, Harakeh S, Azar R. Expression of eukaryotic initiation factor 4E and 4E binding protein 1 in colorectal carcinogenesis. Int J Clin Exp Pathol. 2015;8(1):404-13.
397. Malinowsky K NU, Janssen KP, Bader FG, Spath C, Drecoll E, Keller G, Hofler H, Slotta-Huspenina J, Becker KF. Activation of the PI3K/AKT pathway correlates with prognosis in stage II colon cancer. Br J Cancer. 2014;110(8):2081-9.
398. Lee J LS, Kang SY, Do IG, Lee S, Ha SY, Cho J, Kang WK, Jang J, Ou SH, Kim KM. Identification of ROS1 rearrangement in gastric adenocarcinoma. Cancer. 2013;119(9):1627-35.
399. Parray AA BR, Bhat HF, Wani L, Mokhdomi TA, Mushtaq U, Bhat SS, Kirmani D, Kuchay S, Wani MM, Khanday FA. MKK6 is upregulated in human esophageal, stomach, and colon cancers. Cancer Invest. 2014;32(8):416-22.
400. Williams CS BJ, Demory Beckler M, Almohazey D, Washington MK, Smith JJ, Frey MR. ERBB4 is over-expressed in human colon cancer and enhances cellular transformation. Carcinogenesis. 2015;36(7):710-8.
401. Malapelle U PP, Sgariglia R, Vigliar E, Biglietto M, Carlomagno C, Giuffre G, Bellevicine C, Troncone G. Less frequently mutated genes in colorectal cancer: evidences from next-generation sequencing of 653 routine cases. J Clin Pathol. 2016;69(9):767-71.
402. Gao X ZS, Zhu Z. Genetic variation of ErbB4 confers risk of colorectal cancer in a Chinese Han population. Cancer Biomark. 2014;14(6):435-9.
403. Rokavec M JC, Schroth W, Istrate MA, Haas S, Fischer HP, Vollmert C, Illig T, Hamann U, Ko YD, Glavac D, Brauch H. A novel polymorphism in the promoter region of ERBB4 is associated with breast and colorectal cancer risk. Clinical cancer research : an official journal of the American Association for Cancer Research. 2007;13(24):7506-14.

404. Mitsui K YM, Tatsuguchi A, Shinji S, Gudis K, Tanaka S, Fujimori S, Sakamoto C. Localization of phosphorylated ErbB1-4 and heregulin in colorectal cancer. BMC cancer. 2014;14:863.
405. Kountourakis P PK, Psyrri A, Rontogianni D, Xiros N, Patsouris E, Pectasides D, Economopoulos T. Prognostic significance of HER3 and HER4 protein expression in colorectal adenocarcinomas. BMC cancer. 2006;28(6):46.
406. Pavic K DG, Kohn M. VHR/DUSP3 phosphatase: structure, function and regulation. FEBS J. 2015;282(10):1871-90.
407. Henkens R DP, Arafa M, Moutschen M, Zeddou M, Tautz L, Boniver J, Mustelin T, Rahmouni S. Cervix carcinoma is associated with an up-regulation and nuclear localization of the dual-specificity protein phosphatase VHR. BMC cancer. 2008;8:147.
408. Wang JY YC, Chou HC, Yang CH, Fu YN, Chen YT, Cheng HW, Huang CY, Liu HP, Huang SF, Chen YR. Vaccinia H1-related phosphatase is a phosphatase of ErbB receptors and is down-regulated in non-small cell lung cancer. The Journal of biological chemistry. 2011;286(12):10177-84.
409. Amand M EC, Bajou K, Cerignoli F, Blacher S, Martin M, Dequiedt F, Drion P, Singh P, Zurashvili T, Vandereyken M, Musumeci L, Mustelin T, Moutschen M, Gilles C, Noel A, Rahmouni S. DUSP3/VHR is a pro-angiogenic atypical dual-specificity phophatase. Mol Cancer. 2014;13:108.
410. Slattery ML HJ, Lundgreen A, Fitzpatrick FA, Curtin K, Wolff RK. Genetic variation in a metabolic signaling pathway and colon and rectal cancer risk: mTOR, PTEN, STK11, RPKAA1, PRKAG2, TSC1, TSC2, PI3K and Akt1. Carcinogenesis. 2010;31(9):1604-11.
411. Atreya CE SZ, Xu N, Matli MR, Tikishvili E, Welbourn W, Stone S, Shokat KM, Warren RS. PTEN expression is consistent in colorectal cancer primaries and metastases and associates with patient survival. Cancer Med. 2013;2(4):496-506.
412. Bi Z DL, Gu XM. Clinical significance of MMP-7 and PTEN expression in colorectal cancer. Hepatogastroenterology. 2013;60(121):32-6.
413. Therkildsen C BT, Henrichsen-Schnack T, Ladelund S, Nilbert M. The predictive value of KRAS, NRAS, BRAF, PIK3CA and PTEN for anti-EGFR treatment in metastatic colorectal cancer: A systematic review and meta-analysis. Acta Oncol. 2014;53(7):852-64.
414. Akil H PA, Melin C, Jauberteau MO, Mathonnet M. Fine-tuning roles of endogenous brain-derived neurotrophic factor, TrkB and sortilin in colorectal cancer cell survival. PLoS One. 2011;6(9):e25097.
415. Fujikawa H TK, Toiyama Y, Saigusa S, Inoue Y, Uchida K, Kusunoki M. High TrkB expression levels are associated with poor prognosis and EMT induction in colorectal cancer cells. J Gastroenterol. 2012;47(7):775-84.
416. Fan M SJ, Wang W, Fan J, Wang L, Zhang X, Yang A, Wang W, Zhang R, Li J. Tropomyosin-related kinase B promotes distant metastasis of colorectal cancer through portein kinase B-mediated anoikis suppression and correlates with poor prognosis. Apoptosis. 2014;19(5):860-70.
417. Sasahira T UN, Kurihara M, Matsushima S, Ohmori H, Fujii K, Bhawal UK, Yamamoto K, Kirita T, Kuniyasu H. Tropomyosin receptor kinases B and C are tumor progressive and metastatic marker in colorectal carcinoma. Human pathology. 2013;44(6):1098-106.
418. Tanaka K OY, Toiyama Y, Inoue Y, Saigusa S, Kawamura M, Araki T, Uchida K, Mohri Y, Kusunoki M. Brain-derived neurotrophic factor (BDNF)-induced

tropomyosin-related kinase B (Trk B) signalling is a potential therapeutic target for peritoneal carcinomatosis arising from colorectal cancer. PLoS One. 2014;9(5):e96410.
419. Fang Z LA, Chen J, Zhang X, Liu H, Li H, Hu Y, Zhang X, Zhang J, Qiu L, Mei L, Shao J, Chen X. CREB1 directly activtaes the transcription of ribonucleotide reductase small subunit M2 and promotes the aggressiveness of human colorectal cancer. Oncotarget. 2016;doi: 10.18632/oncotarget.12938.
420. Lu H GV, Disis ML. Targeting serum antibody for cancer diagnosis: a focus on colorectal cancer. Expert Opin Ther Targets. 2007;11(2):235-44.
421. Phelan CM IJ, Lynch HT, Lubinski J, Gronwald J, Moller P, Ghadirian P, Foulkes WD, Armel S, Eisen A, Neuhausen SL, Senter L, Singer CF, Ainsworth P, Kim-Sing C, Tung N, Llacuachaqui M, Chornokur G, Ping S, Narod SA, Hereditary Breast Cancer Study Group. Incidence of colorectal cancer in BRCA1 and BRCA2 mutation carriers: results from a follow-up study. Br J Cancer. 2014;110(2):530-4.
422. Margalef P F-MV, Villanueva A, Garcia-Carbonell R, Iglesias M, Lopez L, Martinez-Iniesta M, Villa-Freixa J, Mulero MC, Andreu M, Torres F, Mayo Mw, Bigas A, Espinosa L. A truncated form of IKKalpha is responsible for specific nuclear IKK activity in colorectal cancer. Cell Rep. 2012;2(4):840-54.
423. Alameda JP M-MR, Fernandez-Acenero MJ, Navarro M, Page A, Jorcano JL, Bravo A, Ramirez A, Casanova ML. Increased IKKalpha expression in the basal layer of the epidermis of transgenic mice enhances the malignant potential of skin tumours. PLoS One. 2011;6(7):e21984.
424. Zhang YJ DQ, Sun DF, Xiong H, Tian XQ, Gao FH, Xu MH, Chen GQ, Han ZG, Fang JY. mTOR signaling pathway is a target for the treatment of colorectal cancer. Ann Surg Oncol. 2009;16(9):2617-28.
425. Pradhan MP PN, Palakal MJ. A systems biology approach to the global analysis of transcription factors in colorectal cancer. BMC cancer. 2012;12:331.
426. Lo Iacono M MV, Vavala T, Gisabella M, Saviozzi S, Bracco E, Novello S, Papotti M, Scagliotti GV. ATF2 contributes to cisplatin resistance in non-small cell lung cancer and celastrol induces cisplatic resensitisation through inhibition of JNK/ATF2 pathway. International journal of cancer Journal international du cancer. 2015;136(11):2598-609.
427. Xu Y LZ, Guo K. The effect of JDP2 and ATF2 on the epithelial-mesenchymal transition of human pancreatic cancer cell lines. Pathol Oncol Res. 2012;18(3):571-7.
428. Wu DS CC, Wu ZJ, Liu B, Gao L, Yang Q, Chen W, Chen JM, Bao Y, Qu L, Wang LH. ATF2 predicts poor prognosis and promotes malignant phenotypes in renal cell carcinoma. J Exp Clin Cancer Res. 2016;35(1):108.
429. Lau E FY, Claps G, Fukuda MN, Perlina A, Donn D, Jilaveanu L, Kluger H, Freeze HH, Ronai ZA. The transcription factor ATF2 promotes melanoma metastasis by suppressing protein fucosylation. Sci Signal. 2015;8(406):ra124.
430. Bhoumik A FB, Derossi C, Breitwieser W, Kluger HM, Davis S, Subtil A, Meltzer P, Krajewski S, Jones N, Ronai Z. Suppressor role of activating transcription factor 2 (ATF2) in skin cancer. Proceedings of the National Academy of Sciences of the United States of America. 2008;105(5):1674-9.
431. Tomas NM MK, Piecha JC, Niggemann B, Zanker KS. Akt and phospholipase Cgamma are involved in the regulation of growth and migration

of MDA-MB-468 breast cancer and SW480 colon cancer cells when cultured with diabetogenic levels of glucose and insulin. BMC Res Notes. 2012;5:214.
432. Bigelow K NT. Increase of gap junction activities in SW480 human colorectal cancer cells. BMC cancer. 2014;14:502.
433. Sirnes S BJ, Kolberg M, Kjenseth A, Lind GE, Svindland a, Brech A, Nesbakken A, Lothe RA, Leithe E, Rivedal E. Connexin 43 acts as a colorectal cancer tumour suppressor and predicts disease outcome. International journal of cancer Journal international du cancer. 2012;131(3):570-81.
434. Simoes AE PD, Gomes SE, Brito H, Carvalho T, French A, Castro RE, Steer CJ, Thibodeau SN, Rodrigues CM, Borralho PM. Aberrant MEK5/ERK5 signalling contributes to human colon cancer progression via NF-KB activation. Cell Death Dis. 2015;6:e1718.
435. Wang Y KY, Ueno T, Suzuki N, Yoshino S, Iizuka N, Zhang X, Oka M, Nakamura K. Differential expression of up-regulated cofilin-1 and down-regulated cofilin-2 characteristic of pancreatic cancer tissues. Oncol Rep. 2011;26(6):1595-9.
436. Mathew S GS, Wang Y, Siddiqui MR, Srinivasan K, Tan L, Khurana S. Potential molecular mechanism for c-Src kinase-mediated regulation of intestinal cell migration. The Journal of biological chemistry. 2008;283(33):22709-22.
437. Lu CW LS, Chien CW, Lin SC, Lee CT, Lin BW, Lee JC, Tsai SJ. Overexpression of pyruvate dehydrogenase kinase 3 increases drug resistance and early recurrence in colon cancer. The American journal of pathology. 2011;179(3):1405-14.
438. Cheng S RJ, Su L, Liu J, Liu Q, Zhou J, Ye X, Zhu N. O-GIcNAcylation of the signalling scaffold protein, GNB2L1 promotes its degredation and increases metastasis of gastric tumours. Biochemical and biophysical research communications. 2016;478(4):1497-502.
439. Jin S MY, Wang X, Liu Z, Wan L, Xiong Y, Zhang Y, Zhou L, Li L. Overexpressed RACK1 is positively correlated with malignant degree of human colorectal carcinoma. Molecular biology reports. 2014;41(5):3393-9.
440. Swaminathan G CC. Rack1 promotes epithelial cell-cell adhesion by regulating E-cadherin endocytosis. Oncogene. 2012;31(3):376-89.
441. Mamidipudi V CC. A novel pro-apoptotic function of RACK1: suppression of Src activity in the intrinsic and Akt pathways. Oncogene. 2009;28(50):4421-33.
442. Cuny GD RM, Ulyanova NP, Patnaik D, Pique V, Casano G, Liu JF, Lin X, Xian J, Glicksman MA, Stein RL, Higgins JM. Structure-activity relationship study of acridine analogs as haspin and DYRK2 kinase inhibitors. Bioorg Med Chem Lett. 2010;20(12):3491-4.
443. Erlich RB KS, Lima FR, Muras AG, Martins RA, Linden R, Chiarini LB, Martins VR, Moura Neto V. STI1 promotes glioma proliferation through MAPK and PI3K pathways. Glia. 2007;55(16):1690-8.
444. Fonseca AC RL, Amaral RF, Assad Kahn S, Lobo D, Martins S, Marcondes de Souza J, Moura-Neto V, Lima FR. Microglial stress inducible protein 1 promotes proliferation and migration in human glioblastoma cells. Neuroscience 2012;200:130-41.
445. Kawabata M IT, Inoue H, Hanai J, Nishihara A, Hanyu A, Takase M, Ishidou Y, Udagawa Y, Oeda E, Goto D, Yagi K, Kato M, Miyazono K. Intracellular signalling

of the TGF-beta superfamily by Smad proteins. Ann N Y Acad Sci. 1999;886:73-82.
446. Laurent-Puig P BH, Cugnenc PH. Sequence of molecular genetic events in colorectal tumourigenesis. Eur J Cancer Prev. 1999;8(Suppl 1):S39-47.
447. Matsuzaki K OK. Transforming growth factor-beta during carcinogenesis: the shift from epithelial to mesenchymal signalling. J Gastroenterol. 2006;41(4):295-303.
448. Yanagi T TK, Wilkie-Grantham R, Hishiki A, Nagai K, Toyonaga E, Chivukula P, Matsuzawa S. Lipid nanoparticle-mediated siRNA transfer against PCTAIRE1/PCTK1/Cdk16 inhibits in vivo cancer growth. Mol Ther Nucleic Acids. 2016;5(6):e327.
449. Sari I BB, Ozkara E, Oztuzcu S, Camci C, Demiryurek AT. Role of rho-kinase gene polymorphisms and protein expressions in colorectal cancer development. Pathobiology. 2013;80(3):138-45.
450. Neuzillet C T-RA, de Mestier L, Cros J, Faivre S, Raymond E. MEK in cancer and cancer therapy. Pharmacol Ther. 2014;141(2):160-71.
451. Temraz S MD, Shamseddine A. Dual inhibition of MEK and PI3K pathway in KRAS and BRAF mutated colorectal cancers. Int J Mol Sci. 2015;16(9):22976-88.
452. Doherty GA BS, Austin SC, Scully GM, Sadlier DM, Neilan TG, Kay EW, Murray FE, Fitzgerald DJ. Regulation of the apoptosis-inducing kinase DRAK2 by cyclooxygenase-2 in colorectal cancer. Br J Cancer. 2009;101(3):483-91.
453. Chang YM KH, Evans CP. Nonreceptor tyrosine kinases in prostate cancer. Neoplasia. 2007;9(2):90-100.
454. Holopainen T L-AV, Zheng W, Heljasvaara R, Jones D, He Y, Tvorogov D, D'Amico G, Wiener Z, Andersson LC, Pihlajaniemi T, Min W, Alitalo K. Deletion of the endothelial Bmx tyrosine kinase decreases tumour angiogenesis and growth. Cancer Res. 2012;72(14):3512-21.
455. Chaudhary D RS, Romero DL. Recent advances in the discovery of small molecule inhibitors of interleukin-1 receptor-associated kinase 4 (IRAK4) as a therapeutic target for inflammation and oncology disorders. Journal of Medicinal Chemistry. 2015;58:96-110.
456. Fazekas K CO, Koves I, Raso E, Timar J. Experimental and clinicopathologic studies on the function of the HGF receptor in human colon cancer metastasis. Clinical & Experimental Metastasis. 2000;18(8):639-49.
457. Takeuchi H BA, Saha S, Turner R, Wiese D, Tanaka M, Kuo C, Wang HJ, Hoon DSB. c-met expression level in primary colon cancer: A predictor of tumour invasion and lymph node metastases. Clinical Cancer Research. 2003;9(4):1480-8.
458. Corso S CP, Giordano S. Cancer therapy: can the challenge be MET? Trends in Molecular Medicine. 2005;11(6):284-92.
459. Sung WW LY, Wu PR, Yen HH, Lai HW, Su TC, Huang RH, Wen CK, Chen CY, Chen CJ, Yeh KT. High nuclear/cytoplasmic ratio of Cdk1 expression predicts poor prognosis in colorectal cancer patients. BMC cancer. 2014;14(951).
460. Lin PC YY, Tyan YC, Hsiao ES, Chu PC, Lee CT, Lee JC, Chen YM, Liao PC. Identification of Phosphorylated Cyclin-Dependent Kinase 1 Associated with Colorectal Cancer Survival Using Label-Free Quantitative Analyses. PLoS One. 2016;11(7):e0158844.

461. Huang MY WJ, Chang HJ, Kuo CW, Tok TS, Lin SR. CDC25A, VAV1, TP73, BRCA1 and ZAP70 gene overexpression correlates with radiation response in colorectal cancer. Oncol Rep. 2011;25(5):1297-306.
462. Laplante M SD. mTOR signaling at a glance. Journal of Cell Science. 2009;122:3589-94.
463. Friedrich T SM, Gutting T, Janssen KP, Behrens HM, Rocken C, Ebert MPA, Burgermeister E. Subcellular compartmentalization of docking protein-1 contributes to progression in colorectal cancer. EBioMedicine. 2016;8:159-72.